NASA TECHNICAL NOTE

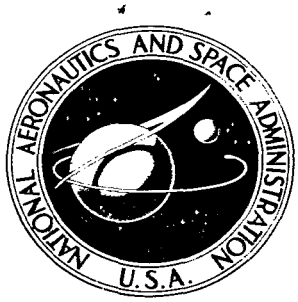

NASA TN D-6098

A COMPARISON OF AIRCRAFT AND GROUND VEHICLE STOPPING PERFORMANCE ON DRY, WET, FLOODED, SLUSH-, SNOW-, AND ICE-COVERED RUNWAYS

Final Report on Project Combat Traction, a Joint USAF-NASA Program

by

Thomas J. Yager, W. Pelham Phillips, and Walter B. Horne

Langley Research Center

and

Howard C. Sparks

Aeronautical Systems Division
Wright-Patterson Air Force Base

NATIONAL AERONAUTICS AND SPACE ADMINISTRATION • WASHINGTON, D. C. • NOVEMBER 1970

NASA TECHNICAL NOTE

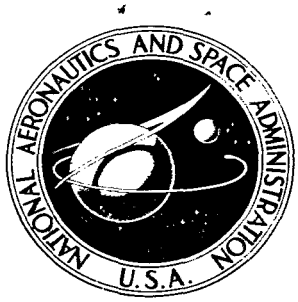

NASA TN D-6098

A COMPARISON OF AIRCRAFT AND GROUND VEHICLE STOPPING PERFORMANCE ON DRY, WET, FLOODED, SLUSH-, SNOW-, AND ICE-COVERED RUNWAYS

Final Report on Project Combat Traction, a Joint USAF-NASA Program

by

Thomas J. Yager, W. Pelham Phillips, and Walter B. Horne

Langley Research Center

and

Howard C. Sparks

Aeronautical Systems Division
Wright-Patterson Air Force Base

NATIONAL AERONAUTICS AND SPACE ADMINISTRATION • WASHINGTON, D. C. • NOVEMBER 1970

1. Report No.	2. Government Accession No.	3. Recipient's Catalog No.
NASA TN D-6098		

4. Title and Subtitle	5. Report Date
A COMPARISON OF AIRCRAFT AND GROUND VEHICLE STOPPING PERFORMANCE ON DRY, WET, FLOODED, SLUSH-, SNOW-, AND ICE-COVERED RUNWAYS	November 1970
	6. Performing Organization Code

7. Author(s)	8. Performing Organization Report No.
Thomas J. Yager, W. Pelham Phillips, Walter B. Horne, and Howard C. Sparks	L-7565
	10. Work Unit No. 126-61-12-05

9. Performing Organization Name and Address	11. Contract or Grant No.
NASA Langley Research Center, Hampton, Va. 23365 USAF Wright-Patterson Air Force Base, Ohio 45433	
	13. Type of Report and Period Covered: Technical Note

12. Sponsoring Agency Name and Address	14. Sponsoring Agency Code
National Aeronautics and Space Administration Washington, D.C. 20546	

15. Supplementary Notes

Appendix D by R. W. Sugg of British Ministry of Aircraft Supply

16. Abstract

A joint USAF-NASA research program has studied the stopping performance of an instrumented C-141A four-engine jet transport and several instrumented ground vehicles on 50 runways in the United States and Europe under dry, wet, flooded, slush, snow, and ice conditions. It is shown that measurement of the stopping distance of a diagonal-braked ground vehicle provides a meaningful measure of the slipperiness of a wet runway, and permits accurate prediction of the stopping distance of an aircraft under varied runway slipperiness conditions as well as a means for realistic calculation of crosswind limitations. It is also shown that aircraft stopping performance on a wet runway can be considerably improved either by grooving the runway or by use of a porous surface course.

17. Key Words (Suggested by Author(s))	18. Distribution Statement
Runway surface treatments Aircraft-ground vehicle stopping performance Runway slipperiness due to adverse weather	Unclassified – Unlimited

19. Security Classif. (of this report)	20. Security Classif. (of this page)	21. No. of Pages	22. Price*
Unclassified	Unclassified	196	$3.00

*For sale by the National Technical Information Service, Springfield, Virginia 22151

CONTENTS

A COMPARISON OF AIRCRAFT AND GROUND VEHICLE STOPPING PERFORMANCE ON DRY, WET, FLOODED, SLUSH-, SNOW-, AND ICE-COVERED RUNWAYS

Final Report on Project Combat Traction,
a Joint USAF-NASA Program

By Thomas J. Yager, W. Pelham Phillips, and Walter B. Horne
Langley Research Center

and

Howard C. Sparks
Aeronautical Systems Division
Wright-Patterson Air Force Base

SUMMARY

A joint USAF-NASA research program has studied the stopping performance of an instrumented C-141A four-engine jet transport and several instrumented ground vehicles on 50 runways in the United States and Europe under dry, wet, flooded, slush, snow, and ice conditions. It is shown that measurement of the stopping distance of a diagonal-braked ground vehicle provides a meaningful measure of the slipperiness of a wet runway, and permits accurate prediction of the stopping distance of an aircraft under varied runway slipperiness conditions as well as a means for realistic calculation of crosswind limitations. It is also shown that aircraft stopping performance on a wet runway can be considerably improved either by grooving the runway or by use of a porous surface course.

INTRODUCTION

Wet-runway operating problems became of primary concern with the introduction of jet aircraft since their landing speeds are usually well above the hydroplaning speed of their tires. In addition, improved flight instruments and instrument landing systems have led to more landings being made under adverse weather conditions. The increased landing speeds coupled with more landings being made on wet runways have resulted in more landing accidents occurring because of the lack of effective braking action. This experience with both military and civil jet aircraft operation indicates that the presently used

performance prediction methods for aircraft take-off and landing accountability on wet or slippery runways are deficient in several respects.

For certification of piston-engine category aircraft for civil operation, performance on dry runways is determined and FAA regulations increase the dry landing distances thus obtained by a factor of 1.67 to provide a safety margin for operation on dry runways, and to provide for the increase in stopping distance required on a wet runway. In January 1966, the FAA instituted the 15-percent rule which increased this factor to 1.92 for jet-turbine-category aircraft operation on wet runways; thus, recognition was made of the fact that jet-engine-powered aircraft were experiencing more difficulty in stopping on wet or slippery runways than the piston-engine aircraft. This civil regulatory approach for wet-runway accountability does not differentiate between runways of different slipperiness and does not account for the loss of directional control due to reduction in sideways traction.

The U.S. Air Force uses the RCR or runway condition reading system to account for wet or slippery runway conditions. RCR numbers are obtained by making maximum braking measurements on the runway with an airport ground vehicle employing a James brake decelerometer at speeds of 20 to 30 miles per hour. The flight manual of every aircraft in the U.S. Air Force inventory contains take-off and landing distance charts based on RCR numbers. Also given are crosswind limitations based on the same RCR numbers. The main problem associated with the RCR system has been that the low-speed measurements of runway slipperiness made by the ground vehicle cannot be uniquely related to the actual slipperiness experienced by the aircraft at the higher speeds of the landing roll, especially on wet runways. As a result, the RCR system can considerably underestimate the actual aircraft landing distance on a wet runway. For the same reason, an unconservative crosswind limitation can be given the pilot for a landing or take-off.

For the past decade, the U.S. Air Force (USAF) and National Aeronautics and Space Administration (NASA) have been cooperating extensively on research of aircraft skidding problems on wet and slippery runways. The USAF furnished aircraft tires, landing gears, wheels, and complete aircraft for study by scientists at specially equipped research facilities of the NASA Langley Research Center and Wallops Station. From this effort, along with outstanding cooperation and assistance of the FAA, NTSB, ATA, and ALPA in this country, and the Ministry of Public Works and Roads, Road Research Laboratories, and Ministry of Aviation Supply in England, many studies were generated which greatly increased the understanding of hydroplaning and other skidding factors.

During the late fifties and early sixties, Langley Research Center conducted research on the landing loads track on full-size aircraft tires which disclosed a significant loss of traction and complete wheel spin-down due to hydroplaning. These results

were confirmed with flight tests. One important early result of this work was the development of the slush drag and dynamic hydroplaning equations. Extensive tests at the landing loads track showed how tire groove patterns and depth affected the ability of the tire to develop friction on wet and flooded surfaces. Friction was found to increase with an increase in the number and depth of grooves. The studies, however, showed the groove patterns to be insignificant in affecting friction when less than approximately 1/16 inch of groove depth remained. In this same period, joint testing by the FAA and NASA of an instrumented four-engine jet transport also investigated hydroplaning in terms of aircraft slush-drag reduction and unbraked wheel spindown. Also, a study of aircraft skidding accidents had revealed that in many cases, there were elliptical areas of reverted rubber on the tire tread. It was evident that the tire had undergone a locked-wheel skid of a lengthy duration. Tests at the NASA landing loads track confirmed the fact that extremely low values of friction occurred when tires contained reverted-rubber patches. Another type of hydroplaning was that associated with thin fluid films between pavement and tire and designated as viscous hydroplaning.

The research indicated that measures other than tire-tread design would have to be taken to solve the total runway hydroplaning problem, which was designated in three types as dynamic hydroplaning, viscous skidding, and reverted-rubber skidding. One approach to solve the problem of low friction under dynamic hydroplaning conditions was to direct a stream of high-pressure air in front of the tire to displace the water on the runway. Subsequent tests made by NASA on their landing loads track and the Douglas Aircraft Company on a DC-7 showed a significant improvement in friction under flooded conditions; however, under wet and damp conditions, viscous and reverted-rubber skidding was still experienced.

It was obvious that the solution to the problem of skidding would not come from tire or aircraft improvement alone. Attention was then focused on the pavement surface. A British study revealed that transverse grooves in the pavement surface provided significant improvement in the traction of a problem runway. Tests on similarly grooved surfaces at the NASA landing loads track under flooded, wet, and damp conditions showed that grooved surfaces greatly alleviated dynamic hydroplaning, viscous skidding, and reverted-rubber skidding.

The next step was to construct a research runway at the NASA Wallops Station. Tests were conducted with three aircraft and several friction-measuring vehicles. Results of these tests and tests at Langley Research Center indicated that grooves in the runway surfaces did indeed improve landing characteristics. (See ref. 1.) As a result, surfaces of runways at several Air Force and civil airports were grooved. The data from the test track and the short test sections at Wallops Station, however, left many questions unanswered as to the relative merits of the different surfaces and surface treatments for a full-length runway.

Project Combat Traction was initiated as a joint U.S. Air Force-NASA project consisting of two parts: (a) Full-stop brake tests were made by an instrumented C-141A aircraft, an RCR test vehicle, and a diagonal-braked test vehicle on civil and military runways in the United States and Europe under dry, artificially wet, natural rain, ice, and snow conditions. Included in the European program were tests conducted jointly with the British Ministry of Aviation Supply on Royal Air Force (RAF) and Royal Navy (RN) Bases using a Mu-meter and a Miles engineering skid trailer. (b) Limited brake tests were conducted on the landing research runway at NASA Wallops Station, with the C-141A to correlate the results with those of similar tests previously conducted on an F-4D and a Convair 990A, and Beech Queen Aire. Most of the research described in the introduction is contained in references 1 to 15.

These programs were designed to meet the following research objectives as specified in reference 16:

(a) Establish and validate a means for predicting aircraft stopping distance for various surfaces by use of a ground vehicle as a means of assessing surface condition.

(b) Assemble a priority list of USAF runways requiring corrective measures to prevent skidding and hydroplaning accidents.

(c) Determine optimum runway surfaces.

(d) Investigate a water-depth warning system or other measuring system.

The preliminary results of Project Combat Traction have been reported in references 17 and 18 and the final results are presented in this paper.

Appendix A presents a compilation of the test data. Methods used to compute the data are presented in appendix B. Civil engineering descriptions of the runways tested, if available, are presented in appendix C. Appendix D presents the results of tests conducted by the British Ministry of Aviation Supply.

SYMBOLS

The data are referred to the body-axis system except the lift and drag coefficients which are referred to the stability-axis system. The estimated center-of-gravity location for the C14A aircraft tests was at $0.28\bar{c}$. All coefficients are based on the projected wing planform area and mean geometric chord. Pitching-moment coefficient $C_{m,g}$ was determined about the intersection of the main-gear strut center line and the ground.

a_x uncorrected longitudinal acceleration, ft/sec^2

$\vec{a}_x$ longitudinal acceleration corrected for accelerometer platform attitude, ft/sec^2

C_D three-point aerodynamic drag coefficient for test configuration (take-off flaps, spoilers deployed), $\frac{Drag}{qS}$

C_L three-point aerodynamic lift coefficient for test configuration (take-off flaps, spoilers deployed), $\frac{Lift}{qS}$

$C_{m,g}$ pitching-moment coefficient about intersection of main-gear strut center line and ground, $\frac{Moment}{qS\bar{c}}$

$\bar{c}$ mean geometric wing chord, 266.5 inches

D uncorrected stopping distance, ft

D_{corr} corrected stopping distance from a brake engagement ground speed of 100 knots to a full stop, ft

ΔD_B incremental distance from brake engagement to $V_G = 100$ knots (positive when $V_{G,B} < 100$ knots; negative when $V_{G,B} > 100$ knots), ft

ΔD_{final} incremental distance from brake release to a full stop (positive always since $V_{G,final} > 0$)

$F_{z,m}$ vertical load on main gear (instantaneous computation during a braking run), lb

g acceleration due to gravity, 32.17 ft/sec^2

h_{cg} vertical displacement of center of gravity from ground, ≈96.0 inches

$K_{a,x}$ accelerometer sensitivity constant, counts/ft/sec^2

p_a ambient pressure during braking test, lb/ft^2

q free-stream dynamic pressure, lb/ft^2

S projected wing planform area, ft^2

$S, S_1, S_2, \ldots S_6$ runway distances (fig. 25)

T_a ambient temperature, ^{o}Rankine

T_n installed idle thrust (from engine manufacturer's data), lb

t time measured from V_{Go}, sec

Δt time increment

V_A airspeed, ft/sec

V_G ground speed, ft/sec

V_w wind velocity component parallel to runway center line (positive, when headwind; negative, when tailwind), ft/sec

ΔV velocity increment

W configuration test weight (estimated from empty weight + crew + cargo + fuel for each test run), lb

$\overline{X}, X_A, X_B, X_C$ stopping distance ratios (fig. 25)

Δx longitudinal distance between nose and main gears, 636.0 inches

Δx_g longitudinal distance from center-of-gravity station to main gear, ≈48.75 inches

y vertical axis

α angle of attack, deg

ϵ thrust misalinement angle, 0^{o}

μ_B braking friction coefficient

μ_R rolling friction coefficient, 0.015 (assumed)

μ_{wet}, μ_{dry}	wet and dry braking friction coefficients, respectively

Subscripts:

o	initial condition
B	condition at brake engagement
Braked	condition measured during maximum braking
final	condition at braked release
R	condition measured during free-rolling tare test
RDG	raw test data
Zero	data zero

ABBREVIATIONS

AC	asphaltic concrete
ALPA	Air Line Pilots Association
ASTM	American Society For Testing Materials
ATA	Air Transport Association
BS	British standard
CBR	California bearing ratio
CL	clay
DBT	double bituminous surface treatment
FAA	Federal Aviation Administration
Grade 200 pen	Penetration petroleum bitumen

K	number indicates subgrade reaction
NASA	National Aeronautics and Space Administration
NTSB	National Transportation Safety Board
PCC	Portland cement concrete
PSP	pierced steel planking
RAE	Royal Aircraft Establishment
RAF	Royal Air Force
RAFB	Royal Air Force Base
RCR	runway condition reading
RN	Royal Navy
R/W	runway
S.O.	Specification officer
USAF	United States Air Force

TEST APPARATUS

Test Vehicles

Aircraft.- A C-141A aircraft (fig. 1(a)) was chosen as the test aircraft for a number of reasons: (1) the four-wheel main-gear bogies of this aircraft provide maximum safety for the kind of testing contemplated; (2) thrust and drag can be determined; (3) the braking and antiskid systems are well suited to the project; and (4) its range and cargo capacity would solve a formidable logistics problem concerning the moving of a 20-man test crew, the test equipment, and a test vehicle from one location to another, in the United States and in Europe, within a short period of time. The test crew included the project pilot, the copilot, two flight engineers, a navigator, a four-man maintenance crew, the project manager, the flight test engineer, a civil engineer from the U.S. Air Force, and a seven-man NASA crew. Test equipment carried onboard the aircraft included data

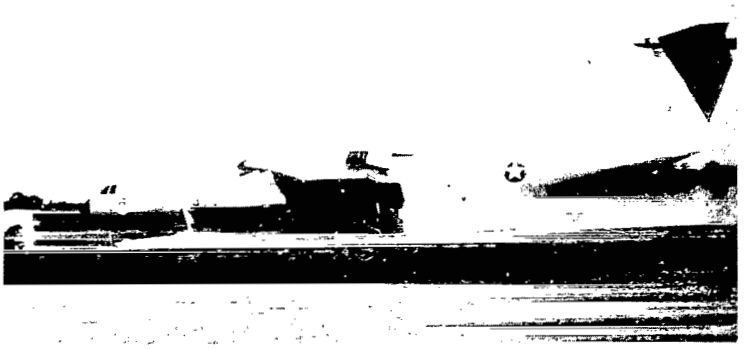

(a) C-141A test aircraft.

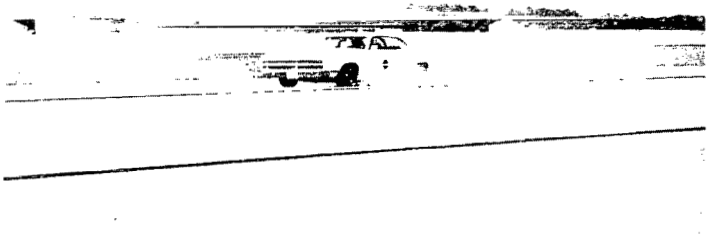

(b) NASA test vehicle.

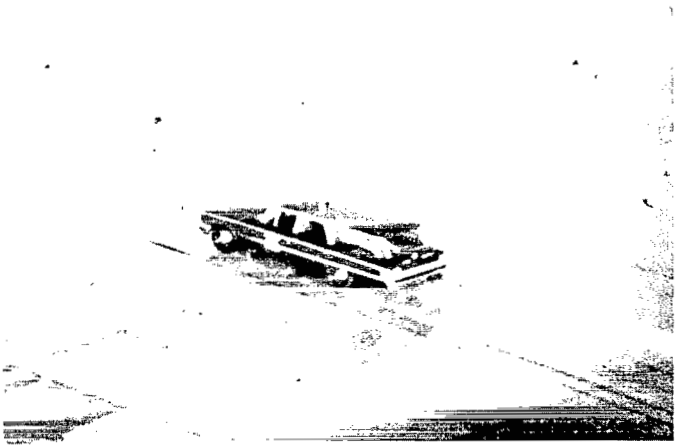

(c) RCR vehicle. L-70-4790

Figure 1.- Test apparatus.

recorders, spare tires for the aircraft and test vehicle, camera equipment, aircraft jacks, runway markers, and film.

Ground vehicles.- Since the 1968 NASA studies at Wallops Station (ref. 1) had clearly demonstrated that wet-dry stopping distance ratios obtained by the diagonal braking technique correlated better with test aircraft wet-dry stopping distance ratios, a 1969 sedan (see fig. 1(b)) was equipped with a diagonal-braking system. The diagonal-braking system was obtained by installing cutoff valves in the brake lines. (See fig. 2.) Thus, by appropriate valve selections, one pair of diagonal wheels on the automobile could be braked while the opposite pair of wheels remained unbraked and freely rolling. They were then free to steer or develop cornering or side forces for maintaining vehicle stability. The diagonal-braked wheels were equipped with the ASTM bald-tread tires (Specification E249) and the unbraked wheels were equipped with conventional rib-tread tires. The use of bald tires on the braked wheels essentially eliminates the effects of tire-tread design on braking traction; hence, repeatable data could be obtained. This diagonal-braking technique makes it possible for the test vehicle to enter locked-wheel skids at high speeds on wet pavements, and even on snow- and ice-covered pavements and still maintain good directional control.

Provisions were made in the diagonal-braked test vehicle instrumentation for the measurement and recording of ground-speed, stopping distance, angular velocity on individual wheels, longitudinal acceleration, and brake pressure.

The Air Force runway condition reading (RCR) vehicle from the local base was utilized in the tests at USAF bases since it represented the system currently employed worldwide by the U.S. Air Force to predict operational stopping distances for aircraft in adverse weather. Each test site provided an RCR vehicle such as the one shown in figure 1(c).

The Mu-meter and Miles engineering skid trailer were tested concurrently with the C-141A and diagonal-braked vehicle at the British Royal Air Force (RAF) and Royal Navy (RN) Bases.

Instrumentation

Aircraft.- Four recorders were used to record the following information with respect to time on $6\frac{1}{2}$-inch-wide photographic film:

Recorder 1 recorded the following:

(a) Event marker, actuated by the flight test engineer, to indicate entry into the test section and passage of each runway marker.

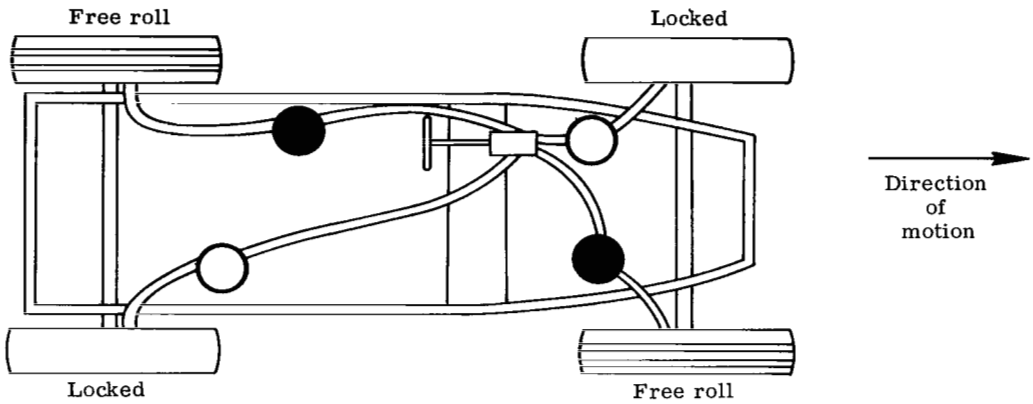

Figure 2.- Braking system for NASA diagonal-braked test vehicle.

(b) Angular velocity of the nose wheel as sensed by a magnetic pickup and a 90-tooth steel ring mounted on the left nose wheel. The output from the magnetic pickup was converted to a direct current voltage proportional to the input frequency; this voltage was recorded on the oscillograph and displayed to the pilot on an instrument calibrated in ground speed.

(c) Angular velocity of each main wheel. The signal from the frequency generator of the antiskid system was converted to a dc voltage proportional to the input frequency and fed to the oscillograph.

(d) Position of the antiskid modulating valve for each main wheel was obtained by recording the dc voltage input to the valve solenoid.

Recorder 2 obtained:

(a) Actuation of the event marker, as for recorder 1.

(b) Longitudinal, lateral, and normal accelerations, as measured by three accelerometers having a range of +1g to -1g, +1/2g to -1/2g, and 0 to 2g, respectively, and a dc output of 0 to 5 volts. The accelerometers were mounted on a single bracket near the center of gravity on the lower side of the wing carrythrough structure at 0.36$\bar{c}$.

(c) Pitch and yaw attitudes (used to correct longitudinal acceleration) were measured by a pitch-yaw attitude gyro with direct-current signals transmitted from a potentiometer.

(d) Nose-wheel steering angle, as measured by a direct current voltage from a potentiometer.

(e) Elevator position, as measured by a potentiometer mounted underneath the cockpit and attached to the elevator control cable. The dc signal was generated by a potentiometer.

(f) Main landing-gear and nose landing-gear strut pressures, which indicated vertical load on the tires. These values were used to calculate coefficient of friction and were measured by a 0 to 3000 psi pressure transducer with a 0 to 5 volt output. The strut filler valve was removed and replaced by a tee; the filler valve was placed in one side of the tee and the transducer in the other side.

(g) A reference for the pitch, yaw, and the accelerometer traces, provided by a vertical gyro.

Recorder 3 recorded:

(a) Event marker actuation, as for recorders 1 and 2.

(b) Pressure of each of the eight brakes, as sensed by a 0 to 3000 psi transducer, which provided a 0 to 5 volt dc output.

(c) An indication of left and right brake system pressures as provided by 0 to 3000 psi transducers, with an output of 0 to 2 volts dc, placed upstream from the modulating valves, to indicate when sufficient brake pressure was available to operate the antiskid system.

(d) The antiskid dump valve position for each main wheel, as indicated by the dc voltage input to the valve solenoid.

Recorder 4, an FM tape recorder, was used to record each actuation of the event marker and the vibration input to the fuselage from the landing gear on some of the runs. The information was provided by two accelerometers with a range of $\pm 2\frac{1}{2}$g mounted high on the strut (near the fuselage) to measure vertical and longitudinal vibrations.

Stopping distance was determined by mounting a brake-actuated switch, a magnetic pickup, and a single-tooth ring mounted on the left nose wheel to count the number of wheel revolutions from brake application to brake release. The data were displayed by an electronic counter and recorded by the flight test engineer.

Ground vehicles.- On the diagonal-braked test vehicle a ten-channel recorder was used to record the following information with respect to time:

(a) Event marker, a pressure switch in the brake system actuated the event marker when the brake was applied, and a timer reactuated it at 1-second intervals as long as braking was applied.

(b) Longitudinal acceleration, as measured by an accelerometer with a range of 0 to 1g.

(c) The angular velocity of each vehicle wheel, as measured by a generator.

(d) Angular velocity of a trailing fifth wheel, as measured by a generator.

(e) Hydraulic pressures, as measured with pressure transducers on the left front brake and right rear brake.

(f) Stopping distance as measured by a mechanical and an electronic wheel revolution counter mounted on a trailing fifth wheel and actuated by a brake pressure switch.

The RCR vehicle instrumentation consisted of a James brake decelerometer mounted on the front floor of an operations vehicle. (See ref. 19.) The data were recorded by the vehicle operator.

Other Instrumentation

Water depth.- Water depth was measured by a gage (ref. 20) designed by NASA for this program. (See fig. 3.) The gage works on the principle of reflectivity. Plexiglass rods of different lengths that protrude through its body are marked with numbers from

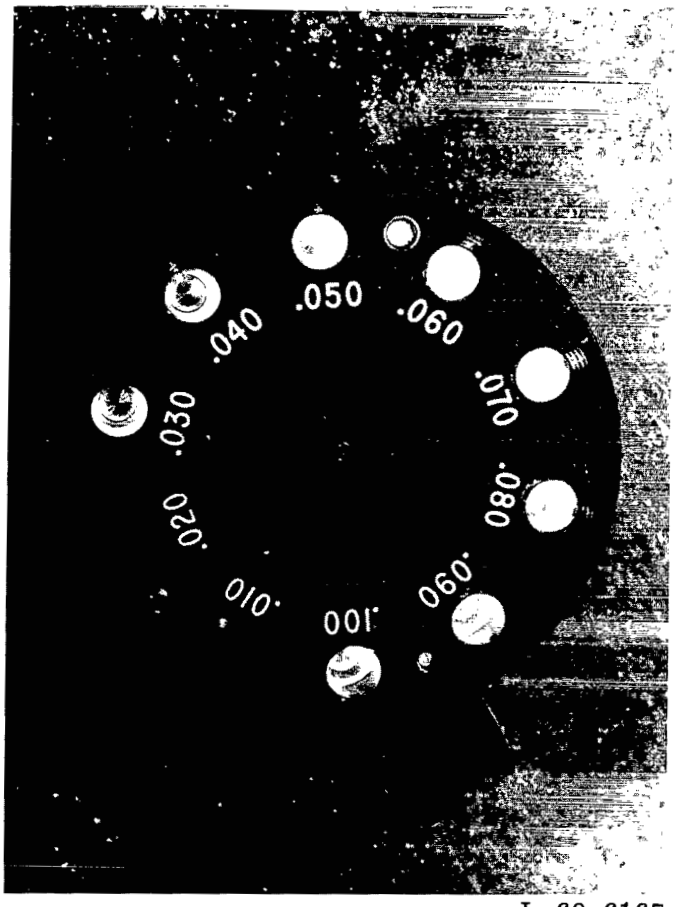

L-69-6167

Figure 3.- NASA water depth gage.

0.010 to 0.100 inch to indicate water depth. Since water is highly reflective and will reflect more light than the runway surface, rods that are not touching the water will appear lighter than those that are touching or submerged in water. The dark rod with the highest number, therefore, indicates the water depth. In figure 3, for example, the gage indicates a water depth of 0.020 inch.

Texture depth.- A runway texture-depth measuring kit (fig. 4), developed by NASA (ref. 21), was used to measure the depth of the surface texture of most of the runways. For this measurement, 1/2 cubic inch of grease was spread on the runway with a rubber squeegee in an area between two strips of masking tape laid 4 inches apart.

When the grease was evenly spread, the area covered was measured. The volume of grease (1/2 cubic inch) was divided by the area covered and the result indicated the average texture depth of the surface.

Photographic coverage.- A vibration-free camera mount was installed in a helicopter for photographic coverage during the wet tests. A motion-picture camera with a 12- to 120-millimeter zoom lens and photographing 24 frames per second was installed on the mount to take overhead color motion pictures of the aircraft landings and brake runs and the brake runs of the diagonal-braked and RCR test vehicles. The helicopter usually flew at an altitude of about 1000 feet so that two runway markers would appear in each picture frame; in case the aircraft instrumentation malfunctioned, this technique would provide enough data to calculate the aircraft velocity when entering the test section and the deceleration and stopping distances. A cameraman on the ground also took color motion pictures of each aircraft and vehicle test run. Only the ground photographic coverage was provided for the ice and snow tests.

The tests at Wallops Station were covered by six 16-millimeter color motion-picture cameras and one television camera. Two hydraulically operated (with azimuth and elevation control) gun mounts were converted to camera mounts and placed about 800 feet from each side of the runway. Each camera mount held two cameras: one, using a 4-inch lens and taking 128 frames per second, was focused on the aircraft; the other, using a 10-inch lens and taking 200 frames per second, was focused on the wheels. The wheels were painted with four white radial stripes to indicate wheel rotation or skid. These cameras tracked the aircraft from just prior to touchdown to test-section exit. A remotely operated end-of-the-runway camera, with a 10-inch lens and taking 48 frames per second, recorded all directional control problems encountered during each test run. The helicopter-mounted color camera was supplemented by a television camera held by the same mount. These cameras provided overhead coverage to record aircraft directional stability and water-spray patterns. The television transmissions were recorded to provide a quick review of the test runs by the ground and flight test crew.

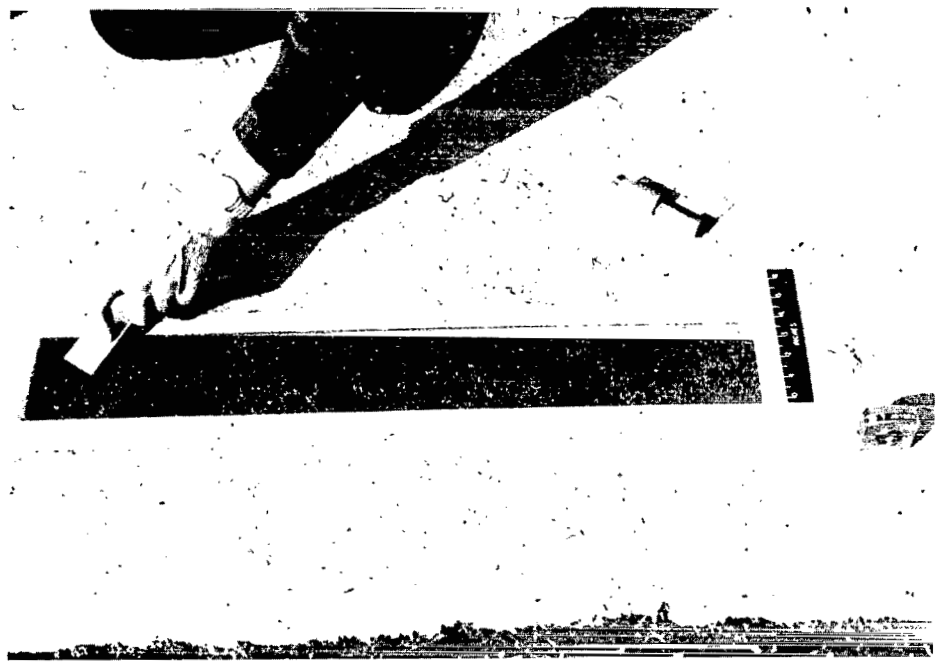

L-70-4791

Figure 4.- Runway texture depth measuring kit.

Runway markers.- Three lead-in markers and seven test-section markers were located along the right-hand side of the runway at 500-foot intervals as shown in figure 5. The first lead-in marker was located 1500 feet from the beginning of test section toward the approach end of the runway. These markers were used to guide the pilot in entering the test section at the proper speed. The test-section markers, lettered A to G, served as reference points to the flight test engineer for actuating the event marker on the airborne recorder and to the ground crew for locating where the brakes were applied and released.

Atmospheric data.- Wind direction and velocity was provided by the airfield control tower and by a hand-held anemometer. Temperature and barometric pressure measurements were also provided by the control tower.

TEST PROCEDURES

Wet and Dry Runways

For the wet and dry runway tests, the aircraft and crew landed at the test base in the afternoon preceding the day of the test. In addition to a printed briefing mailed several weeks prior to the scheduled arrival time, a verbal briefing was held on the afternoon preceding the test for the benefit of the base personnel required to take part in the test and to select the runway test section. Each base furnished water for wetting the runway, a water coordinator, transient aircraft maintenance, operations vehicle driver, a ground cameraman, base photographic facilities, and a helicopter for aerial photographic coverage.

The target start time was 1/2 hour before daylight with a short check-in meeting at Base Operations, where a weather decision was made and portable radios and water-depth gages were issued to the test personnel. The runway crew was dispatched to the runway to lay out the selected test section with portable runway markers.

After the runway markers were in place, the aircraft and helicopter took off. The aircraft made three landings, the first of which was a touch-and-go landing so that the pilot could verify the approach and landing speed required to enter the test section under the proper conditions (100 knots ground speed as measured by the segmented ring on the nose wheel, flaps in take-off position, spoilers up, and engines at idle thrust).

The second landing was a maximum-braking stop on the dry runway. The pilot applied maximum braking as he passed the A marker and held full brakes until the aircraft had slowed to approximately 10 knots. The flight test engineer who occupied the jump seat actuated the event marker as the aircraft cockpit passed each runway marker. An observer stationed beside the runway near the A marker marked with paint the location where the over-the-wing light came on and indicated brake application. Similarly,

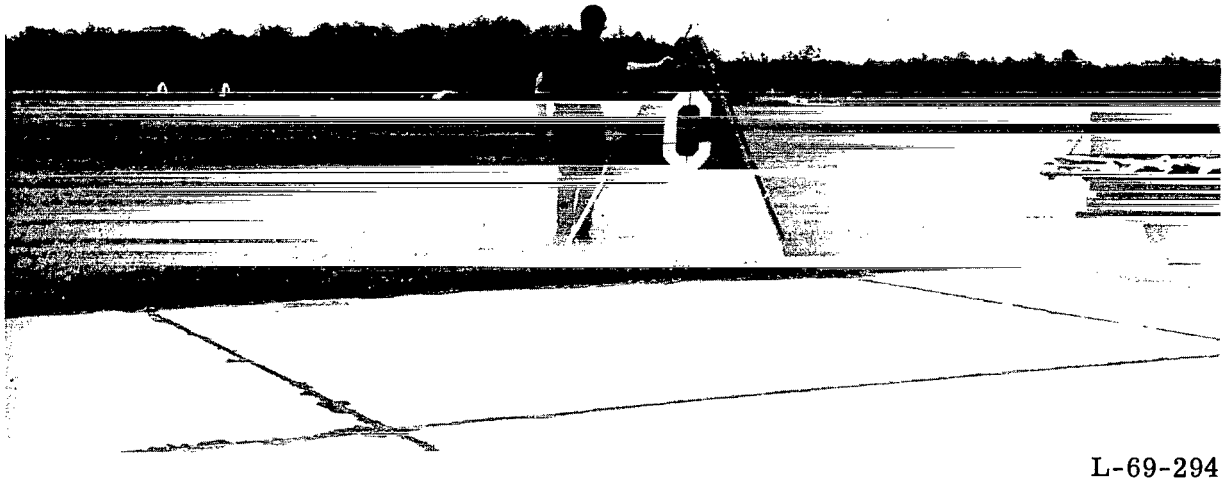

L-69-294

Figure 5.- Runway markers.

another observer near the aircraft expected stopping point marked the location where the over-the-wing light was extinguished and indicated brake release. Stopping distance was then determined by measuring the distance between the first and second marks. Since brake release occurred at a speed of approximately 10 knots, an extrapolation of distance from the velocity recording history was used to determine the remaining distance that would have been required to come to a complete stop. Full braking was not normally used below 10 knots because the antiskid system disarmed and the wheels would lock up and cause excessive tire damage. The stop was followed by a tire and brake inspection by the maintenance crew.

Before the third landing, the aircraft took off to air-cool the brakes. While the brakes were being air-cooled, the water trucks were placed on the runway and the artificial wetting operation was initiated. To provide the necessary wetting without excessive water loss by drainage and evaporation, it was necessary to place approximately 9000 gallons of water on a 40- by 1500- to 2500-foot runway strip within 8 minutes and have the aircraft land within 2 minutes after completion. The pilot was continually advised by tower personnel of the wetting progress so the aircraft could be positioned to land within the prescribed time. The third landing was then made on the wet runway using the technique described for the maximum-braking dry stop. The aircraft then promptly cleared the runway, after which the NASA diagonal-braked test vehicle and the RCR test vehicle made their runs. The elapsed time between aircraft test-section entry and completion of the vehicle runs was never more than 3 minutes and usually less than 2 minutes.

The diagonal-braked test vehicle began each run at 60 miles per hour. The left-front and right-rear wheels were locked with brakes, and the brakes kept fully on until the vehicle came to a complete stop. Stopping distance was measured by the trailing fifth wheel and recorded by the driver. These runs were made slightly outboard of the tracks left by the right main gear. Since the test vehicle stopping distance was about one-third that of the aircraft, the test vehicle, attempting to cover the entire length of stopping path traversed by the aircraft, made as many runs as time permitted. The test vehicle stopping distances were then averaged. At the same time, the RCR test vehicle took a similar series of readings just outboard of the track of the left main gear. Each reading was made in accordance with the technique described in reference 19. RCR readings on the dry runway were taken on the test section just after the aircraft had made its maximum-braking dry stop. Since skidding to a stop on two locked wheels on a dry surface from 60 miles per hour usually rendered the tires unfit for further use, the dry stopping distance of the diagonal-braked test vehicle was determined after all wet runs had been completed by using an adjacent section of runway which had not been wetted. The braked tires were then changed in preparation for the next day's testing. In the tests conducted on British airfields, the Mu-meter and the Miles engineering skid trailer were tested concurrently

with the RCR and diagonal-braked test vehicles. The entire test operation required about 1 hour and 45 minutes to complete.

Snow-, Slush-, and Ice-Covered Runways

Unlike the summer program, where the tests were scheduled several months in advance, the usual procedure for the ice and snow test was to locate an airfield with snow or ice on the runway within 1 or 2 hours flying time of the last runway measured. The base operations officer was then contacted by telephone for permission to test the runway on a noninterference basis; however, because of the efficiency of the snow removal crews, it was usually difficult to find a runway completely covered with ice or snow.

After selecting a snow-covered airfield, the aircraft and test crew would arrive at the site and present a short briefing to the base operations officer covering test procedures and assistance needed. The runway was then surveyed by the diagonal-braked and RCR vehicles before the aircraft was committed to a test. The narrow tread of the C-141A landing gear permitted testing on both sides and the center of the runway. (The usual procedure followed by the snow removal crews was to clear the center portion of the runway first, and to leave the sides covered with snow and ice.) After the survey by the diagonal-braked test vehicle, the aircraft usually made several runs on different sections of the runway to take advantage of the various conditions. Taxiways were also tested by the vehicles and aircraft when the proper conditions were present. The diagonal-braked test vehicle and RCR test vehicle made runs both before and after the aircraft and each test vehicle's readings were averaged. Because the runway surface was covered with ice or snow, dry runs could not be made by the vehicles or the aircraft. Therefore, an average dry stopping distance of 1100 feet was used for the aircraft and 302 feet for the diagonal-braked test vehicle.

NASA Landing Research Runway

The landing research runway at NASA Wallops Station is described in appendix C. The procedure for tests at this facility is described in detail in reference 1.

RESULTS AND DISCUSSION

The present investigation of aircraft and ground vehicle braking performance on runways included full-stop braking tests on active runways in the United States and Europe under dry, wet, slush, snow, and ice conditions; and limited braking tests on short (approximately 350 feet) test surfaces of the research runway at NASA Wallops Station under dry, wet, flooded, and slush-covered runway conditions. The results of these tests and a discussion of the correlation of the techniques are included in the following sections along with an evaluation of the relative slipperiness of surfaces.

Full-Stop Runway Braking Tests

The corrected stopping distances required to brake the C-141A aircraft to a stop from 100 knots ground speed, and the NASA diagonal-braked test vehicle from a speed of 60 miles per hour to a stop are presented in appendix A for each runway tested. It should be noted that two independent methods were used to determine the aircraft stopping distance. In one method, the stopping distance was obtained directly from the nose-wheel revolution counter installed on the C-141A aircraft (and described in the instrumentation section of this paper). In the other method, the stopping distance was obtained from an integration of the aircraft deceleration time history measured during a braking run. Also shown in each figure are the calculated effective tire-ground friction coefficients developed by the aircraft during the braking runs. The computer program required to obtain the aircraft stopping distance and effective friction coefficients from acceleration measurements is described in appendix B.

Also tabulated in the figures of appendix A are the pavement, atmospheric, and aircraft test conditions, along with measured values of RCR and average texture depth of the pavement. A photograph of the runway surface in the area tested by the aircraft and the diagonal-braked test vehicle is also shown. For each figure and runway are presented the results of the core sample analysis, where available. These analyses were made by the USAF Weapons Laboratory for U.S. Air Force runways and by the Ministry of Public Buildings and Works for British runways. Civil engineering descriptions of each runway surface tested under dry and wet conditions are listed in appendix C. Each runway tested is assigned a runway reference number based on its slipperiness determined by tests as shown in table I. Concrete runways are listed separately from asphalt runways. Thus, runway numbers 1 to 16 refer to the concrete runways and numbers 17 to 39 refer to the asphalt runways. Runway 40 is a landing mat surface.

Full-stop aircraft and test vehicle braking tests were also carried out on nine runways and taxiways where the pavement surface was coated with snow, slush, or ice. These runways are assigned runway numbers 41 to 49 as shown in table II.

Dry-runway braking characteristics.- For most of the dry runways, the antiskid system of the C-141A tended to develop maximum braking efficiency at the higher ground speeds. A much lower braking efficiency usually developed at the lower ground speeds because of less effective wheel skid control which resulted in excessive cycling and dumping of wheel brake pressure. This antiskid operational feature on dry runways usually resulted in a decrease in the effective tire-ground friction coefficients generated by the aircraft braking system with decreasing ground speed. (See fig. A1.) This trend is not attributed to brake fade during an aircraft stop since the wheels are not torque limited at low speeds. The test records show that the main gear wheels develop deep skids and frequent wheel lockups at the lower ground speeds as shown in figure 6(a).

TABLE I.- SUMMARY OF DATA OBTAINED ON WET RUNWAYS

Runway	Airport	Material	Surface treatment	Test condition	Average wet-dry stopping distance ratio		RCR dry-wet ratio
					Aircraft (*)	Test vehicle	
1	Dyess AFB	Concrete	Conventional	Artificially wet	2.77	2.70	1.28
2	England AFB	Concrete	Conventional	Artificially wet	2.47	2.16	1.45
3	Marham RAFB	Concrete	Conventional	Artificially wet	2.24	1.93	1.00
4	Offutt AFB	Concrete	Conventional	Artificially wet	2.21	2.15	1.24
5	Ellington AFB	Concrete	Conventional	Light rain	2.17	2.16	2.00
6	Edwards AFB	Concrete	Conventional	Artificially wet	2.15	1.91	1.16
7	Wright-Patterson AFB	Concrete	Conventional	Artificially wet	2.12	1.95	1.04
8	Lockbourne AFB	Concrete	Conventional	Artificially wet	2.05	1.84	1.02
9	Langley AFB	Concrete	Conventional	Artificially wet	1.90	1.95	1.41
9	Langley AFB	Concrete	Conventional	Damp after light rain	1.42	---	---
10	Yeovilton RNB	Concrete	Wire combed	Artificially wet	1.78	1.65	.96
11	Yeovilton RNB	Concrete	Scored transversely	Artificially wet	1.65	1.76	1.15
12	John F. Kennedy Airport	Concrete	Grooved, $1\frac{3}{8}$ in. by 3/8 in. by 1/8 in.	Artificially wet (clean)	1.57	1.75	---
12	John F. Kennedy Airport	Concrete	Grooved, $1\frac{3}{8}$ in. by 3/8 in. by 1/8 in.	Artificially wet (rubber deposits)	1.86	2.20	---
13	Seymour Johnson AFB	Concrete	Grooved, 2 in. by 1/4 in. by 1/4 in.	Artificially wet (clean)	1.38	1.35	1.21
13	Seymour Johnson AFB	Concrete	Grooved, 2 in. by 1/4 in. by 1/4 in.	Artificially wet (rubber deposits)	1.47	1.50	1.21
14	Chicago Midway Airport	Concrete	Grooved, $1\frac{1}{4}$ in. by 1/4 in. by 1/4 in.	Artificially wet	1.25	1.35	---
15	Offutt AFB	Concrete	Grooved, $1\frac{1}{4}$ in. by 1/4 in. by 1/4 in.	Artificially wet	1.20	1.32	1.24
16	Beale AFB	Concrete	Grooved, 1 in. by 1/4 in. by 1/4 in.	Artificially wet	1.11	1.20	1.05
17	Mildenhall USAFE**	Asphalt	Slurry seal	Artificially wet	---	3.15	---
18	Spangdahlem USAFE	Asphalt	1/8 in. German antiskid coat	Artificially wet	2.35	2.50	1.41
19	Elmendorf AFB	Asphalt	Plant mix	Artificially wet	2.32	2.48	1.53

*Average value of revolution-counter and acceleration-time measurements.

**Resurfaced with porous friction course, November 1970.

TABLE I.- SUMMARY OF DATA OBTAINED ON WET RUNWAYS – Concluded

Runway	Airport	Material	Surface treatment	Test condition	Average wet-dry stopping distance ratio		RCR dry-wet ratio
					Aircraft (*)	Test vehicle	
20	Bitburg USAFE	Asphalt	Marshall asphalt	Artificially wet	1.97	1.78	1.09
21	Myrtle Beach AFB	Asphalt	Slurry seal	Damp after light rain	1.08	---	1.05
21	Myrtle Beach AFB	Asphalt	Slurry seal	Artificially wet	1.92	1.67	1.02
22	Waddington RAFB	Asphalt	1/8 in. surface dressing	Artificially wet	1.82	1.87	---
23	Otis AFB	Asphalt	Plant mix	Artificially wet	1.81	1.62	1.18
24	Aviano USAFE	Asphalt	Crushed rock seal coat	Artificially wet	1.76	1.57	1.10
25	Alconbury USAFE	Asphalt	Slurry seal	Artificially wet	1.71	1.68	1.10
26	Farnborough RAE	Asphalt	Plant mix – grooved 1 in. by 1/8 in. by 1/8 in.	Artificially wet	1.69	1.40	1.05
27	Sembach USAFE	Asphalt	1/8 in. German antiskid coat	Artificially wet	1.67	1.50	1.13
28	Pope AFB	Asphalt	Plant mix	Artificially wet	1.56	1.78	1.19
29	Tempelhof Airport	Asphalt	1/8 in. German antiskid coat – grooved $1\frac{1}{2}$ in. by 3/8 in. by 3/8 in.	Artificially wet	1.51	1.65	1.41
30	McChord AFB	Asphalt	Plant mix	Moderate rain	1.49	1.94	---
31	Little Rock AFB	Asphalt	Plant mix	Artificially wet	1.48	1.61	.96
32	Scott AFB	Asphalt	Plant mix	Artificially wet	1.40	1.80	1.16
33	Dover AFB	Asphalt	Plant mix	Artificially wet	1.33	1.50	1.18
34	Nellis AFB	Asphalt	Plant mix	Artificially wet	1.32	1.60	1.02
35	NASA Wallops Station	Asphalt	Slurry seal	Artificially wet	1.28	1.29	1.05
36	Farnborough RAE	Asphalt	$1\frac{1}{4}$ in. porous friction course	Artificially wet	1.18	1.05	.87
37	Shemya AFB	Asphalt	Plant mix	Artificially wet	1.15	1.45	1.07
38	Marham RAFB	Asphalt	3/4 in. porous friction course	Artificially wet	1.12	1.10	1.00
39	Meigs Airport	Asphalt	Plant mix – synthetic aggregate	Artificially wet	---	1.17	---
40	Dyess AFB	Landing mats	Epoxy-grit coated aluminum	Artificially wet	2.05	1.66	1.02

*Average value of revolution-counter and acceleration-time measurements.

TABLE II.- SUMMARY OF DATA OBTAINED ON SNOW, SLUSH, AND ICE-COVERED RUNWAYS

Runway	Airport	Material	Surface treatment	Test condition		Average wet-dry stopping distance ratio		RCR dry-wet ratio
				Temperature, °F	Surface cover	Aircraft (*)	Test vehicle	
41	Malmstrom AFB	Concrete (ramp)	Conventional	27	Packed dry snow	3.71	4.16	6.00
42	Loring AFB	Asphalt	Slurry seal	21	Glazed ice and dry snow	3.51	3.40	4.00
43	Wurtsmith AFB	Concrete	Conventional	23	Packed snow and ice	3.31	3.65	12.00
44	Grissom AFB	Asphalt (taxiway)	Plant mix	22	Packed snow and ice	3.20	3.95	4.80
45	Wright-Patterson AFB	Concrete	Conventional	8	Dry packed snow and ice	2.82	2.90	4.36
46	Glenview NAS	Concrete and asphalt	Conventional	27	Patchy ice and snow	2.39	2.51	----
47	K. I. Sawyer AFB	Asphalt	Slurry seal	11	Patchy packed snow and ice	2.27	1.63	----
47	K. I. Sawyer AFB	Asphalt	Slurry seal	23	Packed snow and ice	2.25	2.27	3.20
48	McGuire AFB	Asphalt	Plant mix	14	Patchy snow and ice	1.84	2.17	2.53
49	Malmstrom AFB	Asphalt (runway)	Plant mix	33	Patchy slush	1.75	1.62	1.72

*Average value of revolution-counter and acceleration-time measurements.

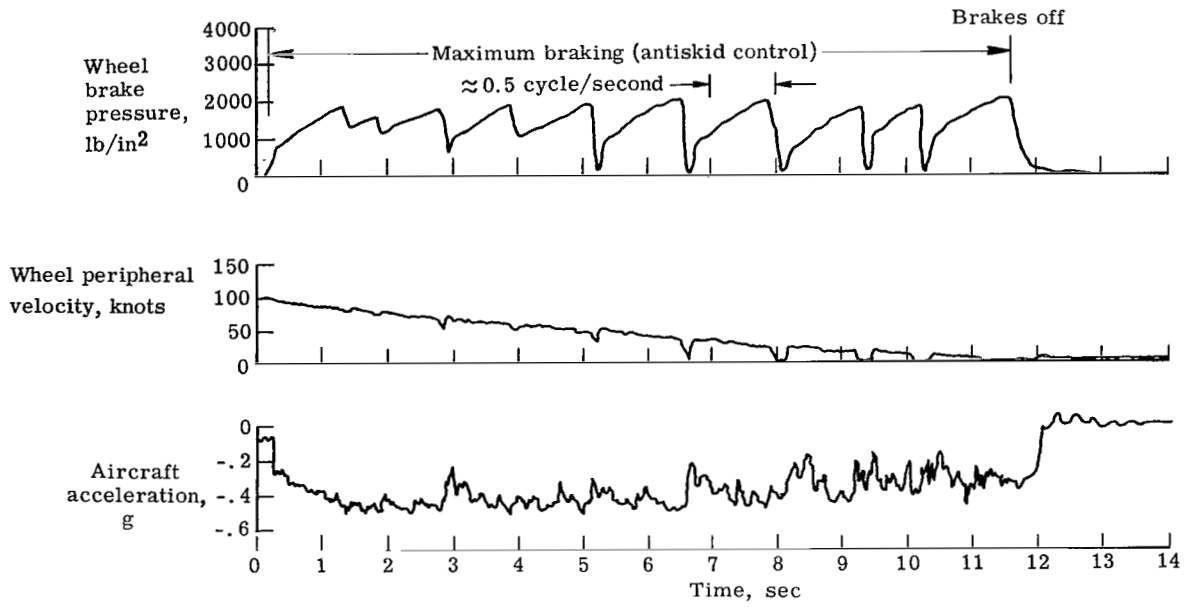

(a) Dry runway condition. Porous friction course at Marham RAFB.

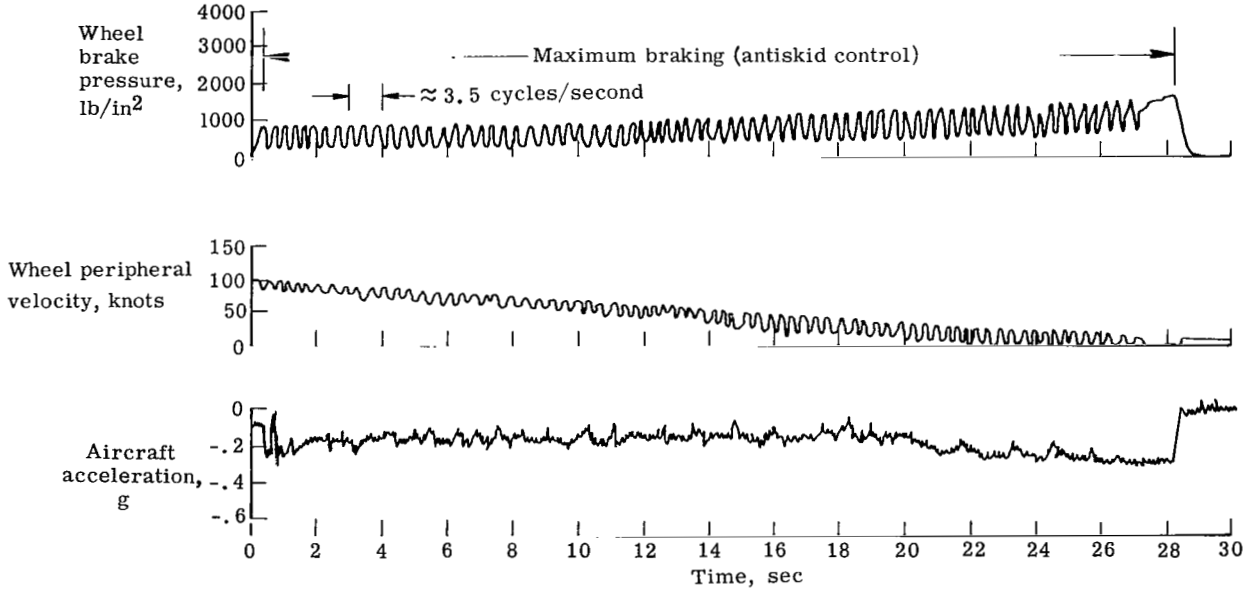

(b) Wet runway condition (low friction). Concrete runway at England AFB.

Figure 6.- Examples of variation in C-141A aircraft wheel brake pressure and velocity and aircraft acceleration during maximum braking conditions on dry, wet, and ice-covered runway surfaces (left rear inboard wheel).

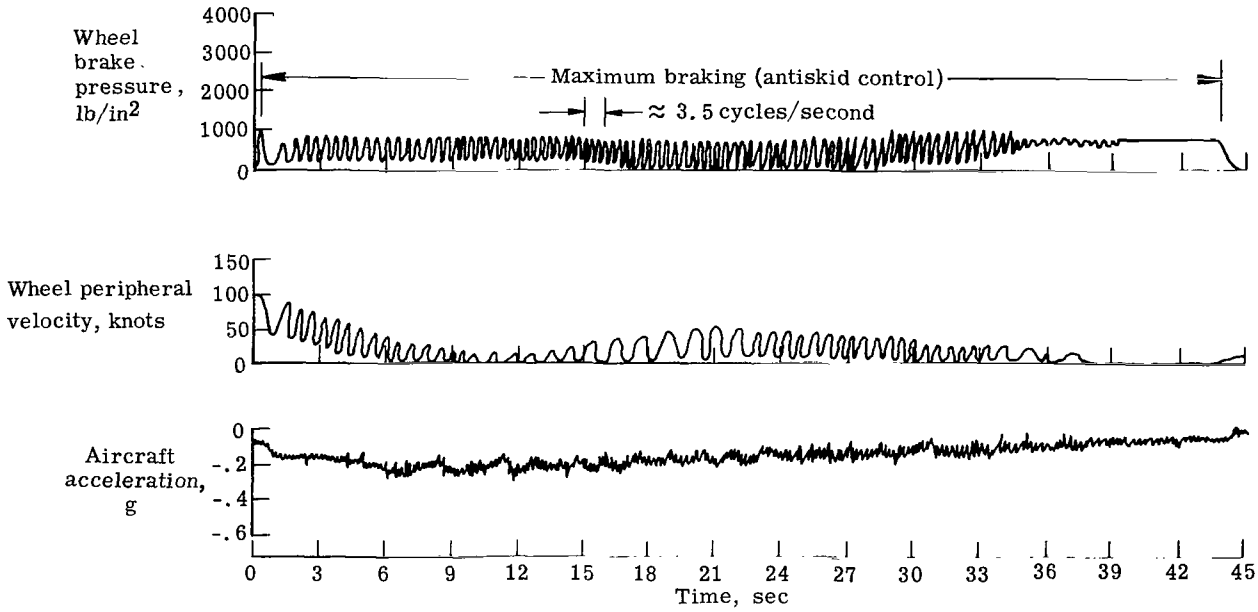

(c) Glazed-ice and snow-covered runway condition. Slurry seal runway at Loring AFB.

Figure 6.- Concluded.

The stopping distances obtained by the C-141A aircraft during braking runs on dry surfaces are given in appendix A. These data produced the average dry stopping distances from 100 knots ground speed as shown in the following table:

Runway surface	Stopping distance, feet		
	Revolution counter	Acceleration time	Average
Asphalt	*1097	1142	1120
Concrete	1022	1092	1058

*Waddington RAFB omitted (Revolution counter reading believed to be in error).

Both the revolution counter and acceleration-time methods of determining aircraft stopping distance indicate that the aircraft requires slightly less distance to stop on dry concrete than on dry asphalt runways. The average of the two methods indicates that the aircraft stopping distance was 1120 feet on asphalt and 1058 feet on concrete, a difference of 62 feet. No distinctive trend could be found for aircraft stopping distance on dry runways with changes in either ambient air temperature (see fig. 7) or aircraft gross weight. It is apparent that deviations in stopping distance on dry runways must occur from differences, as yet undetermined, in antiskid efficiency, wheel brake wear, and effects of pavement surface condition and contamination such as dust, oil films, rubber deposits, and so forth. It should also be mentioned that the aircraft tires were installed on the aircraft in an unused condition; however, some tires were new whereas others were re-caps. The tires were replaced when 50 percent worn. Tire construction effects and different rubber compounding used on the tires tested could also contribute to the deviations in stopping distance encountered. As noted in appendix B, runway slope information provided for the different runways was insufficient to allow slope corrections to be made to the raw data and this fact could also account for some small part of the aircraft stopping distance variations.

The braking system utilized on the NASA diagonal-braked test vehicle caused the diagonal pair of ASTM smooth tread tires to be locked upon brake application by the driver. Thus, the kinetic energy developed by the test vehicle at 60-miles-per-hour brake-application speed on a dry runway was absorbed in a small contact patch on each of the two smooth tread tires. A typical time history of a dry runway braking stop by the diagonal-braked test vehicle is shown in figure 8(a). It can be seen that the deceleration of the test vehicle decreases with time from the initial high value at brake application speed until at some lower speed, the deceleration increases and reaches a peak value similar in magnitude to the initial deceleration peak at brake engagement speed. It is

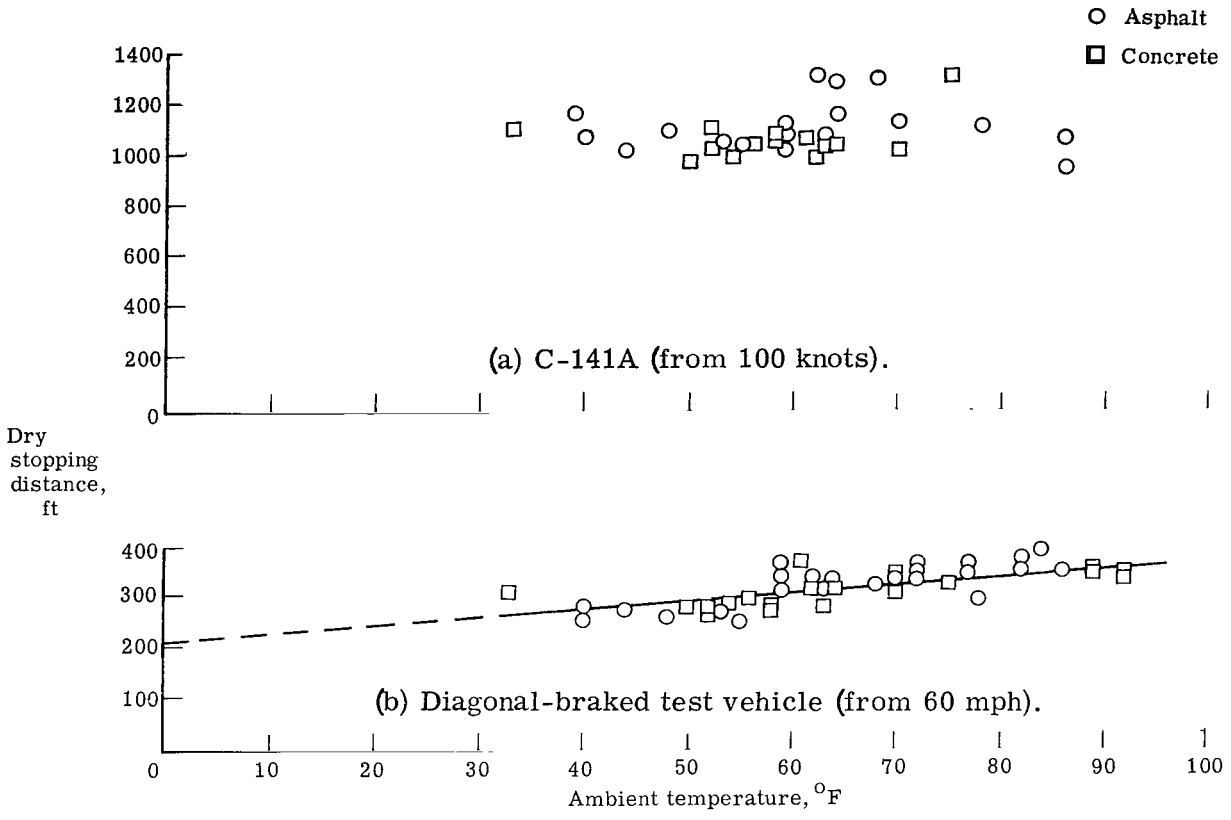

Figure 7.- Effects of runway ambient air temperature on aircraft and test vehicle dry runway stopping distance.

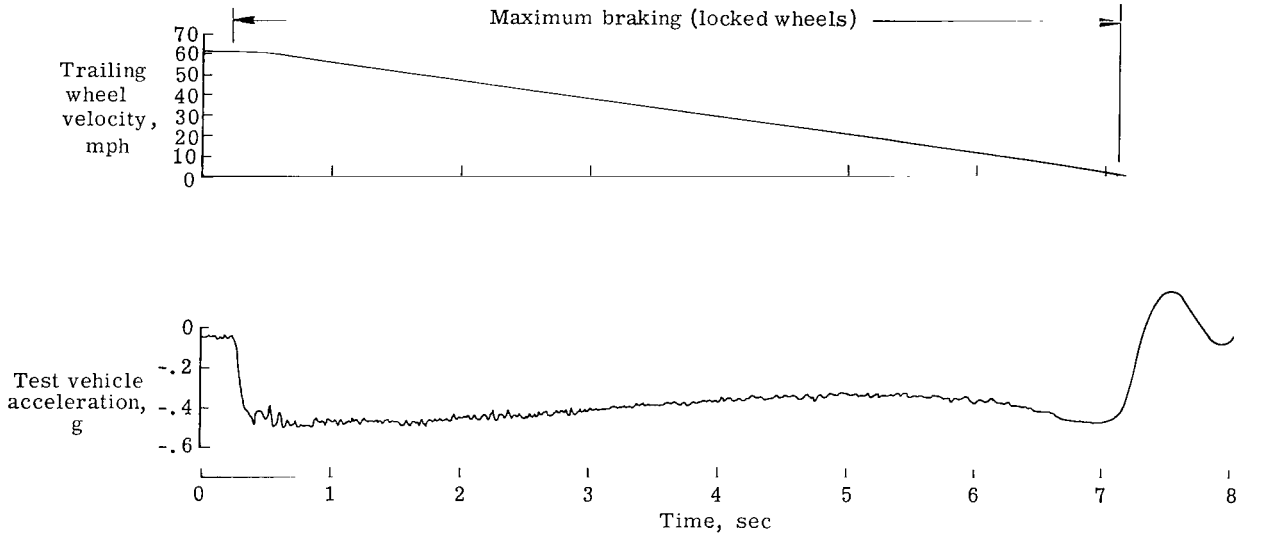

(a) Dry runway condition. Concrete runway at England AFB.

Figure 8.- Examples of variation in diagonal-braked test vehicle velocity and acceleration under locked-wheel braking conditions on dry, wet, and ice-covered runways.

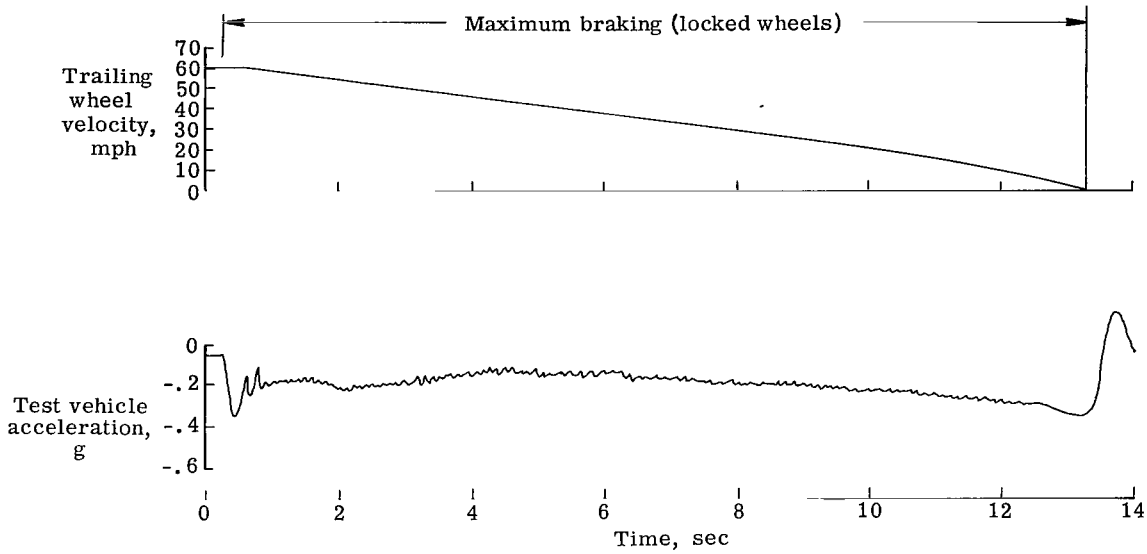

(b) Wet runway condition. Concrete runway at England AFB.

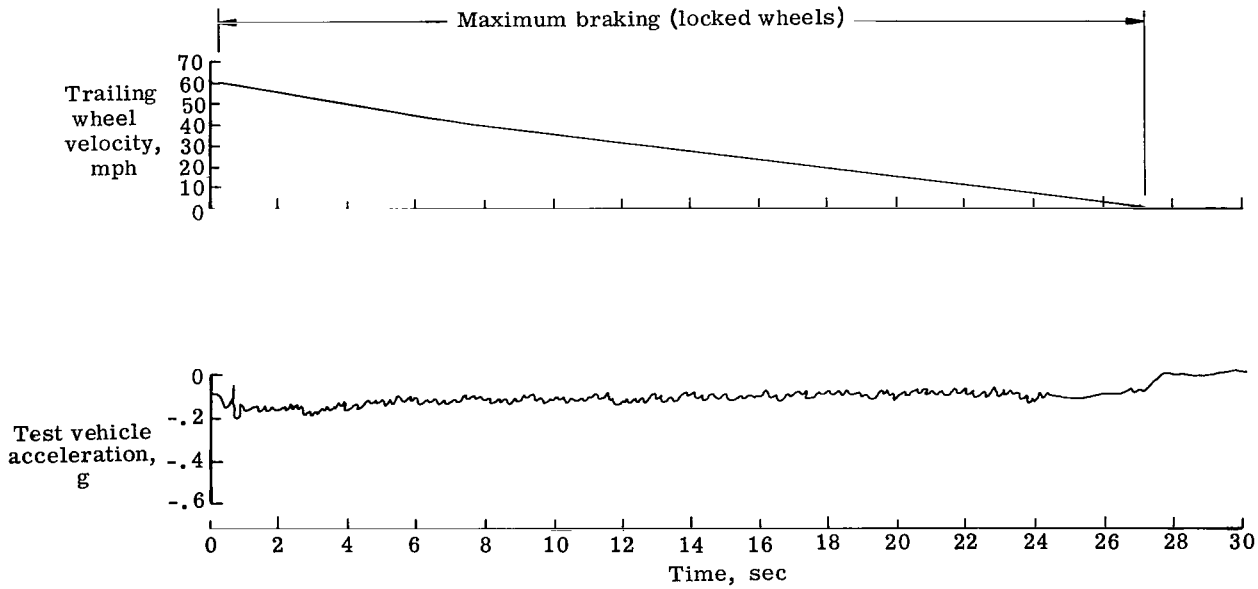

(c) Glazed-ice and snow-covered runway condition. Slurry seal runway at Loring AFB.

Figure 8.- Concluded.

felt that this loss in test vehicle deceleration comes from a loss in tire-ground friction coefficient associated with high rubber temperatures in the skidding tire contact patch.

The locked-wheel operation of the NASA diagonal-braked test vehicle differed from the typical antiskid controlled braking of the C-141A aircraft tires where the rotating tires continuously introduced new rubber into the tire-ground contact area. At low ground speeds, locked-wheel skids sometimes occurred for a fraction of a second. In contrast to the aircraft stopping distance results on dry runways, which showed no effect of runway ambient air temperature, the test vehicle stopping distance on dry surfaces tends to increase with increasing runway ambient air temperature as shown in figure 7. No discernible difference in stopping distance could be detected for the test vehicle between dry asphalt and dry concrete runway surfaces. The variation in diagonal-braked test vehicle stopping distances with air temperature can be approximated by the empirical equation

$$D_{vehicle,dry} = 208 + 1.45T_r \qquad (1)$$

where T_r is the runway ambient air temperature in degrees Fahrenheit, and $D_{vehicle,dry}$ is the stopping distance (from 60 mph) in feet. Equation (1) was derived from the range of runway ambient air temperature (33° F to 92° F) studied in this investigation. It is noted in figure 7 that considerable data scatter exists from the values predicated by equation (1). The aircraft tires used were from several different tire manufacturers, whereas the ASTM tires used on the test vehicle were constructed by one tire company according to rigid and detailed ASTM specifications on tire construction and tread rubber composition. Therefore the data scatter shown for the vehicle dry stopping distance cannot be attributed to the vehicle test tires. It is probable that factors such as measurement accuracy, wind velocity and direction, runway slope, and possibly changes in vehicle rolling resistance contributed to the scatter of the vehicle dry-stopping-distance data.

Wet-runway braking characteristics.- Before attempting to describe the aircraft performance on wet runways, it is first necessary to define runway wetness. Under damp or wet pavement conditions, viscous hydroplaning or skidding is the predominant factor contributing to losses of vehicle tire braking and steering capability. For predominantly viscous hydroplaning conditions, the texture of the pavement and the skid resistance of the exposed aggregate determine the degree of slipperiness of the pavement. Only thin water films (less than 0.01 inch thick) are required for viscous hydroplaning effects to produce drastic tire friction losses on smooth pavements. A damp-runway condition is defined as having a moist (discolored) surface where the average water depth is 0.01 inch or less on the pavement as measured by the NASA water depth gage. (See fig. 3.) A wet-runway condition is defined as having a moist surface where the average water depth lies between 0.01 and 0.1 inch as measured by the NASA water depth gage. When the average

water depths on typical runway surfaces exceed 0.1 inch, additional losses in tire braking and cornering performance occur because of dynamic hydroplaning on worn aircraft tires. New tires with full tread depth require larger average water depths from 0.2 to 0.3 inch for dynamic hydroplaning to occur. A flooded runway is therefore defined as having an average water depth on the pavement greater than 0.1 inch as measured by the NASA water depth gage.

The wet-runway conditions can be simulated by artificial wetting as was done for most of the runways tested in this investigation. The average water depths obtained by artificially wetting runways in the test program were 0.039 inch for ungrooved concrete pavements, 0.035 inch for ungrooved asphalt pavements, damp to 0.01 inch for grooved pavements with the exception of the John F. Kennedy and Farnborough shallow grooved runways which averaged approximately 0.03 inch, and porous asphalt runways which averaged 0.025 inch. It is interesting to note that a light rain produced a damp surface on the Ellington Air Force Base runway, whereas a moderate rain on the McChord Air Force Base asphalt runway produced an average water depth of 0.02 inch. The McChord airport tower rain gage indicated that the rainfall precipitation rate at time of testing was approximately 0.3 inch per hour. From this correlation it is apparent that the artificial wetting technique utilized in this investigation was the equivalent of light to moderate natural rainfalls on the runways with conventional surfaces. The artificial wetting technique was only able to produce a damp condition on deeply grooved runway surfaces.

The braking characteristics of the C-141A aircraft on wet runways can be considerably different than those on dry runways, especially for smooth textured runways where viscous hydroplaning effects predominate. For example, figure 6(b) shows the time history of the aircraft longitudinal deceleration and left rear inboard wheel brake pressure and velocity developed during a braking stop on the wet runway at England Air Force Base (wet-dry stopping distance ratio, 2.47). It can be seen that the antiskid cycling increased from approximately 1/2 cycle per second for the dry runway (fig. 6(a)) to approximately 3.5 cycles per second for the wet runway (fig. 6(b)). As the aircraft speed decreased during the braked roll, the wheel skids became progressively deeper until at approximately 30 knots ground speed, the wheel was cycling under full skid (locked-wheel) conditions.

NASA research reported in reference 18 indicates that aircraft tires encounter a complete loss in cornering or side-force capability when the braked wheels operate at slip ratios greater than 0.25. (See fig. 9.) These data explain the tendency for the aircraft to weathercock into the wind when braking on slippery runways in crosswinds. The deceleration trace in figure 6(b) indicates that tire friction improved as the aircraft speed decreased. (Also, see fig. A1(b).) This trend was characteristic of all wet runways

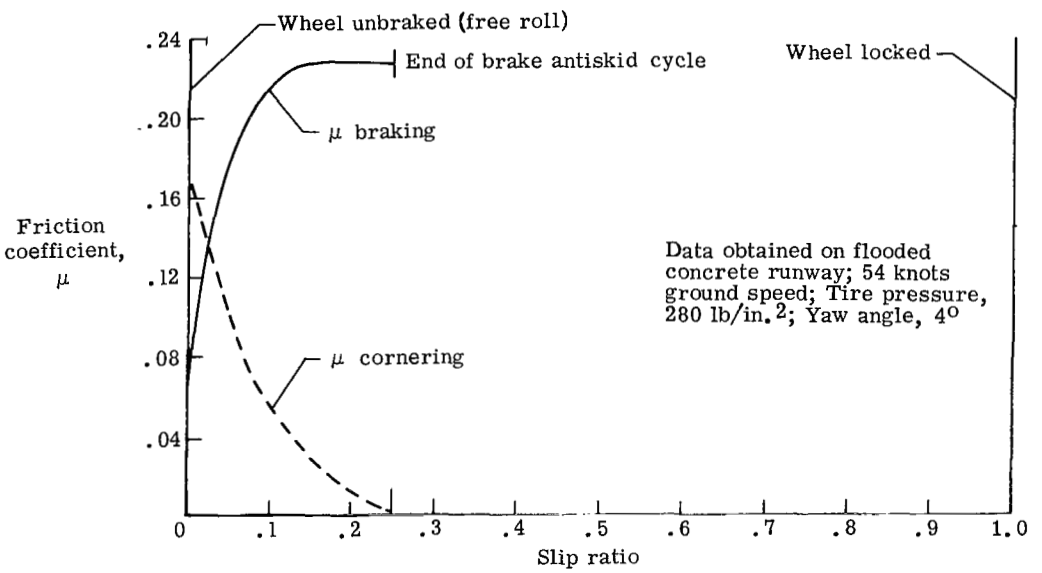

Figure 9.- Loss of cornering friction of main landing gear tire of fighter aircraft.

except for the deeply grooved and porous surfaces which showed no loss in effective friction coefficient with increasing aircraft ground speed.

The deceleration of the diagonal-braked test vehicle on wet runways under diagonal-braked conditions exhibited the same trend as observed for the aircraft, that is, the deceleration or tire friction increased with decreasing vehicle ground speed. This effect is shown in figure 8(b). This trend is characteristic of the friction losses associated with viscous hydroplaning. At low speeds both the rolling tire and the skidding tire have more time to break through the thin water film lying between the tire and pavement than at high speeds. Consequently, more and more adhesion of friction is regained between the tire and pavement as ground speed decreases.

Snow-, slush-, and ice-covered runway braking characteristics.- The slipperiest runway conditions encountered by the C-141A aircraft in this investigation developed when the runways were covered with snow and ice. A typical time history of wheel brake pressure, velocity, and aircraft longitudinal deceleration is shown in figure 6(c) for the aircraft braking run at Loring Air Force Base for a glazed-ice- and snow-covered runway condition at 21° F. The time history indicates that the aircraft is in a more slippery condition (stopping distance ratio, 3.51) than for a wet runway (fig. A1(nn)). The antiskid system, although cycling the brake pressure at 3.5 cycles per second, allowed the wheel to spin down to practically locked-wheel conditions approximately 7 seconds after brake application. This trend indicates that the aircraft would weathercock in a crosswind. The aircraft during the Loring braking run was exposed to a direct crosswind component of approximately 6 knots and developed $6\frac{1}{2}^{\circ}$ yaw into the wind. The pilot used aerodynamic controls and nose-wheel steering and had no problem maintaining directional control during the braking stop. In contrast to the wet-runway trends in which the tire friction coefficient increases as ground speed is decreased, the deceleration data in figure 6(c) indicates that on snow and ice, the friction coefficient tends to be either constant with speed or to decrease slightly with decreasing ground speed.

The nose-wheel steering on the C-141A aircraft was very effective on snow- and ice-covered runways for small nose-wheel steering angles. The fact that nose-wheel steering is lost at larger steering angles was encountered after a landing on the snow- and ice-covered runway at Glenview Naval Air Station. The landing was accomplished without any directional problems. However, it took extensive maneuvering to turn the aircraft from the runway onto the taxiway because the nose wheel would slide instead of turning the aircraft at the large steering angle required. The turn was finally accomplished by the use of asymmetrical forward and reverse thrusts from the engines.

The diagonal-braked test vehicle exhibited braking characteristics on snow and ice similar to those for the C-141A aircraft. This effect is illustrated in figure 8(c) from the time history for the braked run for the vehicle at Loring Air Force Base and on glazed ice

and snow in figure A1(nn). On most of the snow- and ice-covered runways, a definite trend for the skidding tire friction coefficient to decrease with decreasing ground speed was evident. In fact, the lowest skidding friction coefficients measured were just before the vehicle came to a complete stop. It is felt that this result was caused by the skidding tires having more time at lower speeds to pressure melt the surface of the snow or ice in the ground contact areas and thus create a water film for the tires to slide on.

The test vehicle driver had little difficulty maintaining directional control of the diagonal-braked vehicle during braking tests on the slipperiest snow and ice-covered runways tested as long as he used small steering wheel inputs. Steering capability was also lost for the vehicle as was just described for the aircraft when large steering angles were applied. The most difficulty experienced by the vehicle on snow and ice was accelerating up to the test speed of 60 miles per hour. For this low friction condition, the driver had difficulty applying proper throttle to allow the vehicle to accelerate without spinning the rear wheels with subsequent "fishtailing" or "spin out." Acceleration distances required to obtain 60 miles per hour on snow and ice were as much as 4000 to 5000 feet.

Limited Braking Tests at Wallops Landing Research Runway

Since extensive braking tests had already been conducted for aircraft (ref. 1) under simulated all-weather test conditions on the landing research runway, it appeared advantageous to perform similar tests for the C-141A aircraft to provide a comparison of braking characteristics with the previous test aircraft. The landing research runway at NASA Wallops Station (shown schematically in fig. C1) is composed of level test sections which exhibit surface and composition differences. Also provided are removable dams for the retention of surface wetness conditions. Pavements with surface finish and composition differences were installed with grooved and ungrooved sections. A complete description of the landing research runway may be found in reference 1.

Effects of grooving.- The effects of 1/4 inch by 1/4 inch by 1 inch pitch grooves on C-141A longitudinal deceleration and main-gear wheel velocity in raw data format are shown in figure 10. Figure 10(a) shows considerable deceleration gains in the concrete test region containing 1/4 inch by 1/4 inch by 1 inch pitch grooves as compared with the otherwise similarly prepared ungrooved surface for wet and puddled, flooded, and slush-covered conditions. These maximum antiskid braking runs were conducted over limited test-section lengths on the landing research runway at speeds near those for normal-landing brake engagement.

Comparisons of braking coefficient data on dry surfaces and on wet and puddled surfaces for three of the aircraft tested on the landing research runway are shown in figure 11. The friction coefficients for the C-141A on a dry surface increases with increasing velocity (fig. 11(a)) whereas the friction coefficients for the 990A (fig. 11(b))

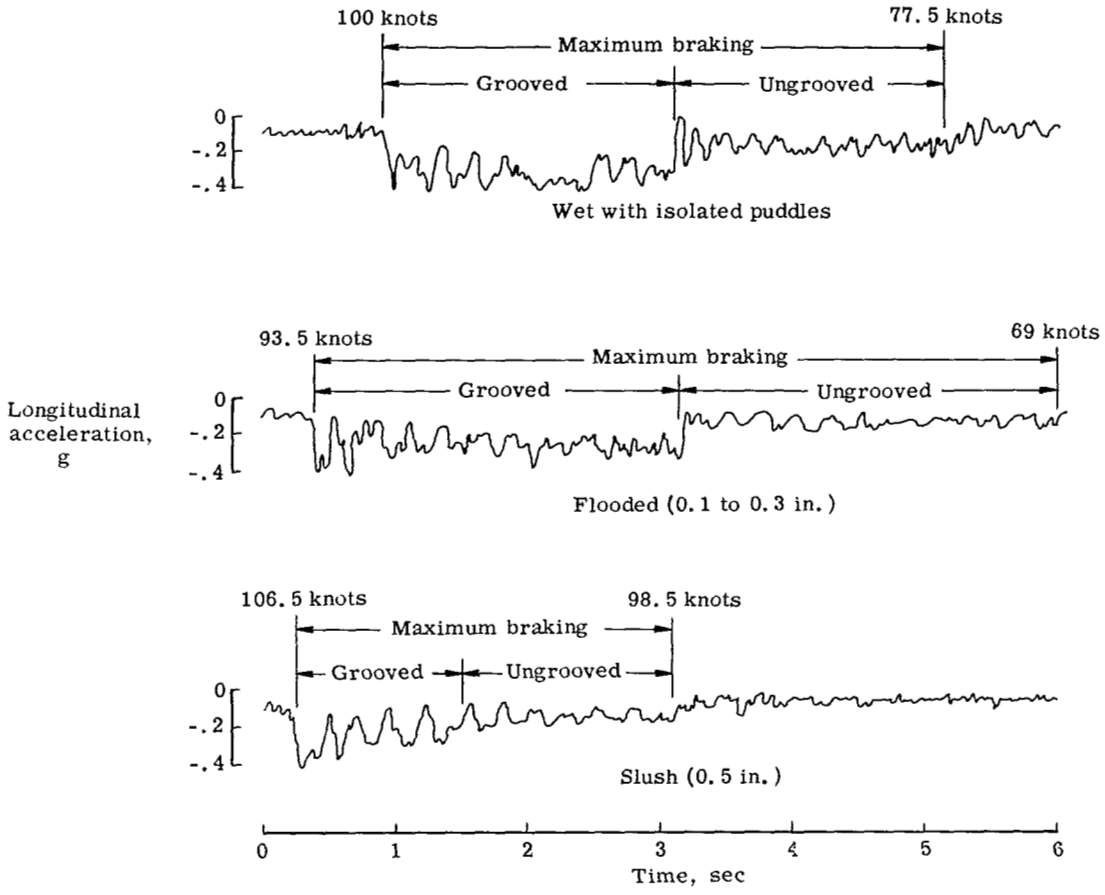

(a) General trends.

Figure 10.- Effects of grooving on raw data time histories.

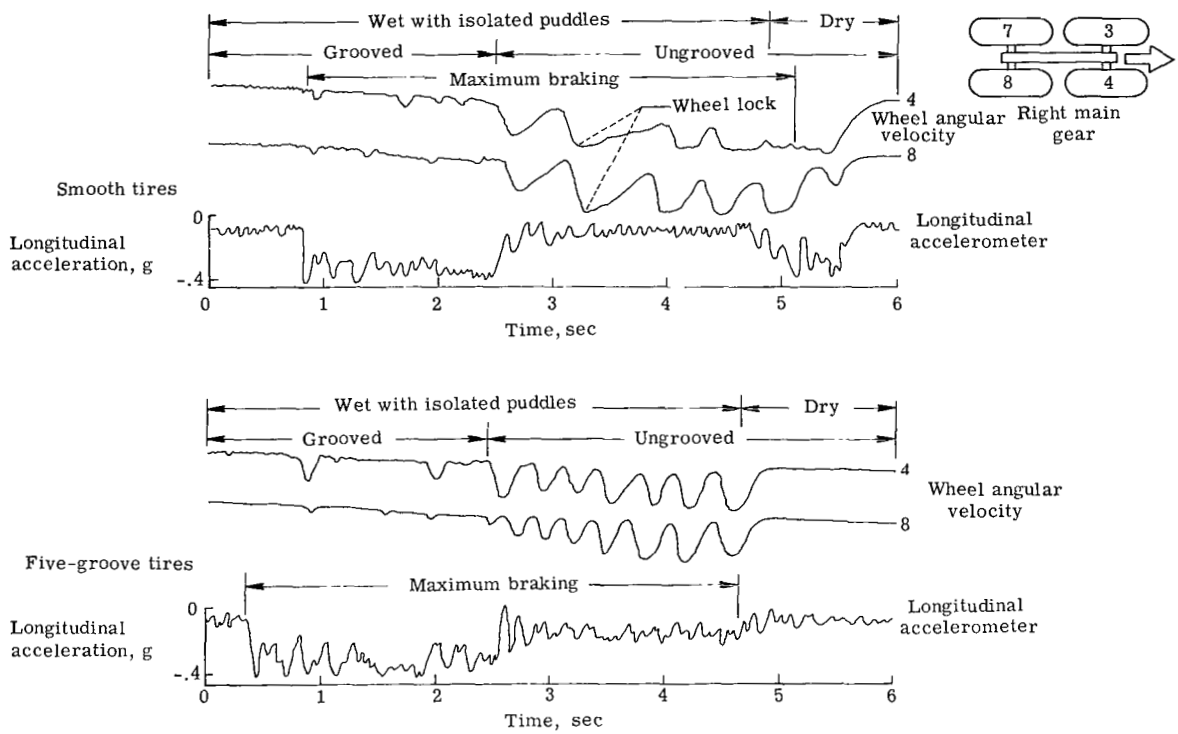

(b) Tread effects (wet).

Figure 10.- Continued.

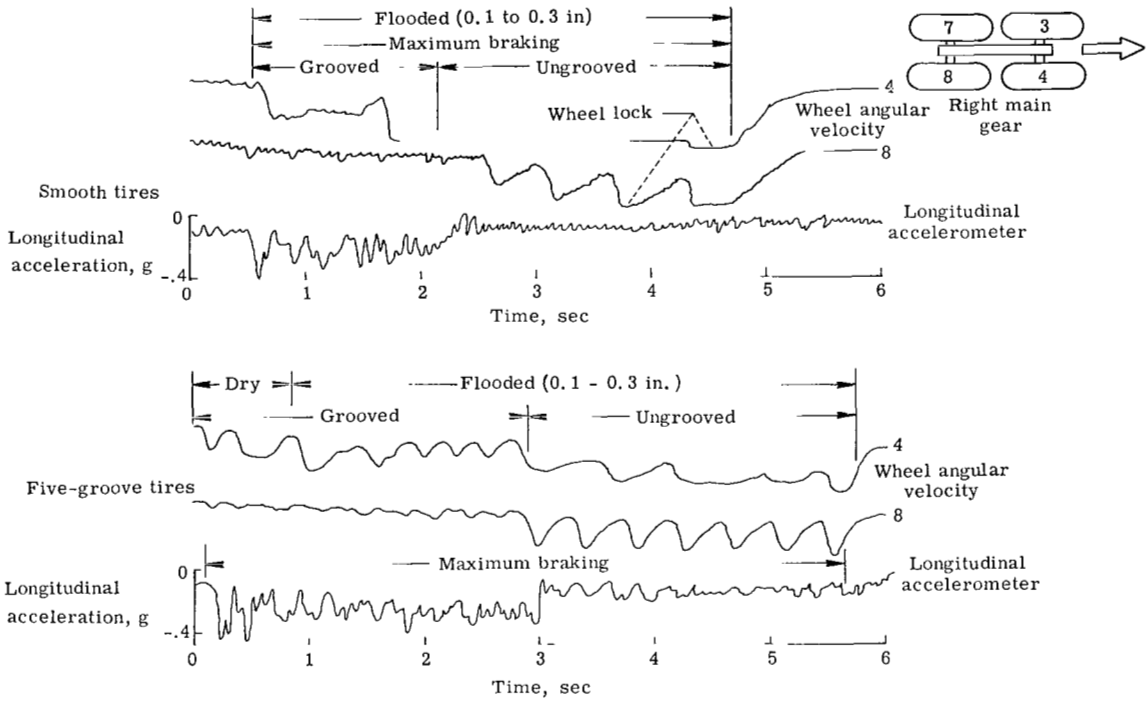

(c) Tread effects (flooded).

Figure 10.- Concluded.

and the F-4D (fig. 11(c)) decrease with increasing velocity. This difference in dry braking effectiveness levels is attributed, as was previously noted, for full-stop braking test results, to C-141A antiskid efficiency losses in the lower speed range rather than to brake fade.

The friction coefficient data obtained from the C-141A tests on the original nine surfaces of the landing research runway surfaces (A to I) for wet and puddled test conditions resulted in a relative slipperiness rating of the surfaces which was consistent with results obtained for the 990A and F-4D (parts (b) and (c) of fig. 11). The most significant result which is once more very much in evidence is the increase in C-141A braking effectiveness under wet and puddled conditions attributable to 1/4 inch by 1/4 inch by 1 inch pitch transverse grooving; that is, compare grooved surface data for surfaces H, G, C, and B with results obtained from the similar textured and wetted ungrooved surfaces I, F, D, and A. The gripstop surface E also provides some improvement in braking effectiveness for the wet and puddled tests.

Surface J which was added to the landing research runway test surface after completion of the 990A and F-4D test programs exhibits a grooved surface similar to the Seymour Johnson Air Force Base runway groove configuration (1/4 inch by 1/4 inch by 2 inch pitch grooves for 2 feet followed by 2 feet of ungrooved concrete). A comparison of C-141A wet and puddled braking effectiveness data obtained on surface J is made in figure 12 with similarly obtained data from a 1/4 inch by 1/4 inch by 1 inch concrete surface (representative of the Beale Air Force Base runway configuration) and an ungrooved concrete surface. The Seymour Johnson groove configuration provides considerable improvement in braking friction coefficient over the ungrooved concrete surface; however, the continuous 1/4 inch by 1/4 inch by 1 inch pitch configuration provides a further increase in braking effectiveness over the speed range investigated for wet and puddled concrete surfaces. It is of further interest to note that full-stop braking test results on the Seymour Johnson Air Force Base runway provided higher friction coefficients for the surface in a damp or wet condition (fig. A1(m)) than the tests on the same configuration on the landing research runway at the NASA Wallops Station. This difference is attributed to the drainage capability of the Seymour Johnson runway provided by the grooving with transverse slope, whereas a more uniform wetness condition was maintained during the level surface tests on the landing research runway.

The comparison of flooded grooved and ungrooved surfaces (fig. 13) indicates that the C-141A, as did the 990A and F-4D, achieved significantly higher braking friction coefficients on grooved as opposed to ungrooved surfaces. Surface E, the gripstop asphalt surface, affords slight improvements in braking effectiveness over ungrooved asphalt (surface F) at high speed $\left(V_G \approx 80 \text{ to } 100 \text{ knots}\right)$ under flooded conditions.

Path-clearing effects.- The effects of forward-tire path clearing for the C-141A twin-tandem main gear bogies are shown by comparing figures 10(b) with 10(c). The

Surface	Material	Treatment	Grooves
A	Concrete	Canvas belt	Ungrooved
B	Concrete	Canvas belt	1 in. by 1/4 in. by 1/4 in.
C	Concrete	Burlap drag	1 in. by 1/4 in. by 1/4 in.
D	Concrete	Burlap drag	Ungrooved
E	Asphalt	Gripstop	Ungrooved
F	Asphalt	Small aggregate	Ungrooved
G	Asphalt	Small aggregate	1 in. by 1/4 in. by 1/4 in.
H	Asphalt	Large aggregate	1 in. by 1/4 in. by 1/4 in.
I	Asphalt	Large aggregate	Ungrooved
J	Concrete	Burlap drag	2 in. by 1/4 in. by 1/4 in. (Seymour Johnson AFB groove configuration)

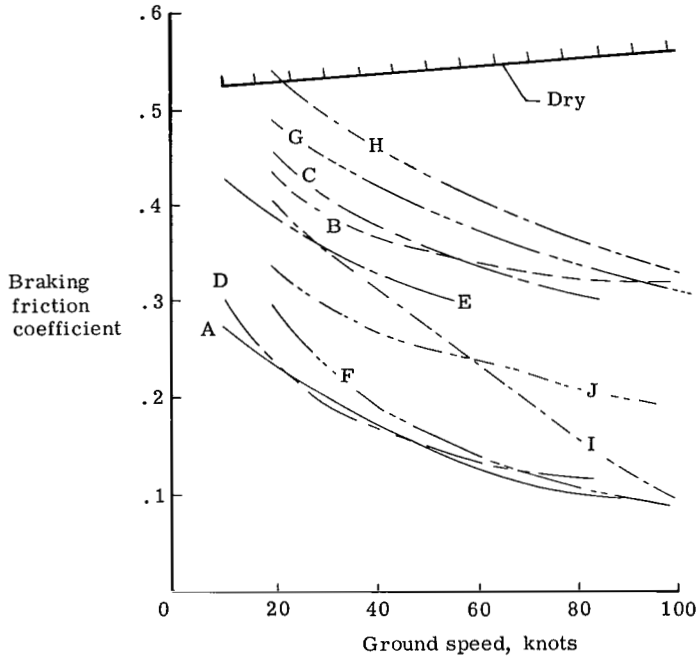

(a) C-141A.

Figure 11.- Comparison of braking friction coefficients on wet and puddled runways obtained for three aircraft.

	Surface	Material	Treatment	Grooves
———	A	Concrete	Canvas belt	Ungrooved
– – – –	B	Concrete	Canvas belt	1 in. by 1/4 in. by 1/4 in.
— – —	C	Concrete	Burlap drag	1 in. by 1/4 in. by 1/4 in.
—— – –	D	Concrete	Burlap drag	Ungrooved
— · —	E	Asphalt	Gripstop	Ungrooved
— -- —	F	Asphalt	Small aggregate	Ungrooved
— --- —	G	Asphalt	Small aggregate	1 in. by 1/4 in. by 1/4 in.
—— —–	H	Asphalt	Large aggregate	1 in. by 1/4 in. by 1/4 in.
—·—· —·	I	Asphalt	Large aggregate	Ungrooved

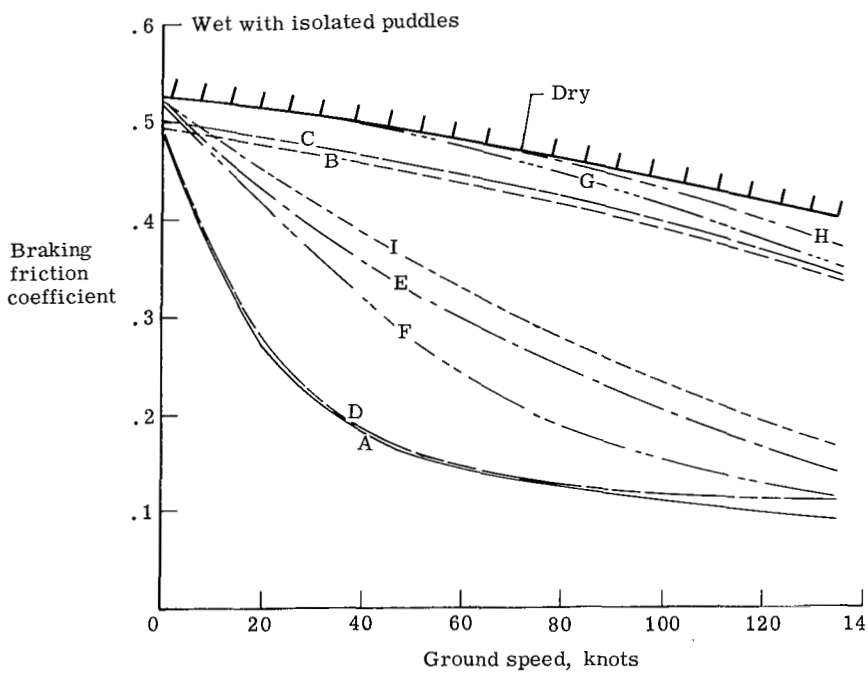

(b) 990A.

Figure 11.- Continued.

Surface	Material	Treatment	Grooves
A	Concrete	Canvas belt	Ungrooved
B	Concrete	Canvas belt	1 in. by 1/4 in. by 1/4 in.
C	Concrete	Burlap drag	1 in. by 1/4 in. by 1/4 in.
D	Concrete	Burlap drag	Ungrooved
E	Asphalt	Gripstop	Ungrooved
F	Asphalt	Small aggregate	Ungrooved
G	Asphalt	Small aggregate	1 in. by 1/4 in. by 1/4 in.
H	Asphalt	Large aggregate	1 in. by 1/4 in. by 1/4 in.
I	Asphalt	Large aggregate	Ungrooved

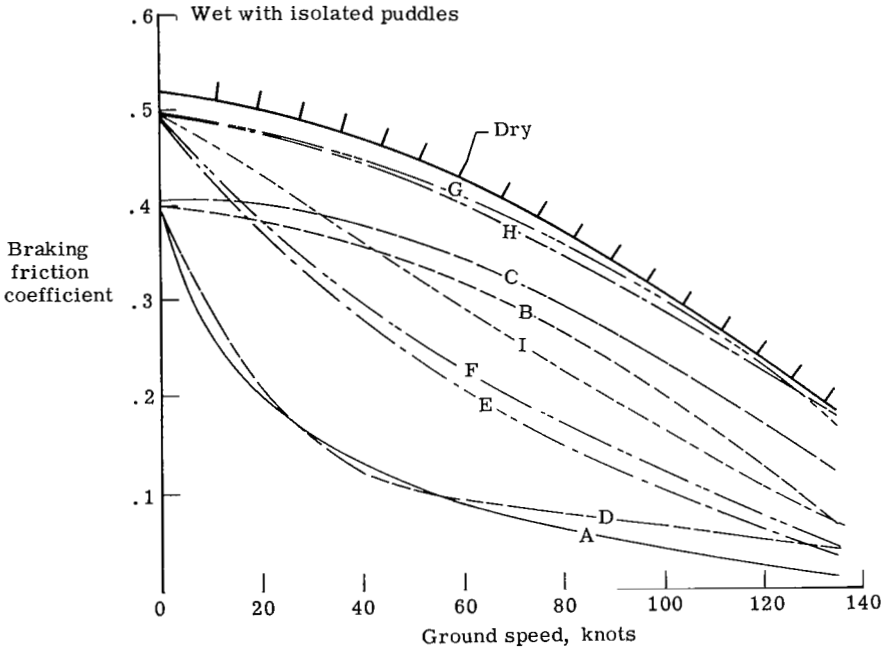

(c) F-4D.

Figure 11.- Concluded.

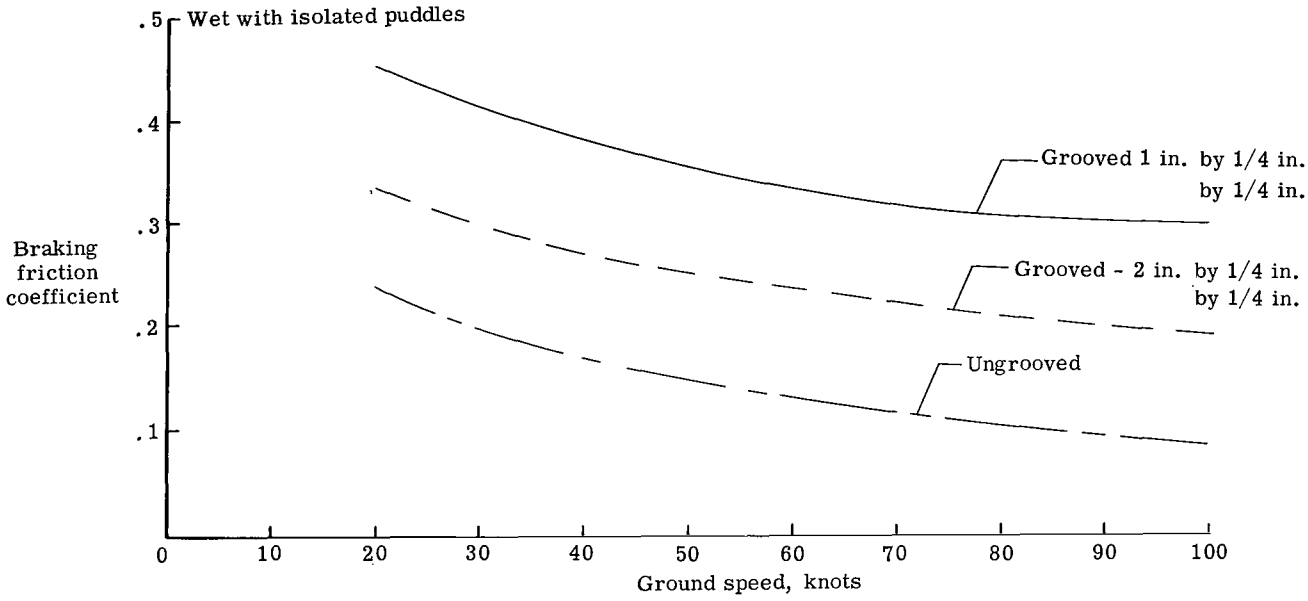

Figure 12.- Effect of runway groove configuration on C-141A aircraft braking on landing research runway at NASA Wallops Station.

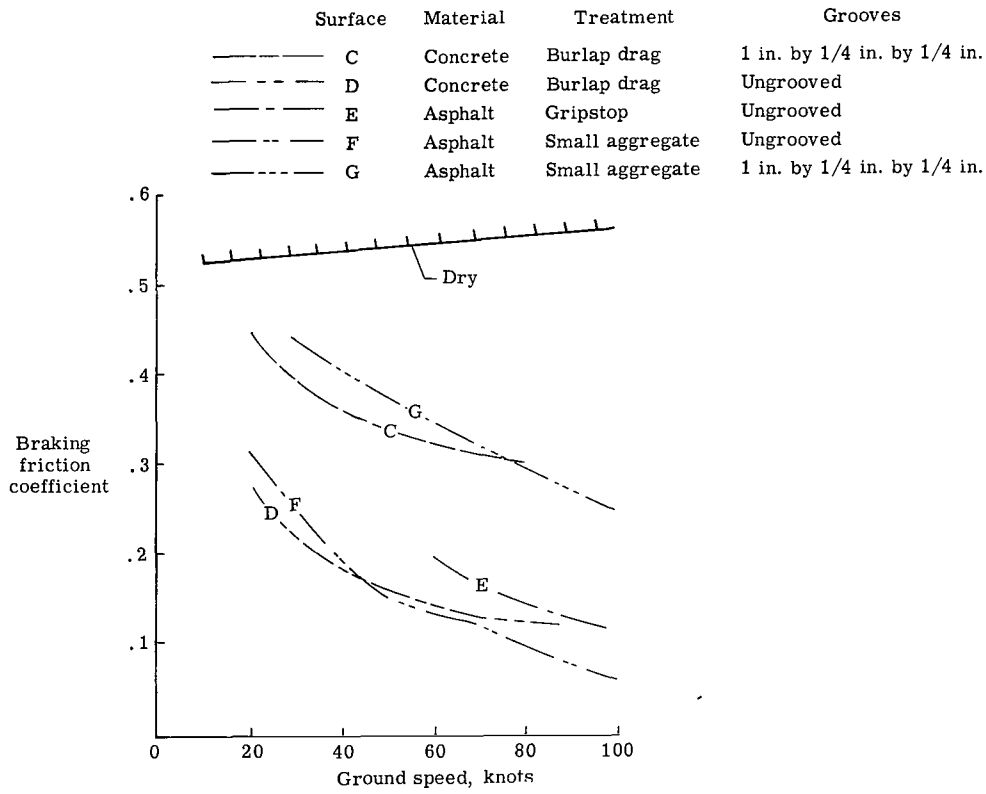

(a) C-141A.

Figure 13.- Comparison of braking friction coefficients on flooded runways (0.1 in. to 0.3 in. water depth) for three aircraft.

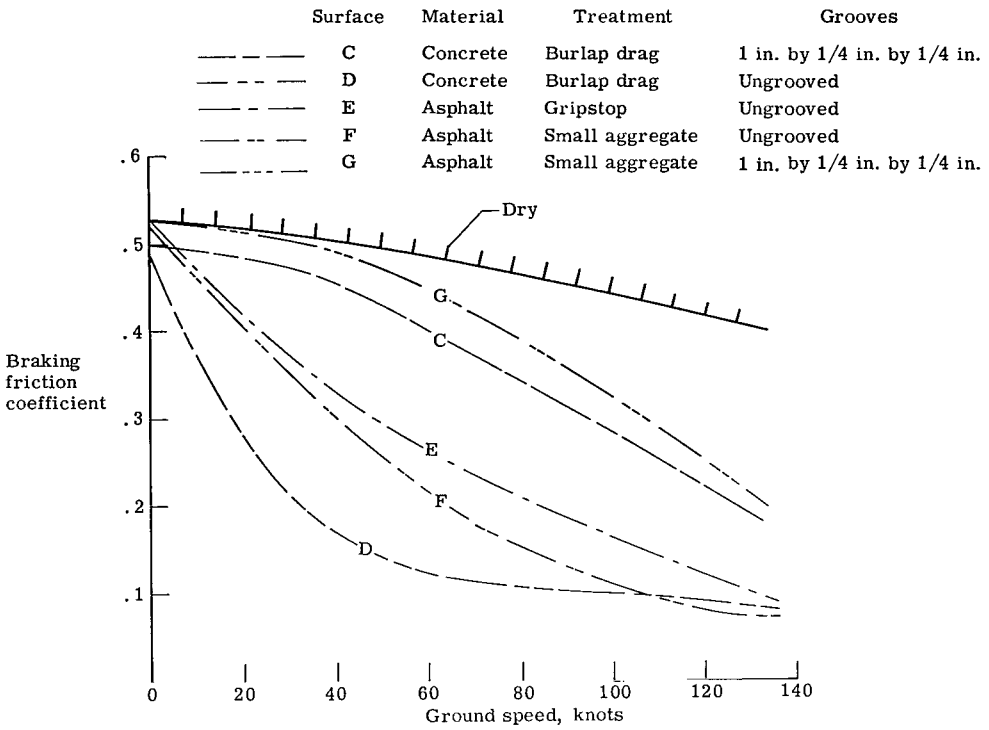

(b) 990A.

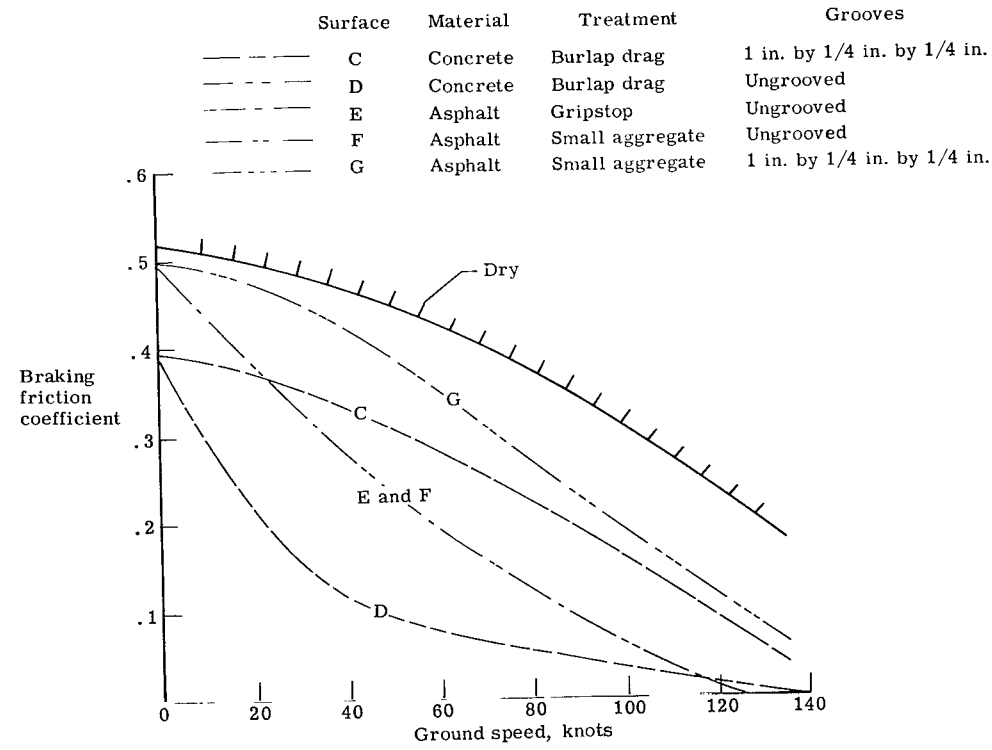

(c) F-4D.

Figure 13.- Concluded.

trailing-wheel spindown characteristics, represented by trace 8, on the two figures are noted to be similar on flooded and wet test surfaces. This observation emphasizes the desirability of the path clearing of the forward bogie wheels (and, therefore, the twin-tandem or a tandem bogie design) since the rear tires appear to be operating in a wet and puddled braking environment on a flooded runway.

Effects of tire-tread design.- Some effects of tire-tread design are shown in figures 10(b) and 10(c) for comparative C-141A braking runs with either smooth or five-groove tires on wet with isolated puddles and flooded concrete surfaces. More prolonged wheel lockups are noted to occur for the smooth-tread tires operating on the wet-ungrooved surface (top right of fig. 10(b)) as compared with the five-groove tire tread on the same wet surface (bottom right of fig. 10(b)). As a result, a loss in longitudinal deceleration (hence, braking effectiveness) is noted for the C-141A equipped with smooth tires. However, when comparing the smooth and five-groove tire braking characteristics on the wet grooved concrete surface (left half of fig. 10(b)), no appreciable tire spindowns or losses in airplane deceleration are observed. This result indicates that pavement grooving is an effective way to minimize the braking losses that normally occur between new and worn aircraft tires on wet-runway surfaces. Figure 10(c) shows the braking characteristics of both smooth and five-groove tires on flooded ungrooved and grooved concrete pavements. As indicated by comparing the velocity traces for the forward wheels (trace 4), more prolonged spindowns (or lockups) are noted to occur for the smooth forward tire than for the forward five-groove tire (bottom of fig. 10(c)) on both the ungrooved and grooved flooded concrete pavements.

The comparative braking effectiveness of smooth and five-groove tires on wet and puddled surfaces is shown in figures 14(a) and 14(b) for the C-141A and 990A, respectively. These comparisons for operations on ungrooved pavements indicate considerable gains in braking effectiveness levels using five-groove tires as compared with smooth tires (simulated worn tires) for both aircraft. Calculations made in reference 1 indicate that the losses in braking effectiveness for the smooth-tire condition just shown increases the stopping distance of the 990A aircraft on the wet ungrooved concrete runway approximately 1500 feet over that required for the unworn five-groove tire design. No significant losses in braking effectiveness are noted between five-groove and smooth-tire braking operations on wet-grooved surfaces for either aircraft. (See fig. 14.) Therefore, no significant increases in stopping distance would be expected for smooth or worn tire operations on the wet-grooved surface.

Aircraft and RCR Correlation

Wet and flooded runways.- The 1968 NASA and Air Force studies at Wallops Station (ref. 1) indicate that very poor correlation existed between aircraft stopping distance

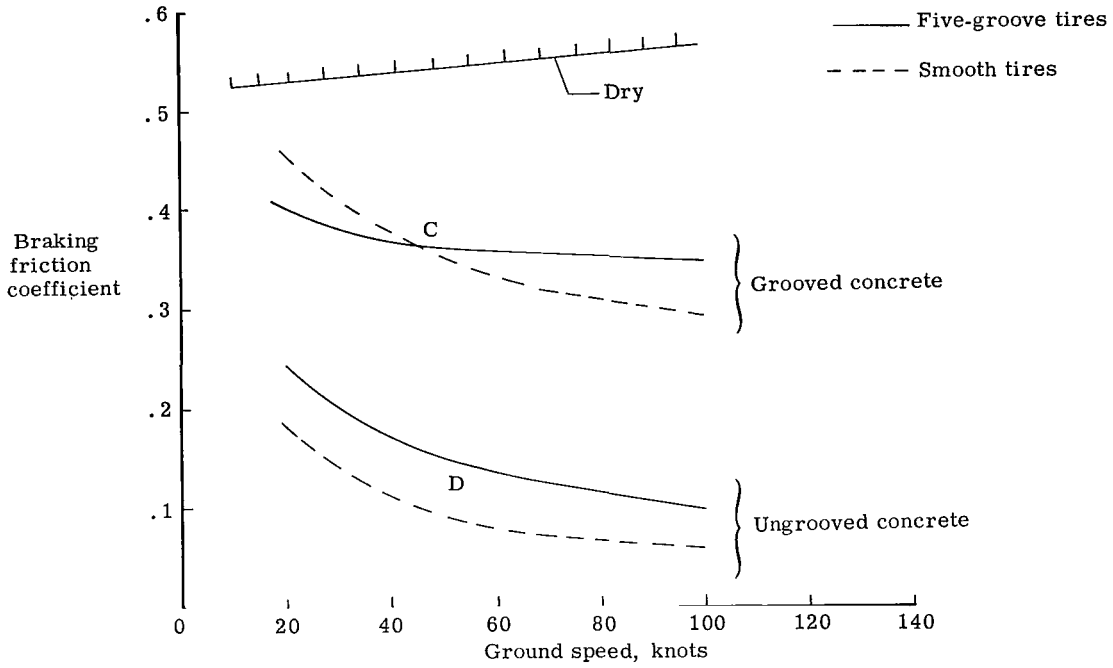

(a) C-141A.

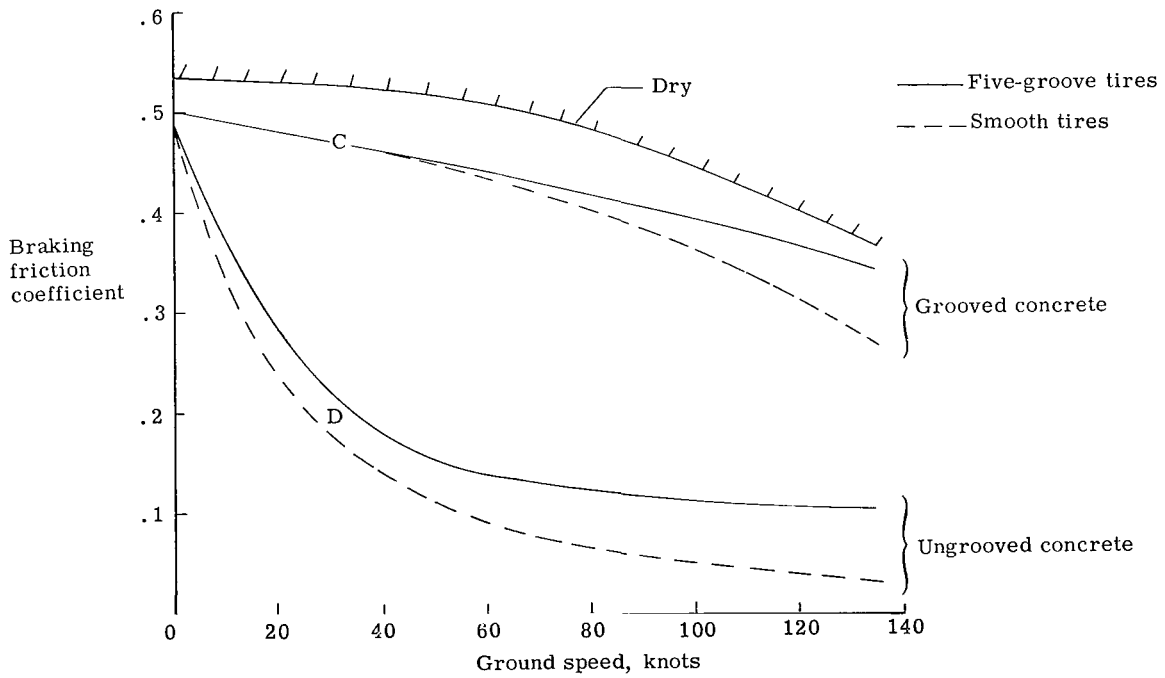

(b) 990A.

Figure 14.- Tire-tread effects on wet and puddled runways for twin-tandem bogie arrangements.

measurements and runway condition readings (RCR) for the nine runway surfaces studied under wet and flooded conditions as shown in figure 15. A similarly poor correlation was also found in the present investigation where C-141A stopping distance and RCR measurements were obtained on 36 runways under artificially or naturally wet conditions as shown in table I and figure 16. A statistical analysis of the data of figure 16 was made and the line through the point 1, 1 with least mean square error had a slope of 2.809. The root mean square error in the aircraft stopping distance ratio was 0.56 about this line. The deviation about the line of perfect agreement is much greater. The results just described indicate that RCR measurements made on wet runway surfaces with the James brake decelerometer can considerably underestimate aircraft stopping performance.

Snow-, slush-, and ice-covered runways.- The limited tests conducted on snow-, slush-, and ice-covered surfaces show much better correlation between the C-141A and the RCR vehicle. In fact, instead of underestimating aircraft performance, as the RCR was found to do on wet runways, the RCR system on snow- and ice-covered pavements, overestimated aircraft stopping performance. (See fig. 16.) The RCR system thus yields a conservative result when used to predict aircraft performance on snow- and ice-covered runway surfaces. It is important to note that a relatively narrow range of snow and ice temperatures was included in this investigation (8° F to 33° F).

Comments on the RCR system.- The data obtained from aircraft and ground vehicles during the present investigation offer an explanation for the unconservative performance of the RCR system in predicting aircraft stopping capability on wet runways and the conservative performance of the RCR system on snow- and ice-covered runways. The RCR system has a James brake decelerometer (damped pendulum instrument) installed securely on the floor of the front part of an airport ground vehicle, usually a station wagon. The brakes of the vehicle are firmly applied until all four wheels are fully locked at a ground speed ranging between 20 and 30 miles per hour on the runway to be tested. The maximum reading of the instrument, which is the deceleration in ft/sec^2, is noted; this value is the RCR number. The vehicle must be equipped with standard or snow tires in good repair. The standard tires just described have an efficient tread design for improving tire traction on wet pavements. At a vehicle speed of 20 to 30 mph, it can be expected on wet pavements that the vehicle performance will be influenced more by tire-tread design than by the basic runway slipperiness. As a further example of this point, consider the data shown in figure A1(h) for the Lockbourne Air Force Base wet concrete runway. At a ground speed of 20 knots, there is little difference between the aircraft wet and dry friction coefficients (lower part of fig. A1(h)); this result is the same as that indicated by the RCR vehicle at approximately the same speed, 23 dry and 22.5 wet. However, it will be noticed that at high speeds (up to 100 knots), the wet runway is very slippery to the aircraft as indicated by the much lower friction coefficients obtained. This condition results in a relatively high stopping distance ratio (2.05) which

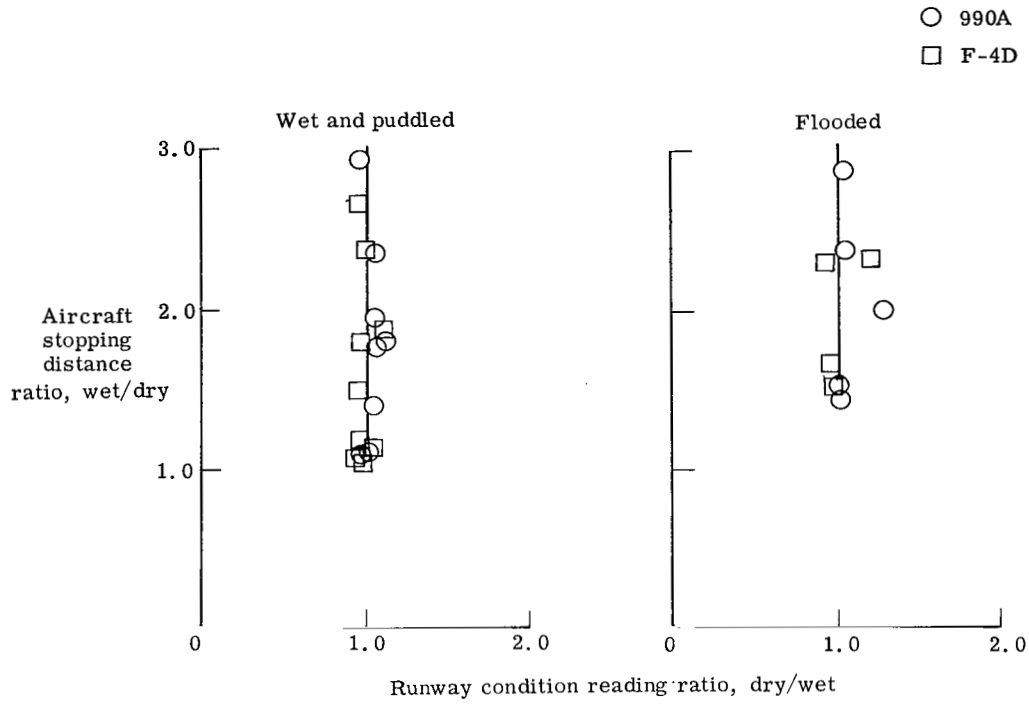

Figure 15.- Comparison of aircraft stopping distance ratios with RCR ratios. Vehicle test conditions: velocity, 30 mph; four-wheel skid; typical production tires; tire pressure, 24 lb/in^2; tire vertical load, 1012 lb (1968 NASA-Air Force Study, ref. 1).

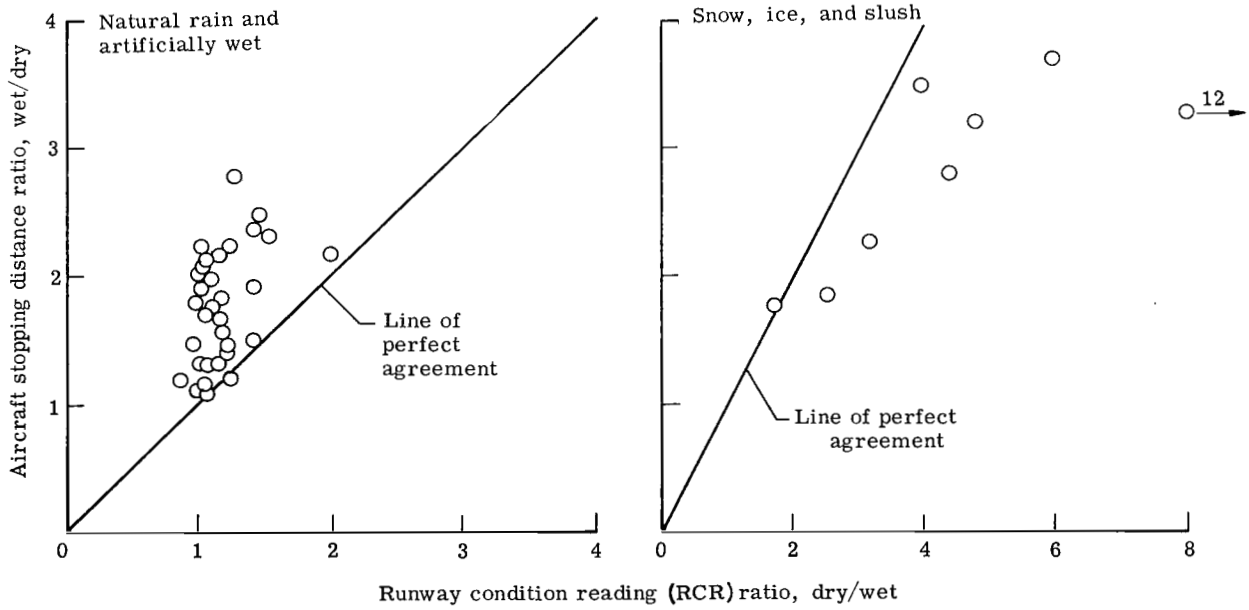

Figure 16.- Correlation between C-141A aircraft and RCR test vehicle.

contrasts with the RCR measurements that were made at the lower speed and indicated essentially a dry-runway condition (23 dry and 22.5 wet).

NASA research on viscous hydroplaning (ref. 9) indicates that the smoother the pavement surface the greater the tire friction loss to viscous hydroplaning and the less effective tire-tread design becomes. The most perfect example of viscous hydroplaning is a tire braking on wet glare ice. For this condition no difference in friction level can be detected between tires with smooth-tread (bald) or brand new rib-tread tires. The smooth-textured runway surface at Dyess Air Force Base (fig. A1(a)) approaches this condition when wet. It can be seen that the aircraft indicated the runway as slippery with a stopping distance ratio of 2.77. The RCR ratio measured for the runway was 1.28. The correlation between the aircraft and RCR vehicle is poor for this runway, but it can be seen that the RCR is reporting the runway more slippery when wet than when dry.

On snow- and ice-covered runways, the situation is very different. The aircraft results on the glazed-ice- and snow-covered runway at Loring (see figs. 6(c) and A1(nn)) indicate that the effective aircraft friction coefficient is nearly constant with ground speed. Under diagonal braking, the tests were made with the NASA test vehicle with the diagonal pair of smooth-tread tires locked and skidding on the runway. As discussed earlier in the paper, this operational condition resulted in the lowest snow and ice friction coefficients being obtained when the vehicle came to a stop. This low-friction result was attributed to the skidding tire having time at low speeds to melt the surface layer of the snow- and ice-covered pavement and provide additional friction-lowering lubrication. It is felt that the RCR vehicle locking its wheels at 20 mph is also in this pressure-melting condition. It can be seen from figure 6(c), that the C-141A follows a similar trend (see aircraft deceleration trace) when the wheels become fully locked at low speed (time 38 seconds). As can be seen from table II, the RCR dry-wet ratio reports the slipperiness of the runway as 4.0, a more conservative result than the wet-dry stopping ratio of 3.51 reported by the aircraft on the same surface.

Aircraft and NASA Diagonal-Braked Test-Vehicle Correlation

The development of the diagonal-braked test vehicle stopping distance as a means for rating runway slipperiness and estimating aircraft performance on slippery runways is described in references 14 and 18. In contrast to the RCR system which is proven to be not effective on wet surfaces, the diagonal-braked test vehicle technique correlates well with different aircraft for all runway surface conditions of wetness, slush, snow, and ice studied as shown in figure 17. A more detailed analysis of the correlation of the aircraft and diagonal-braked test vehicle obtained from test results of the present investigation is presented herein.

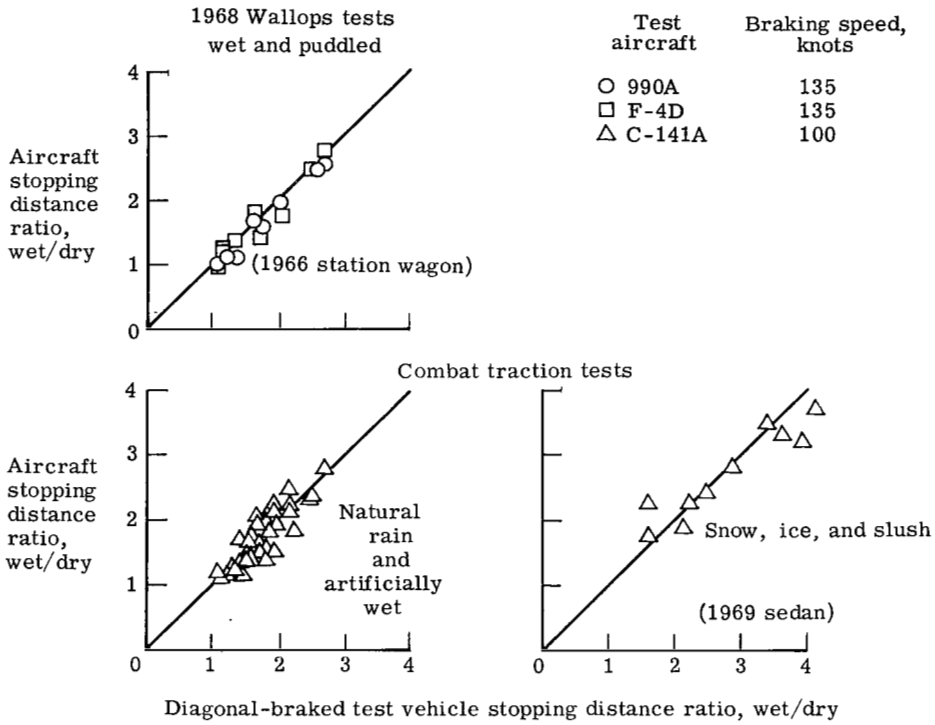

Figure 17.- Correlation between aircraft and test vehicle stopping distance ratios. The diagonal-braked test vehicle stopping distance ratio was determined by using a dry stopping distance of 302 feet for the snow, ice, and slush tests.

Artificially and naturally wet surfaces.- The manner in which the diagonal-braked test vehicle and the C-141A aircraft correlate in rating the slipperiness of pavement surfaces is illustrated by comparing the aircraft and test vehicle deceleration time histories obtained at Offutt Air Force Base and shown in figures 18(a) and 18(b), respectively. Wet and dry tests on the Offutt Air Force Base runway were conducted by the C-141A and test vehicle on September 10, 1969. These tests were repeated February 20, 1970, after the runway was transverse grooved to a $1\frac{1}{4}$ inch by 1/4 inch by 1/4 inch groove pattern. It can be seen from figure 17 that excellent correlation between the aircraft and the diagonal-braked test vehicle exists. Figure 19 and table I show the correlation obtained between the C-141A and the diagonal-braked test vehicle by using data from the present investigation obtained on 40 artificially wet or natural-rain-covered runways. The statistical analysis of the data of figure 19 with the line through the point 1,1 with least mean square error had a slope of 0.993. The root mean square error in the aircraft stopping distance ratio was only 0.19.

Snow-, ice-, and slush-covered surfaces.- Very good correlation between the C-141A aircraft and the diagonal-braked test vehicle was also found for the runways tested under slush, snow, and ice conditions as shown in figures 17 and 19 and table II. It should be pointed out that for both aircraft and test vehicle, dry stopping distance data were unobtainable because of the condition of the runways. Accordingly, the wet-dry stopping distance ratio for the aircraft was calculated by using an average dry stopping distance value of 1100 feet. The average stopping distance for all dry runs made by the diagonal-braked test vehicle in this investigation was 302 feet. The wet-dry stopping distance ratios used in figures 17 and 19 and table II for the test vehicle are based on this dry distance figure. It can be seen that on this basis, excellent correlation is achieved between the test vehicle and aircraft for snow-, ice-, and slush-covered runways.

The trend for the diagonal-braked test vehicle dry stopping distance to vary with ambient air temperature according to equation (1) as discussed earlier is of concern in this regard. The test vehicle wet-dry stopping distance ratios on slush, snow, and ice surfaces were recomputed by using the value of the test vehicle dry stopping distance obtained from equation (1) for the actual runway ambient air temperatures given in table II. The correlation between the test vehicle and the aircraft wet-dry stopping distance ratios on this basis is shown in figure 20. Also shown in the figure for comparison is the RCR dry-wet ratio obtained under the same conditions (from table II). It can be seen that for this case, the diagonal-braked test vehicle prediction of runway slipperiness is in agreement with the RCR method, and both ground vehicle methods overestimate aircraft stopping distance on slush-, snow-, and ice-covered runways. This result indicates the need for further correlation trials to be conducted between other aircraft and the diagonal-braked test vehicle on snow-, ice-, and slush-covered surfaces to determine

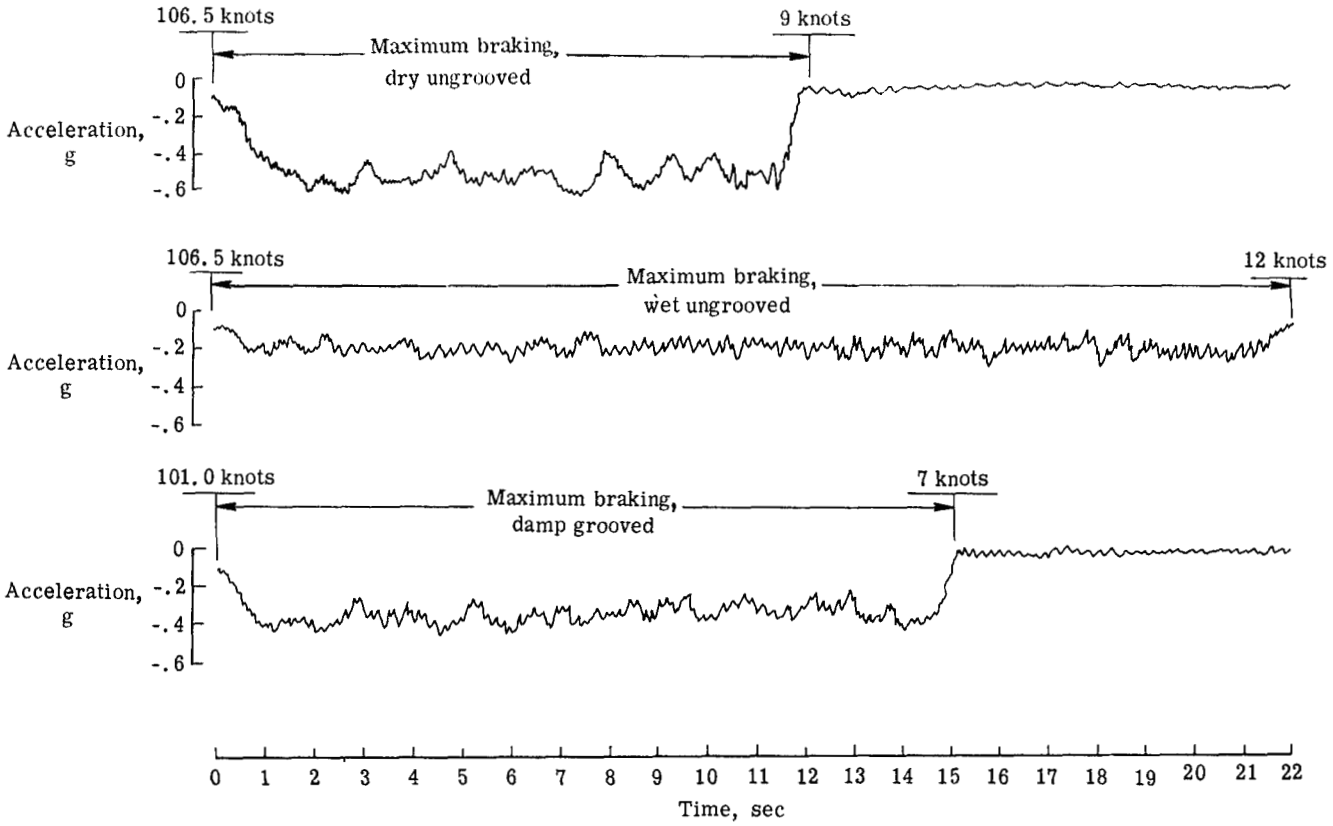

(a) C-141A aircraft.

Figure 18.- Braking at Offutt AFB on ungrooved and grooved runway surfaces under dry and wet conditions.

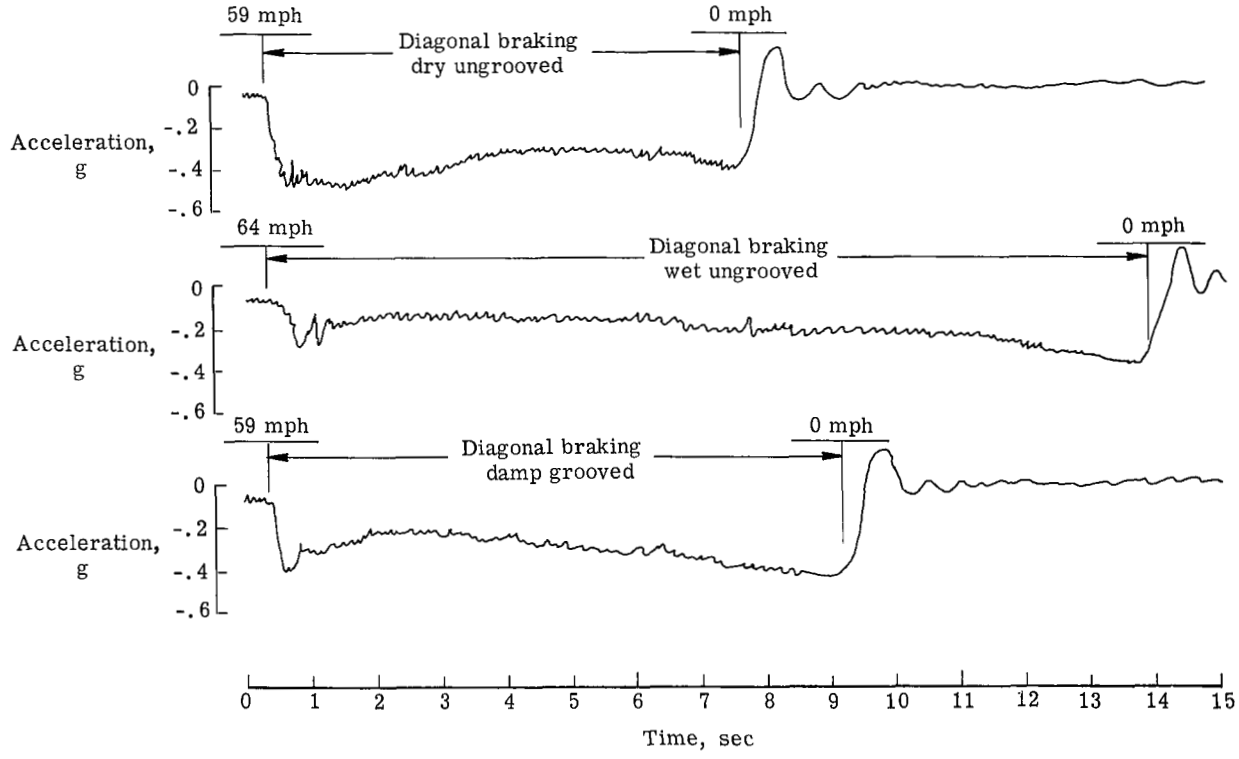

(b) Diagonal-braked test vehicle.

Figure 18.- Concluded.

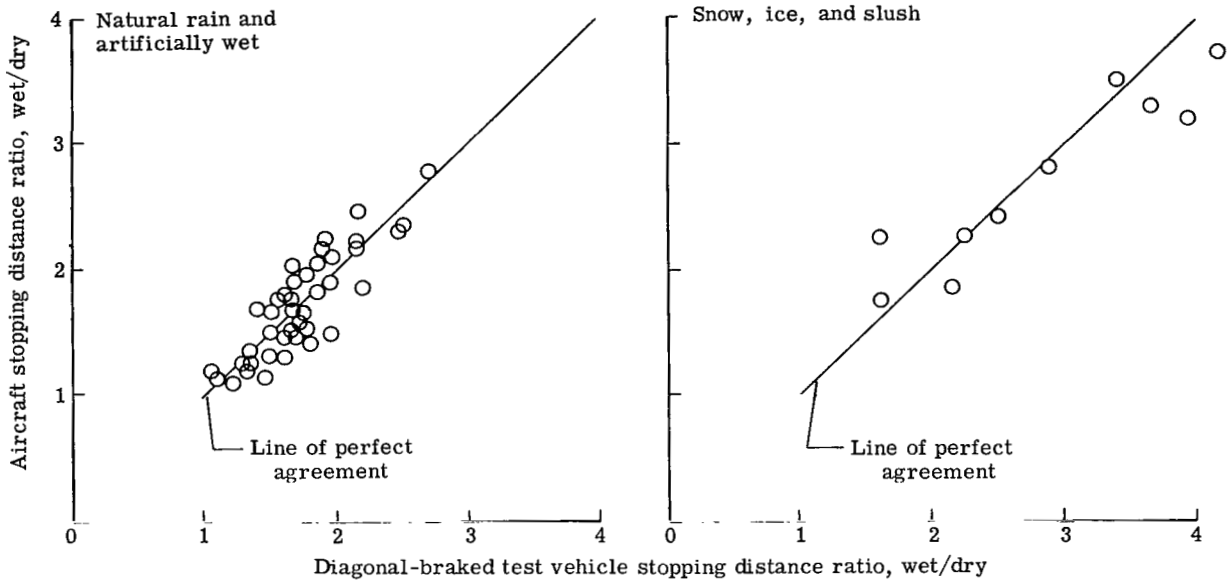

Figure 19.- Correlation between C-141A aircraft and the diagonal-braked test vehicle.

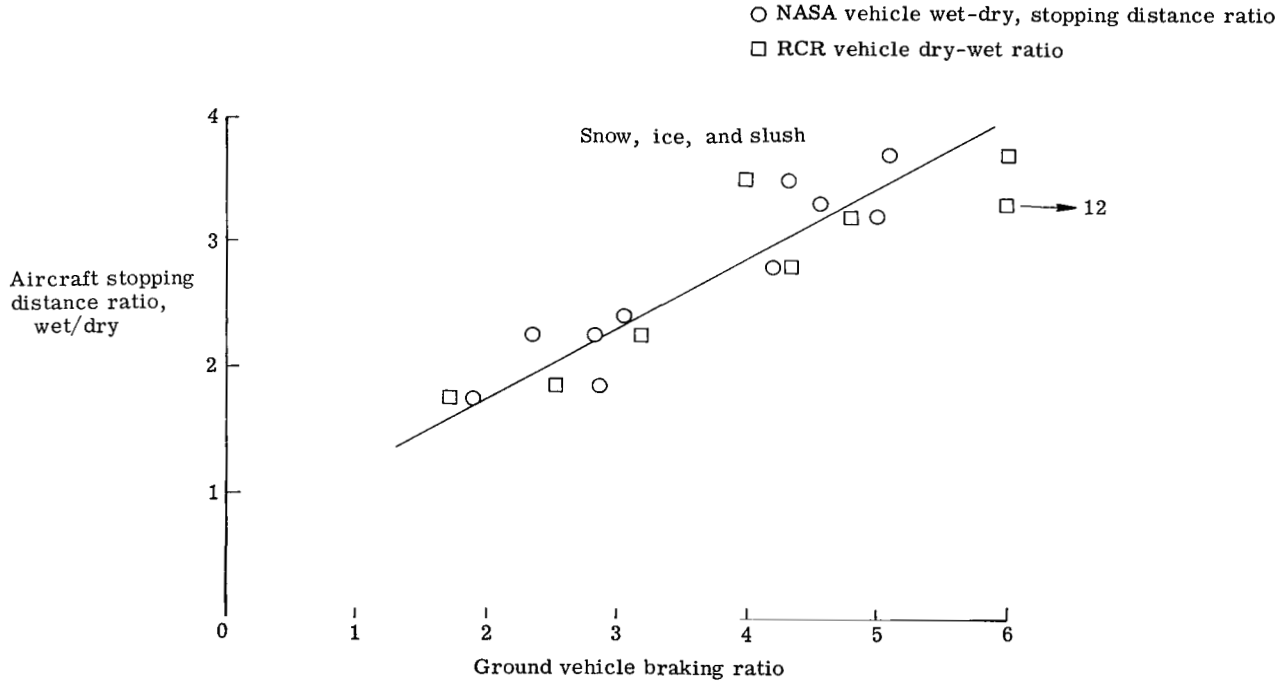

Figure 20.- Correlation between aircraft and ground vehicle braking ratio. Diagonal-braked test vehicle wet-dry stopping distance ratio based on dry stopping distance, $D_{vehicle,dry} = 208 + 145T_r$.

which dry stopping distance for the test vehicle (average dry value or temperature compensated) best agrees with aircraft stopping performance.

The correlation obtained between the C-141A and the diagonal-braked test vehicle on slippery runways can also be demonstrated by using data obtained with the auxiliary aircraft and test vehicle instrumentation used in the present investigation. For example, both the aircraft and test vehicle measured vehicle ground speed as a function of time. In figure 21, tire braking loss is computed from vehicle velocity time histories by using the relationship

$$\text{Braking loss} = \left\{1 - \frac{\left[\left(\frac{\Delta V}{\Delta t}\right)_{\text{Braked}} - \left(\frac{\Delta V}{\Delta t}\right)_{\text{Unbraked}}\right]_{\text{Wet}}}{\left[\left(\frac{\Delta V}{\Delta t}\right)_{\text{Braked}} - \left(\frac{\Delta V}{\Delta t}\right)_{\text{Unbraked}}\right]_{\text{Dry}}}\right\} \times 100 \qquad (2)$$

These data are plotted against vehicle wet-dry stopping distance ratios obtained from the test vehicle and aircraft by using revolution counter data for stopping distance. (See fig. A1.) A rather remarkable relationship is shown in figure 21. The 5000-lb test vehicle predicts the braking loss experienced by a 200 000-lb aircraft to within about ±10 percent accuracy at the larger (slipperier) wet-dry stopping distance ratios of interest. This relationship is of great importance since NASA research (ref. 1) shows little difference between tire braking and cornering (side-force) friction coefficients for similar wetness and speed conditions. Thus, figure 21 could be expressed as cornering traction loss as well as braking loss and thus could predict losses in tire steering and side-force capability necessary to estimate aircraft crosswind limitations on slippery runways.

It is felt that the technique described in this investigation to wet artificially a runway surface and obtain wet and dry diagonal-braked test vehicle stopping distances (wet-dry stopping distance ratio) within a short period of time (within 1 hour) has proven to be a reliable way to rate wet-runway slipperiness in terms of aircraft stopping performance. For example, the Edwards Air Force Base runway was tested by the test vehicle and aircraft on September 20, 1969. The test vehicle and aircraft developed wet-dry stopping distance ratios of 1.91 and 2.15, respectively. (See fig. A1(f).) This runway was retested by the test vehicle in June 1970. Under similar artificial wetting conditions (0.03-inch water depth), the test vehicle at this latter date developed a wet-dry stopping distance ratio of 2.10. It is of considerable interest to note that the dry stopping distance for the test vehicle was 269 feet in September 1969 and 316 feet in June 1970 even though the ambient air temperatures were approximately the same (58° F in September 1969 and 52° F to 64° F in June 1970). Preliminary data indicate that the diagonal-braked test

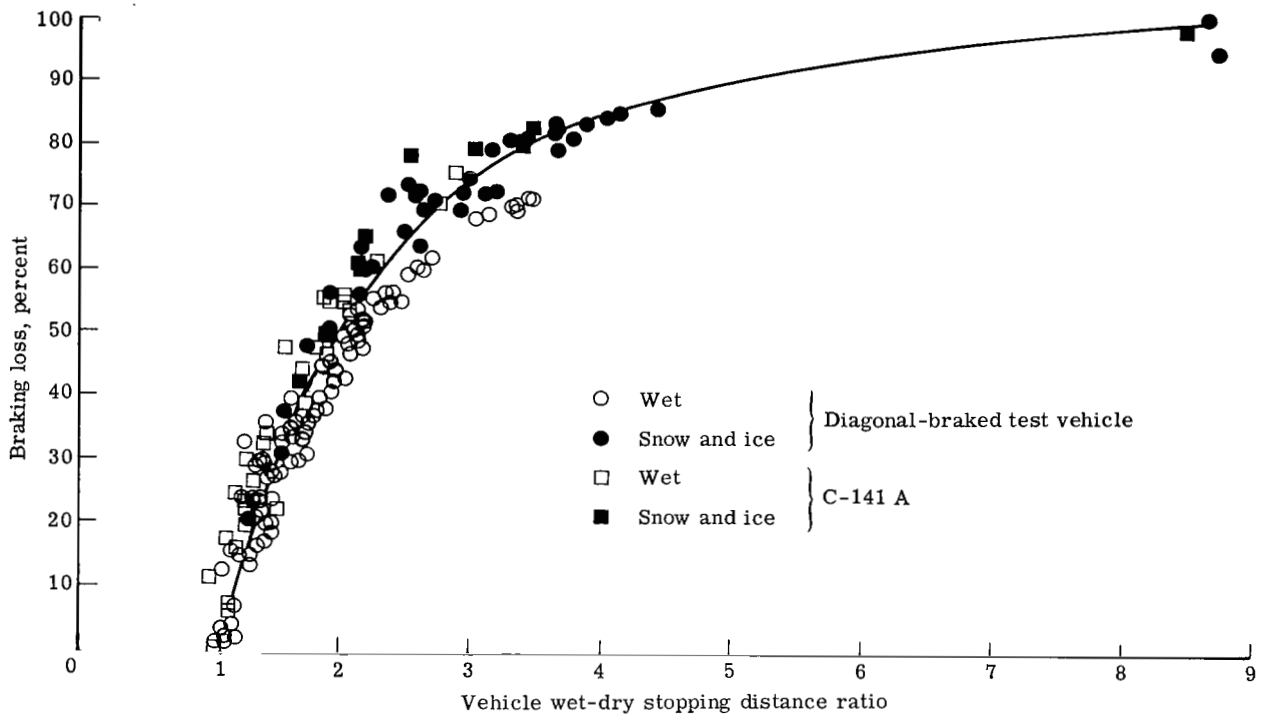

Figure 21.- Effect of runway slipperiness on stopping distances and tire traction of C-141A aircraft and NASA diagonal-braked test vehicle.

vehicle achieved a reasonable correlation with the C-5A aircraft, test vehicle (2.09) and C-5A (1.88) for the runway wetted with a water-foam mixture. These results are encouraging because even though the test vehicle dry stopping distances varied considerably between tests at Edwards, the wet-dry stopping distances were reasonably close in magnitude.

When the diagonal-braked test vehicle is used operationally to predict aircraft performance at time of take-off and landing, it will most likely be impossible to make a test vehicle dry-runway stopping distance test in close time proximity to the wet-runway braking test. The question thus arises as to what value of the test vehicle dry-runway stopping distance should be assigned for the wet-dry stopping distance ratio. It is felt that the test vehicle wet- and dry-stopping distance measurements should be made on the same runway under similar artificial wetness conditions for a wide range of ambient air temperatures to answer this question properly for operational use.

A recent study made with the diagonal-braked test vehicle on a local airport runway during varying natural rain conditions (see fig. 22) indicates that the stopping distance ratio of the test vehicle increases with increasing rainfall precipitation rate and water depth on the runway. This result, although not unexpected, points out two areas of interest. First, the changing slipperiness of the runway with precipitation rate demonstrates the need to assess runway slipperiness at time of aircraft take-off and landing. Second, it has been proposed to correlate the diagonal-braked test vehicle stopping distance ratio with rainfall precipitation rate at a given airport runway. Once a correlation is established, the runway slipperiness condition during a rain can be determined from the rainfall precipitation rate without the need of making test vehicle stopping tests other than occasional calibration runs. This correlation would be of great help at busy airports. Also of interest in this figure is the fact that a 1.44-inch-per-hour precipitation rate produced an average water depth on the runway of 0.17. This depth is sufficient to produce aircraft hydroplaning. As discussed in the limited braking section of this paper, research is needed to determine the correlation of the diagonal-braked test vehicle with aircraft of different landing-gear wheel geometry on flooded runways because of wheel-path-clearing effects.

Equivalent RCR

As discussed earlier in the paper, U.S. Air Force aircraft flight manual take-off and landing distance charts are based on RCR numbers. This section of the paper develops a method for converting diagonal-braked test vehicle wet-dry stopping distance ratios to equivalent RCR values. These charts are constructed on the basis of a linear variation of RCR and aircraft braking coefficient as shown in sketch (a).

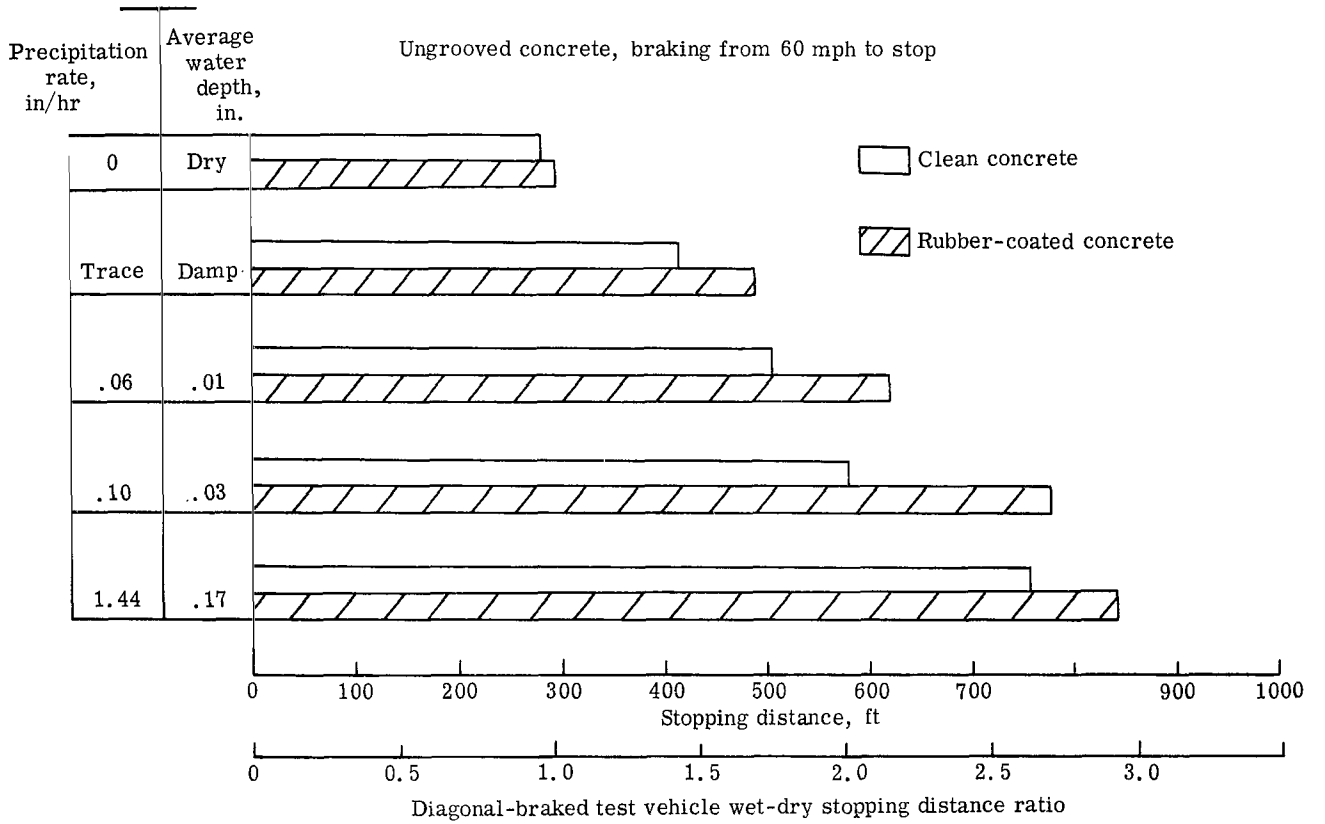

Figure 22.- Slipperiness of airport runway during natural rain.

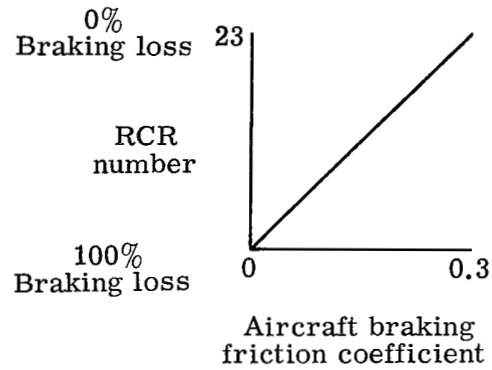

Sketch (a)

For example, an aircraft during certification trials demonstrates an average braking friction coefficient of 0.3 during its dry-runway braking tests. The James brake-decelerometer-equipped vehicle during stops on dry runways usually develops an RCR number of 23. The landing distance chart for an RCR number of 11.5 is calculated on the basis of an average braking coefficient of 0.15. (See sketch (a).) The chart in figure 23 is developed by means of sketch (a) and figure 21 from which an equivalent RCR number can be obtained for a given vehicle wet-dry stopping distance ratio. This chart may be used for all aircraft whose flight manual RCR stopping distance data are developed according to the method outlined in sketch (a).

In September 1970, this conversion of stopping distance ratio to equivalent RCR was checked for the F-106 aircraft by the following procedure. Figure 24 describes a typical aircraft landing. The landing is composed of three segments; air distance, transition distance, and braking distance. The air distance is defined as the distance required for the aircraft to descend from a point 50 feet above the runway threshold to touchdown with the main landing gear. The transition distance is the distance required from touchdown to derotate the aircraft (nose-wheel touchdown) and apply wheel brakes. The braking distance is defined as the distance required to bring the aircraft to a stop after brake application. The total of the three segments is defined as the landing distance. Actually, only the dry braking distance is affected by runway surface slipperiness. A series of landings were made with the F-106 and the distance to brake application point from the runway threshold noted. This distance was subtracted from the aircraft flight manual landing distance (from threshold) to obtain dry stopping distance for the aircraft landing condition (gross weight). By using the procedure given in figure 25, it is possible to determine the average diagonal-braked test vehicle wet-dry stopping distance ratio $\overline{X}$ on a given runway from the aircraft brake application point. The diagonal-braked test vehicle was used to test the runway at Hamilton Air Force Base in September 1970. Preliminary data from this test indicates that runway 12 under a wet condition gave a stopping distance ratio of $\overline{X} = 2.15$. The dry distance for the F-106 obtained in the manner described earlier was multiplied by 2.15 to obtain the wet stopping distance for the aircraft on this runway. The

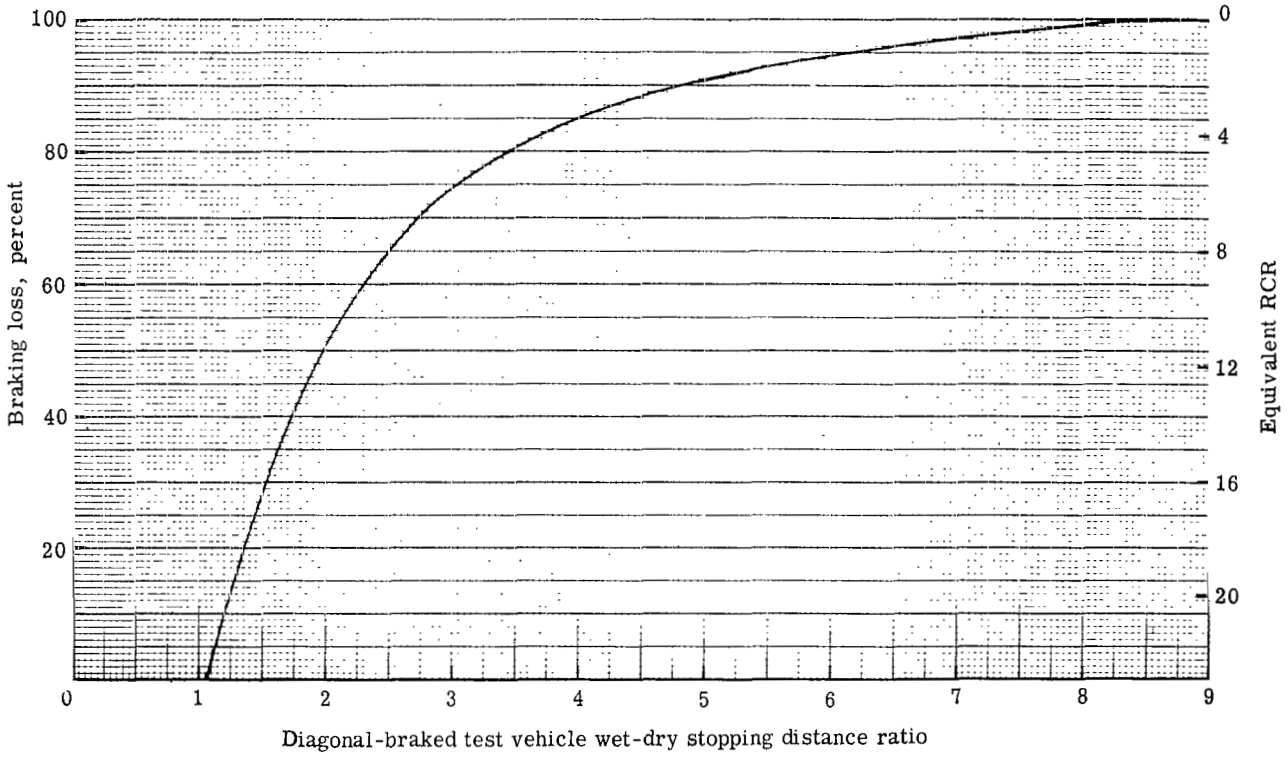

Figure 23.- Conversion of diagonal-braked test vehicle wet-dry stopping distance ratio to the equivalent RCR.

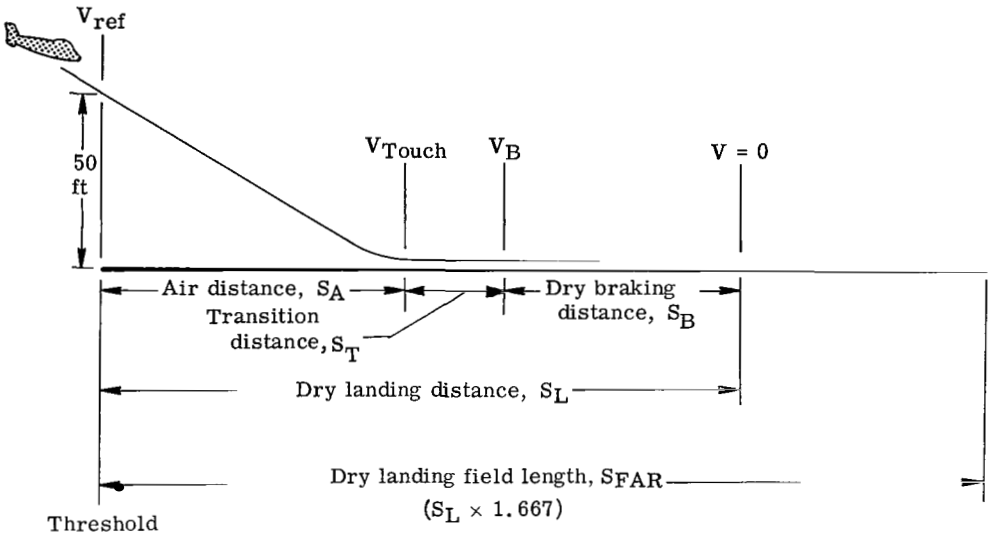

Figure 24.- Aircraft landing terminology.

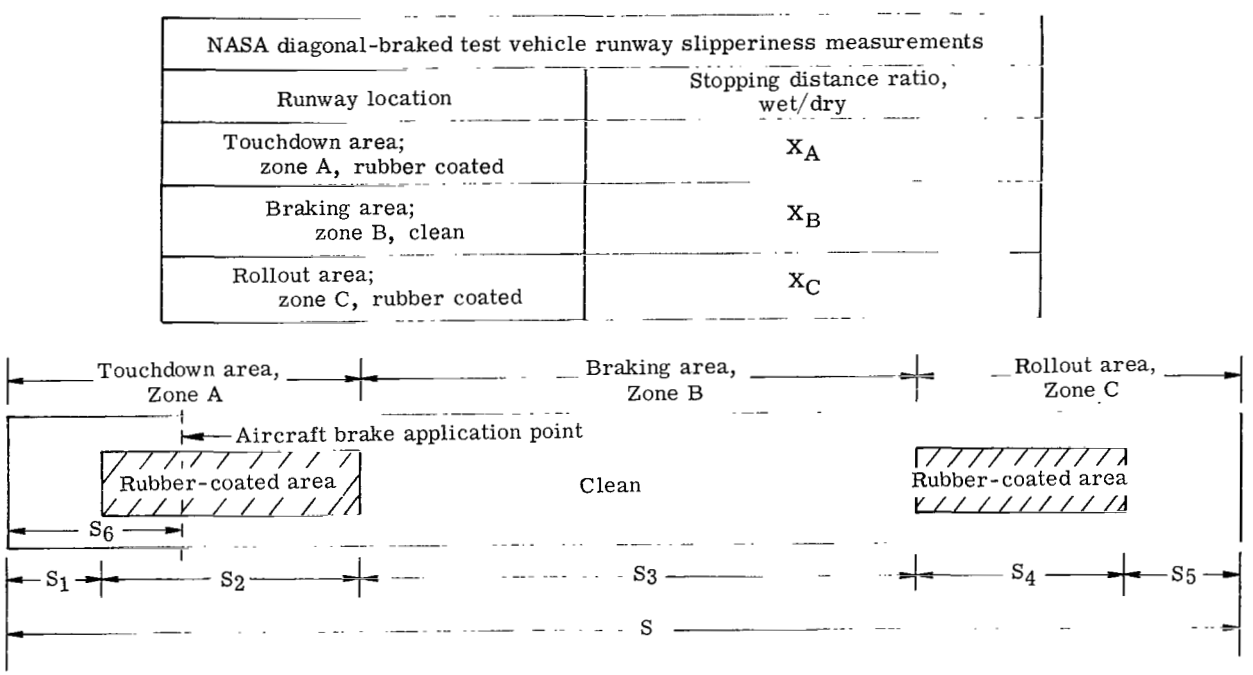

Figure 25.- Method for calculating the average diagonal-braked test vehicle wet-dry stopping distance ratio $\overline{X}$ for a given aircraft landing condition.

$$\overline{X} = \frac{(S_1 + S_2 - S_6)X_A + (S_3 + S_5)X_B + S_4X_C}{S - S_6}$$

air distance and transition distance were then added to obtain the wet landing distance. This wet landing distance was entered into the flight manual at the aircraft landing condition to obtain an equivalent RCR of 11. The wet-dry stopping distance ratio of 2.15 obtained was entered in figure 23 to obtain an equivalent RCR of approximately 11.5. The agreement thus shown is very encouraging. However, operational use of the equivalent RCR method would depend upon further validation of the technique with other aircraft types.

British Ministry of Aviation Supply Evaluation of Runway Conditions

Two different British ground vehicle friction measuring devices, the friction meter (Mu-meter) and the Miles engineering skid trailer, were tested concurrently with the C-141A aircraft, RCR vehicle, and diagonal-braked test vehicle at all British Royal Air Force and Naval Bases studied in this investigation. The British Ministry of Aviation Supply report describing the Mu-meter and RCR vehicle evaluation of runway slipperiness at these bases is given in appendix D. The Ministry of Aviation Supply report did not present an evaluation of the runway surfaces by the Miles engineering skid trailer.

Runway Surface Treatment Evaluation

Data from the present investigation indicate that aircraft stopping distances on dry concrete pavements were usually only slightly less than those obtained on dry asphalt pavements. Slipperiness of runways thus becomes important only when pavements become wet, flooded, or covered with slush, snow, ice, or other contaminants.

Conventional surface treatments (wet conditions).- The runways studied in this investigation are ranked according to slipperiness (wet-dry stopping distance ratio) in table I, first for concrete pavements, and then for asphalt pavements. These data, along with visual observations of the runway surface during test, surface photographs, and the core sample analysis shown in appendix A as well as the engineering data given in appendix C, show that some concrete and asphalt runways although constructed according to conventional surface treatment procedures were slippery when wet. Such slippery surfaces, whether constructed of concrete or asphalt, have several features in common. These features are: lack of surface texture, use of smooth or polished stones in the exposed aggregate of the surface, and relatively poor water drainage. NASA research (ref. 9) indicates that smooth pavements and smooth or polished aggregate stones lack the gritty texture required for aircraft tires to puncture and displace from the tire footprint the thin viscous water film that may create viscous hydroplaning or viscous skidding. The lack of surface texture also makes the tire-pavement combination more susceptible to dynamic hydroplaning when finite water depths cover the pavement. Open-textured pavements, for example, provide many small escape paths for the bulk water

trapped in the tire-ground contact patch to drain outside the footprint and delay dynamic hydroplaning from occurring until greater ground speeds are achieved or deeper water depths are encountered on the pavement. An indication of the effect of surface texture on pavement slipperiness is given by the data shown in figure 26 which shows the variation of aircraft wet-dry stopping distance ratio (table I) with average pavement surface texture depth. As the average texture depth of the pavement increases, the wet-dry stopping distance ratio of the aircraft decreases. The scatter of the data in figure 26 is mainly attributed to the fact that the NASA grease technique used measures gross surface porosity and hence does not distinguish between smooth or polished pavement surfaces having aggregates which are ineffective against viscous hydroplaning, and smooth but gritty surfaces having aggregates which are effective against viscous hydroplaning. The rubber-coated touchdown areas of runways provide another example of the effect of surface texture on pavement slipperiness. These rubber desposits tend to fill the voids and to round the small sharp asperities of a runway surface; thus, the surface texture is made smoother and more susceptible to both viscous and dynamic hydroplaning effects. An ungrooved runway recently tested by the NASA diagonal-braked test vehicle under wet and damp conditions exhibited the following wet-dry stopping distance ratios: rubber-contaminated concrete, 3.46 wet and 3.36 damp; and for clean concrete, 2.42 wet and 1.88 damp. The ratio of 3.36 achieved on this damp rubber-coated concrete runway was larger (more slippery) than that obtained on many of the snow- and ice-covered runways tested in this investigation. (See table II.) It can be seen from table I that the rubber deposits on the grooved runways at John F. Kennedy and Seymour Johnson Airports also increased the pavement slipperiness of these runways. Note that the increase in slipperiness due to rubber deposits is not as severe on the grooved runways investigated as on the ungrooved surfaces.

Conventional surface treatments (flooded or slush-covered conditions).- Under heavy rainfall precipitation rates, conventional runway surface treatments cannot drain the water from the pavement quickly enough to prevent the pavement from flooding and completely covering even open-textured runway surfaces with finite water depths. Under this condition, dynamic hydroplaning reduces aircraft tire-ground braking capability at high speeds as shown in figure 13(c) for the F-4D aircraft. The same situation is true for slush-covered runways as well since slush may act as a viscous fluid.

Conventional surface treatments (snow- and ice-covered conditions).- When snow or ice accumulate on a runway surface to a depth and density that prevents aircraft tires from actually contacting the bare pavement surface, it is obvious that the particular pavement surface treatment underlying the snow or ice cover will have no effect on the aircraft or ground vehicle braking action. The safety hazards that snow and ice create on a runway surface are readily apparent from the magnitude of the aircraft wet-dry stopping distance ratios which are as high as 3.71 (table II). It is noted that these values were

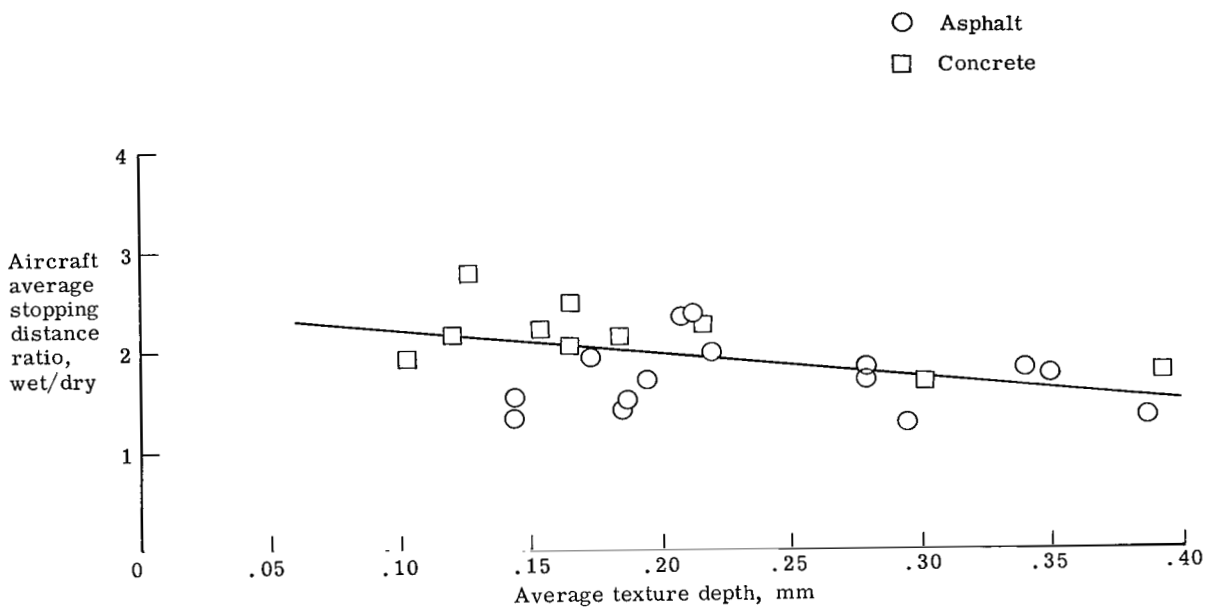

Figure 26.- Variation of aircraft wet-dry stopping distance ratio with runway surface average texture depth (NASA grease test).

obtained for a relatively cold temperature range from 8^{o} to 27^{o} Fahrenheit where the snow and ice covers are relatively dry. If a sudden thaw were to occur, the warm temperatures would tend to produce first a water film on the packed snow or ice and later a slush condition. A water film on ice (based on wet-ice friction-coefficient data from ref. 9) is estimated to produce wet-dry stopping distance ratios for the aircraft of 8.5 as shown in figure 21. It is important therefore to remove or treat the snow or ice condition on runways and taxiways as quickly as possible.

Unconventional surface treatments (wet or flooded conditions).- Runway surfaces found to provide the best aircraft stopping performance under damp or wet conditions in this investigation were grooved and porous asphalt friction course surfaces. Both grooved and porous surfaces were observed to drain rapidly during times of heavy natural rain so that surface flooding which occurs on conventional surface treatments under such conditions did not normally occur except in isolated small runway low-spot (bird bath) areas.

The aircraft stopping performance on damp or wet grooved pavements was found to be dependent upon the groove arrangement (groove spacing and depth of groove) selected. (See table I.) Best aircraft stopping distance performance was achieved by using 1/4 inch wide by 1/4 inch deep transverse grooves spaced 1 inch apart. These results are in agreement with earlier NASA research on groove configurations described in reference 1. The alternating groove pattern (2 inch by 1/4 inch by 1/4 inch) used at Seymour Johnson Air Force Base and described in appendix C, although shown to be effective (table I) for a damp runway condition, was found to be considerably less effective for a wet runway condition during tests at Wallops Station (see fig. 12) than the 1 inch by 1/4 inch by 1/4 inch groove pattern. As previously described, the limited braking tests at Wallops Station on the C-141A, F-4D, and 990A aircraft indicated that grooved pavements were considerably superior to ungrooved pavements under flooded runway conditions in developing tire-ground braking forces. The porous asphalt surfaces were not tested under flooded runway conditions in this investigation. It is felt, however, that the porous asphalt friction course surface would be effective under flooded conditions because of the internal drainage capacity of this surface configuration.

It should be mentioned that synthetic aggregates, such as used in the asphalt surface at Meigs Airport, may be a solution for runway construction areas in which the local aggregate is smooth and possesses low friction qualities. Such aggregates could be used in porous friction course or open-textured asphalt surface treatments.

Unconventional surface treatments (slush, snow, or ice conditions).- The limited braking tests at Wallops Station show that for the C-141A and 990A aircraft, grooved pavements are superior to ungrooved pavements when under a slush cover. (See fig. 27.) The porous asphalt friction course was not studied under a slush condition in this

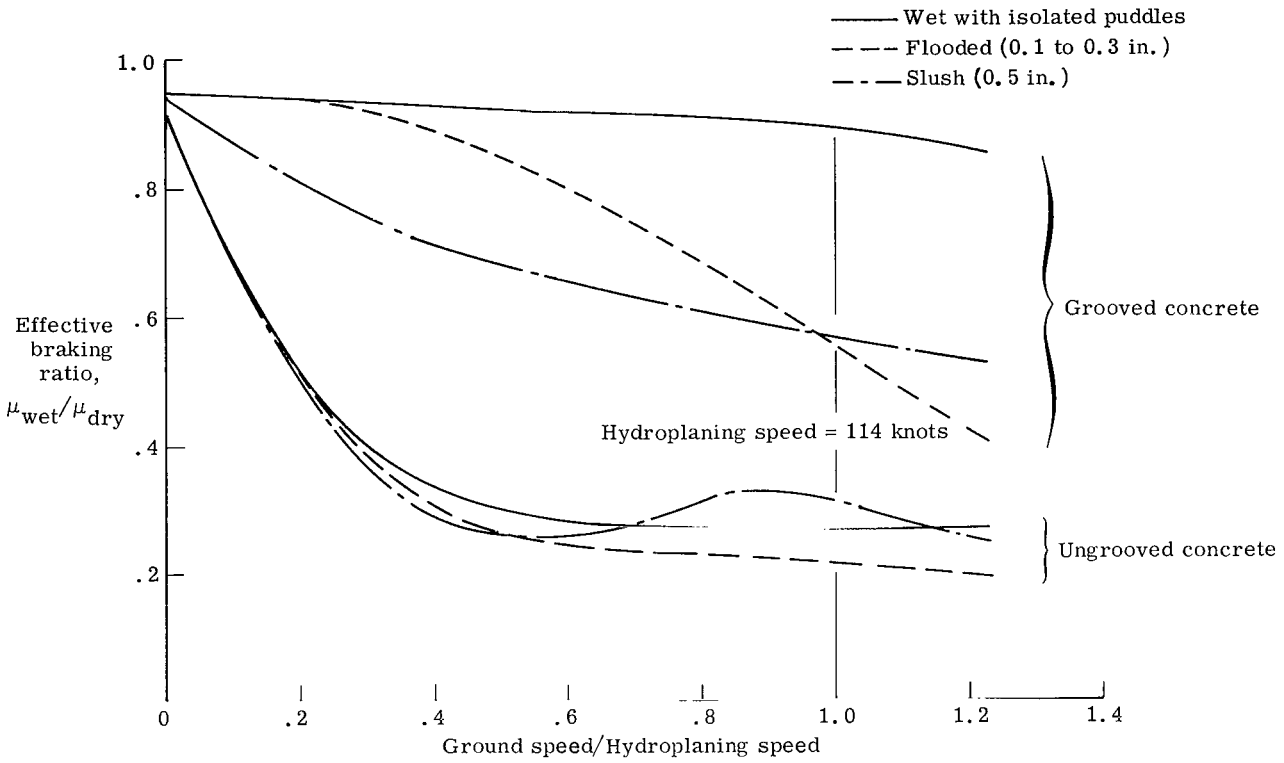

(a) 990A aircraft; five-groove tire; inflation pressure, 160 lb/in^2.

Figure 27.- Effect of runway grooves on aircraft braking performance.

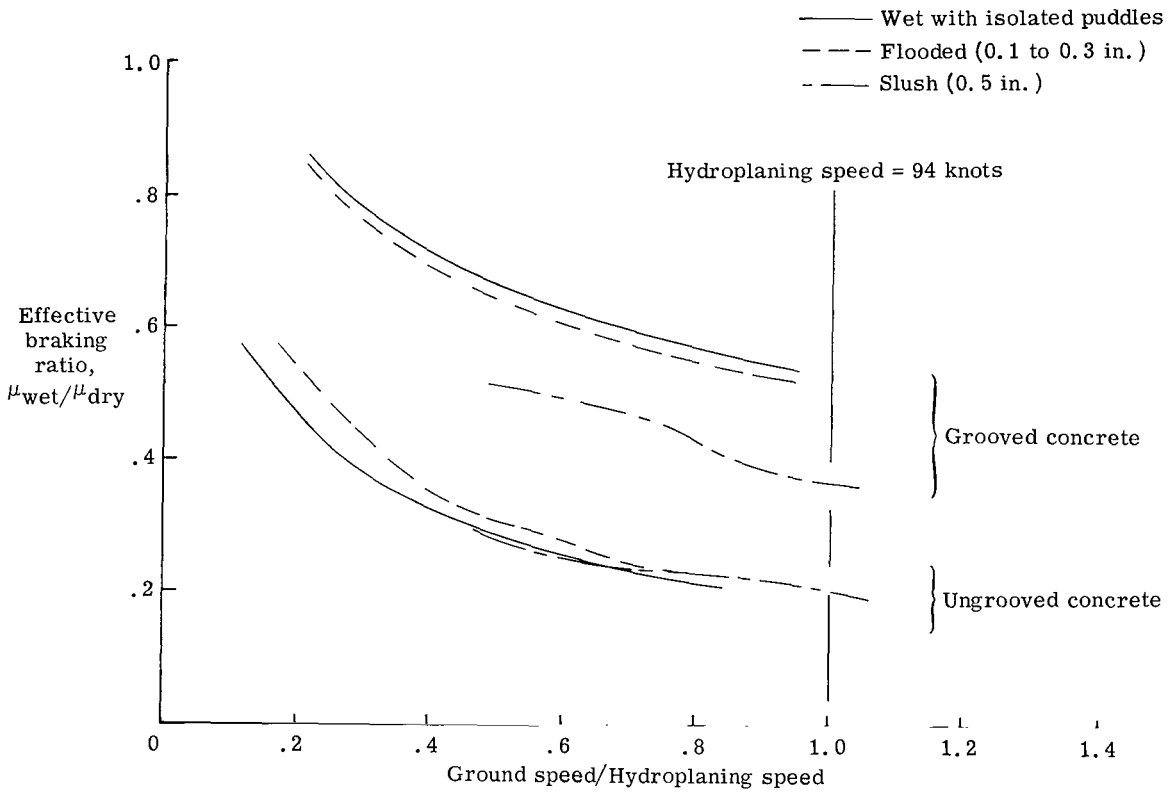

(b) C-141A aircraft; five-groove tire; inflation pressure, 110 lb/in^2.

Figure 27.- Concluded.

investigation. The fact that grooved and porous pavement treatments drain quickly also means that they dry quickly, and as a result, ice formation on the runway during cold temperatures should be alleviated. It has been noted (ref. 1) that when thin ice forms on grooved runways at, near, or slightly below freezing ambient air temperatures, tire passage over the ice-covered grooved pavement shatters the ice in the tire-ground contact zone and friction is improved. Tire passage on an adjacent ungrooved pavement under the same thin-ice temperature conditions did not disturb the ice bond to the pavement and friction was very low. The same type of improvement in aircraft and ground vehicle performance furnished by grooved pavements under this ice condition has also been observed on the porous asphalt friction course surface at Marham RAFB. Unfortunately, snow conditions were not available for test on unconventional surfaces.

Unconventional surface treatments (other factors).- As of July 1970, 23 concrete and asphalt runways have been grooved worldwide. (See table III.) The experience thus far (ref. 1) shows that pavement deterioration from grooving, especially on concrete surfaces, has not been a significant problem. Grooved plant mix asphalt runways with dense aggregate such as those at Farnborough, Washington National, and Kansas City have had no significant pavement deterioration problems. Asphalt taxiway grooves have failed and collapsed when the grooving treatment was applied to thin asphalt slurry-seal runway coatings. Groove-collapsing-type failures also have occurred on the runway at Tempelhof. (See fig. A1(bb).) In this instance, the grooving treatment was installed on the surface of a plant-mix asphalt runway that had a 1/8-inch German antiskid coating applied to the original surface. The surface photographs in figure A1(bb) show that the 1/8-inch antiskid coating has slipped with respect to the original surface and has flowed into the runway grooves. The grooves in the original plant-mix asphalt underlying the surface coating have maintained integrity.

Reference 1 reports that the most significant new aircraft operational problem that can be attributed to pavement grooving is the chevron cutting of aircraft tires at the moment of touchdown during landing. NASA research indicates that chevron cutting occurs only on the larger size aircraft tires where large wheel moment of inertias produce high wheel spin-up drag loads on aircraft tire treads at touchdown. Preliminary results of a study being conducted at the NASA landing loads track on a large 49×17 aircraft tire (see fig. 28) indicate that damages from chevron cutting are functions of touchdown speed, inflation pressure, and tread rubber compound. Damage index in figure 28 is simply the product of the chevron cut damaged area of the tire tread and the deepest chevron cut. The index furnishes an indication of the volume of tire-tread rubber affected. Tire I in figure 28 used a tread rubber compound in wide use before pavement grooving was initiated on runways. Tire II in figure 28 used a new tread rubber compound expressly made to alleviate chevron cutting. It is apparent from these results that tread rubber compounding is a promising way to alleviate this aircraft operational problem.

TABLE III.- GROOVED RUNWAYS – July 1970

[All runways have transverse groove patterns with rectangular cross section unless otherwise noted]

Type	Location	Material	Year grooved	Groove pattern		
				Pitch, in.	Width, in.	Depth, in.
Military (Continental)	Beale AFB, Calif.	Concrete	1968	1	1/4	1/4
	Seymour-Johnson AFB, N.C.	Concrete and asphalt	1968	*2	1/4	1/4
	Offutt AFB, Neb.	Concrete	1969	$1\frac{1}{4}$	1/4	1/4
Military (Overseas)	Ubon, Thailand	Concrete	1966	*2	1/4	1/4
	Udorn, Thailand	Concrete	1966	*2	1/4	1/4
	Shemya, Alaska	Asphalt	1970	$1\frac{1}{4}$	1/4	1/4
	Kadena, Okinawa	Concrete and asphalt	1970	$1\frac{1}{4}$	1/4	1/4
	Bien Hoa AB, S. Vietnam	Concrete	1967	*2	1/4	1/4
Civil	Washington National	Asphalt	1967	1	1/8	1/8
	Kansas City Municipal Airport	Concrete and asphalt	1967	1	1/8	1/4
	John F. Kennedy Airport, N.Y.C.	Concrete	1967	**$1\frac{3}{8}$	3/8 top 3/16 bottom	1/8
	Kanewha Airport, Charleston, W. Va.	Concrete and asphalt	1968 and 1969	$1\frac{1}{4}$	1/4	1/4
	Midway Airport, Chicago, Ill.	Concrete	1968	$1\frac{1}{4}$	1/4	1/4
	Atlanta, Ga.	Concrete	1969	**$1\frac{1}{4}$	3/8 top 1/8 bottom	1/4
	Nashville, Tenn.	Concrete and asphalt	1969	$1\frac{1}{4}$	1/4	1/4
	Dallas, Texas	Concrete	1969	$1\frac{1}{4}$	1/4	1/4
	O' Hare Airport Chicago, Ill.	Asphalt	1969	$1\frac{1}{4}$	1/4	1/4
	Harry S. Truman Airport, Virgin Islands	Concrete and asphalt	1970	$1\frac{1}{4}$	1/4	1/4
Foreign	Farnborough, England	Asphalt	1961	1	1/8	1/8
	Birmingham, England	Asphalt	1967	1	1/8	1/8
	Manchester, England	Asphalt	1961 and 1965	1	1/8	1/8
	Tempelhof, Germany	Asphalt	1968	$1\frac{1}{2}$	3/8	3/8
	Wellington, New Zealand	Asphalt	1969 and 1970	1	1/8	1/8

*Groove 2 feet; skip 2 feet.
**V-shape groove cross section.

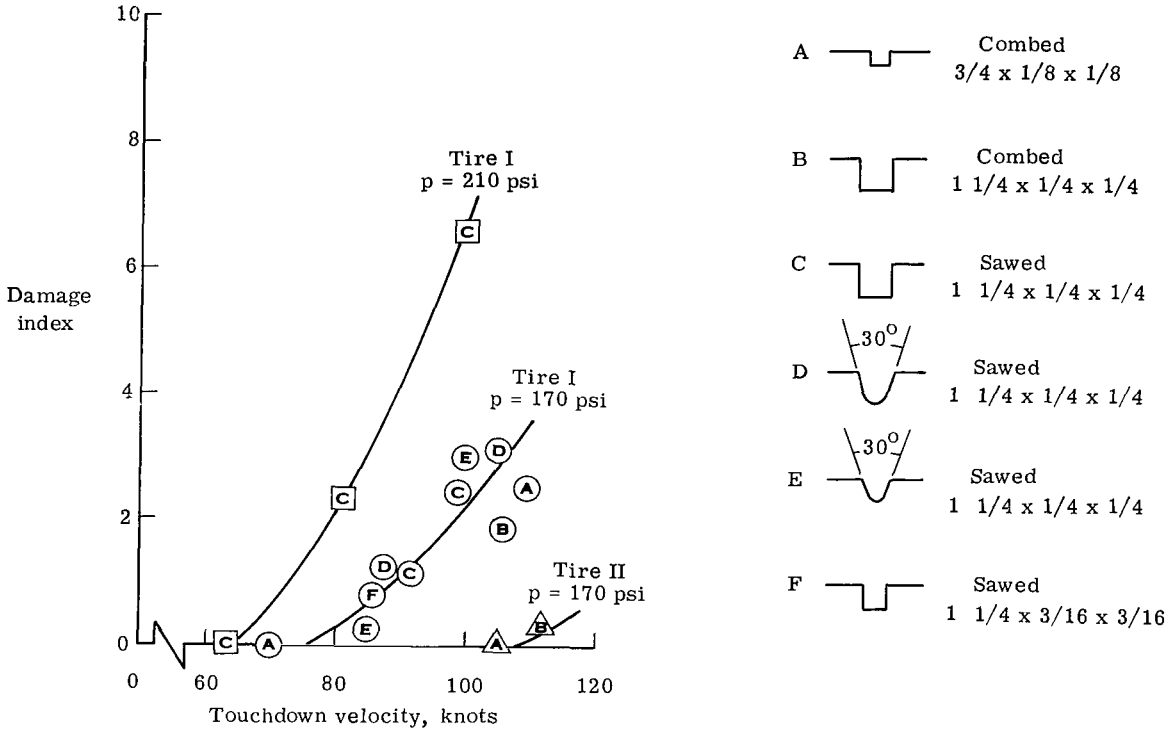

Figure 28.- Tire chevron cutting on grooved surfaces. 49 × 17 tire; vertical velocity, 2.5 ft/sec. Measurements are in inches for runway surfaces unless otherwise noted.

Based on operational experiences, the USAF has noted that Offutt Air Force Base and Beale Air Force Base have experienced chevron cutting on the larger tire sizes due to runway grooves. The groove patterns at these bases are 1/4 inch by 1/4 inch on $1\frac{1}{4}$ inch centers and 1/4 inch by 1/4 inch on 1 inch centers. Limited testing during the Combat Traction tests consisted of two landings on the grooved runway at Wallops Station which resulted in minor tire cuts. More tests were scheduled at Beale Air Force Base but could not be accomplished because the airplane was down for maintenance. From the reports received, the severity of cutting is a function of tread rubber composition, tire size, and the number of consecutive touch-and-go landings made. The cuts are small and shallow and are usually worn off when full stop landings are accomplished. The most severe cuts reported are the result of several consecutive touch-and-go landings.

A problem noted for the porous asphalt friction course surfaces studied in this investigation was from fuel spillage on the runway that occurred during a helicopter mishap. The fuel dissolved the asphaltic binder of the friction course and loosened the aggregate. The section of the runway surface involved in the fuel spillage had to be repaved.

It may be noted that two techniques are available for providing standard low levels of runway slipperiness. Runway grooving has been shown to develop similar results for different runways. For example, the concrete runway at Offutt (runway 15, table I) and the Chicago Midway (runway 14, table I) were grooved to similar patterns and gave remarkably similar results. Also a porous asphalt friction course has been shown to provide similar results for different runways (runways 36 and 38, table I).

CONCLUSIONS AND RECOMMENDATIONS

Full-stop brake tests were made by the C-141A aircraft, the runway condition reading (RCR) vehicle, and the diagonal-braked test vehicle on civil and military runways in the United States and Europe under dry, artifically wet, natural rain, ice, and snow conditions. Included in the European program were tests conducted jointly with the British Ministry of Aviation Supply on Royal Air Force and Royal Navy Bases using a Mu-meter and the Miles engineering skid trailer. Limited brake tests were also conducted on the landing research runway at NASA Wallops Station, Virginia, with the C-141A aircraft. An analysis of the test results indicates the following:

1. Runway condition reading (RCR) now in use by the U.S. Air Force is not an adequate method for predicting aircraft stopping distance on a wet runway, but it can be used to conservatively predict stopping distance on ice- and snow-covered runways.

2. A diagonal-braked vehicle can be used to predict aircraft stopping distance and crosswind limitations for wet, ice-, and snow-covered runways and can be used to measure runway slipperiness.

3. Grooved pavements and porous asphalt surfaces were the most effective surface treatments investigated in alleviating surface flooding and wet runway slipperiness.

4. Aircraft stopping distance generally increases with increasing water depth on the runway.

On the basis of these test results, the following recommendations are made:

1. Engineer, design, and test a diagonal-braked vehicle which will be suitable for Air Force operations use.

2. Continue research and development of runway groove designs and spacing and of tire-tread compounds to alleviate tire cutting and excessive tire wear.

3. Develop a rainfall-precipitation-rate—water-depth measuring system for runways to provide real-time runway condition information and reduce the number of operational measurements needed with the diagonal-braked test vehicle.

4. Gather data (tire wear, pilot comments, ambient temperature variations, rainfall and rainfall rate, snowfall, effect of jet-exhaust impingement and resistance of the asphaltic binders to aircraft fuels) on the existing Air Force porous runways and continue research on porous runways.

5. Test additional aircraft with various landing-gear configurations, tire sizes, and tire groove patterns on full-length dry, wet, flooded, ice-, and snow-covered runways to verify correlation with a diagonal-braked test vehicle.

6. With the replacement of RCR vehicles by diagonal-braked test vehicles, change RCR to stopping distance factor (SDF) by issuance of appropriate supplements to the flight handbooks of military and civil aircraft affected.

7. Measure the slipperiness of each Air Force runway with an instrumented diagonal-braked vehicle to assemble a priority list of runways in need of surface treatment.

Langley Research Center,
National Aeronautics and Space Administration,
Hampton, Va., November 7, 1970.

APPENDIX A

COMPILATION OF TEST DATA

The data compiled and tabulated for each test runway are presented in this appendix in the order of aircraft wet-dry stopping distance ratios as listed in tables I and II. Figure A1 shows the data compiled on each runway. This compilation includes the following data: a photograph and description of the pavement surface condition; texture depth measurements; wind direction and velocity; ambient temperature; aircraft heading and gross weight; aircraft and diagonal-braked test vehicle stopping distances and ratios; RCR data; and curves showing the variation of aircraft stopping distance and braking friction coefficient with ground speed. These curves, based on the recorded aircraft deceleration levels, were obtained from the computational procedure described in appendix B. If available, core sample analysis data and photographs are also included for the test runways. Test data are not presented for runways 17 (Mildenhall Air Force Base) and 39 (Meigs Airport) as the aircraft was not tested. Data for runway 49 are included with those of runway 41 (Malmstrom Air Force Base). Note that for runway 15, data are included for two different aircraft gross weight conditions.

DYESS AFB, TEXAS			RUNWAY 16/34			DATE 9-24 & 25-69		STOPPING DISTANCE, FT			STOPPING DISTANCE RATIO			RCR
R/W REF. NO.	PAVEMENT SURFACE			WIND		TEMP., °F / ALT. SET., in. Hg	AIRCRAFT	AIRCRAFT		TEST VEHICLE	AIRCRAFT		TEST VEHICLE	
	MATERIAL	TEXTURE DEPTH, mm	CONDITION (WATER DEPTH), in.	DIR.	VEL., knots		HEADING	GROSS WEIGHT, lb	REVOLUTION COUNTER	ACCELERATION-TIME	REVOLUTION COUNTER	REVOLUTION COUNTER	ACCELERATION-TIME	REVOLUTION COUNTER	
1	CONCRETE	0.127	DRY	—	0	58 / 30.03	340	200,300	1019	1150	276	2.89	2.65	2.70	23
			WET (.05)	140	4	60 / 29.88	340	193,400	2943	3040	746				18

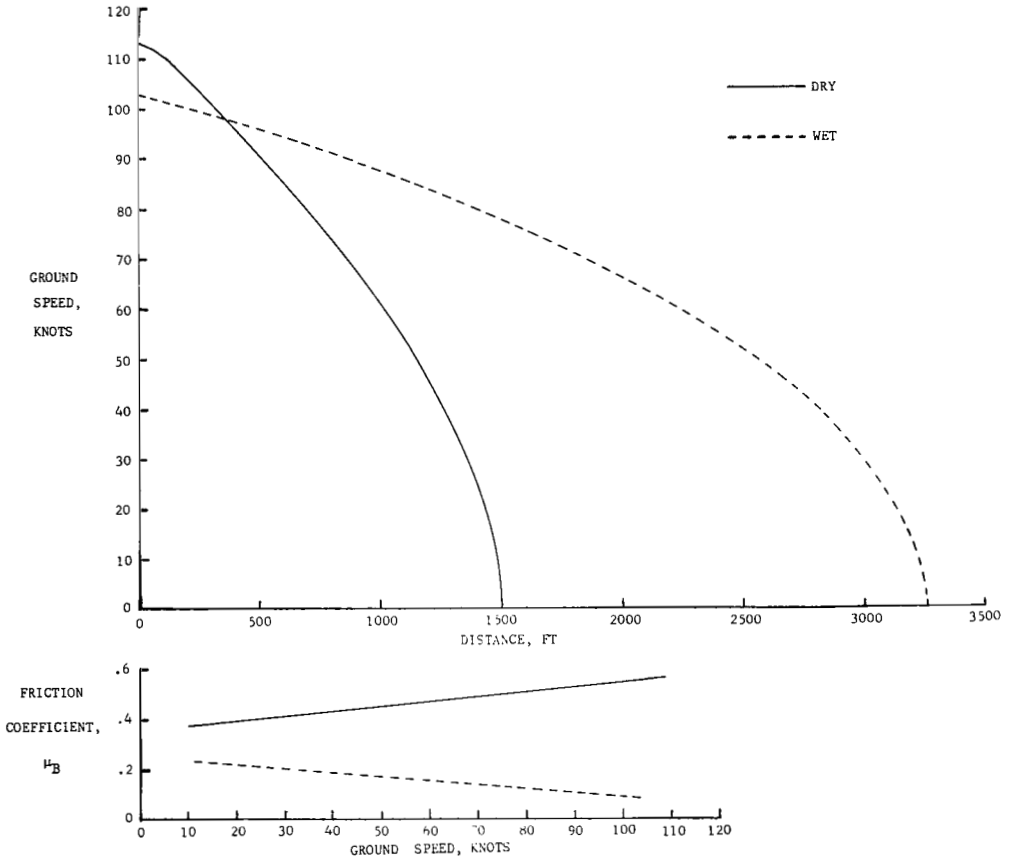

(a) Runway 1; Dyess Air Force Base.

Figure A1.- Runway and vehicle data for runways tested.

DYESS AFB, TEXAS RUNWAY: 16/34 DATE 9-24 & 25-69

SUMMARY OF PAVEMENT TRACTION FACTORS BASED ON CORE SAMPLE ANALYSIS

PAVEMENT TYPE	PREDOMINANT CHARACTERISTICS	FACTORS	CLASSIFICATION FOR WET OPERATION
Portland Cement Concrete Burlap-Drag Finish	Poor surface drainage. Exposed particles of fine sand. Rubber coatings. Fine grained texture.	The surface texture characteristics of the sample of portland cement concrete from Dyess AFB are described as follows: (1) A burlap-drag finish on a fine grained sand-mortar surface. (2) Very little surface texture resulting from exposed particles of sand. Fine texture with some rubber coating. (3) The surface configurations resulting from the burlap-drag finish offer very little surface drainage from the wheel track. The structural characteristics reflected at a depth of 1-1/2 in. below the surface are as follows: (1) The coarse aggregate skeleton consists of a mixture of rounded particles of quartz gravel and fragments of calcareous material. Maximum particle diameter is about 2-1/2 in. (2) The dense graded mix offers no subsurface drainage.	Medium-Poor

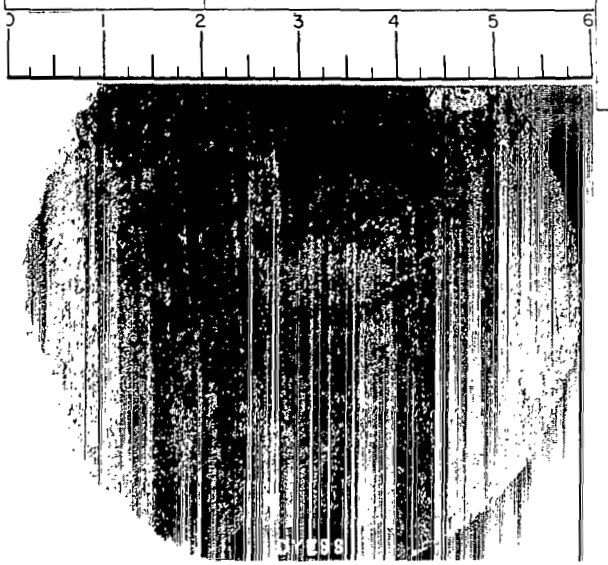

CORE SAMPLE SURFACE

CORE SAMPLE SURFACE PROFILE

(a) Concluded.

Figure A1.- Continued.

ENGLAND AFB, LOUISIANA				RUNWAY 14/32				DATE 10-13-69		STOPPING DISTANCE, FT			STOPPING DISTANCE RATIO			RCR
R/W REF. NO.	PAVEMENT SURFACE			WIND		TEMP., °F	ALT. SET., in. Hg	AIRCRAFT		AIRCRAFT		TEST VEHICLE	AIRCRAFT		TEST VEHICLE	
	MATERIAL	TEXTURE DEPTH, mm	CONDITION (WATER DEPTH), in.	DIR.	VEL., knots			HEADING	GROSS WEIGHT, lb	REVOLUTION COUNTER	ACCELERATION-TIME	REVOLUTION COUNTER	REVOLUTION COUNTER	ACCELERATION-TIME	REVOLUTION COUNTER	
2	CONCRETE	0.166	DRY AND DAMP	290	6	63	29.98	320	200,400	978	1080	277	2.46*	2.49*	2.16	22
			WET (.05)	310	5	63	29.99	320	193,800	2705	2740	598				15

*Based on S_{DRY} = 1100 ft

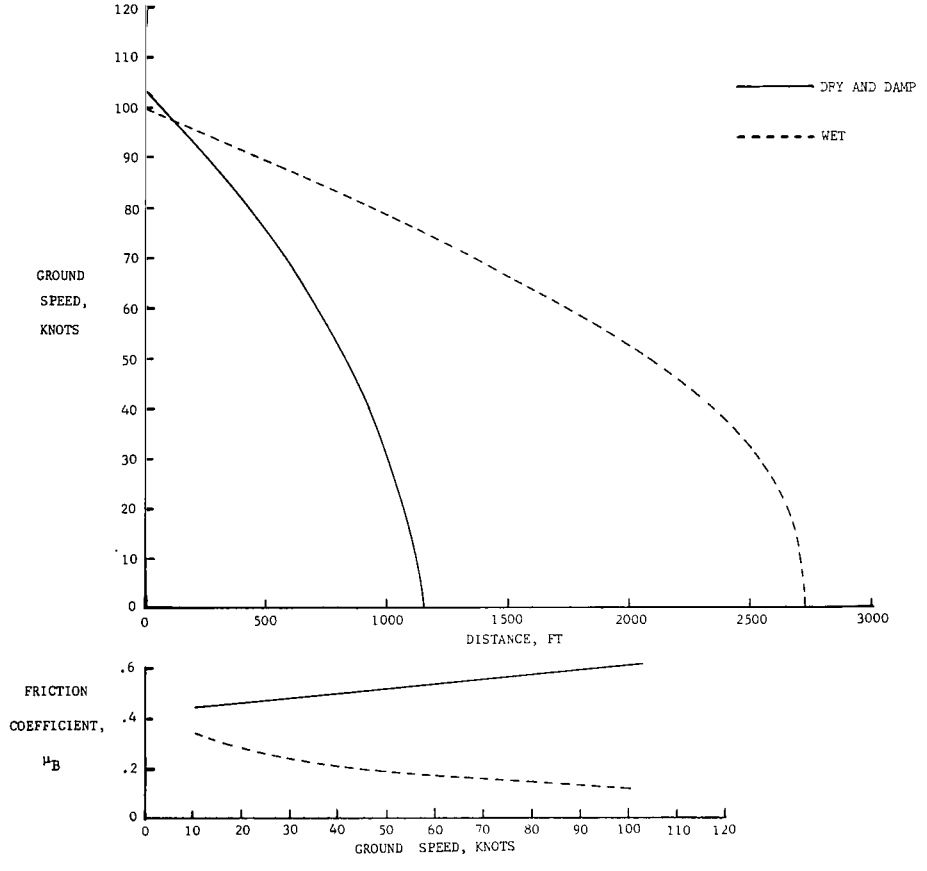

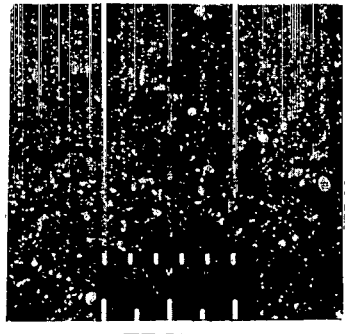

TEST SURFACE

(b) Runway 2; England Air Force Base.

Figure A1.- Continued.

ENGLAND AFB, LOUISIANA RUNWAY: 14/32 DATE: 10-13-69

SUMMARY OF PAVEMENT TRACTION FACTORS BASED ON CORE SAMPLE ANALYSIS

PAVEMENT TYPE	PREDOMINANT CHARACTERISTICS	FACTORS	CLASSIFICATION FOR WET OPERATION
Portland Cement Concrete	Poor surface drainage. Exposed particles of fine sand and some cavitation resulting from dislodgement of particles. Fine grained texture.	The surface texture characteristics of the portland cement concrete from England AFB are described as follows: (1) The fine grained surface texture is defined by exposed particles of sand and mortar cavitation resulting from particle dislodgement. (2) The surface texture affords little surface drainage. The structure characteristics reflected at a depth of 1-1/2 in. below the surface are as follows: (1) The coarse aggregate skeleton consists of rounded particles of quartz gravel well graded between 1/4 and 1 in. in diameter. (2) The dense particles and matrix offer no subsurface drainage.	Medium-Poor

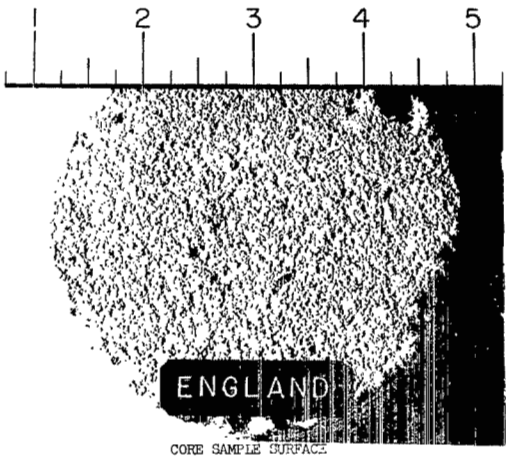

CORE SAMPLE SURFACE


CORE SAMPLE SURFACE PROFILE

(b) Concluded.

Figure A1.- Continued.

MARHAM RAFB, ENGLAND				RUNWAY 2/20			DATE 7-22-69		STOPPING DISTANCE, FT			STOPPING DISTANCE RATIO			RCR
R/W REF. NO.	PAVEMENT SURFACE			WIND		TEMP., °F	ALT. SET., in. Hg	AIRCRAFT		AIRCRAFT		TEST VEHICLE	AIRCRAFT		TEST VEHICLE	
	MATERIAL	TEXTURE DEPTH, mm	CONDITION (WATER DEPTH), in.	DIR.	VEL., knots			HEADING	GROSS WEIGHT, lb	REVOLUTION COUNTER	ACCELERATION-TIME	REVOLUTION COUNTER	REVOLUTION COUNTER	ACCELERATION-TIME	REVOLUTION COUNTER	
3	CONCRETE	0.217	DRY	230	5	61	30.04	200	189,400	1030	1110	363	2.29	2.20	1.93	23
			WET (.04) / WET (.05)	240 / 220	7 / 5	61 / 62	30.04 / 30.05	200	184,400 / 178,800	2360	2440	702				23

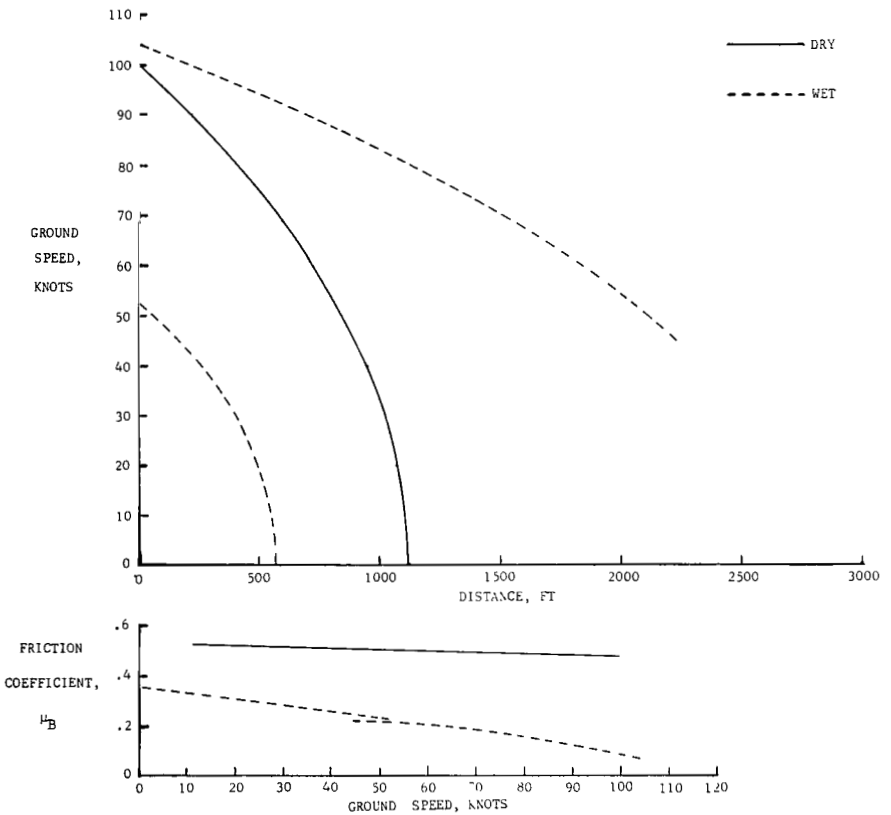

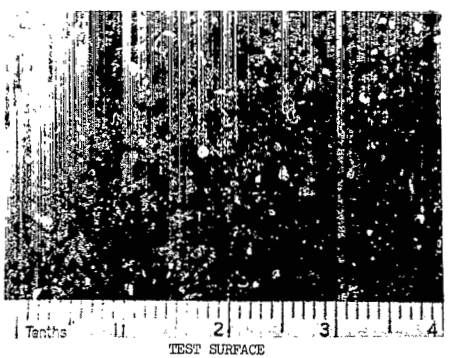

(c) Runway 3; Marham Royal Air Force Base.

Figure A1.- Continued.

OFFUTT AFB, NEBRASKA				RUNWAY 12/30			DATE 9-10-69		STOPPING DISTANCE, FT			STOPPING DISTANCE RATIO			RCR
R/W REF. NO.	PAVEMENT SURFACE			WIND		TEMP., °F	ALT. SET., in. Hg	AIRCRAFT	AIRCRAFT		TEST VEHICLE	AIRCRAFT		TEST VEHICLE	
	MATERIAL	TEXTURE DEPTH, mm	CONDITION (WATER DEPTH), in.	DIR.	VEL., knots			HEADING	GROSS WEIGHT, lb	REVOLUTION COUNTER	ACCELERATION-TIME	REVOLUTION COUNTER	REVOLUTION COUNTER	ACCELERATION-TIME	REVOLUTION COUNTER	
4	UNGROOVED CONCRETE	0.154	DRY	050	1	54	30.18	300	194,300	974	1000	280	2.28	2.36	2.15	26
			WET (.04)	085	1	56	30.18	300	189,500	2220	2360	601				21

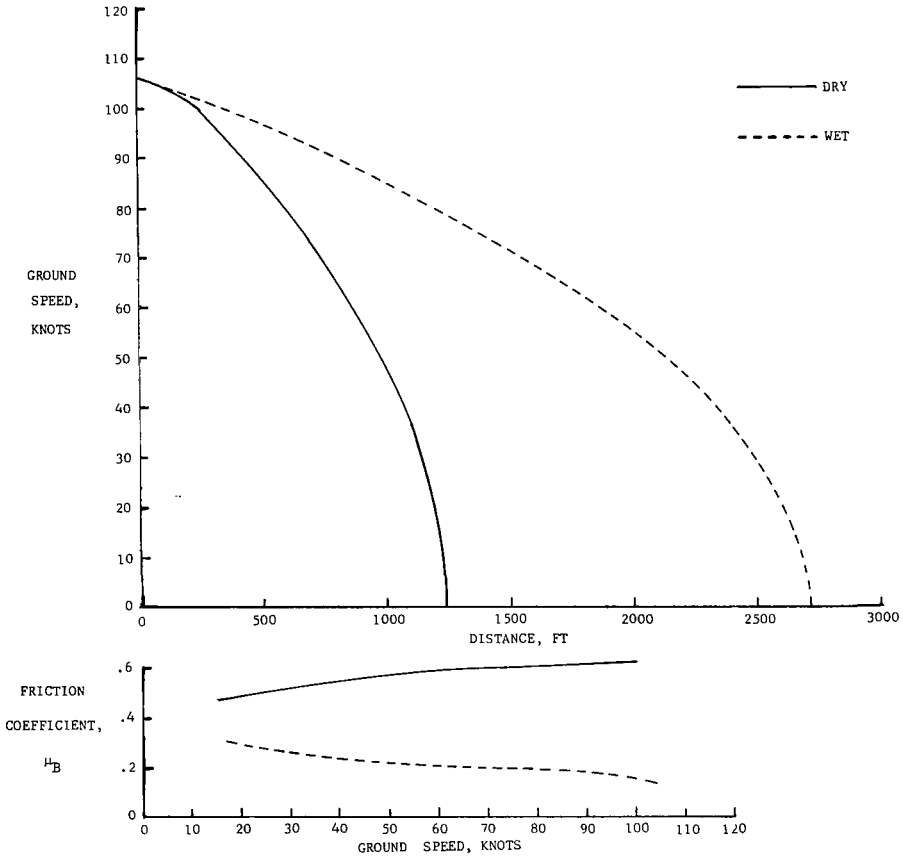

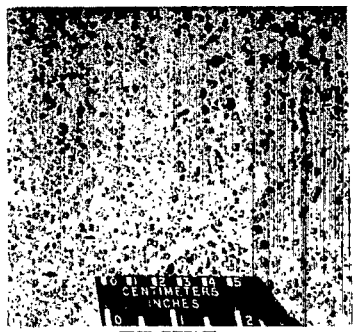

TEST SURFACE

(d) Runway 4; Offutt Air Force Base.

Figure A1.- Continued.

OFFUTT AFB, NEBRASKA RUNWAY: 12/30 DATE: 9-10-69

SUMMARY OF PAVEMENT TRACTION FACTORS BASED ON CORE SAMPLE ANALYSIS

PAVEMENT TYPE	PREDOMINANT CHARACTERISTICS	FACTORS	CLASSIFICATION FOR WET OPERATION
Portland Cement Concrete	Medium surface drainage. Exposed particles of rounded aggregate. Medium grained surface texture.	The surface texture characteristics of the sample of portland cement concrete from Offutt AFB are described as follows: (1) The medium grained surface texture is defined by exposed particles of fine gravel (approximately 1/8 to 3/8 in.). The exposed particles are, in general, rounded and polished. (2) The interparticle depressions afford a limited amount of surface drainage. The structural characteristics reflected at a depth of 1-1/2 in. below the surface are as follows: (1) The aggregate skeleton consists of a mixture of fine gravel and fragments of calcareous rock (approximately 15 percent calcareous). (2) The dense graded pavement offers no subsurface drainage even though there is evidence of air voids (bubbles) in the matrix.	Medium-Poor

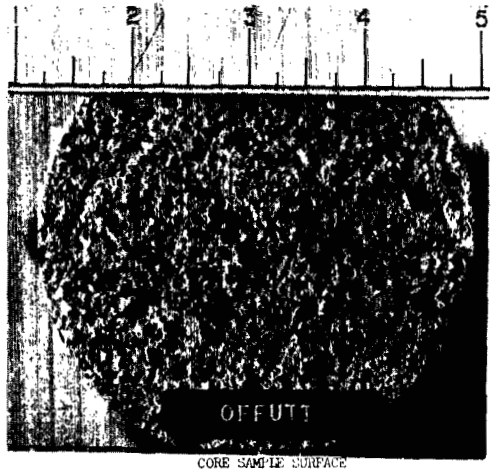

CORE SAMPLE SURFACE

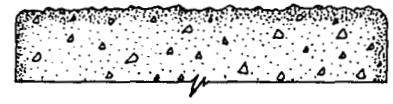
CORE SAMPLE SURFACE PROFILE

(d) Concluded.

Figure A1.- Continued.

ELLINGTON AFB, TEXAS RUNWAY 4/22								DATE 2-6-70		STOPPING DISTANCE, FT		STOPPING DISTANCE RATIO			RCR
R/W REF. NO.	PAVEMENT SURFACE			WIND		TEMP., °F	ALT. SET., in. Hg	AIRCRAFT		AIRCRAFT		TEST VEHICLE	AIRCRAFT		TEST VEHICLE	
	MATERIAL	TEXTURE DEPTH, mm	CONDITION (WATER DEPTH), in.	DIR.	VEL., knots			HEADING	GROSS WEIGHT, lb	REVOLUTION COUNTER	ACCELERATION-TIME	REVOLUTION COUNTER	REVOLUTION COUNTER	ACCELERATION-TIME	REVOLUTION COUNTER	
5	CONCRETE	———	DAMP	090	11	57	30.23	040	198,800	2320	2460	626	2.11*	2.24*	2.16*	11

*Based on S_{DRY} of 1100 ft for aircraft and 291 ft for test vehicle

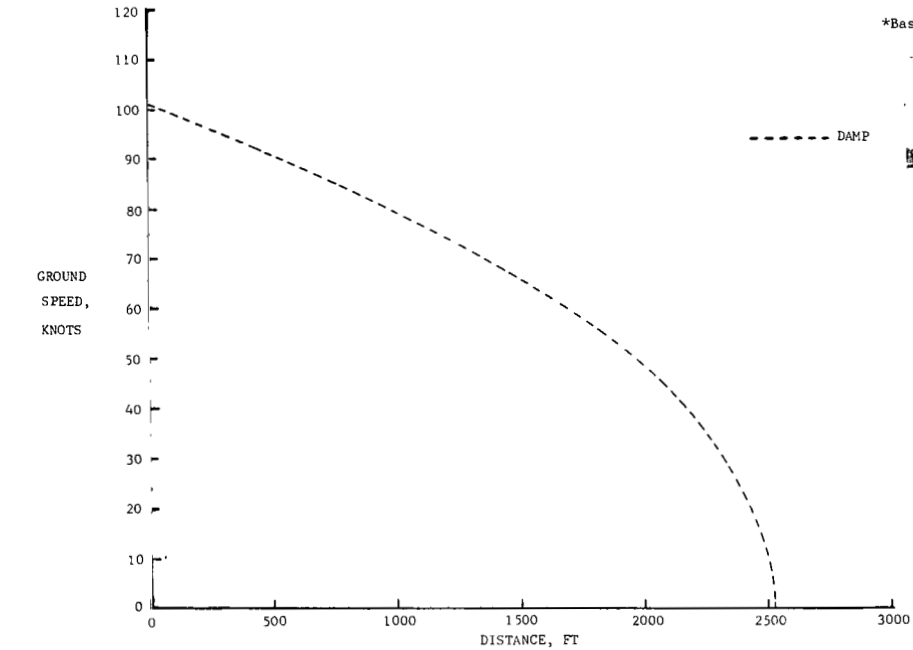

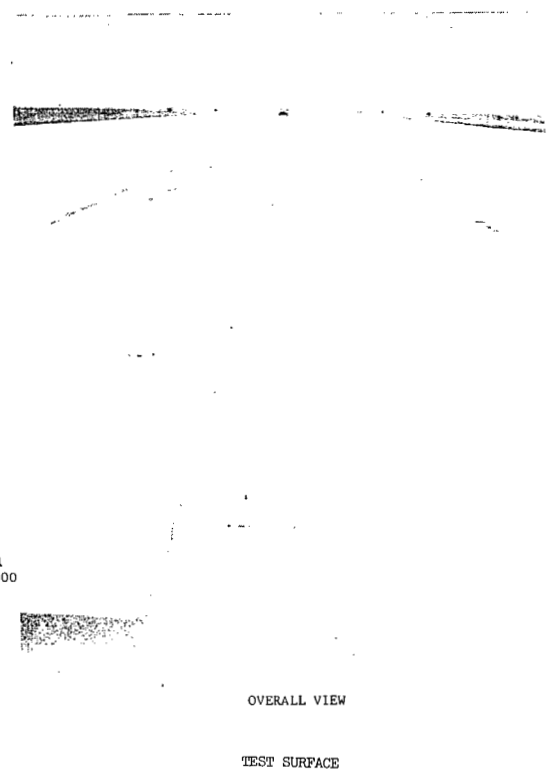

(e) Runway 5; Ellington Air Force Base.

Figure A1.- Continued.

EDWARDS AFB, CALIFORNIA				RUNWAY 4/22				DATE 9-20-69		STOPPING DISTANCE, FT			STOPPING DISTANCE RATIO			RCR
R/W REF. NO.	PAVEMENT SURFACE			WIND		TEMP., °F	ALT. SET., in. Hg	AIRCRAFT		AIRCRAFT		TEST VEHICLE	AIRCRAFT		TEST VEHICLE	
	MATERIAL	TEXTURE DEPTH, mm	CONDITION (WATER DEPTH), in.	DIR.	VEL., knots			HEADING	GROSS WEIGHT, lb	REVOLUTION COUNTER	ACCELERATION-TIME	REVOLUTION COUNTER	REVOLUTION COUNTER	ACCELERATION-TIME	REVOLUTION COUNTER	
6	CONCRETE	0.119	DRY	200	20	58	29.84	220	196,500	1038	1070	269	2.04	2.26	1.91	22
			WET (.03)	210	13	58	29.84	220	191,700	2120	2420	512				18

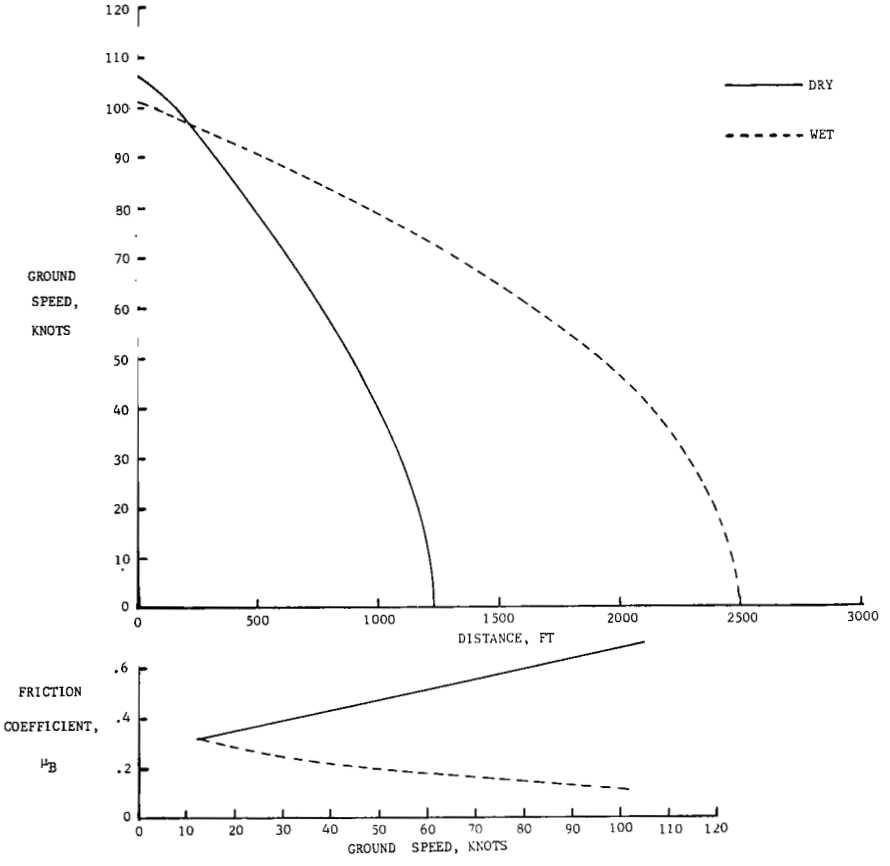

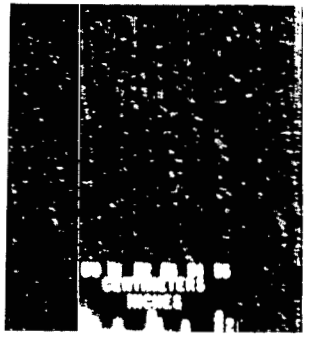

TEST SURFACE

(f) Runway 6; Edwards Air Force Base.

Figure A1.- Continued.

WRIGHT-PATTERSON AFB, OHIO				RUNWAY 5L/23R		DATE 10-3-69				STOPPING DISTANCE, FT			STOPPING DISTANCE RATIO			RCR
R/W REF. NO.	PAVEMENT SURFACE			WIND		TEMP., °F	ALT. SET., in. Hg	AIRCRAFT		AIRCRAFT		TEST VEHICLE	AIRCRAFT		TEST VEHICLE	
	MATERIAL	TEXTURE DEPTH, mm	CONDITION (WATER DEPTH), in.	DIR.	VEL., knots			HEADING	GROSS WEIGHT, lb	REVOLUTION COUNTER	ACCELERATION-TIME	REVOLUTION COUNTER	REVOLUTION COUNTER	ACCELERATION-TIME	REVOLUTION COUNTER	
7	CONCRETE	0.185	DRY	—	0	56	30.05	050	194,600	989	1090	288	2.07	2.17	1.95	26
			WET (.05)	120	1	56	30.05	050	190,500	2045	2360	564				24

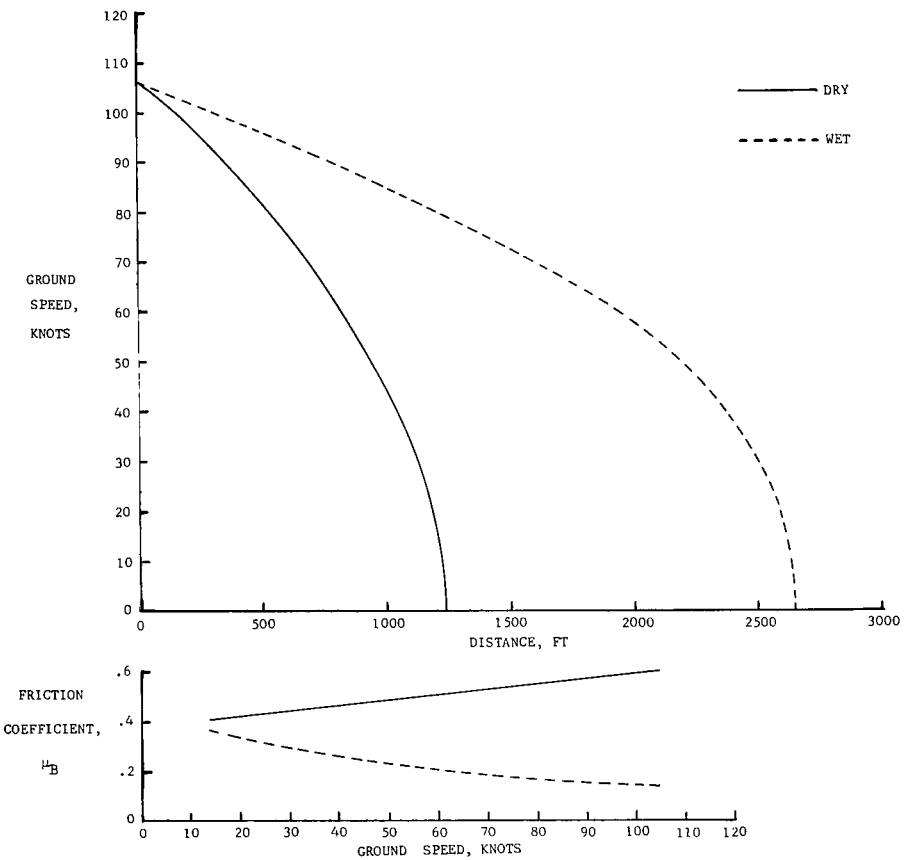

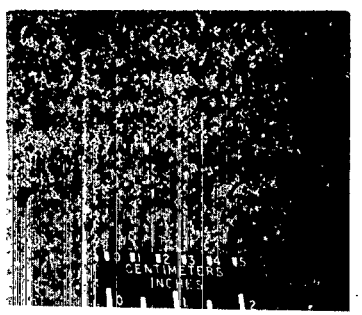

TEST SURFACE

(g) Runway 7; Wright-Patterson Air Force Base.

Figure A1.- Continued.

LOCKBOURNE AFB, OHIO				RUNWAY 5R/23L		DATE 9-30-69			STOPPING DISTANCE, FT			STOPPING DISTANCE RATIO			RCR
R/W REF. NO.	PAVEMENT SURFACE			WIND		TEMP., °F	ALT. SET., in. Hg	AIRCRAFT	AIRCRAFT		TEST VEHICLE	AIRCRAFT		TEST VEHICLE	
	MATERIAL	TEXTURE DEPTH, mm	CONDITION (WATER DEPTH), in.	DIR.	VEL., knots			HEADING	GROSS WEIGHT, lb	REVOLUTION COUNTER	ACCELERATION-TIME	REVOLUTION COUNTER	REVOLUTION COUNTER	ACCELERATION-TIME	REVOLUTION COUNTER	
8	CONCRETE	0.165	DRY	220	3.5	52	30.03	230	202,800	1072	1140	267	2.04	2.07	1.84	23
			WET (.03)	210	3	52	30.03	230	196,800	2183	2340	491				22.5

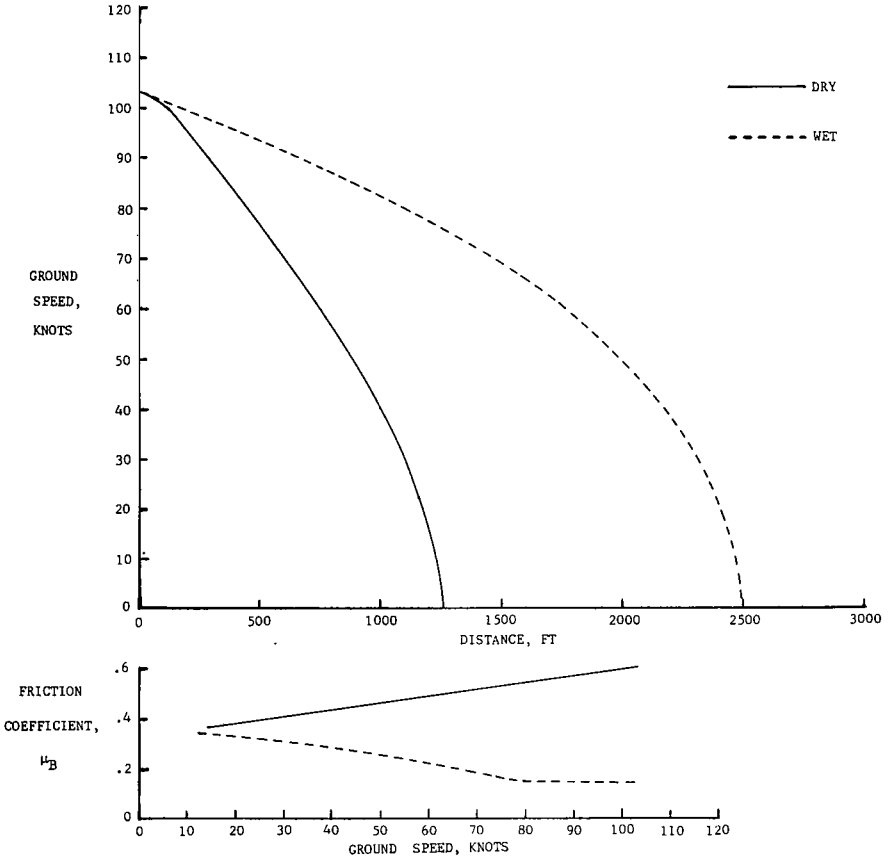

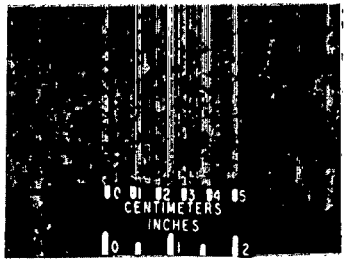

TEST SURFACE

(h) Runway 8; Lockbourne Air Force Base.

Figure A1.- Continued.

LOCKBOURNE AFB, OHIO RUNWAY: 5R/23L DATE: 9-30-69

SUMMARY OF PAVEMENT TRACTION FACTORS BASED ON CORE SAMPLE ANALYSIS

PAVEMENT TYPE	PREDOMINANT CHARACTERISTICS	FACTORS	CLASSIFICATION FOR WET OPERATION
Portland Cement Concrete	Medium to poor surface drainage. Exposed particles of rounded aggregate. Medium grained surface texture.	The surface texture characteristics of the sample of portland cement concrete from Lockbourne AFB are described as follows: (1) The medium grained surface texture is defined by exposed particles of fine aggregate (less than 1/4 in.). The majority of the particles have rounded and/or polished faces exposed. (2) The surface configurations afford little or no surface drainage. The structural characteristics reflected at a depth of 1-1/2 in. below the surface are as follows: (1) The coarse aggregate skeleton consists of a mixture of quartz gravel, igneous rocks, and rounded particles of calcareous rocks (approximately 90 percent calcareous). Maximum diameter is 1-1/2 in. (2) No subsurface drainage resulting from porosity in the aggregate or the matrix.	Medium-Poor

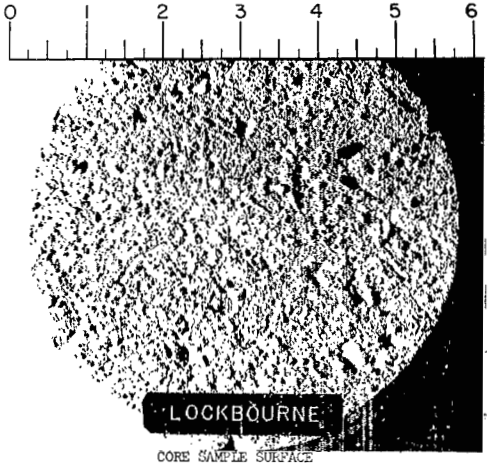

CORE SAMPLE SURFACE

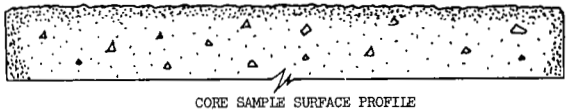

CORE SAMPLE SURFACE PROFILE

(h) Concluded.

Figure A1.- Continued.

LANGLEY AFB, VIRGINIA			RUNWAY 7/25				DATE 1-28-70 & 7-8-69		STOPPING DISTANCE, FT			STOPPING DISTANCE RATIO			RCR
R/W REF. NO.	PAVEMENT SURFACE			WIND		TEMP., °F	ALT. SET., in. Hg	AIRCRAFT	AIRCRAFT		TEST VEHICLE	AIRCRAFT		TEST VEHICLE	
	MATERIAL	TEXTURE DEPTH, mm	CONDITION (WATER DEPTH), in.	DIR.	VEL., knots			HEADING	GROSS WEIGHT, lb	REVOLUTION COUNTER	ACCELERATION-TIME	REVOLUTION COUNTER	REVOLUTION COUNTER	ACCELERATION-TIME	REVOLUTION COUNTER	
9	CONCRETE	0.103	DRY	120	8	48	30.26	070	187,000	1282	1350	310	1.81*	2.00*	1.95*	——
			WET (.05)	350	6	75	30.02	070	178,000	1983	2200	619				17

*Based on S_{DRY} of 1100 ft for aircraft and 317 ft for test vehicle

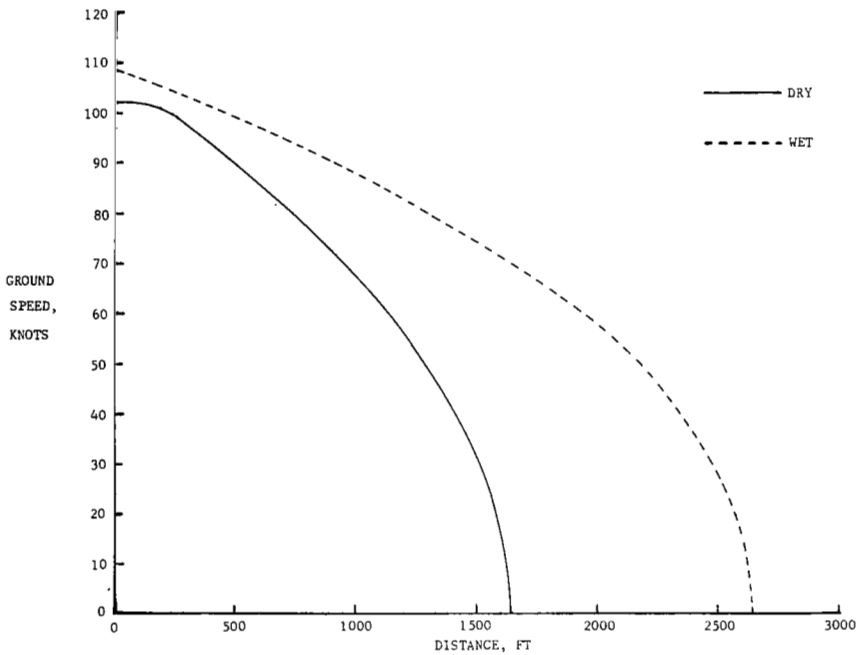

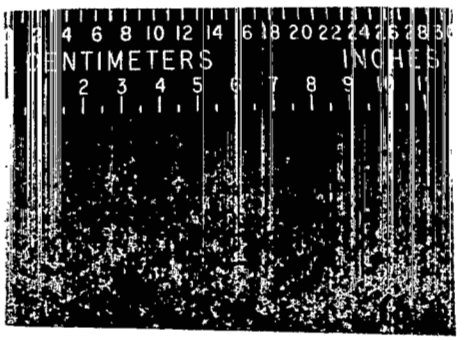

TEST SURFACE

(i) Runway 9; Langley Air Force Base.

Figure A1.- Continued.

LANGLEY AFB, VIRGINIA RUNWAY: 7/25 DATE: 7-8-69 & 1-28-70

SUMMARY OF PAVEMENT TRACTION FACTORS BASED ON CORE SAMPLE ANALYSIS

PAVEMENT TYPE	PREDOMINANT CHARACTERISTICS	FACTORS	CLASSIFICATION FOR WET OPERATION
Portland Cement Concrete	Medium surface drainage. Exposed particles of sharp and rounded aggregate. Medium grained texture.	The surface texture characteristics of the portland cement concrete from Langley AFB are described as follows: (1) The medium grained surface texture is defined by exposed particles of fine aggregate (less than 1/8 in.). The exposed particles reflect rounded as well as fractured faces. (2) The interparticle depressions provide some surface drainage. The surface characteristics reflected at a depth of 1-1/2 in. below the surface are as follows: (1) The coarse aggregate skeleton consists of quartz gravel and fragments of igneous rock. Maximum diameter is 2-1/2 in. (2) No subsurface drainage is reflected in the dense particles or the matrix.	Medium

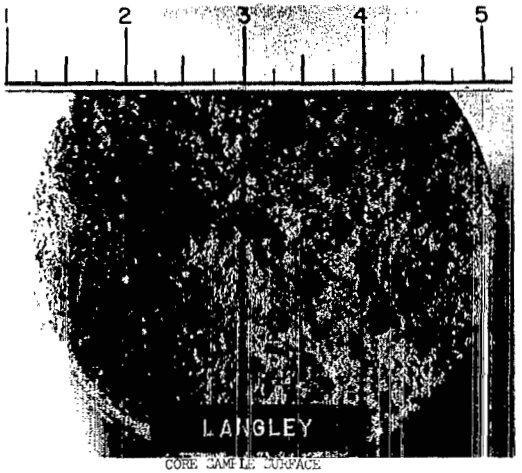

CORE SAMPLE SURFACE

CORE SAMPLE SURFACE PROFILE

(i) Concluded.

Figure A1.- Continued.

YEOVILTON RNB, ENGLAND				RUNWAY 9/27				DATE 7-19-69		STOPPING DISTANCE, FT			STOPPING DISTANCE RATIO			RCR
R/W REF. NO.	PAVEMENT SURFACE			WIND		TEMP., °F	ALT. SET., in. Hg	AIRCRAFT		AIRCRAFT		TEST VEHICLE	AIRCRAFT		TEST VEHICLE	
	MATERIAL	TEXTURE DEPTH, mm	CONDITION (WATER DEPTH), in.	DIR.	VEL., knots			HEADING	GROSS WEIGHT, lb	REVOLUTION COUNTER	ACCELERATION-TIME	REVOLUTION COUNTER	REVOLUTION COUNTER	ACCELERATION-TIME	REVOLUTION COUNTER	
10	WIRE COMBED CONCRETE	0.305	DRY	240	4	64	30.16	090	180,000	1023	1060	312	1.87	1.70	1.65	22
			WET (.02) / DAMP	230 / 230	5 / 6	64 / 64	30.16 / 30.16	090 / 270	175,500 / 172,400	1914	1800	513				23

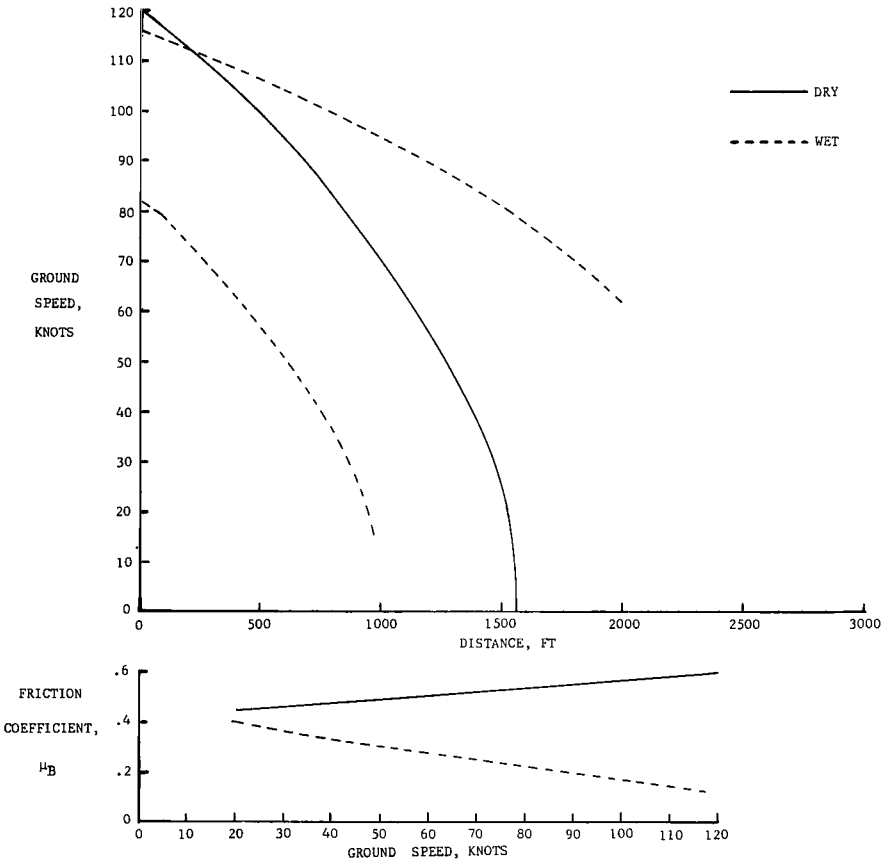

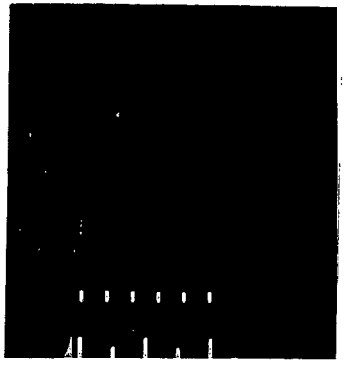

TEST SURFACE

(j) Runway 10; Yeovilton Royal Naval Base.

Figure A1.- Continued.

YEOVILTON RNB, ENGLAND				RUNWAY 9/27				DATE 7-19-69		STOPPING DISTANCE, FT			STOPPING DISTANCE RATIO			RCR
R/W REF. NO.	PAVEMENT SURFACE			WIND		TEMP., °F	ALT. SET., in. Hg	AIRCRAFT		AIRCRAFT		TEST VEHICLE	AIRCRAFT		TEST VEHICLE	
	MATERIAL	TEXTURE DEPTH, mm	CONDITION (WATER DEPTH), in.	DIR.	VEL., knots			HEADING	GROSS WEIGHT, lb	REVOLUTION COUNTER	ACCELERATION-TIME	REVOLUTION COUNTER	REVOLUTION COUNTER	ACCELERATION-TIME	REVOLUTION COUNTER	
11	SCORED CONCRETE	0.394	DRY	240	5	62	30.16	270	191,400	950	1030	312	1.59	1:71	1.76	23
			WET (.04)	220	6	64	30.16	270	186,300	1513	1760	548				20

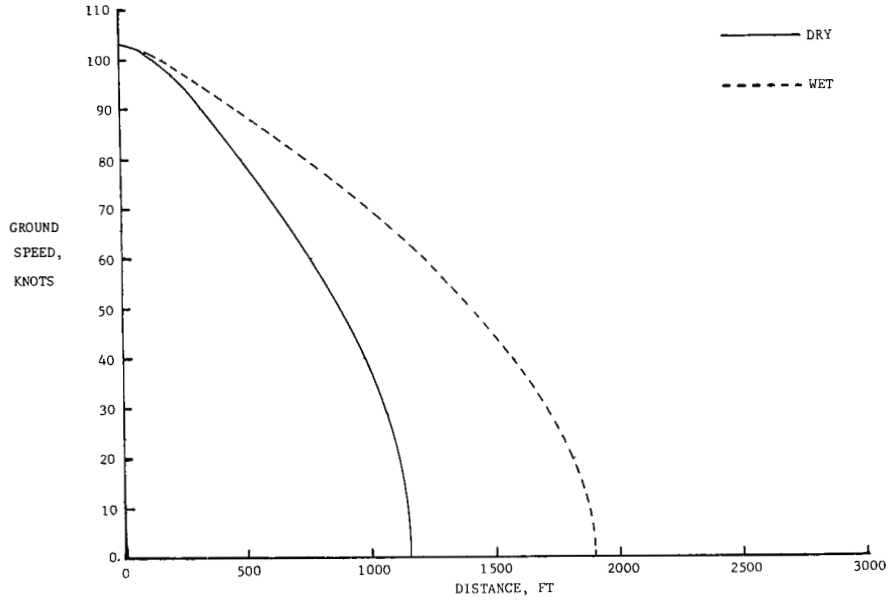

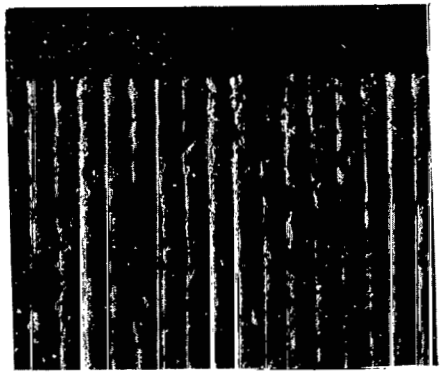

TEST SURFACE

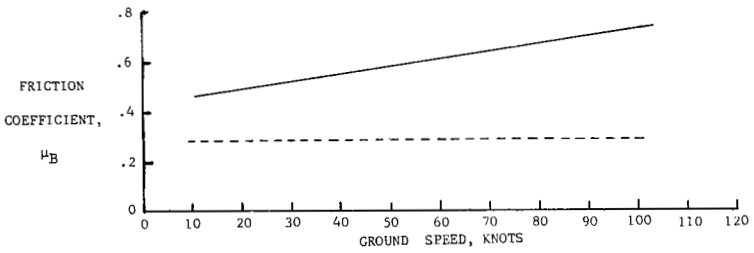

(k) Runway 11; Yeovilton Royal Naval Base.

Figure A1.- Continued.

JOHN F. KENNEDY AIRPORT, NEW YORK			RUNWAY 4R/22L			Date 7-10-69			STOPPING DISTANCE, FT			STOPPING DISTANCE RATIO			RCR
R/W REF. NO.	PAVEMENT SURFACE			WIND		TEMP., °F	ALT. SET., in. Hg	AIRCRAFT			AIRCRAFT		TEST VEHICLE	AIRCRAFT		TEST VEHICLE	
	MATERIAL	TEXTURE DEPTH, mm	CONDITION (WATER DEPTH), in.	DIR.	VEL., knots			HEADING	GROSS WEIGHT, lb	REVOLUTION COUNTER	ACCELERATION-TIME	REVOLUTION COUNTER	REVOLUTION COUNTER	ACCELERATION-TIME	REVOLUTION COUNTER	
12	GROOVED CONCRETE	——	DRY	200	3	70	30.09	220	188,400	——	1010	304	——	1.76	1.75	——
			WET (.03)	200	4	70	30.09	220	182,300	1606	1780	532				——
	RUBBER		WET (.04)	180	4	71	30.10	220	175,600	1882	2000	668	——	1.98	2.20	——

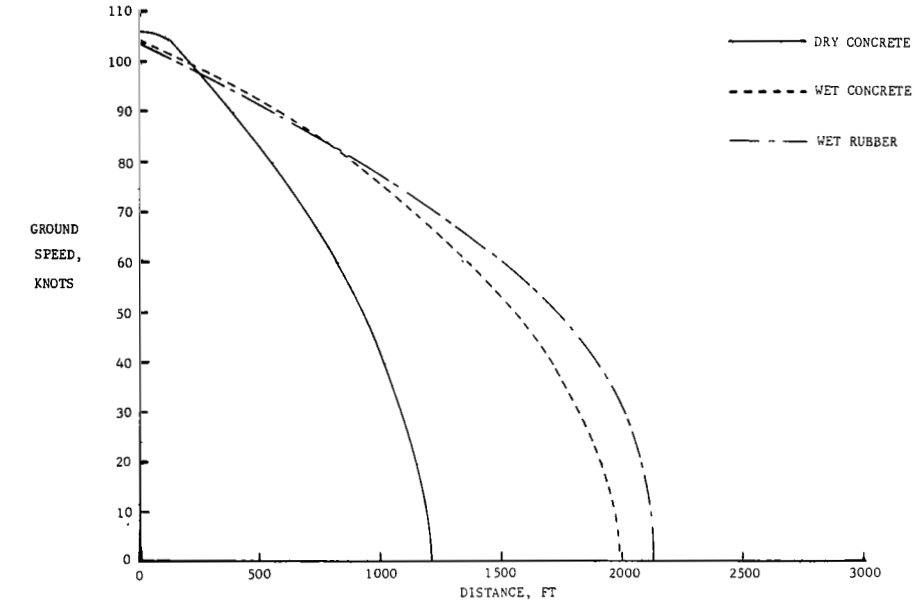

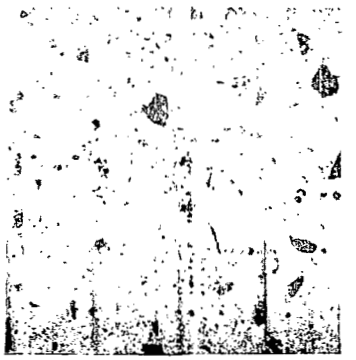

CLEAN

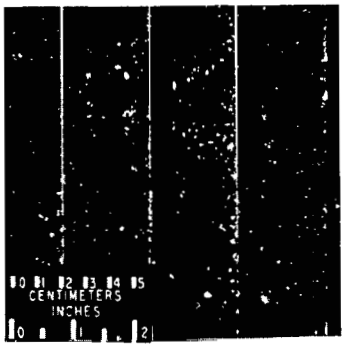

TOUCHDOWN AREA-RUBBER COATED

TEST SURFACE

(l) Runway 12; John F. Kennedy Airport.

Figure A1.- Continued.

SEYMOUR JOHNSON AFB, NORTH CAROLINA			RUNWAY 8/26			DATE 7-9-69		STOPPING DISTANCE, FT			STOPPING DISTANCE RATIO			RCR
	PAVEMENT SURFACE			WIND		TEMP.,	ALT.	AIRCRAFT			AIRCRAFT			
R/W REF. NO.	MATERIAL	TEXTURE DEPTH, mm	CONDITION (WATER DEPTH), in.	DIR.	VEL., knots	°F	SET., in. Hg	HEADING	GROSS WEIGHT, lb	REVOLUTION COUNTER	ACCELERATION-TIME	TEST VEHICLE REVOLUTION COUNTER	REVOLUTION COUNTER	ACCELERATION-TIME	TEST VEHICLE REVOLUTION COUNTER	
13	GROOVED CONCRETE	0.102	DRY	020	6	70	30.08	080	195,400	990	1050	331	1.33	1.43	1.35	20
			WET (.02)	020	6	70	30.08	080	184,600	1321	1510	447				17
	RUBBER		WET (.02)	040	6	70	30.09	080	179,400	1388	1620	498	1.40	1.54	1.50	16

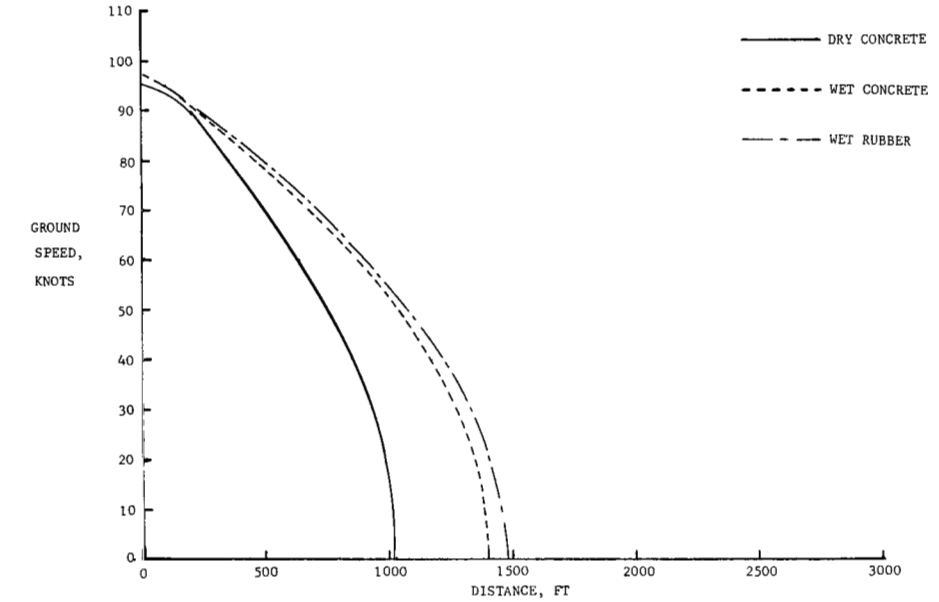

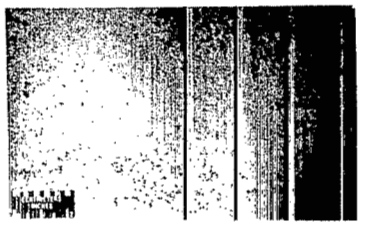

CLEAN

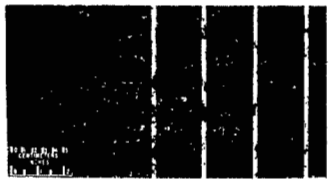

TOUCHDOWN AREA-RUBBER COATED

TEST SURFACE

(m) Runway 13; Seymour Johnson Air Force Base.

Figure A1.- Continued.

S OUR JOHNSON AFB, NORTH CAROLINA RUNWAY: 8/26 DATE: 7-9-69

SUMMARY OF PAVEMENT TRACTION FACTORS BASED ON CORE SAMPLE ANALYSIS

PAVEMENT TYPE	PREDOMINANT CHARACTERISTICS	FACTORS	CLASSIFICATION FOR WET OPERATION
Grooved Portland Cement Concrete	Good surface drainage. Grooves combined with exposed particles of sharp aggregate. Coarse to fine grained surface texture.	The surface texture characteristics reflected in the sample of grooved portland cement concrete from Seymour Johnson AFB are described as follows: (1) Sawed grooves, 1/4 x 1/4 in. spaced 2 in. apart. (2) The surface texture is defined by the grooves and exposed particles of sharp sand and fine aggregate. (3) The combination of grooves and the fine grained surface texture provide a high level of surface drainage. The structural characteristics at a depth of 1-1/2 in. below the surface are described as follows: (1) The coarse aggregate skeleton consists of fragmented particles of quartz and quartz gravel. (2) There is no subsurface drainage capability in the aggregate particles or the matrix.	Good

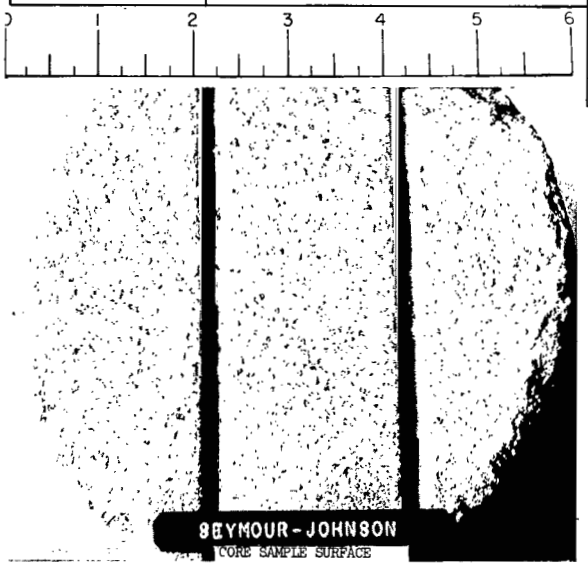

CORE SAMPLE SURFACE PROFILE

(m) Concluded.

Figure A1.- Continued.

CHICAGO MIDWAY AIRPORT, ILLINOIS				RUNWAY 13R/31L			DATE 9-9-69		STOPPING DISTANCE, FT			STOPPING DISTANCE RATIO			RCR
R/W REF. NO.	PAVEMENT SURFACE			WIND		TEMP., °F	ALT. SET., in. Hg	AIRCRAFT	AIRCRAFT		TEST VEHICLE	AIRCRAFT		TEST VEHICLE	
	MATERIAL	TEXTURE DEPTH, mm	CONDITION (WATER DEPTH), in.	DIR.	VEL., knots			HEADING	GROSS WEIGHT, lb	REVOLUTION COUNTER	ACCELERATION-TIME	REVOLUTION COUNTER	REVOLUTION COUNTER	ACCELERATION-TIME	REVOLUTION COUNTER	
14	GROOVED CONCRETE	——	DRY	340	7	50	30.11	310	194,500	960	990	274	1.23	1.26	1.35	—
			WET (.01)	310	12	50	30.11	310	187,700	1174	1250	370				—

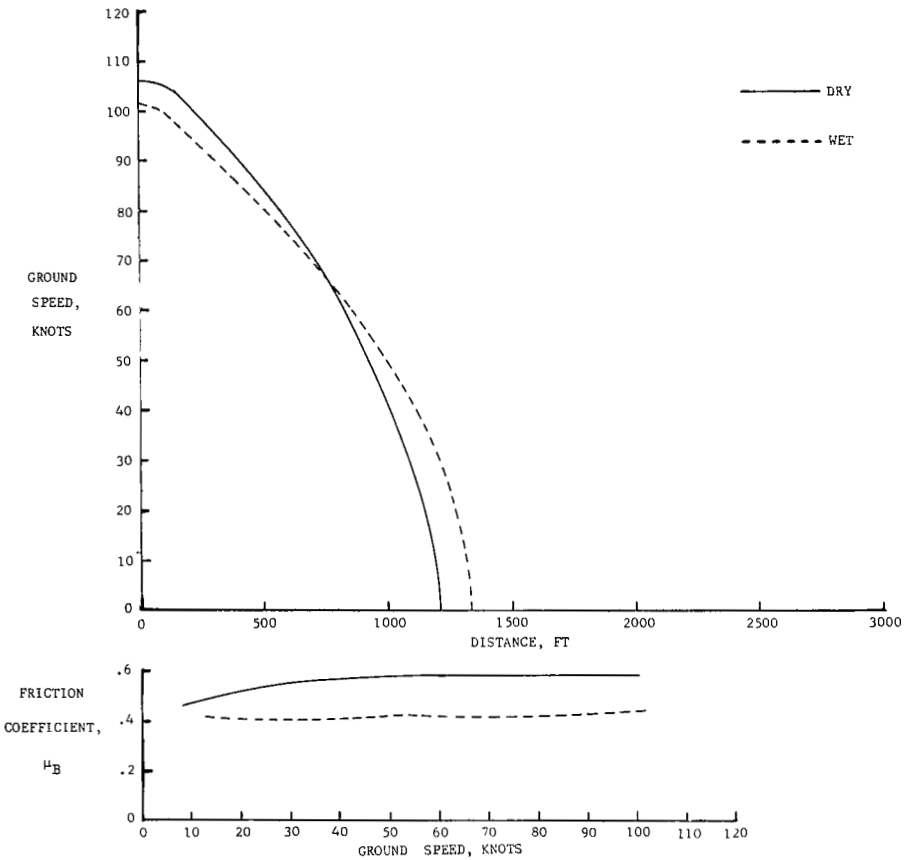

TEST SURFACE

(n) Runway 14; Chicago Midway Airport.

Figure A1.- Continued.

OFFUTT AFB, NEBRASKA RUNWAY 12/30							DATE 2-20-70		STOPPING DISTANCE, FT			STOPPING DISTANCE RATIO			RCR
R/W REF. NO.	PAVEMENT SURFACE			WIND		TEMP., °F	ALT. SET., in. Hg	AIRCRAFT		AIRCRAFT		TEST VEHICLE	AIRCRAFT		TEST VEHICLE	
	MATERIAL	TEXTURE DEPTH, mm	CONDITION (WATER DEPTH), in.	DIR.	VEL., knots			HEADING	GROSS WEIGHT, lb	REVOLUTION COUNTER	ACCELERATION-TIME	REVOLUTION COUNTER	REVOLUTION COUNTER	ACCELERATION-TIME	REVOLUTION COUNTER	
15	GROOVED CONCRETE	—	DRY	220	13	33	30.49	300	193,800	1028	1160	306	1.22	1.18	1.32	20
			DAMP	220	16	33	30.49	300	189,100	1258	1370	404				26

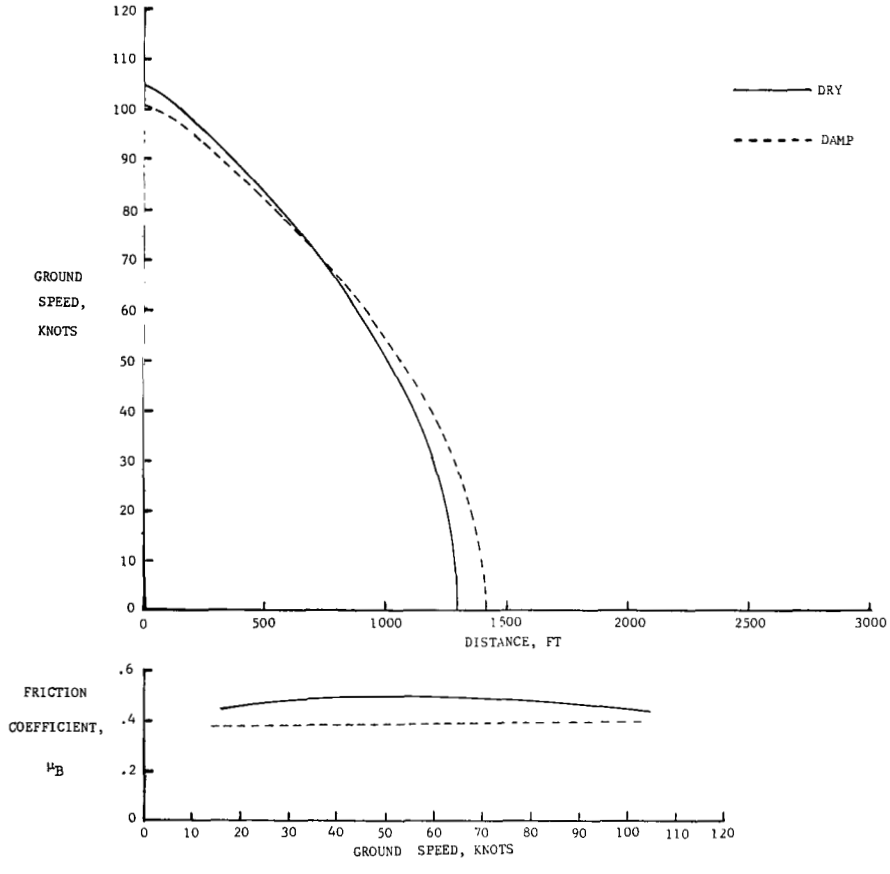

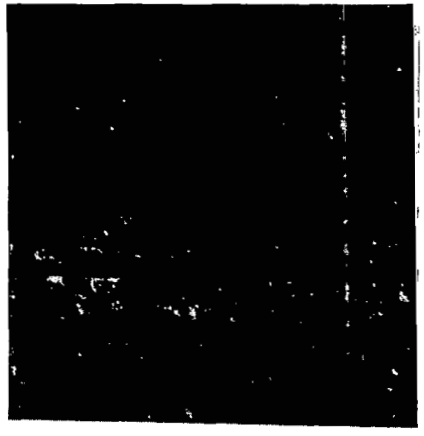

TEST SURFACE

(o) Runway 15; Offutt Air Force Base.

Figure A1.- Continued.

OFFUTT AFB, NEBRASKA RUNWAY 12/30							DATE 2-20-70		STOPPING DISTANCE, FT			STOPPING DISTANCE RATIO			RCR
R/W REF. NO.	PAVEMENT SURFACE			WIND		TEMP., °F	ALT. SET., in. Hg	AIRCRAFT		AIRCRAFT		TEST VEHICLE	AIRCRAFT		TEST VEHICLE	
	MATERIAL	TEXTURE DEPTH, mm	CONDITION (WATER DEPTH), in.	DIR.	VEL., knots			HEADING	GROSS WEIGHT, lb	REVOLUTION COUNTER	ACCELERATION-TIME	REVOLUTION COUNTER	REVOLUTION COUNTER	ACCELERATION-TIME	REVOLUTION COUNTER	
15	GROOVED CONCRETE	—	DRY	205	7	45	30.42	300	237,800	1170	1190	—	1.20	1.20	—	—
			DAMP	200	5	46	30.40	300	232,600	1408	1430	—				—

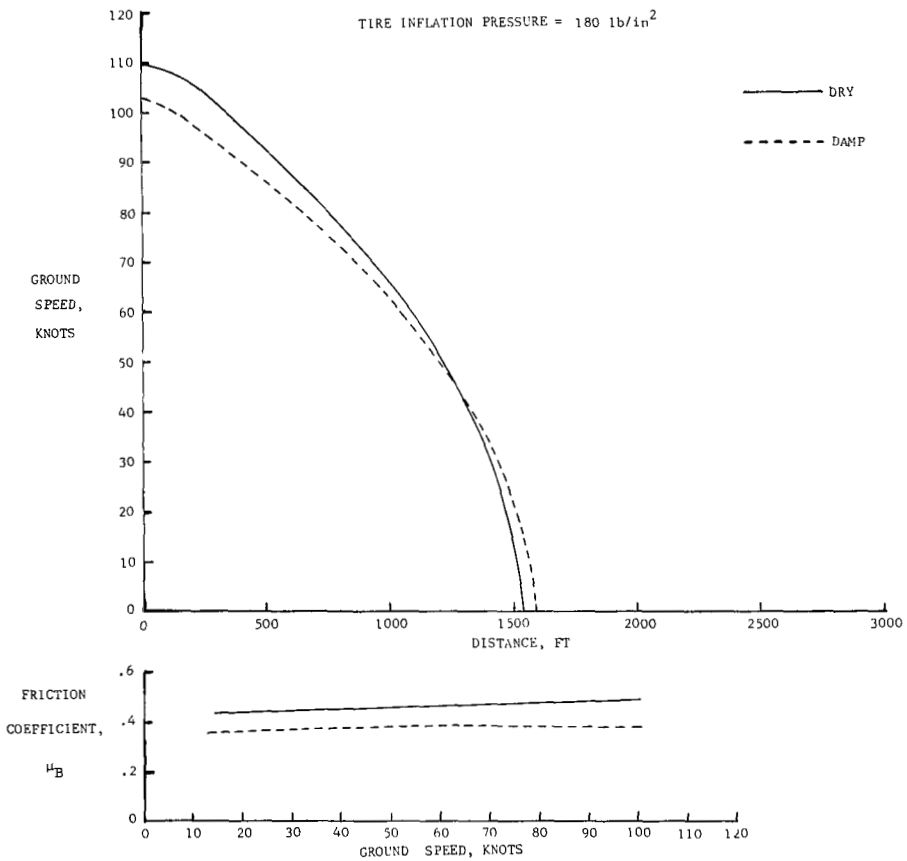

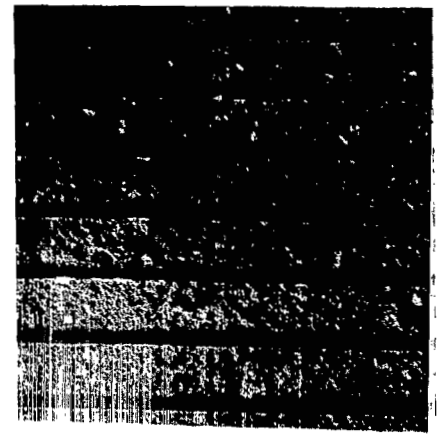

TEST SURFACE

(o) Concluded.

Figure A1.- Continued.

BEALE AFB, CALIFORNIA				RUNWAY 14/32			DATE 10-11-69			STOPPING DISTANCE, FT			STOPPING DISTANCE RATIO			RCR
R/W REF. NO.	PAVEMENT SURFACE			WIND		TEMP., °F	ALT. SET., in. Hg	AIRCRAFT		AIRCRAFT		TEST VEHICLE	AIRCRAFT		TEST VEHICLE	
	MATERIAL	TEXTURE DEPTH, mm	CONDITION (WATER DEPTH), in.	DIR.	VEL., knots			HEADING	GROSS WEIGHT, lb	REVOLUTION COUNTER	ACCELERATION-TIME	REVOLUTION COUNTER	REVOLUTION COUNTER	ACCELERATION-TIME	REVOLUTION COUNTER	
16	GROOVED CONCRETE	—	DRY	320	13	52	29.94	320	200,200	975	1080	258	1.15	1.07	1.20	23
			WET (PUDDLED)	310	9	57	29.95	320	194,200	1122	1160	311				22

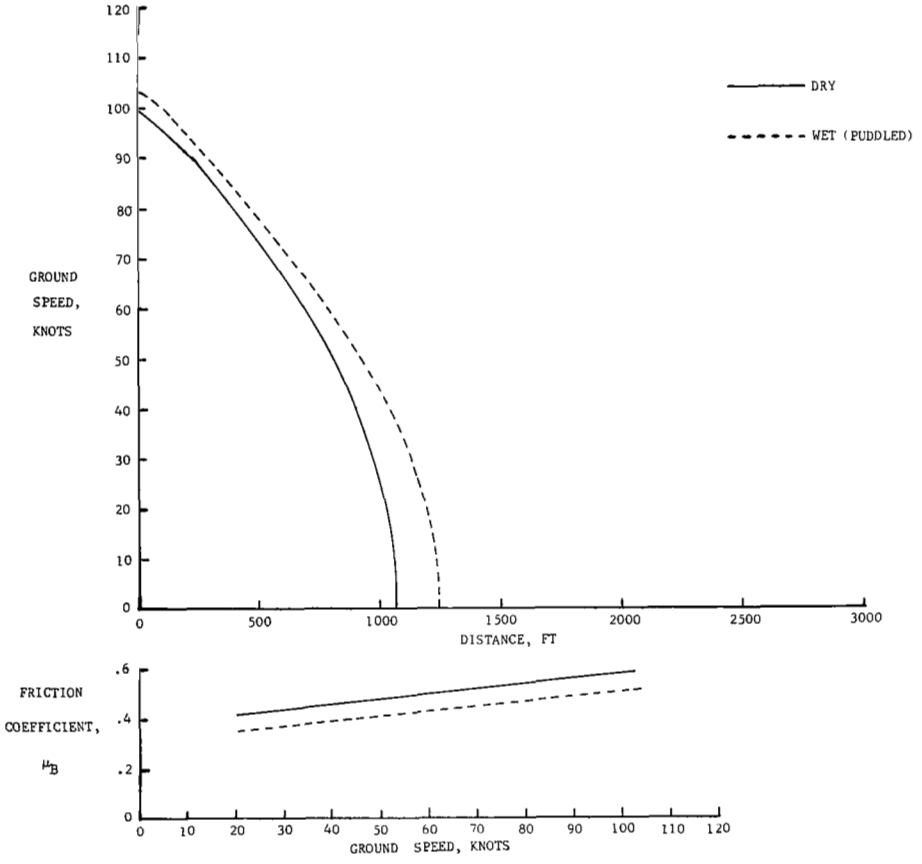

TEST SURFACE

(p) Runway 16; Beale Air Force Base.

Figure A1.- Continued.

BEALE AFB, CALIFORNIA RUNWAY: 14/32 DATE 10-11-69

SUMMARY OF PAVEMENT TRACTION FACTORS BASED ON CORE SAMPLE ANALYSIS

PAVEMENT TYPE	PREDOMINANT CHARACTERISTICS	FACTORS	CLASSIFICATION FOR WET OPERATION
Grooved Portland Cement Concrete	Good surface drainage. Grooves combined with exposed particles of sharp, fine aggregate. Coarse to fine grained surface texture.	The surface texture characteristics of the grooved portland cement concrete from Beale AFB are described as follows: (1) Sawed grooves, 1/4- X 1/4-in. with 1-in. spacing. (2) Fine grained texture resulting from exposed particles of sharp sand. (3) Transverse drainage paths (grooves) to reduce the buildup of dynamic fluid pressure. The structural characteristics reflected at a depth of 1-1/2 in. below the surface are as follows: (1) The coarse aggregate skeleton consists of quartz gravel and igneous rock fragments (non-calcareous). Maximum particle diameter is 2 in. (2) Aggregates are hard, rounded, and well graded from coarse to fine. No subsurface drainage capability reflected in aggregate skeleton or matrix.	Good

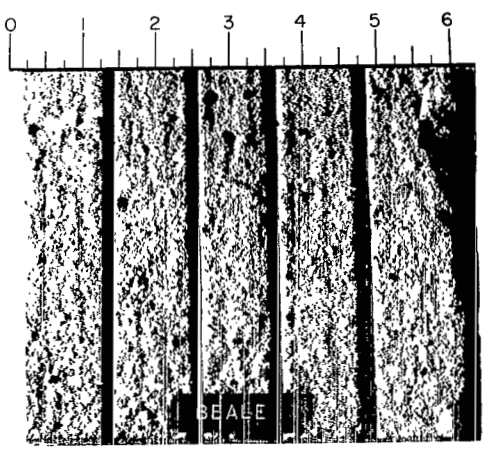

CORE SAMPLE SURFACE

CORE SAMPLE SURFACE PROFILE

(p) Concluded.

Figure A1.- Continued.

SPANGDAHLEM USAFE BASE, GERMANY				RUNWAY 5/23				DATE 7-31-69		STOPPING DISTANCE, FT			STOPPING DISTANCE RATIO			RCR
R/W REF. NO.	PAVEMENT SURFACE			WIND		TEMP., °F	ALT. SET., in. Hg	AIRCRAFT		AIRCRAFT		TEST VEHICLE	AIRCRAFT		TEST VEHICLE	
	MATERIAL	TEXTURE DEPTH, mm	CONDITION (WATER DEPTH), in.	DIR.	VEL., knots			HEADING	GROSS WEIGHT, lb	REVOLUTION COUNTER	ACCELERATION-TIME	REVOLUTION COUNTER	REVOLUTION COUNTER	ACCELERATION-TIME	REVOLUTION COUNTER	
18	SLURRY SEAL	0.214	DRY	030	5	64	30.08	050	194,300	1220	1360	322	2.37*	2.32*	2.50	24
			WET (.02)	020	6	64	30.08	050	184,900	2610	2550	800				17

*Based on S_{DRY} = 1100 ft

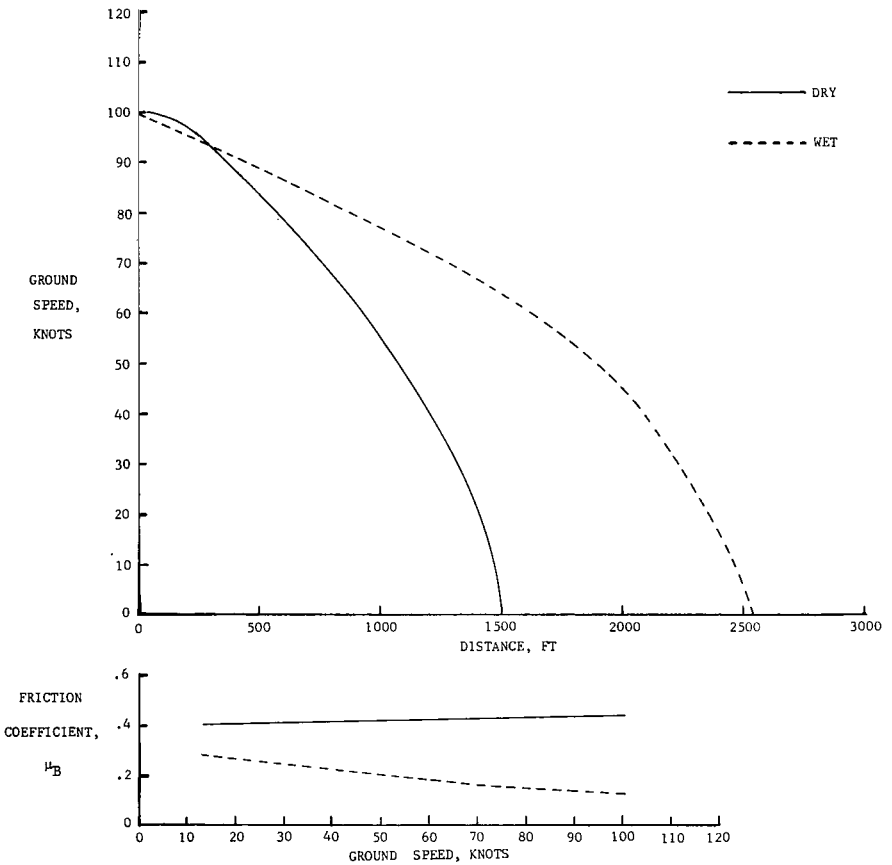

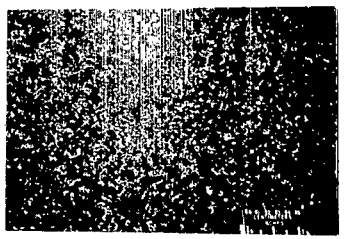

TEST SURFACE

(q) Runway 18; Spangdahlem Air Force Base.

Figure A1.- Continued.

ELMENDORF AFB, ALASKA			RUNWAY 5/23		DATE 9-19-69				STOPPING DISTANCE, FT			STOPPING DISTANCE RATIO			RCR
R/W REF. NO.	PAVEMENT SURFACE			WIND		TEMP., °F	ALT. SET., in. Hg	AIRCRAFT			TEST VEHICLE	AIRCRAFT		TEST VEHICLE	
	MATERIAL	TEXTURE DEPTH, mm	CONDITION (WATER DEPTH), in.	DIR.	VEL., knots			HEADING	GROSS WEIGHT, lb	REVOLUTION COUNTER	ACCELERATION-TIME	REVOLUTION COUNTER	REVOLUTION COUNTER	ACCELERATION-TIME	REVOLUTION COUNTER	
19	ASPHALT	0.208	DRY	180	2	39	29.71	050	189,300	1226	1080	279	2.16*	2.48*	2.48	26
			WET (.04)	140	2	42	29.73	050	184,700	2380	2730	692				17.5

*Based on S_{DRY} = 1100 ft

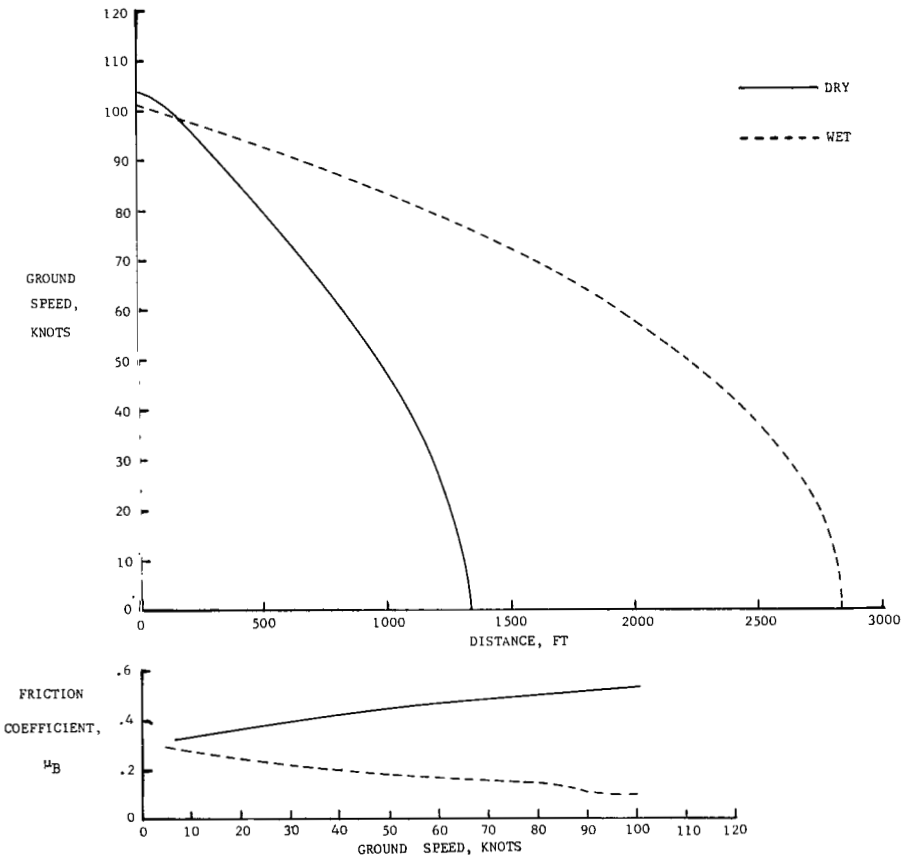

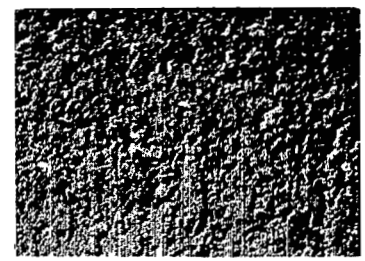

TEST SURFACE

(r) Runway 19; Elmendorf Air Force Base.

Figure A1.- Continued.

ELMENDORF AFB, ALASKA RUNWAY: 5/23 DATE: 9-19-69

SUMMARY OF PAVEMENT TRACTION FACTORS BASED ON CORE SAMPLE ANALYSIS

PAVEMENT TYPE	PREDOMINANT CHARACTERISTICS	FACTORS	CLASSIFICATION FOR WET OPERATION
Asphaltic Concrete	Medium surface drainage. Exposed particles of rounded aggregate. Medium grained texture.	The surface texture characteristics reflected in the sample of asphaltic concrete from Elmendorf AFB are described as follows: (1) The medium grained surface texture is defined primarily by exposed particles of rounded aggregate. (2) The surface texture does offer some surface drainage, but the exposed particles of rounded aggregate are susceptible to thin-film lubrication. The structural characteristics at a depth of 1-1/2 in. below the surface are described as follows: (1) The coarse aggregate skeleton consists of rounded and fragmented particles of igneous rock ranging between 1/8 and 3/4 in. in diameter. (2) The dense graded mix offers no subsurface drainage.	Medium-Poor

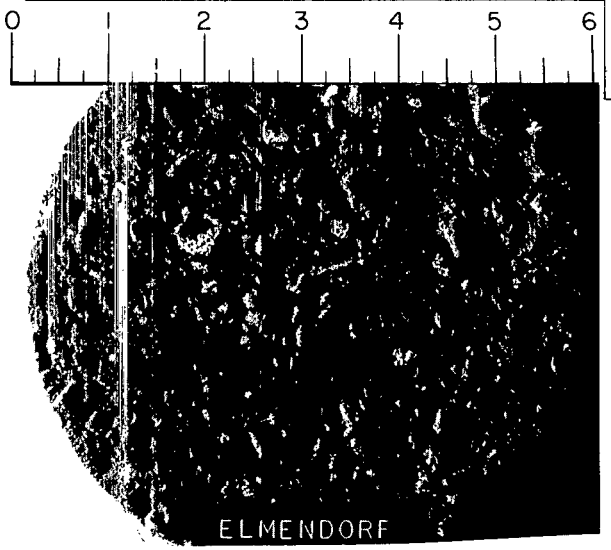

CORE SAMPLE SURFACE

CORE SAMPLE SURFACE PROFILE

(r) Concluded.

Figure A1.- Continued.

BITBURG USAFE BASE, GERMANY				RUNWAY 6/24			DATE 7-30-69		STOPPING DISTANCE, FT			STOPPING DISTANCE RATIO			RCR
R/W REF. NO.	PAVEMENT SURFACE			WIND		TEMP., °F	ALT. SET., in. Hg	AIRCRAFT	AIRCRAFT		TEST VEHICLE	AIRCRAFT		TEST VEHICLE	
	MATERIAL	TEXTURE DEPTH, mm	CONDITION (WATER DEPTH), in.	DIR.	VEL., knots			HEADING	GROSS WEIGHT, lb	REVOLUTION COUNTER	ACCELERATION-TIME	REVOLUTION COUNTER	REVOLUTION COUNTER	ACCELERATION-TIME	REVOLUTION COUNTER	
20	ANTISKID COAT	0.220	DRY	230	4	59	30.07	240	194,600	1060	1100	336	1.83	2.12	1.78	24
			WET (.04)	230	4	59	30.07	240	189,000	1940	2330	577				22

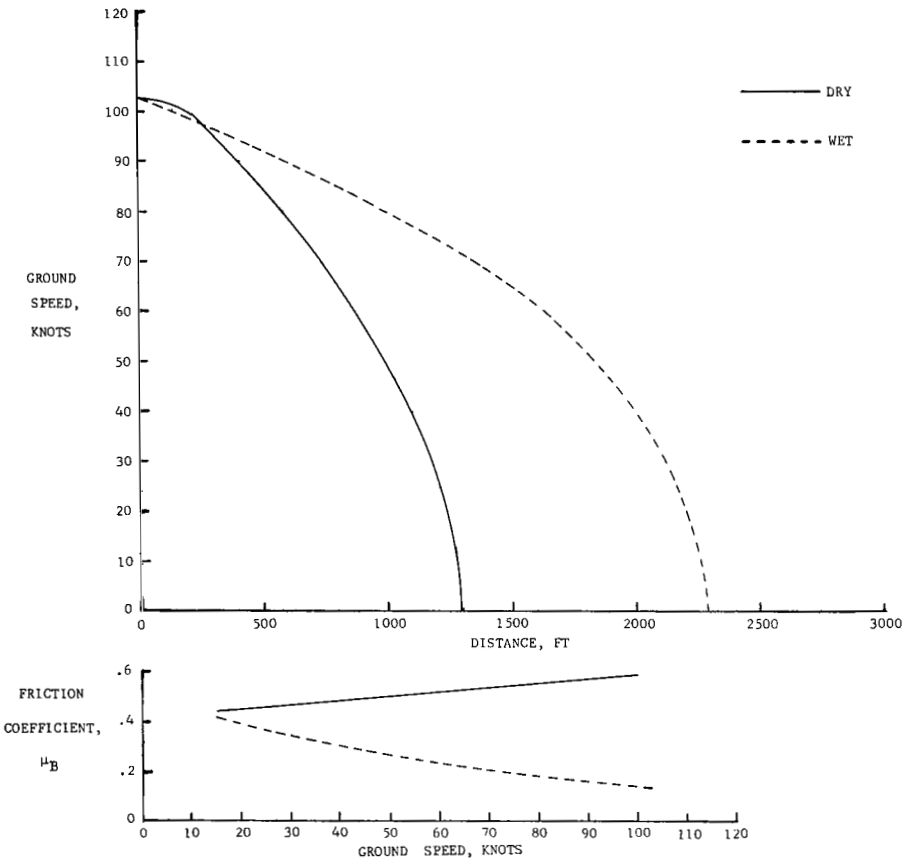

TEST SURFACE

(s) Runway 20; Bitburg Air Force Base.

Figure A1.- Continued.

MYRTLE BEACH AFB, SOUTH CAROLINA			RUNWAY 17/35			Date 10-8-69 & 1-28-70		STOPPING DISTANCE, FT			STOPPING DISTANCE RATIO			RCR
R/W REF. NO.	PAVEMENT SURFACE			WIND		TEMP., °F	ALT. SET., in. Hg	AIRCRAFT		AIRCRAFT		TEST VEHICLE	AIRCRAFT		TEST VEHICLE	
	MATERIAL	TEXTURE DEPTH, mm	CONDITION (WATER DEPTH), in.	DIR.	VEL., knots			HEADING	GROSS WEIGHT, lb	REVOLUTION COUNTER	ACCELERATION-TIME	REVOLUTION COUNTER	REVOLUTION COUNTER	ACCELERATION-TIME	REVOLUTION COUNTER	
21	SLURRY SEAL	0.173	DRY	140	5	59	30.20	170	201,000	1108	1150	304	1.88	1.96	1.67	
			WET (.06)	280	1	68	30.07	170	191,600	2083	2250	507				23.5
			DAMP (<.01)	350	2	68	30.07	170	195,200	1123	1320	———	1.02	1.15	———	23

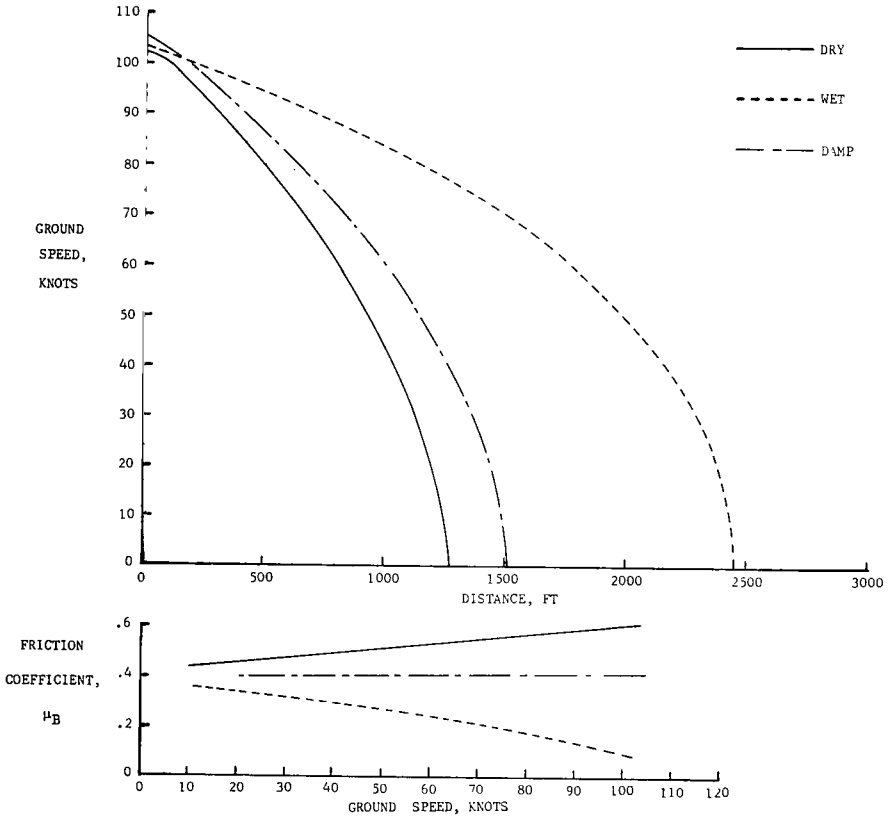

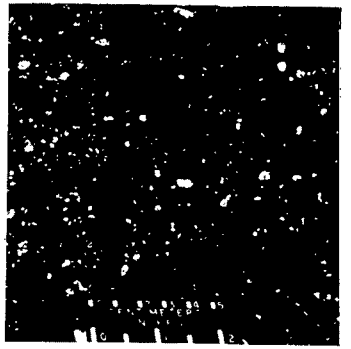

TEST SURFACE

(t) Runway 21; Myrtle Beach Air Force Base.

Figure A1.- Continued.

MYRTLE BEACH AFB, SOUTH CAROLINA RUNWAY: 17/35 DATE: 10-8-69

SUMMARY OF PAVEMENT TRACTION FACTORS BASED ON CORE SAMPLE ANALYSIS

PAVEMENT TYPE	PREDOMINANT CHARACTERISTICS	FACTORS	CLASSIFICATION FOR WET OPERATION
Asphaltic Concrete	Medium surface drainage. Exposed particles of sharp aggregate. Medium grained surface texture.	The surface texture characteristics of the sample of asphaltic concrete from Myrtle Beach AFB are described as follows: (1) The medium grained surface texture is defined by small (less than 1/4 in.) fractured particles of quartz. Aggregate exposure is facilitated by an erosion of the sand-asphalt matrix. (2) The interparticle depressions provide a low level of surface drainage. The structural characteristics below the surface are described as follows: (1) The aggregate skeleton consists of fractured and rounded particles of quartz ranging between 1/4 and 3/4 in. in diameter. (2) The dense graded mix offers no subsurface drainage.	Medium-Good

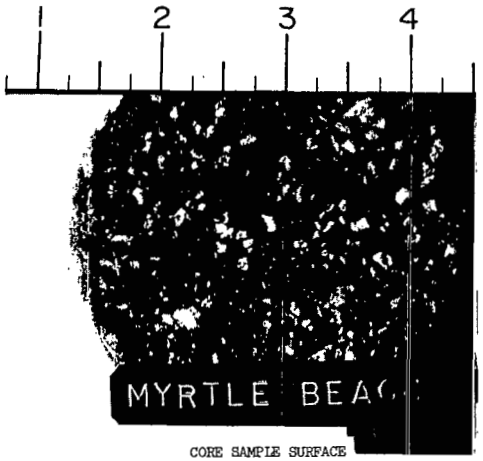

CORE SAMPLE SURFACE

CORE SAMPLE SURFACE PROFILE

(t) Concluded.

Figure A1.- Continued.

WADDINGTON RAFB, ENGLAND				RUNWAY 3/21				DATE 7-25-69		STOPPING DISTANCE, FT			STOPPING DISTANCE RATIO			RCR
R/W REF. NO.	PAVEMENT SURFACE			WIND		TEMP., °F	ALT. SET., in. Hg	AIRCRAFT		AIRCRAFT		TEST VEHICLE	AIRCRAFT		TEST VEHICLE	
	MATERIAL	TEXTURE DEPTH, mm	CONDITION (WATER DEPTH), in.	DIR.	VEL., knots			HEADING	GROSS WEIGHT, lb	REVOLUTION COUNTER	ACCELERATION-TIME	REVOLUTION COUNTER	REVOLUTION COUNTER	ACCELERATION-TIME	REVOLUTION COUNTER	
22	1/8" GRIT COAT	0.279	DRY	140	5	72	30.10	210	193,500	1555	1170	328	1.88*	1.87*	1.87	—
			WET (.03)	140	6	72	30.10	210	188,200	2070	2060	615				—

*Based on S_{DRY} = 1100 ft

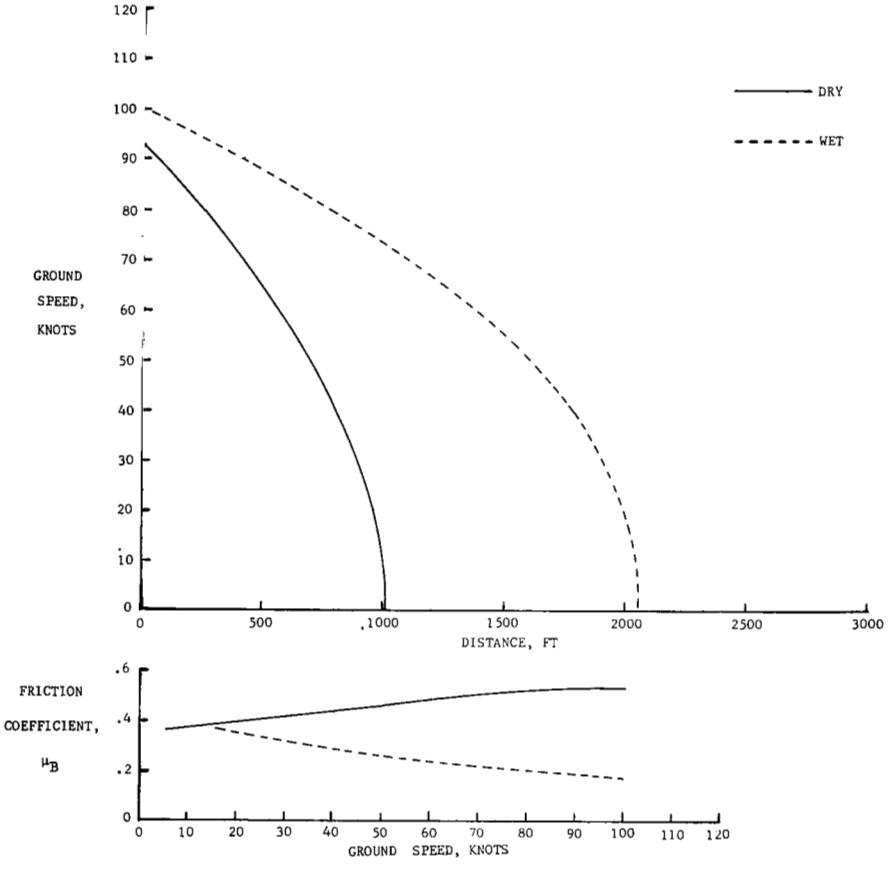

(u) Runway 22; Waddington Royal Air Force Base.

Figure A1.- Continued.

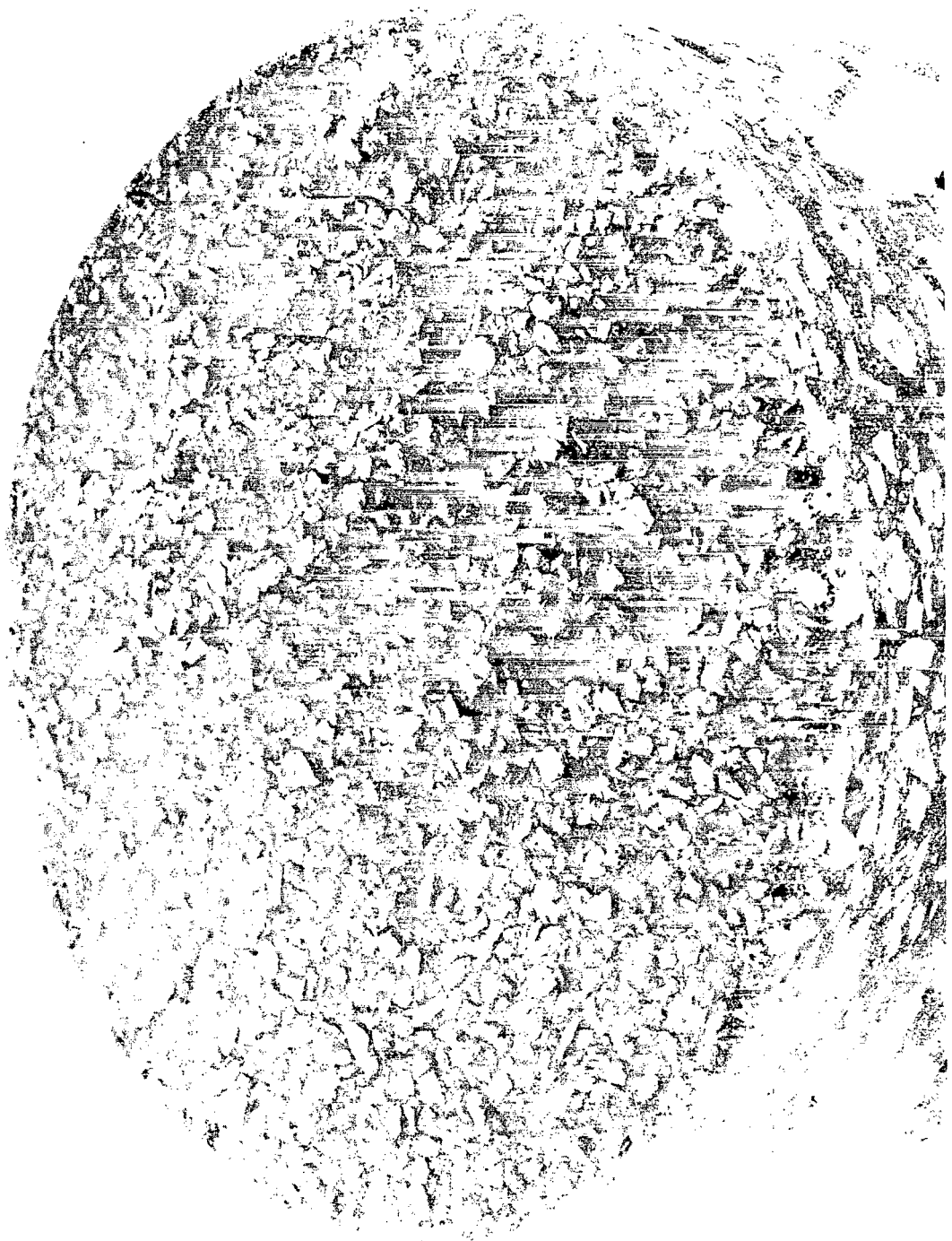

(u) Concluded.

Figure A1.- Continued.

OTIS AFB, MASSACHUSETTS				RUNWAY 14/32			DATE 10-7-69		STOPPING DISTANCE, FT			STOPPING DISTANCE RATIO			RCR
R/W REF. NO.	PAVEMENT SURFACE			WIND		TEMP., °F	ALT. SET., in. Hg	AIRCRAFT	AIRCRAFT		TEST VEHICLE	AIRCRAFT		TEST VEHICLE	
	MATERIAL	TEXTURE DEPTH, mm	CONDITION (WATER DEPTH), in.	DIR.	VEL., knots			HEADING	GROSS WEIGHT, lb	REVOLUTION COUNTER	ACCELERATION-TIME	REVOLUTION COUNTER	REVOLUTION COUNTER	ACCELERATION-TIME	REVOLUTION COUNTER	
23	ASPHALT	0.338	DRY	150	4	53	30.25	320	204,900	1013	1080	262	1.88	1.75	1.62	26
			WET (.03)	160	8	53	30.25	320	201,100	1910	1890	424				22

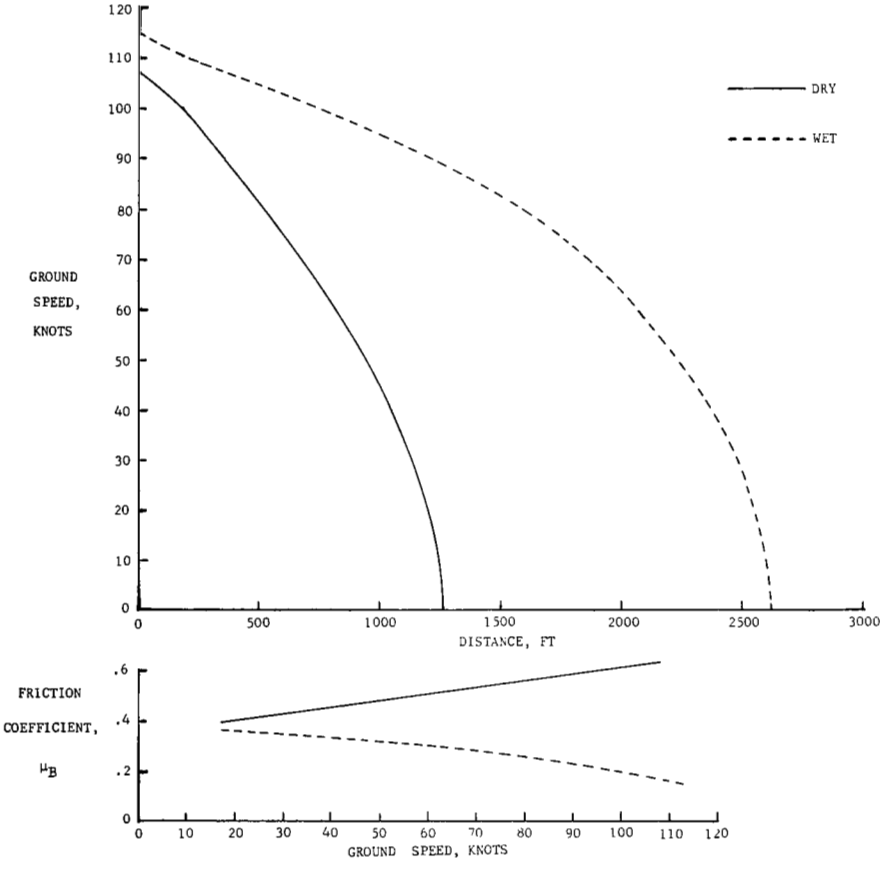

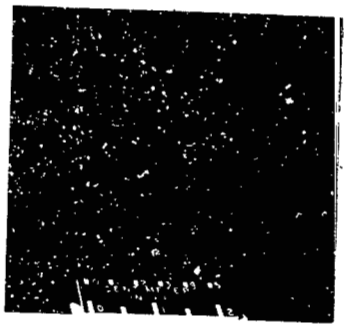

TEST SURFACE

(v) Runway 23; Otis Air Force Base.

Figure A1.- Continued.

OTIS AFB, MASSACHUSETTS RUNWAY: 14/32 DATE: 10-7-69

SUMMARY OF PAVEMENT TRACTION FACTORS BASED ON CORE SAMPLE ANALYSIS

PAVEMENT TYPE	PREDOMINANT CHARACTERISTICS	FACTORS	CLASSIFICATION FOR WET OPERATION
Asphaltic Concrete	Poor surface drainage. Exposed particles of sharp sand. Fine grained surface texture.	The surface texture characteristics reflected in the sample of asphaltic concrete from Otis AFB are described as follows: (1) The fine grained surface texture is defined by the exposed particles of sand in the matrix and small cavities or depressions reflected in the surface. (2) The exposed particles of sand are sharp. However, the surface texture offers little or no surface drainage. The structural characteristics below the surface are described as follows: (1) The coarse aggregate skeleton consists of rounded and fragmented particles of igneous rock ranging between 1/8 and 3/4 in. in diameter. (2) The dense graded mix offers no subsurface drainage.	Medium

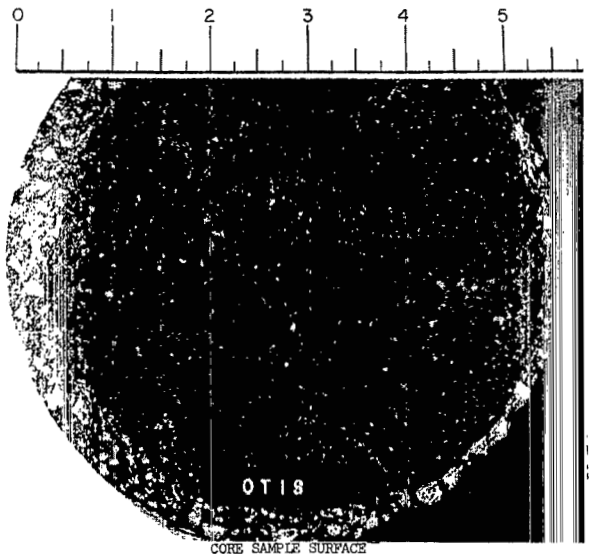

CORE SAMPLE SURFACE

CORE SAMPLE SURFACE PROFILE

(v) Concluded.

Figure A1.- Continued.

AVIANO USAFE BASE, ITALY				RUNWAY 5/23				DATE 8-4-69		STOPPING DISTANCE, FT			STOPPING DISTANCE RATIO			RCR
R/W REF. NO.	PAVEMENT SURFACE			WIND		TEMP., °F	ALT. SET., in. Hg	AIRCRAFT		AIRCRAFT		TEST VEHICLE	AIRCRAFT		TEST VEHICLE	
	MATERIAL	TEXTURE DEPTH, mm	CONDITION (WATER DEPTH), in.	DIR.	VEL., knots			HEADING	GROSS WEIGHT, lb	REVOLUTION COUNTER	ACCELERATION-TIME	REVOLUTION COUNTER	REVOLUTION COUNTER	ACCELERATION-TIME	REVOLUTION COUNTER	
24	ASPHALT	0.349	DRY	030	2	70	30.01	050	193,300	1100	1170	343	1.74	1.78	1.57	23
			WET (.04)	0	1	71	30.01	050	184,600	1910	2080	539				21

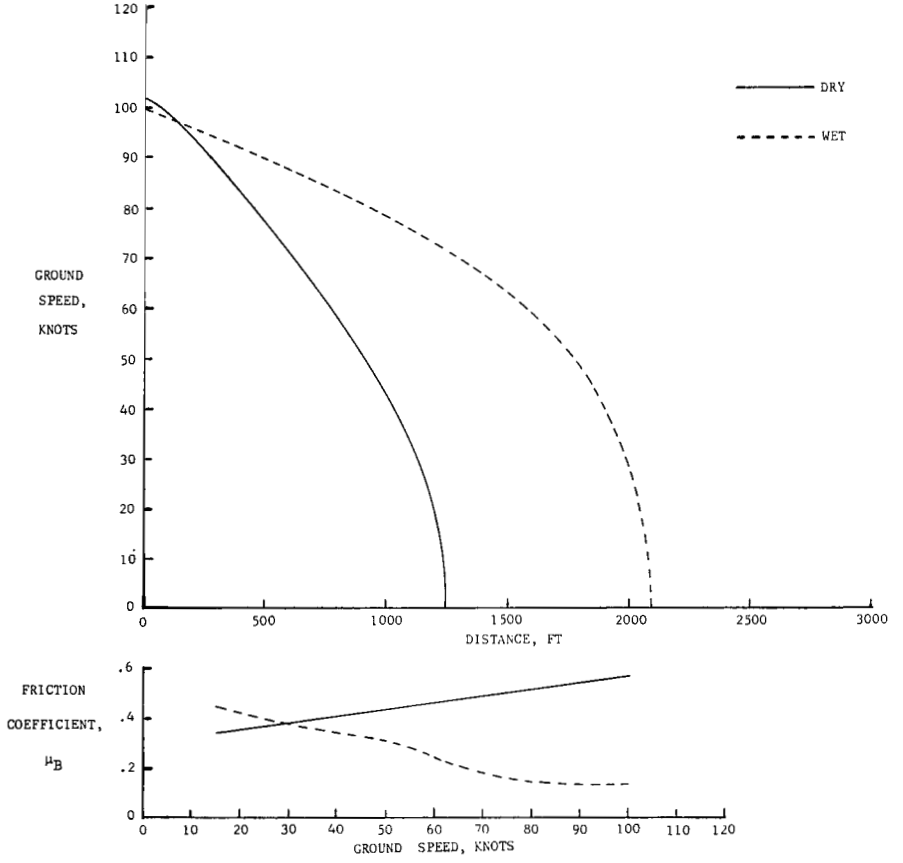

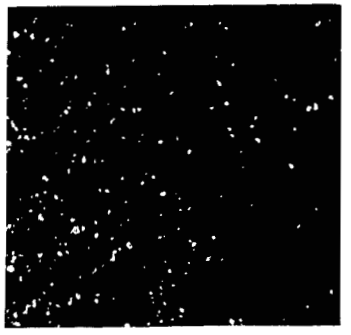

TEST SURFACE

(w) Runway 24; Aviano Air Force Base.

Figure A1.- Continued.

ALCONBURY USAFE BASE, ENGLAND			RUNWAY 12/30			DATE 7-24-69	STOPPING DISTANCE, FT				STOPPING DISTANCE RATIO			RCR
R/W REF. NO.	PAVEMENT SURFACE			WIND		TEMP., °F	ALT. SET., in. Hg	AIRCRAFT		AIRCRAFT		TEST VEHICLE	AIRCRAFT		TEST VEHICLE	
	MATERIAL	TEXTURE DEPTH, mm	CONDITION (WATER DEPTH), in.	DIR.	VEL., knots			HEADING	GROSS WEIGHT, lb	REVOLUTION COUNTER	ACCELERATION-TIME	REVOLUTION COUNTER	REVOLUTION COUNTER	ACCELERATION-TIME	REVOLUTION COUNTER	
25	SLURRY SEAL	0.195	DRY	350	5	64	30.04	300	200,400	1133	1180	330	1.73	1.69	1.68	25
			WET (.05)	020	6	64	30.05	300	193,600	1960	2000	554				23

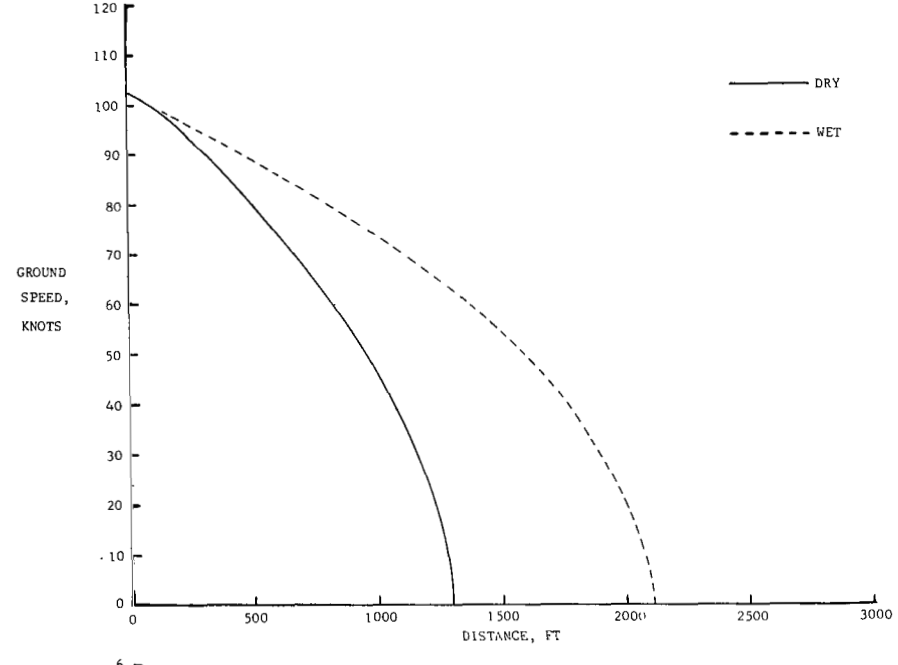

TEST SURFACE

(x) Runway 25; Alconbury Air Force Base.

Figure A1.- Continued.

FARNBOROUGH RAFB, ENGLAND			RUNWAY 7/25			DATE 7-16-69			STOPPING DISTANCE, FT			STOPPING DISTANCE RATIO			RCR
R/W REF. NO.	PAVEMENT SURFACE			WIND		TEMP., °F	ALT. SET., in. Hg	AIRCRAFT	AIRCRAFT		TEST VEHICLE	AIRCRAFT		TEST VEHICLE	
	MATERIAL	TEXTURE DEPTH, mm	CONDITION (WATER DEPTH), in.	DIR.	VEL., knots			HEADING	GROSS WEIGHT, lb	REVOLUTION COUNTER	ACCELERATION-TIME *	REVOLUTION COUNTER	REVOLUTION COUNTER	ACCELERATION-TIME *	REVOLUTION COUNTER	
26	GROOVED ASPHALT	—	DRY	300	5	78	29.76	250	199,200	950	—	346	1.69	—	1.40	20
			WET (.03)	340	3	79	29.76	250	191,700	1602	—	485				19

*Recorder inoperative

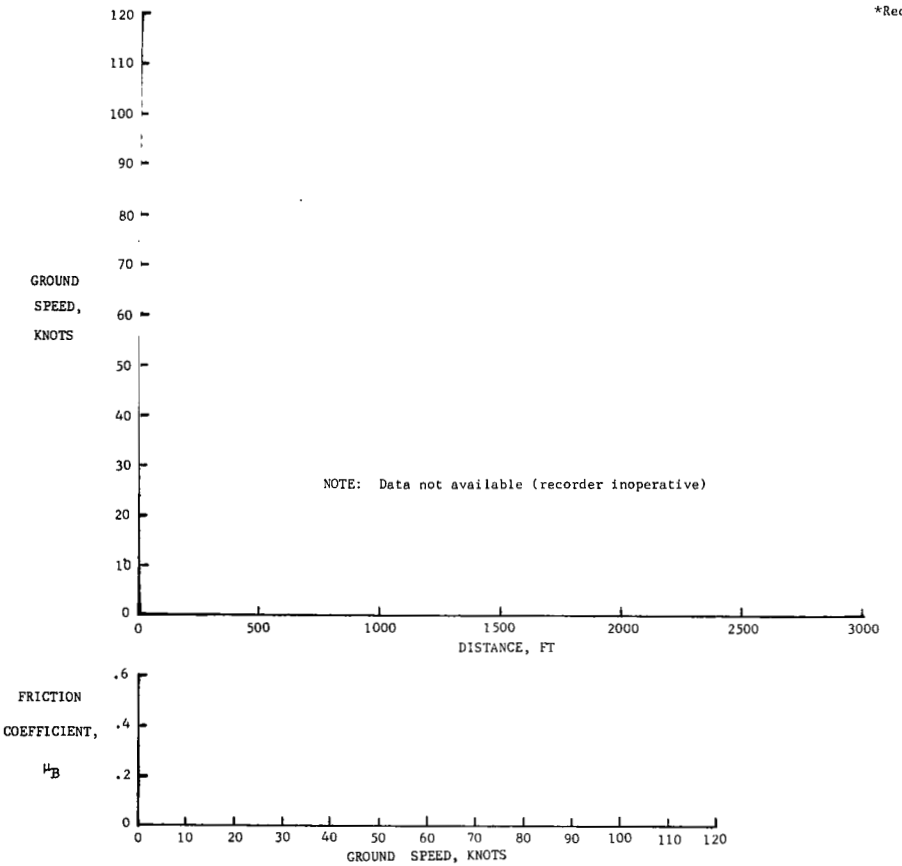

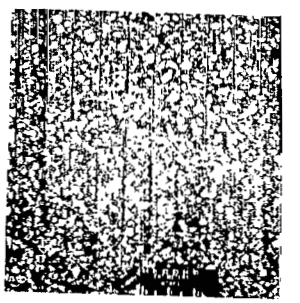

TEST SURFACE

(y) Runway 26; Farnborough Air Force Base.

Figure A1.- Continued.

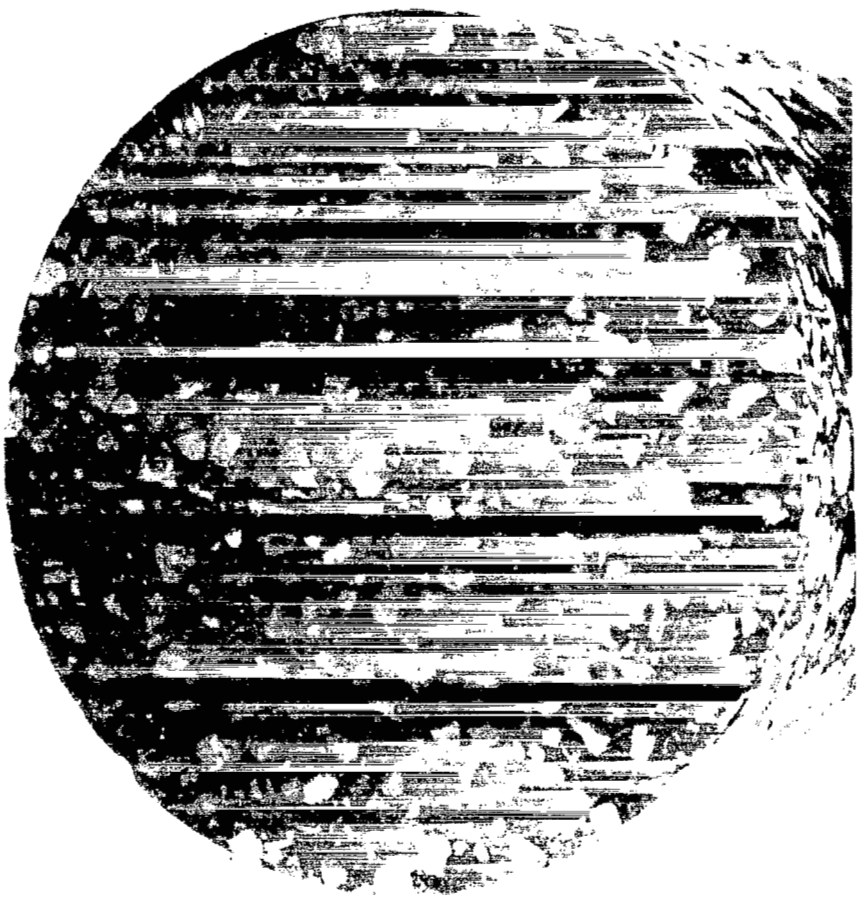

(y) Concluded.

Figure A1.- Continued.

SEMBACH USAFE BASE, GERMANY				RUNWAY 7/25					DATE 7-28-69	STOPPING DISTANCE, FT			STOPPING DISTANCE RATIO			RCR
R/W REF. NO.	PAVEMENT SURFACE			WIND		TEMP., °F	ALT. SET., in. Hg	AIRCRAFT		AIRCRAFT		TEST VEHICLE	AIRCRAFT		TEST VEHICLE	
	MATERIAL	TEXTURE DEPTH, mm	CONDITION (WATER DEPTH), in.	DIR.	VEL., knots			HEADING	GROSS WEIGHT, lb	REVOLUTION COUNTER	ACCELERATION-TIME	REVOLUTION COUNTER	REVOLUTION COUNTER	ACCELERATION-TIME	REVOLUTION COUNTER	
27	ANTISKID COAT	0.228	DRY	160	2	62	30.16	250	197,600	1353	1290	336	1.65*	1.70*	1.50	23
			WET (.02)	140	2	62	30.16	250	190,600	1810	1870	502				20

*Based on S_{DRY} = 1100 ft

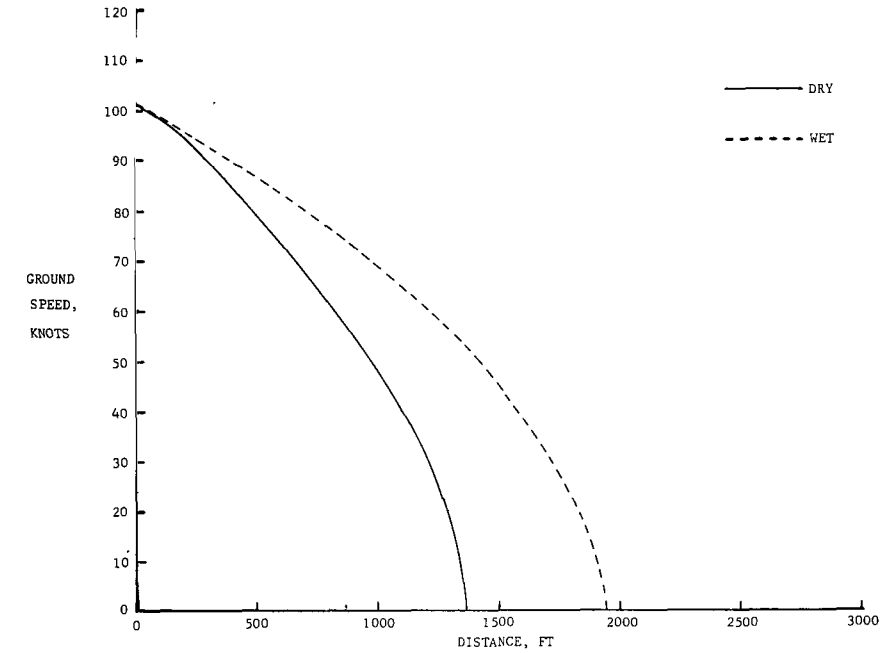

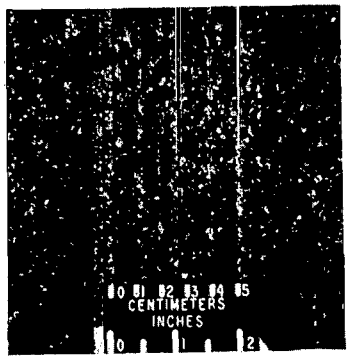

TEST SURFACE

(z) Runway 27; Sembach Air Force Base.

Figure A1.- Continued.

POPE AFB, NORTH CAROLINA				RUNWAY 4/22			DATE 10-10-69		STOPPING DISTANCE, FT			STOPPING DISTANCE RATIO			RCR
R/W REF. NO.	PAVEMENT SURFACE			WIND		TEMP., °F	ALT. SET., in. Hg	AIRCRAFT	AIRCRAFT		TEST VEHICLE	AIRCRAFT		TEST VEHICLE	
	MATERIAL	TEXTURE DEPTH, mm	CONDITION (WATER DEPTH), in.	DIR.	VEL., knots			HEADING	GROSS WEIGHT, lb	REVOLUTION COUNTER	ACCELERATION-TIME	REVOLUTION COUNTER	REVOLUTION COUNTER	ACCELERATION-TIME	REVOLUTION COUNTER	
28	ASPHALT	0.144	DRY	270	3	48	30.11	220	201,800	1098	1070	251	1.47	1.65	1.78	26
			WET (.05)	225	1	50	30.12	220	195,200	1610	1770	447				21

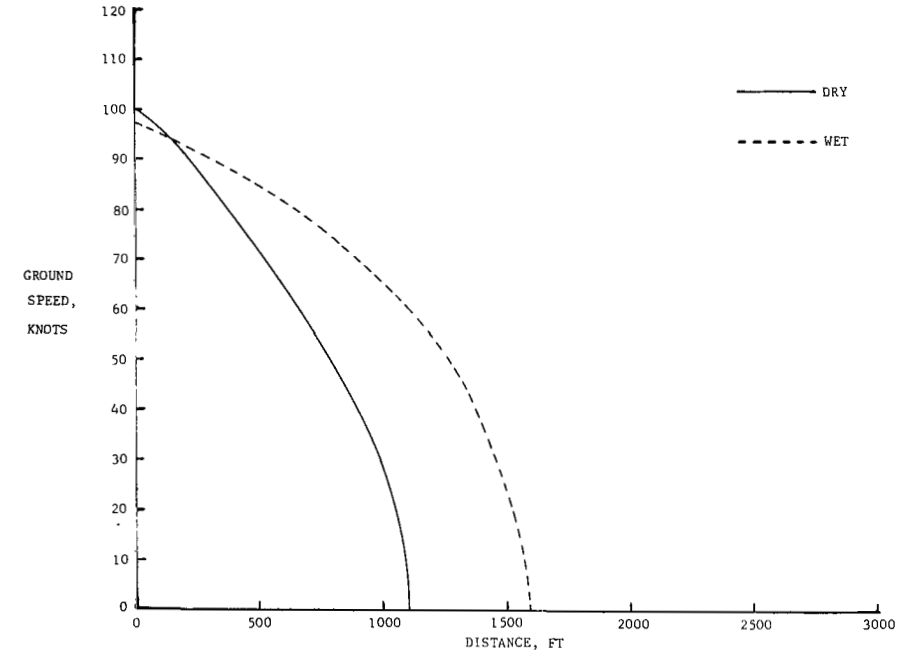

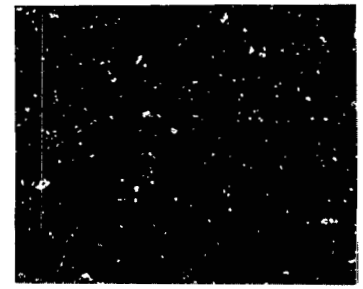

TEST SURFACE

(aa) Runway 28; Pope Air Force Base.

Figure A1.- Continued.

POPE AFB, NORTH CAROLINA RUNWAY: 4/22 DATE: 10-10-69

SUMMARY OF PAVEMENT TRACTION FACTORS BASED ON CORE SAMPLE ANALYSIS

PAVEMENT TYPE	PREDOMINANT CHARACTERISTICS	FACTORS	CLASSIFICATION FOR WET OPERATION
Asphaltic Concrete	Poor surface drainage. Exposed particles of fine sand. Fine grained surface texture.	The surface texture characteristics reflected in the sample of asphaltic concrete from Pope AFB are described as follows: (1) The surface texture is defined by the sand-asphalt matrix that was forced to the surface during compaction. There is very little particle angularity extending above the matrix. (2) The fine grained surface texture offers little or no surface drainage. The structural characteristics at a depth of 1-1/2 in. below the surface are described as follows: (1) The aggregate skeleton consists of a mixture of rounded and fragmented particles of quartz and quartz gravel ranging between 1/4 and 1 in. in diameter. (2) The dense graded mix offers no subsurface drainage.	Medium-Poor

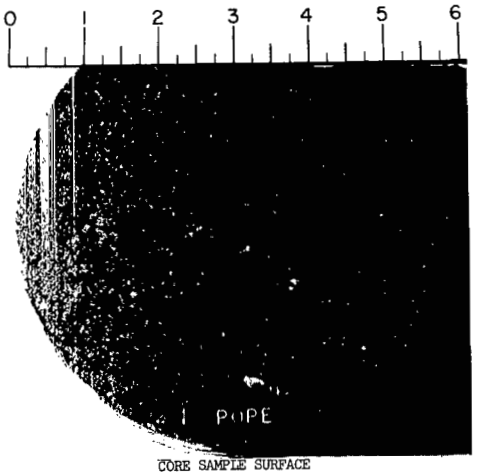

CORE SAMPLE SURFACE


CORE SAMPLE SURFACE PROFILE

(aa) Concluded.

Figure A1.- Continued.

TEMPELHOF CENTRAL AIRPORT, GERMANY				RUNWAY 9R/24L				DATE 7-29-69		STOPPING DISTANCE, FT			STOPPING DISTANCE RATIO			RCR
R/W REF. NO.	PAVEMENT SURFACE			WIND		TEMP., °F	ALT. SET., in. Hg	AIRCRAFT		AIRCRAFT		TEST VEHICLE	AIRCRAFT		TEST VEHICLE	
	MATERIAL	TEXTURE DEPTH, mm	CONDITION (WATER DEPTH), in.	DIR.	VEL., knots			HEADING	GROSS WEIGHT, lb	REVOLUTION COUNTER	ACCELERATION-TIME	REVOLUTION COUNTER	REVOLUTION COUNTER	ACCELERATION-TIME	REVOLUTION COUNTER	
29	GROOVED ASPHALT	0.221	DRY	120	9	68	30.04	090	194,400	1232	1380	320	1.48*	1.53*	1.65	25
			WET (.01)	130	6	69	30.04	090	186,700	1512	1680	529				18

*Based on S_{DRY} = 1100 ft

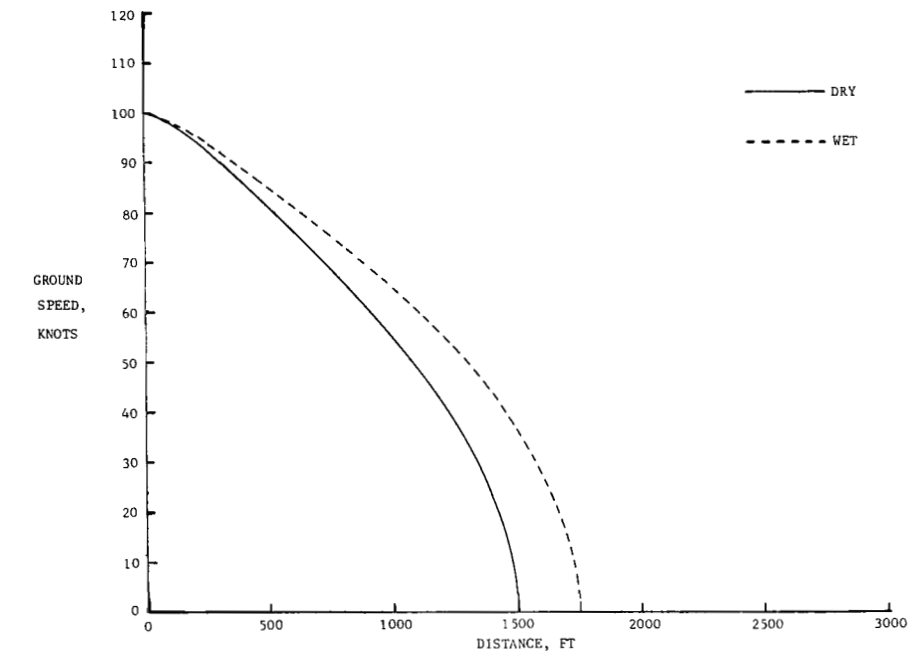

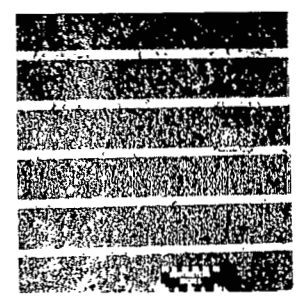

Side of runway
(Untrafficked area)

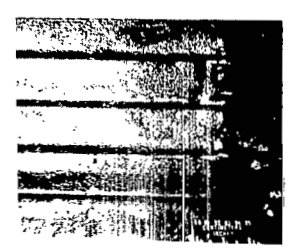

10-feet from runway center line
(Trafficked area)

TEST SURFACE

(bb) Runway 29; Tempelhof Central Airport.

Figure A1.- Continued.

McCHORD AFB, WASHINGTON			RUNWAY 16/34		DATE 2-17-70				STOPPING DISTANCE, FT			STOPPING DISTANCE RATIO			RCR
R/W REF. NO.	PAVEMENT SURFACE			WIND		TEMP., °F	ALT. SET., in. Hg	AIRCRAFT		AIRCRAFT		TEST VEHICLE	AIRCRAFT		TEST VEHICLE	
	MATERIAL	TEXTURE DEPTH, mm	CONDITION (WATER DEPTH), in.	DIR.	VEL., knots			HEADING	GROSS WEIGHT, lb	REVOLUTION COUNTER	ACCELERATION-TIME	REVOLUTION COUNTER	REVOLUTION COUNTER	ACCELERATION-TIME	REVOLUTION COUNTER	
30	ASPHALT	———	NATURAL RAIN (.02)	170	7	42	30.19	160	198,000	1610	1670	523	1.47*	1.51*	1.94*	15

*Based on S_{DRY} of 1100 ft for aircraft and 269 ft for test vehicle

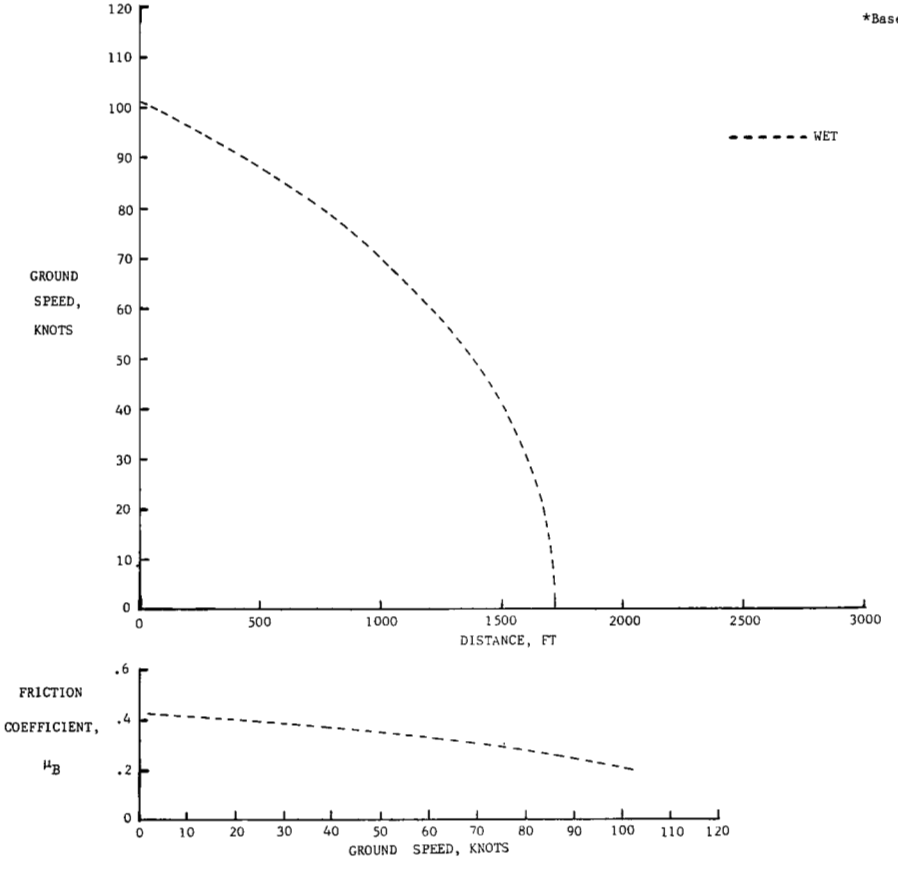

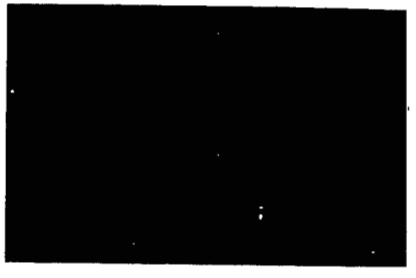

TEST SURFACE

(cc) Runway 30; McChord Air Force Base.

Figure A1.- Continued.

LITTLE ROCK AFB, ARKANSAS				RUNWAY 6/24				DATE 9-26-69		STOPPING DISTANCE, FT			STOPPING DISTANCE RATIO			RCR
R/W REF. NO.	PAVEMENT SURFACE			WIND		TEMP., °F	ALT. SET., in. Hg	AIRCRAFT		AIRCRAFT		TEST VEHICLE	AIRCRAFT		TEST VEHICLE	
	MATERIAL	TEXTURE DEPTH, mm	CONDITION (WATER DEPTH), in.	DIR.	VEL., knots			HEADING	GROSS WEIGHT, lb	REVOLUTION COUNTER	ACCELERATION-TIME	REVOLUTION COUNTER	REVOLUTION COUNTER	ACCELERATION-TIME	REVOLUTION COUNTER	
31	ASPHALT	0.187	DRY	—	0	55	29.99	240	195,900	1007	1080	247	1.44	1.51	1.61	22
			WET (.04)	—	0	56	30.01	240	186,700	1448	1630	397				23

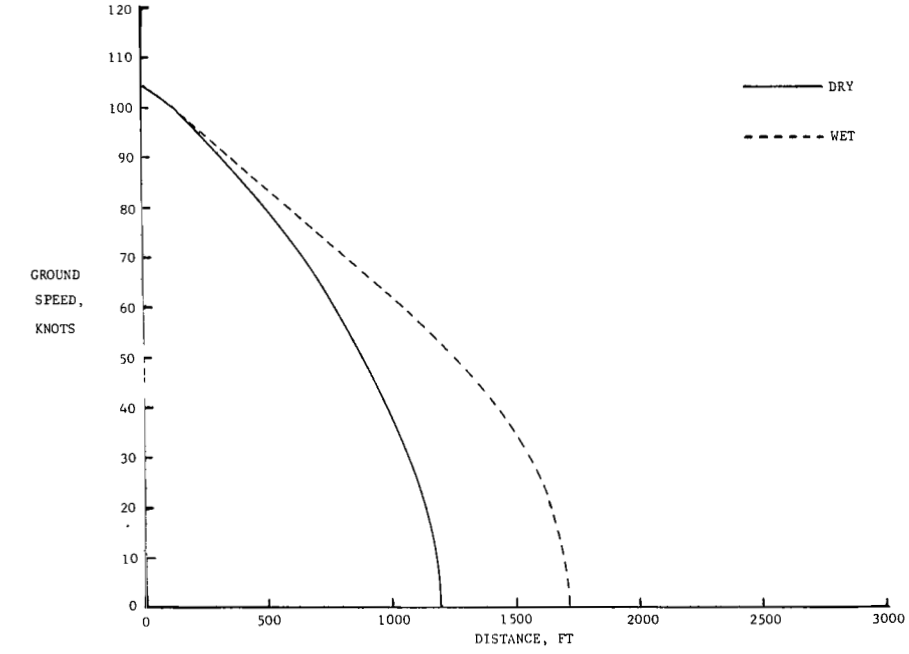

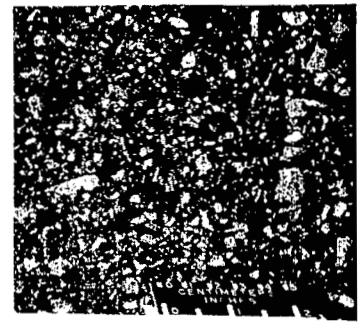

TEST SURFACE

(dd) Runway 31; Little Rock Air Force Base.

Figure A1.- Continued.

LITTLE ROCK, ARKANSAS RUNWAY: 6/24 DATE: 9-26-69

SUMMARY OF PAVEMENT TRACTION FACTORS BASED ON CORE SAMPLE ANALYSIS

PAVEMENT TYPE	PREDOMINANT CHARACTERISTICS	FACTORS	CLASSIFICATION FOR WET OPERATION
Asphaltic Concrete	Medium surface drainage. Exposed particles of sharp or fractured aggregate. Medium grained surface texture.	The surface texture characteristics of the asphaltic concrete from Little Rock AFB are described as follows: (1) The medium grained surface texture is defined by exposed particles of crushed aggregate. (2) The surface texture offers some surface drainage. The medium grained surface texture is a result of exposed particles of crushed rock. The structural characteristics below the surface are described as follows: (1) The coarse aggregate skeleton consists of fragmented particles of igneous rock well graded in size and ranging between 1/8 and 3/4 in. in diameter. (2) The dense graded overlay offers no subsurface drainage.	Medium

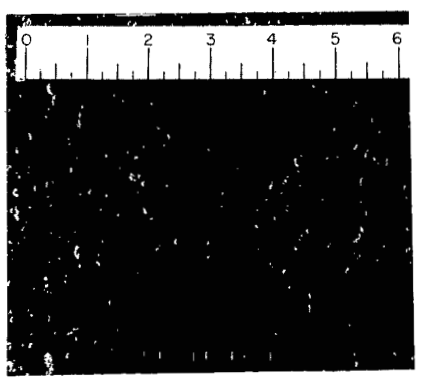

CORE SAMPLE SURFACE

CORE SAMPLE SURFACE PROFILE

(dd) Concluded.

Figure A1.- Continued.

SCOTT AFB, ILLINOIS			RUNWAY 13/31			DATE 10-14-69			STOPPING DISTANCE, FT			STOPPING DISTANCE RATIO			RCR
R/W REF. NO.	PAVEMENT SURFACE			WIND		TEMP., °F	ALT. SET., in. Hg	AIRCRAFT			AIRCRAFT		TEST VEHICLE	AIRCRAFT		TEST VEHICLE	
	MATERIAL	TEXTURE DEPTH, mm	CONDITION (WATER DEPTH), in.	DIR.	VEL., knots			HEADING	GROSS WEIGHT, lb	REVOLUTION COUNTER	ACCELERATION-TIME	REVOLUTION COUNTER	REVOLUTION COUNTER	ACCELERATION-TIME	REVOLUTION COUNTER	
32	SLURRY SEAL	0.184	DRY	330	4	40	30.33	310	200,600	1058	1080	248	1.30	1.50	1.80	22
			WET (.06)	0	7	40	30.33	310	195,700	1376	1620	447				19

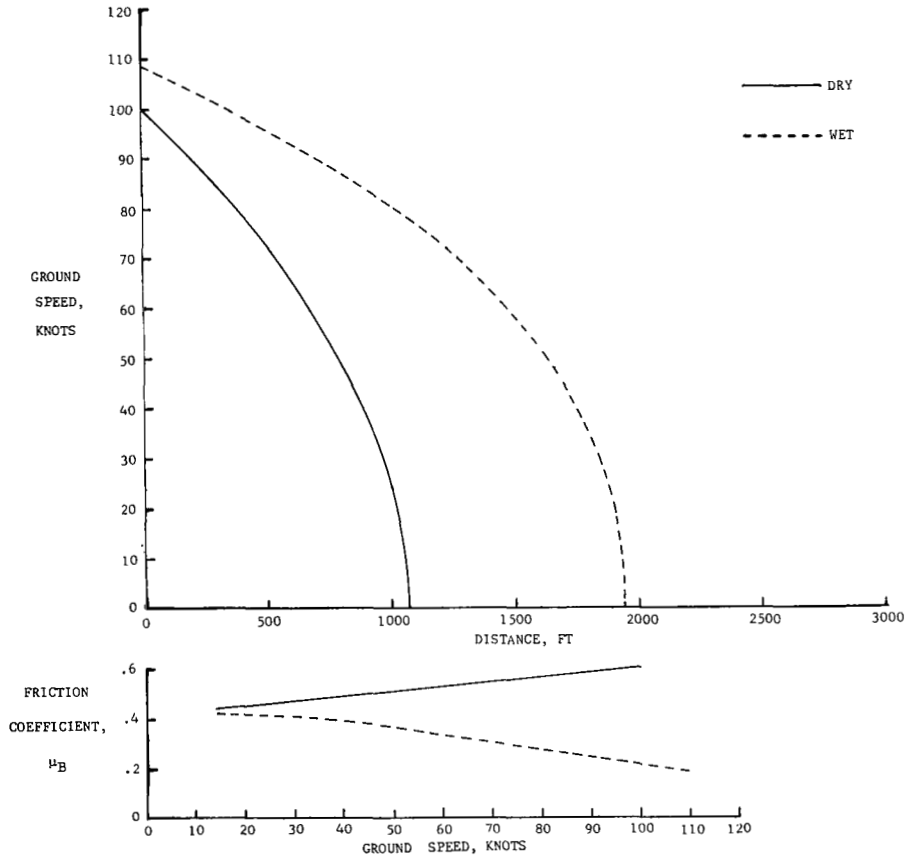

TEST SURFACE

(ee) Runway 32; Scott Air Force Base.

Figure A1.- Continued.

SCOTT AFB, ILLINOIS RUNWAY: 13/31 DATE: 10-14-69

SUMMARY OF PAVEMENT TRACTION FACTORS BASED ON CORE SAMPLE ANALYSIS

PAVEMENT TYPE	PREDOMINANT CHARACTERISTICS	FACTORS	CLASSIFICATION FOR WET OPERATION
Asphaltic Concrete	Medium to poor surface drainage. Exposed particles of limestone reflecting some wear or polish. Medium grained surface texture.	The surface texture characteristics reflected in the sample of asphaltic concrete from Scott AFB are described as follows: (1) The surface texture is defined by the exposed particles of crushed limestone (very little particle angularity above the surface). (2) The relatively smooth surface, resulting from the asphalt matrix and aggregate wear, offers very little surface drainage. The structural characteristics reflected at a depth of 1-1/2 in. below the surface are described as follows: (1) The coarse aggregate skeleton consists of fragmented particles of limestone (calcareous rock) ranging between 1/8 and 1 in. in diameter. (2) The dense graded mix offers no subsurface drainage.	Medium-Poor

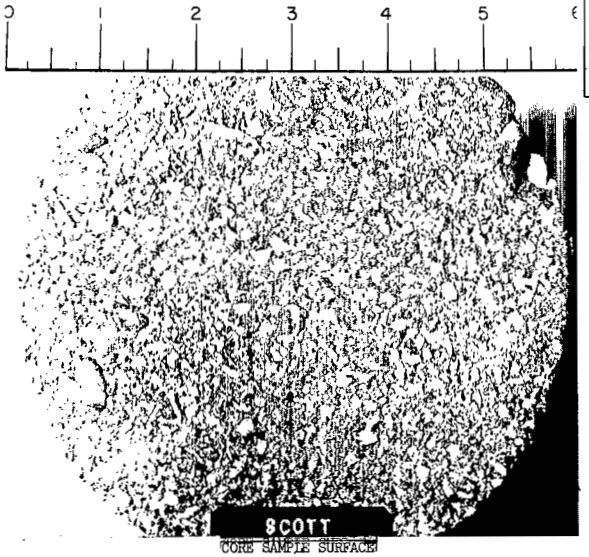

CORE SAMPLE SURFACE

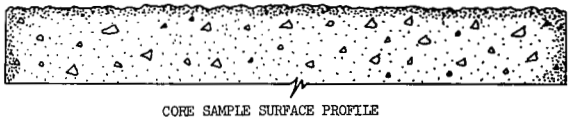
CORE SAMPLE SURFACE PROFILE

(ee) Concluded.

Figure A1.- Continued.

DOVER AFB, DELAWARE				RUNWAY 1/19				DATE 10-6-69		STOPPING DISTANCE, FT			STOPPING DISTANCE RATIO			RCR
R/W REF. NO.	PAVEMENT SURFACE			WIND		TEMP., °F	ALT. SET., in. Hg	AIRCRAFT		AIRCRAFT		TEST VEHICLE	AIRCRAFT		TEST VEHICLE	
	MATERIAL	TEXTURE DEPTH, mm	CONDITION (WATER DEPTH), in.	DIR.	VEL., knots			HEADING	GROSS WEIGHT, lb	REVOLUTION COUNTER	ACCELERATION-TIME	REVOLUTION COUNTER	REVOLUTION COUNTER	ACCELERATION-TIME	REVOLUTION COUNTER	
33	ASPHALT	0.387	DRY	230	2	44	30.29	010	198,400	998	1030	265	1.30	1.36	1.50	22.5
			WET (.04)	200	1	44	30.29	010	195,400	1293	1400	397				19

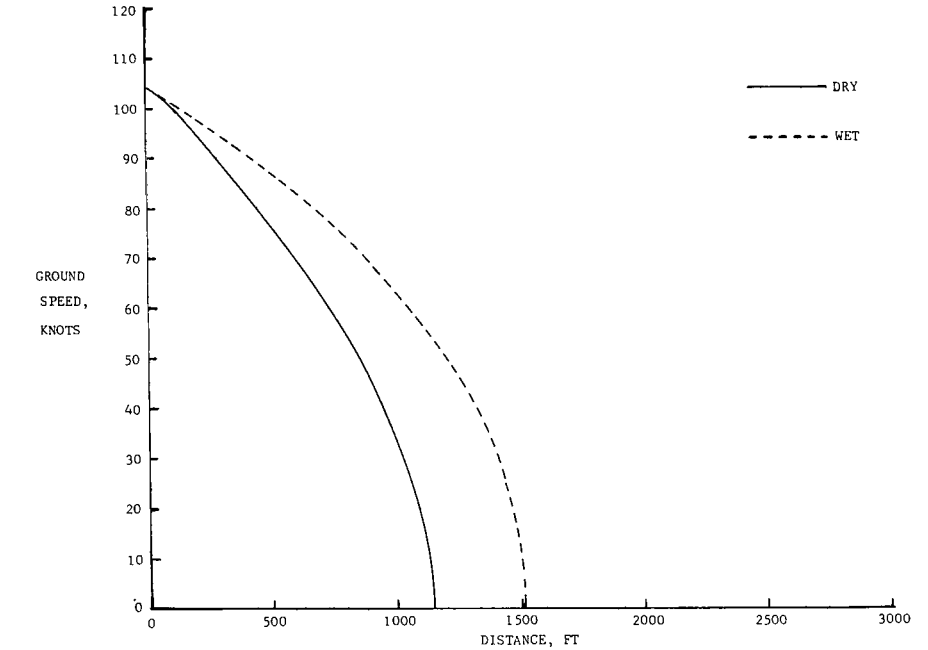

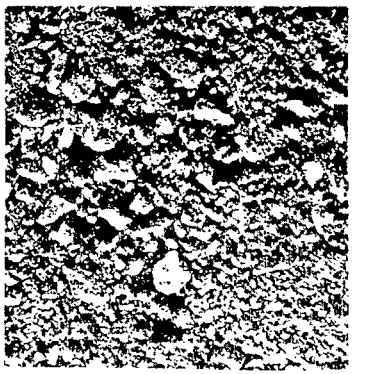

TEST SURFACE

(ff) Runway 33; Dover Air Force Base.

Figure A1.- Continued.

DOVER AFB, DELAWARE RUNWAY: 1/19 DATE: 10-6-69

SUMMARY OF PAVEMENT TRACTION FACTORS BASED ON CORE SAMPLE ANALYSIS

PAVEMENT TYPE	PREDOMINANT CHARACTERISTICS	FACTORS	CLASSIFICATION FOR WET OPERATION
Asphaltic Concrete	Medium surface drainage. Exposed particles of sharp aggregate. Medium grained texture.	The surface texture characteristics reflected in the sample of asphaltic concrete from Dover AFB are described as follows: (1) The medium level of surface texture is defined by exposed particles of fragmented rock approximately 1/4 in. in diameter. (2) The interparticle depressions provide some escape for fluid displacement. The structural characteristics reflected at a depth of 1-1/2 in. below the surface are as follows: (1) The coarse aggregate skeleton consists of crushed igneous rock. The majority of the particles are between 1/4 and 3/4 in. in diameter with a small percentage greater than 1 in. in diameter. (2) The dense graded mix offers no subsurface drainage.	Medium-Good

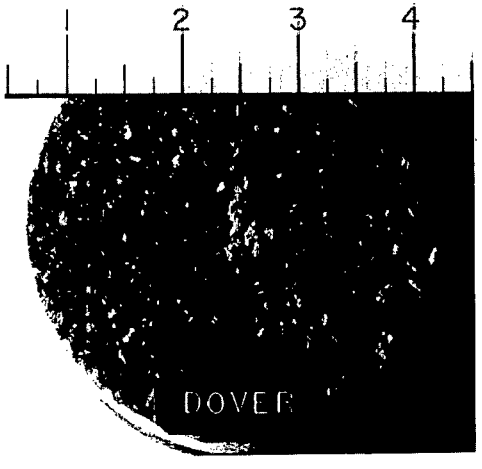

CORE SAMPLE SURFACE

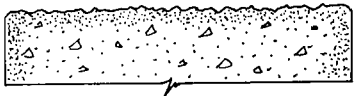

CORE SAMPLE SURFACE PROFILE

(ff) Concluded.

Figure A1.- Continued.

NELLIS AFB, NEVADA				RUNWAY 3R/21L			DATE 9-18-69		STOPPING DISTANCE, FT			STOPPING DISTANCE RATIO			RCR
R/W REF. NO.	PAVEMENT SURFACE			WIND		TEMP., °F	ALT. SET., in. Hg	AIRCRAFT	AIRCRAFT		TEST VEHICLE	AIRCRAFT		TEST VEHICLE	
	MATERIAL	TEXTURE DEPTH, mm	CONDITION (WATER DEPTH), in.	DIR.	VEL., knots			HEADING	GROSS WEIGHT, lb	REVOLUTION COUNTER	ACCELERATION-TIME	REVOLUTION COUNTER	REVOLUTION COUNTER	ACCELERATION-TIME	REVOLUTION COUNTER	
34	ASPHALT	0.144	DRY	—	0	63	29.96	030	197,500	1073	1090	308	1.30	1.33	1.60	26
			WET (.02)	—	0.	67	29.96	030	189,700	1400	1450	493				25

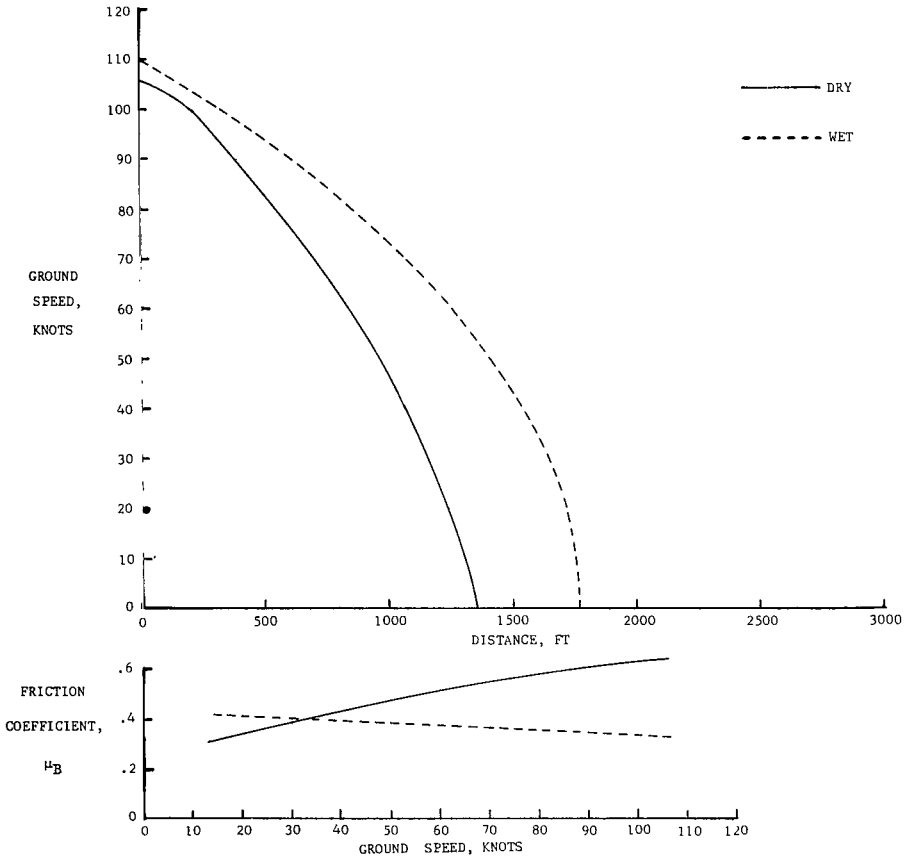

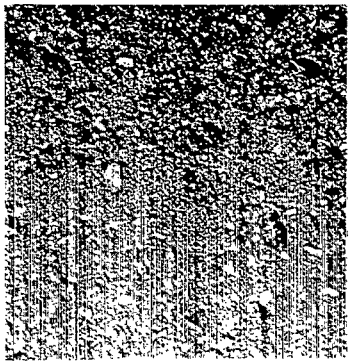

TEST SURFACE

(gg) Runway 34; Nellis Air Force Base.

Figure A1.- Continued.

NELLIS AFB, NEVADA RUNWAY: 3R/21L DATE: 9-18-69

SUMMARY OF PAVEMENT TRACTION FACTORS BASED ON CORE SAMPLE ANALYSIS

PAVEMENT TYPE	PREDOMINANT CHARACTERISTICS	FACTORS	CLASSIFICATION FOR WET OPERATION
Asphaltic Concrete	Medium to poor surface drainage. Exposed particles of sand and some rounded aggregate. Medium grained surface texture.	The surface texture characteristics of the sample of asphaltic concrete from Nellis AFB are described as follows: (1) The medium grained surface texture is defined primarily by the fine-aggregate-asphalt matrix forced to the surface during compaction. (2) A limited amount of surface drainage results from depressions adjacent to exposed particles of coarse aggregate. The structural characteristics reflected at a depth of 1-1/2 in. below the surface are as follows: (1) The well graded coarse aggregate skeleton consists of a mixture of rounded particles of igneous and calcareous rock (approximately 40 percent calcareous). (2) The dense graded mix offers no subsurface drainage even though there is evidence of air bubbles or voids in the matrix.	Medium

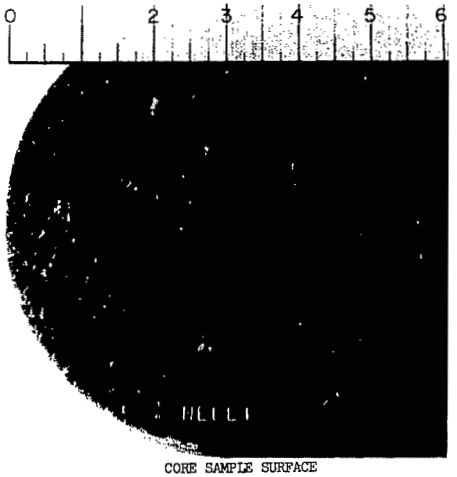

CORE SAMPLE SURFACE


CORE SAMPLE SURFACE PROFILE

(gg) Concluded.

Figure A1.- Continued.

NASA - WALLOPS STATION, VIRGINIA			RUNWAY 10/28			DATE 7-1-69 & 9-4-69		STOPPING DISTANCE, FT			STOPPING DISTANCE RATIO			RCR
R/W REF. NO.	PAVEMENT SURFACE			WIND		TEMP., °F	ALT. SET., in. Hg	AIRCRAFT		AIRCRAFT		TEST VEHICLE	AIRCRAFT		TEST VEHICLE	
	MATERIAL	TEXTURE DEPTH, mm	CONDITION (WATER DEPTH), in.	DIR.	VEL., knots			HEADING	GROSS WEIGHT, lb	REVOLUTION COUNTER	ACCELERATION-TIME	REVOLUTION COUNTER	REVOLUTION COUNTER	ACCELERATION-TIME	REVOLUTION COUNTER	
35	SLURRY SEAL	0.295	DRY	280	10	78	30.03	100	185,400	1080	1140	290	1.23	1.32	1.29	23
			WET (.02)	—	0	76	30.15	100	184,400	1330	1500	374				22

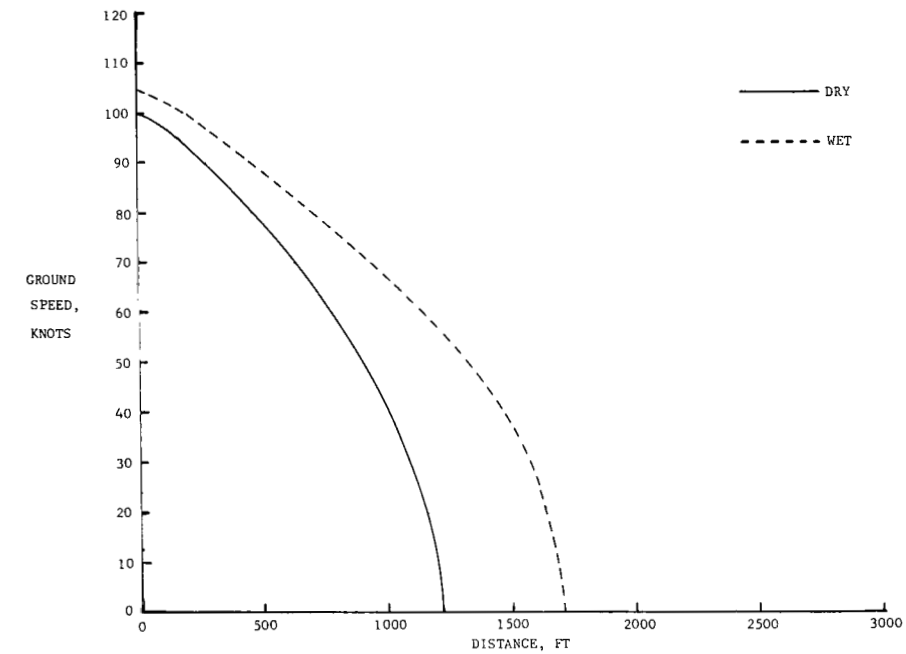

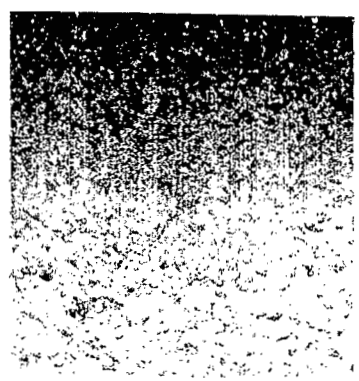

TEST SURFACE

(hh) Runway 35; NASA Wallops Station.

Figure A1.- Continued.

FARNBOROUGH RAFB, ENGLAND				RUNWAY 0/18				DATE 7-16-69		STOPPING DISTANCE, FT			STOPPING DISTANCE RATIO			RCR
R/W REF. NO.	PAVEMENT SURFACE			WIND		TEMP., °F	ALT. SET., in. Hg	AIRCRAFT		AIRCRAFT		TEST VEHICLE	AIRCRAFT		TEST VEHICLE	
	MATERIAL	TEXTURE DEPTH, mm	CONDITION (WATER DEPTH), in.	DIR.	VEL., knots			HEADING	GROSS WEIGHT, lb	REVOLUTION COUNTER	ACCELERATION-TIME	REVOLUTION COUNTER	REVOLUTION COUNTER	ACCELERATION-TIME	REVOLUTION COUNTER	
36	POROUS ASPHALT	———	DRY	240	10	86	29.78	180	187,600	1046	1080	346	1.17	1.20	1.05	20
			WET (.03)	240	7	86	29.78	180	185,900	1227	1300	364				23

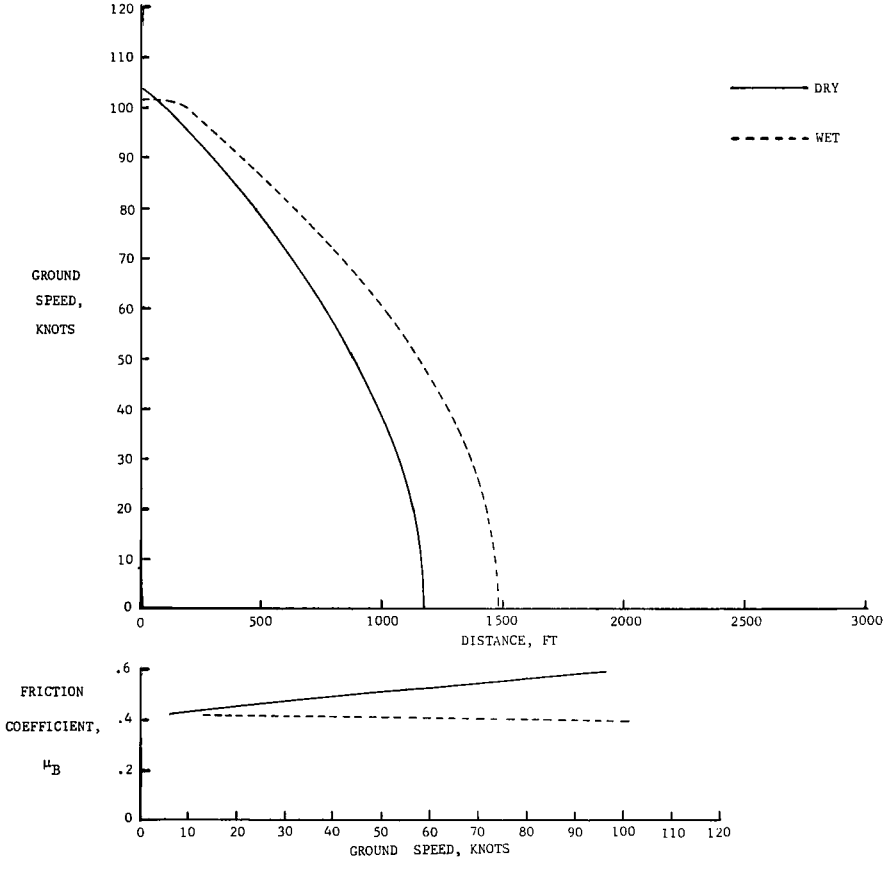

Test surface photograph not available.

(ii) Runway 36; Farnborough Royal Air Force Base.

Figure A1.- Continued.

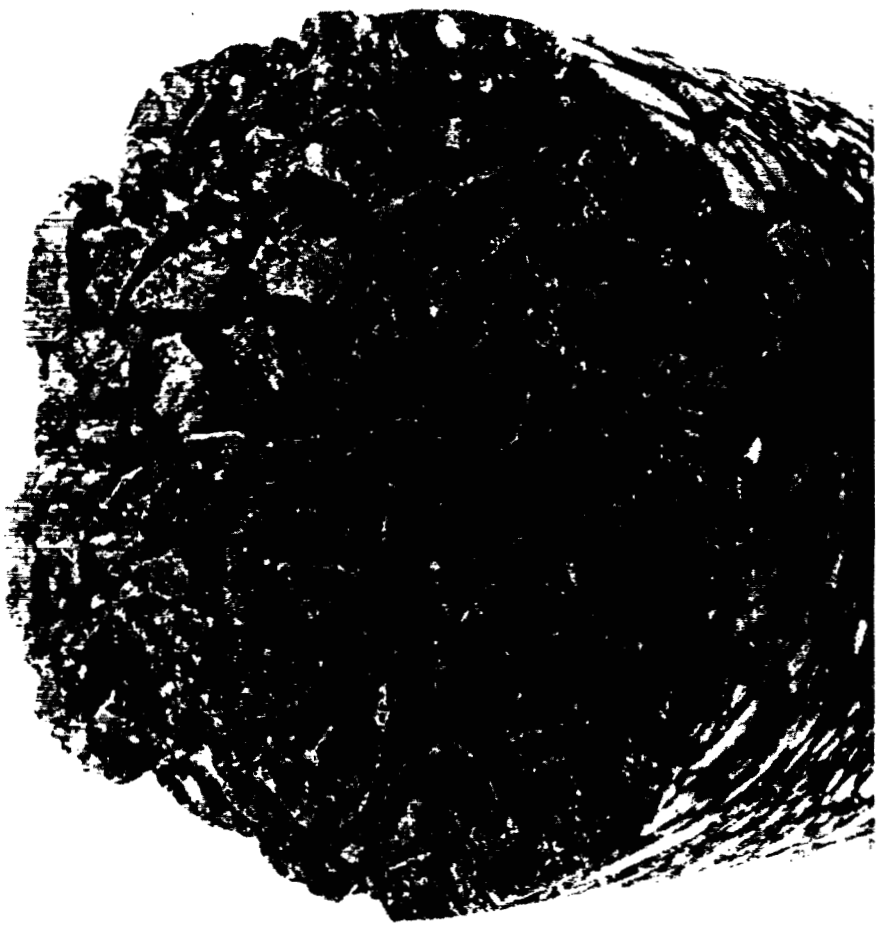

(ii) Concluded.

Figure A1.- Continued.

SHEMYA AFB, ALASKA RUNWAY 10/28							DATE 2-16-70		STOPPING DISTANCE, FT			STOPPING DISTANCE RATIO			
R/W REF. NO.	PAVEMENT SURFACE			WIND		TEMP., °F	ALT. SET., in. Hg	AIRCRAFT		AIRCRAFT		TEST VEHICLE	AIRCRAFT		TEST VEHICLE	RCR
	MATERIAL	TEXTURE DEPTH, mm	CONDITION (WATER DEPTH), in.	DIR.	VEL., knots			HEADING	GROSS WEIGHT, lb	REVOLUTION COUNTER	ACCELERATION-TIME	REVOLUTION COUNTER	REVOLUTION COUNTER	ACCELERATION-TIME	REVOLUTION COUNTER	
37	BASALT ASPHALT	—	DAMP(< .01)	0	14	36	28.92	280	192,000	1262	1270	370	1.14*	1.15*	1.42*	22
			DAMP & PUDDLED	350	9	32	28.92	280	196,000	1200	1290	377	1.09*	1.17*	1.48*	23

*Based on S_{DRY} of 1100 ft for aircraft and 260 and 254 ft for test vehicle

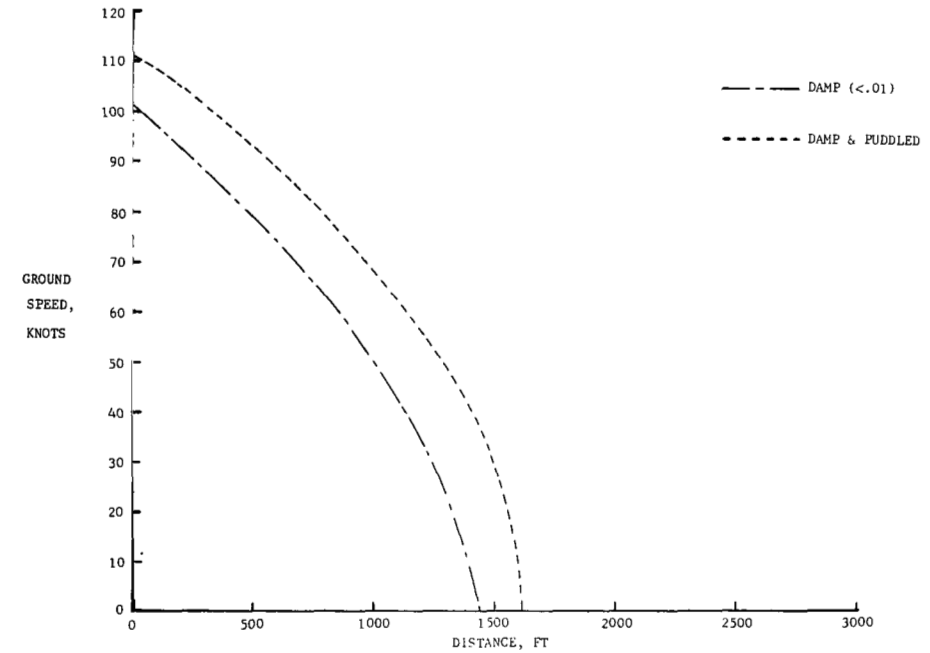

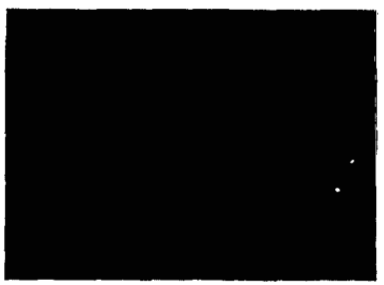

TEST SURFACE

(jj) Runway 37; Shemya Air Force Base.

Figure A1.- Continued.

SHEMYA AFB, ALASKA RUNWAY: 10/28 DATE: 2-16-70

SUMMARY OF PAVEMENT TRACTION FACTORS BASED ON CORE SAMPLE ANALYSIS

PAVEMENT TYPE	PREDOMINANT CHARACTERISTICS	FACTORS	CLASSIFICATION FOR WET OPERATION
Asphaltic Concrete	Good surface drainage. Exposed particles of degraded aggregate and some cavitation resulting from aggregate degradation. Coarse grained texture.	The surface texture characteristics of the sample of asphaltic concrete pavement from Shemya AFB are described as follows: (1) The medium to coarse grained surface texture is attributed to intraparticle fracturing and spalling of the exposed aggregate. (2) There is very little particle angularity extending above the matrix. (3) The depressions resulting from aggregate spalling provide a limited amount of surface drainage. The structural characteristics at a depth of 1-1/2 in. below the surface are described as follows: (1) The coarse aggregate skeleton consists of fractured particles of igneous rock well graded from 1/8 to 3/4 in. in diameter. (2) Some evidence of aggregate fracturing which may be attributed to overrolling or freeze/thaw damage. (3) The dense graded mix offers no subsurface drainage.	Medium-Good

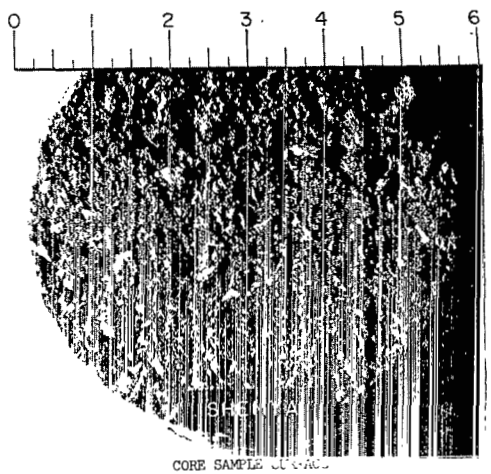

CORE SAMPLE SURFACE

CORE SAMPLE SURFACE PROFILE

(jj) Concluded.

Figure A1.- Continued.

MARHAM RAFB, ENGLAND				RUNWAY 6/24					DATE 7-22-69	STOPPING DISTANCE, FT			STOPPING DISTANCE RATIO			RCR
R/W REF. NO.	PAVEMENT SURFACE			WIND		TEMP., °F	ALT. SET., in. Hg	AIRCRAFT		AIRCRAFT		TEST VEHICLE	AIRCRAFT		TEST VEHICLE	
	MATERIAL	TEXTURE DEPTH, mm	CONDITION (WATER DEPTH), in.	DIR.	VEL., knots			HEADING	GROSS WEIGHT, lb	REVOLUTION COUNTER	ACCELERATION-TIME	REVOLUTION COUNTER	REVOLUTION COUNTER	ACCELERATION-TIME	REVOLUTION COUNTER	
38	POROUS ASPHALT	1.073	DRY	220	5	59	30.04	240	199,900	1005	1030	366	1.07	1.17	1.10	23
			WET (.02)	210	7	59	30.04	240	194,400	1073	1200	404				23

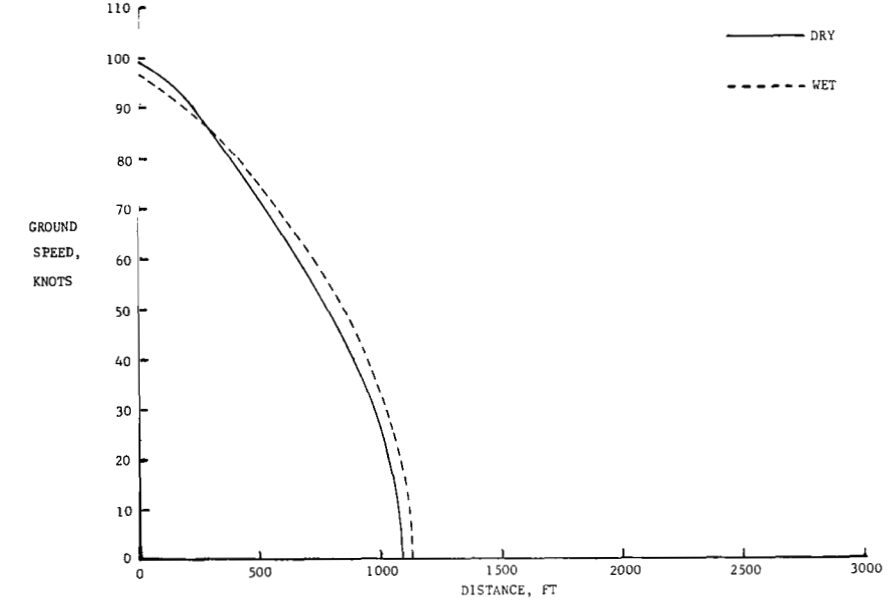

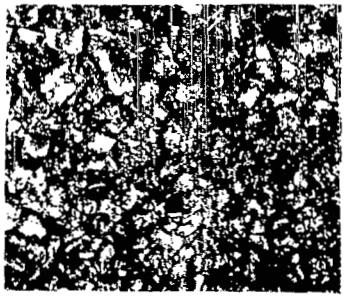

TEST SURFACE

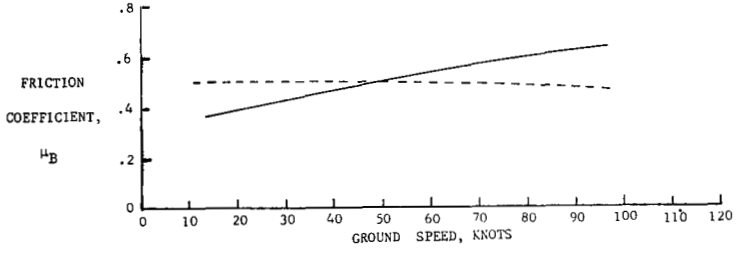

(kk) Runway 38; Marham Royal Air Force Base.

Figure A1.- Continued.

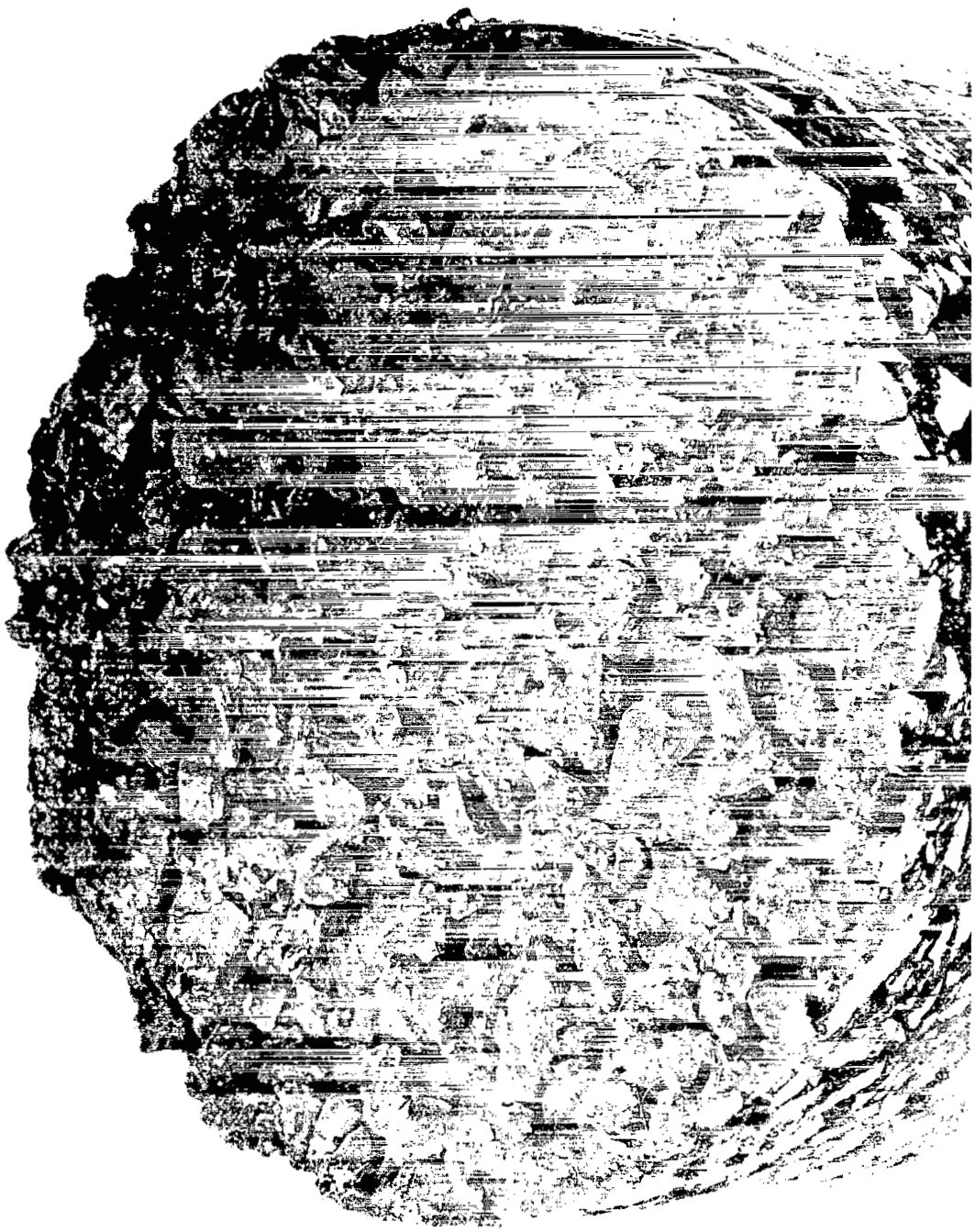

(kk) Concluded.

Figure A1.- Continued.

DYESS AFB, TEXAS				RUNWAY 16/34				DATE 6-25-69		STOPPING DISTANCE, FT			STOPPING DISTANCE RATIO			RCR
R/W REF. NO.	PAVEMENT SURFACE			WIND		TEMP., °F	ALT. SET., in. Hg	AIRCRAFT		AIRCRAFT		TEST VEHICLE	AIRCRAFT		TEST VEHICLE	
	MATERIAL	TEXTURE DEPTH, mm	CONDITION (WATER DEPTH), in.	DIR.	VEL., knots			HEADING	GROSS WEIGHT, lb	REVOLUTION COUNTER	ACCELERATION-TIME	REVOLUTION COUNTER	REVOLUTION COUNTER	ACCELERATION-TIME	REVOLUTION COUNTER	
40	LANDING MATS	0.085	DRY	140	4	73	29.89	340	187,900	1119	1250	295	2.11	1.99	1.66	23
			WET (.02)	140	4	74	29.89	340	182,600	2365	2490	489				23

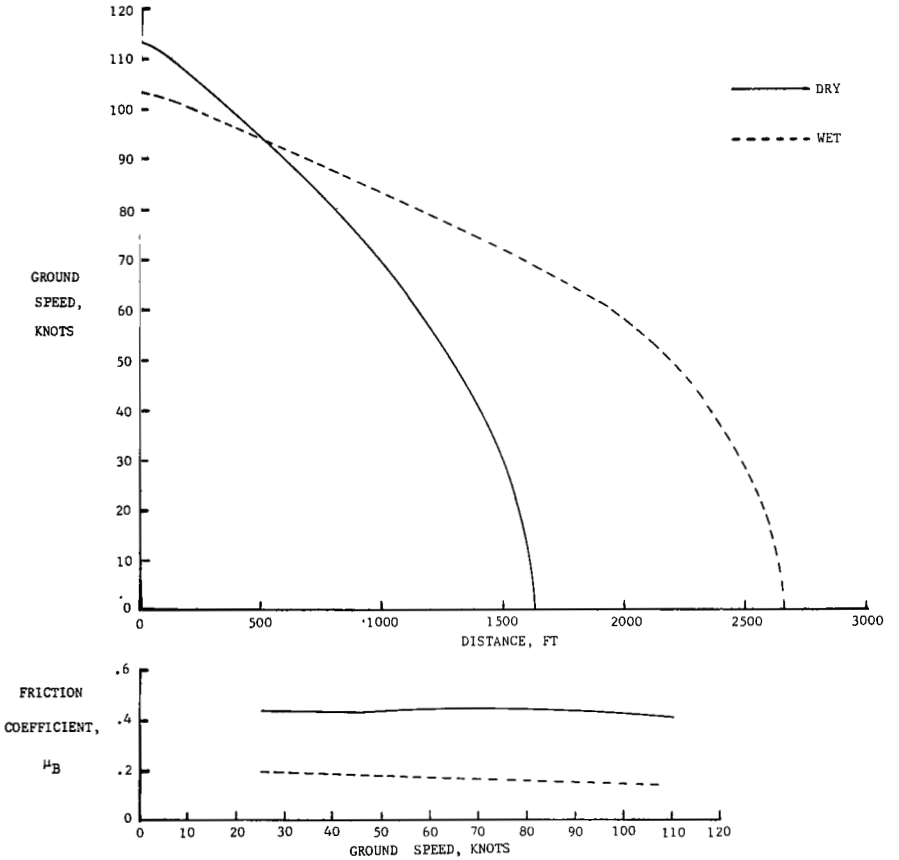

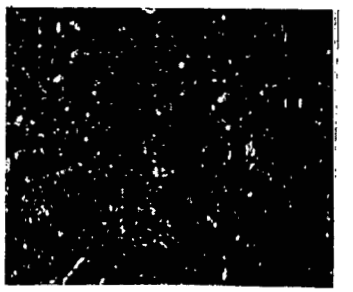

TEST SURFACE

(11) Runway 40; Dyess Air Force Base.

Figure A1.- Continued.

MALMSTROM AFB, MONTANA			RUNWAY 2/20 & RAMP				DATE 2-18-70 & 2-19-70		STOPPING DISTANCE, FT			STOPPING DISTANCE RATIO			RCR
R/W REF. NO.	PAVEMENT SURFACE			WIND		TEMP., °F	ALT. SET., in. Hg	AIRCRAFT		AIRCRAFT		TEST VEHICLE	AIRCRAFT		TEST VEHICLE	
	MATERIAL	TEXTURE DEPTH, mm	CONDITION (WATER DEPTH), in.	DIR.	VEL., knots			HEADING	GROSS WEIGHT, lb	REVOLUTION COUNTER	ACCELERATION-TIME	REVOLUTION COUNTER	REVOLUTION COUNTER	ACCELERATION-TIME	REVOLUTION COUNTER	
49	ASPHALT (R/W)	—	PATCHY SLUSH (0.1)	220	10	33	30.12	200	195,000	1765	2090	488	1.61*	1.90*	1.62*	14
41	CONCRETE (RAMP)	—	PACKED DRY SNOW AND ICE	200	10	27	30.05	020	221,800	3930	4230	1255	3.57*	3.84*	4.16*	4

*Based on S_{DRY} of 1100 ft for aircraft and 302 ft for test vehicle

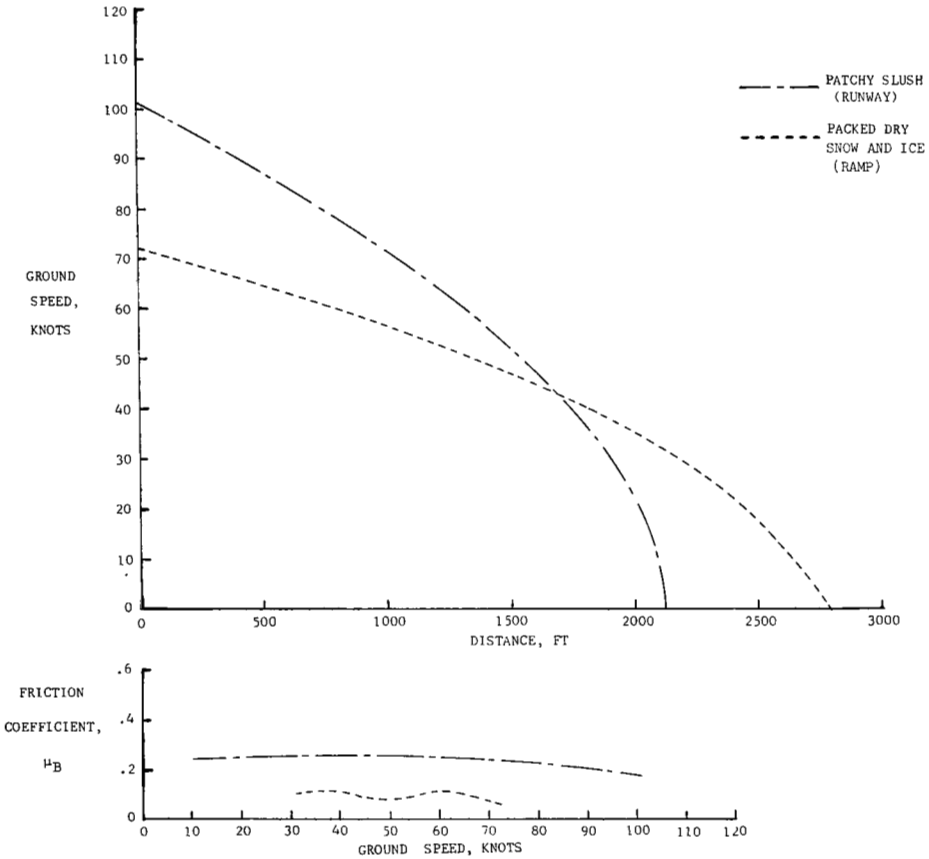

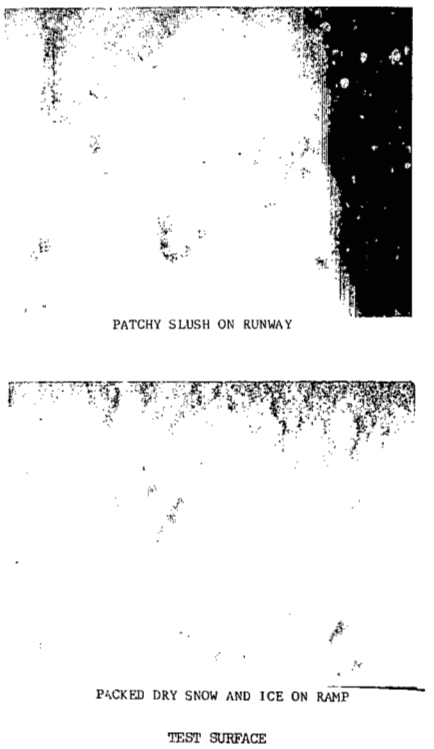

(mm) Runways 49 and 41; Malmstrom Air Force Base.

Figure A1.- Continued.

LORING AFB, MAINE			RUNWAY 1/19				DATE 1-30-70		STOPPING DISTANCE, FT			STOPPING DISTANCE RATIO			RCR
R/W REF. NO.	PAVEMENT SURFACE			WIND		TEMP., °F	ALT. SET., in. Hg	AIRCRAFT	AIRCRAFT		TEST VEHICLE	AIRCRAFT		TEST VEHICLE	
	MATERIAL	TEXTURE DEPTH, mm	CONDITION (WATER DEPTH), in.	DIR.	VEL., knots			HEADING	GROSS WEIGHT, lb	REVOLUTION COUNTER	ACCELERATION-TIME	REVOLUTION COUNTER	REVOLUTION COUNTER	ACCELERATION-TIME	REVOLUTION COUNTER	
42	SLURRY SEAL	——	GLAZED ICE AND SNOW	330	8	21	29.65	010	198,000	3610	4120	1027	3.28*	3.75*	3.40*	6

*Based on S_{DRY} of 1100 ft for aircraft and 302 ft for test vehicle

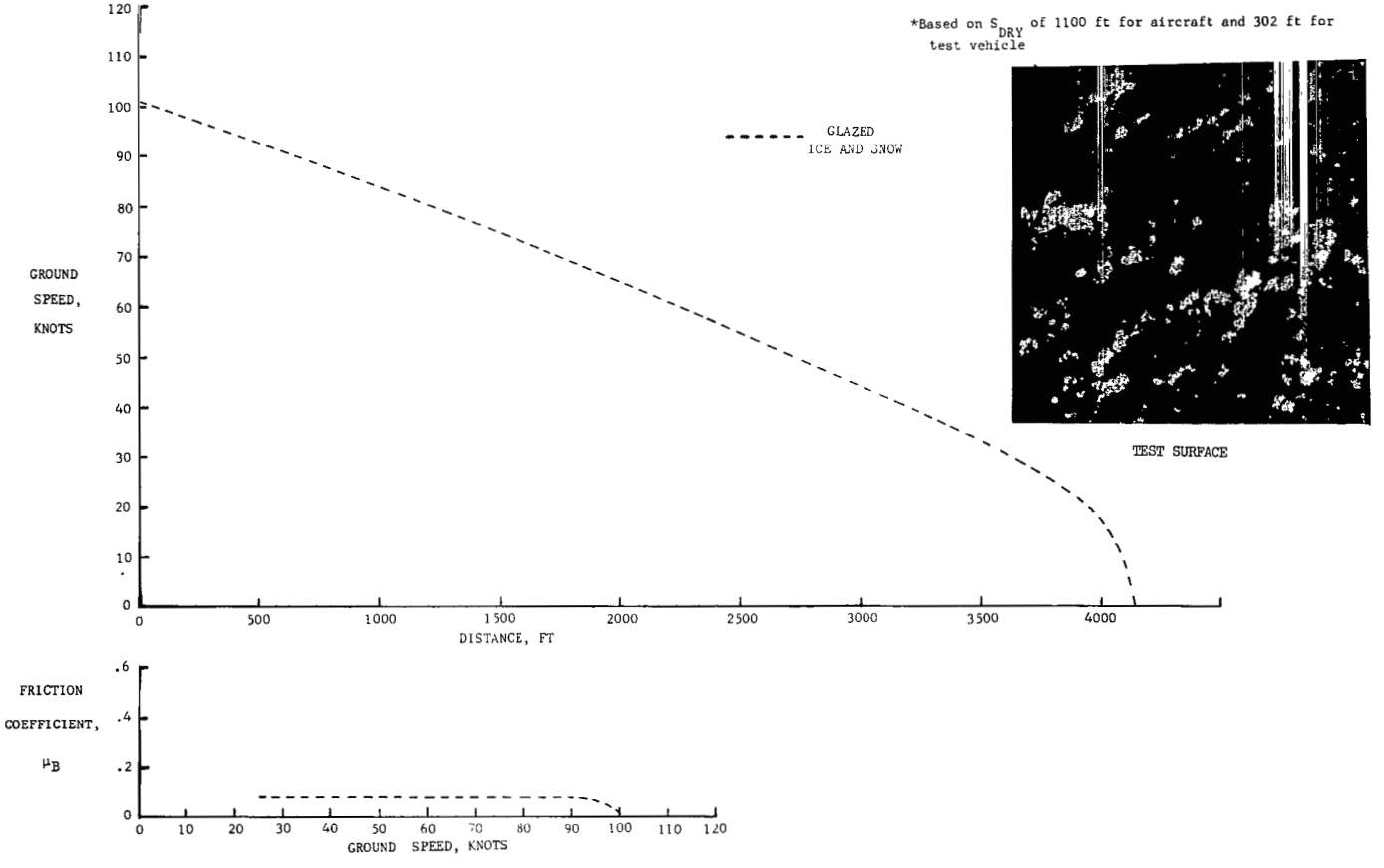

(nn) Runway 42; Loring Air Force Base.

Figure A1.- Continued.

WURTSMITH AFB, MICHIGAN			RUNWAY 6/24				DATE 2-2-70		STOPPING DISTANCE, FT			STOPPING DISTANCE RATIO			RCR
R/W REF. NO.	PAVEMENT SURFACE			WIND		TEMP., °F	ALT. SET., in. Hg	AIRCRAFT	AIRCRAFT		TEST VEHICLE	AIRCRAFT		TEST VEHICLE	
	MATERIAL	TEXTURE DEPTH, mm	CONDITION (WATER DEPTH), in.	DIR.	VEL., knots			HEADING	GROSS WEIGHT, lb	REVOLUTION COUNTER	ACCELERATION-TIME	REVOLUTION COUNTER	REVOLUTION COUNTER	ACCELERATION-TIME	REVOLUTION COUNTER	
43	CONCRETE	—	PACKED SNOW AND ICE	0	15	23	29.47	060	205,000	3520	3760	1100	3.20*	3.41*	3.65*	2

*Based on S_{DRY} of 1100 ft for aircraft and 302 ft for test vehicle

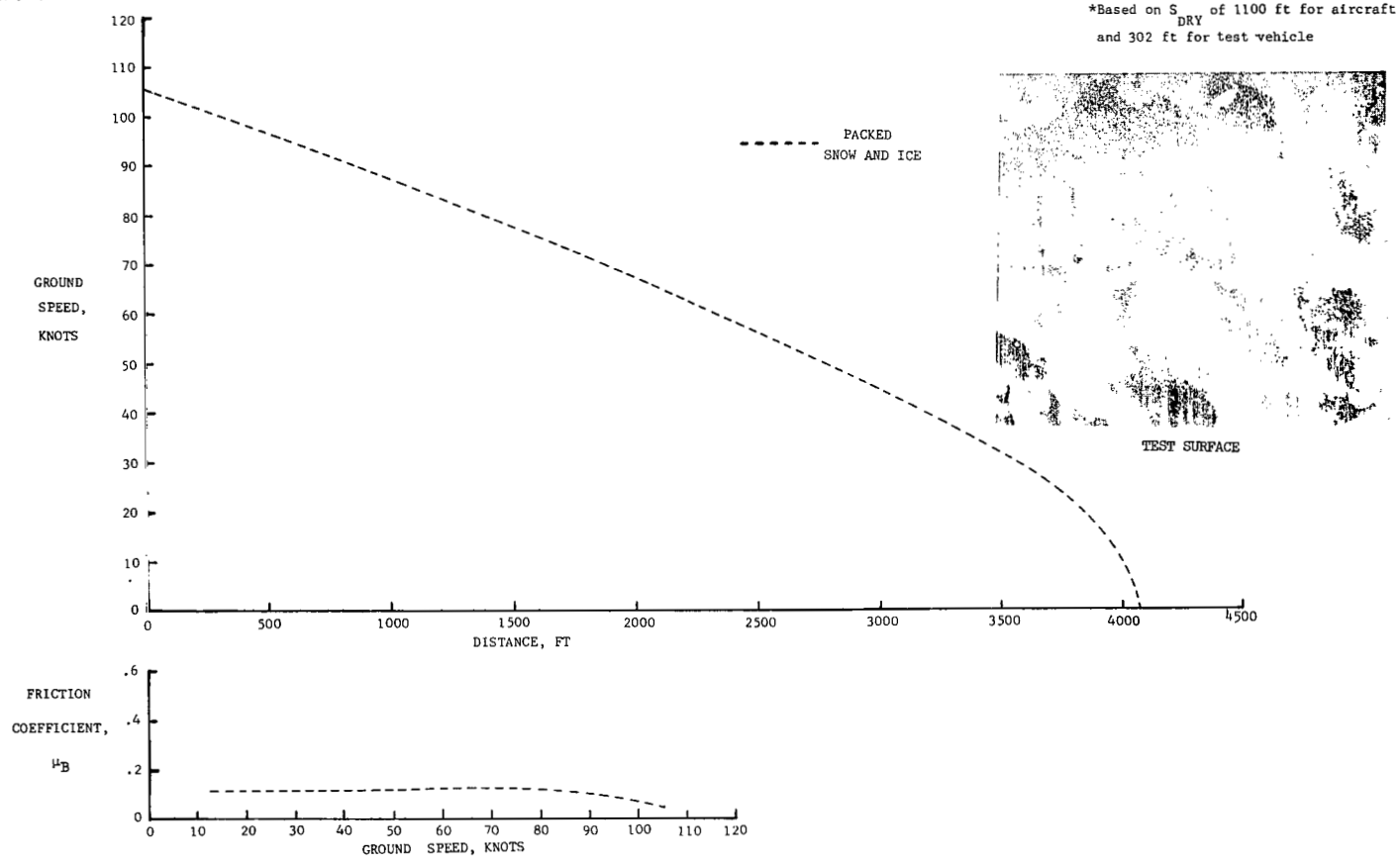

(oo) Runway 43; Wurtsmith Air Force Base.

Figure A1.- Continued.

GRISSOM AFB, INDIANA			TAXIWAY 4/22					DATE 2-10-70		STOPPING DISTANCE, FT			STOPPING DISTANCE RATIO			RCR
R/W REF. NO.	PAVEMENT SURFACE			WIND		TEMP., °F	ALT. SET., in. Hg	AIRCRAFT		AIRCRAFT		TEST VEHICLE	AIRCRAFT		TEST VEHICLE	
	MATERIAL	TEXTURE DEPTH, mm	CONDITION (WATER DEPTH), in.	DIR.	VEL., knots			HEADING	GROSS WEIGHT, lb	REVOLUTION COUNTER	ACCELERATION-TIME	REVOLUTION COUNTER	REVOLUTION COUNTER	ACCELERATION-TIME	REVOLUTION COUNTER	
44	ASPHALT	—	SOLID ICE & SNOW	280	8	22	29.89	220	200,000	—	3520	1190	—	3.20*	3.95*	5

*Based on S_{DRY} of 1100 ft for aircraft and 302 ft for test vehicle

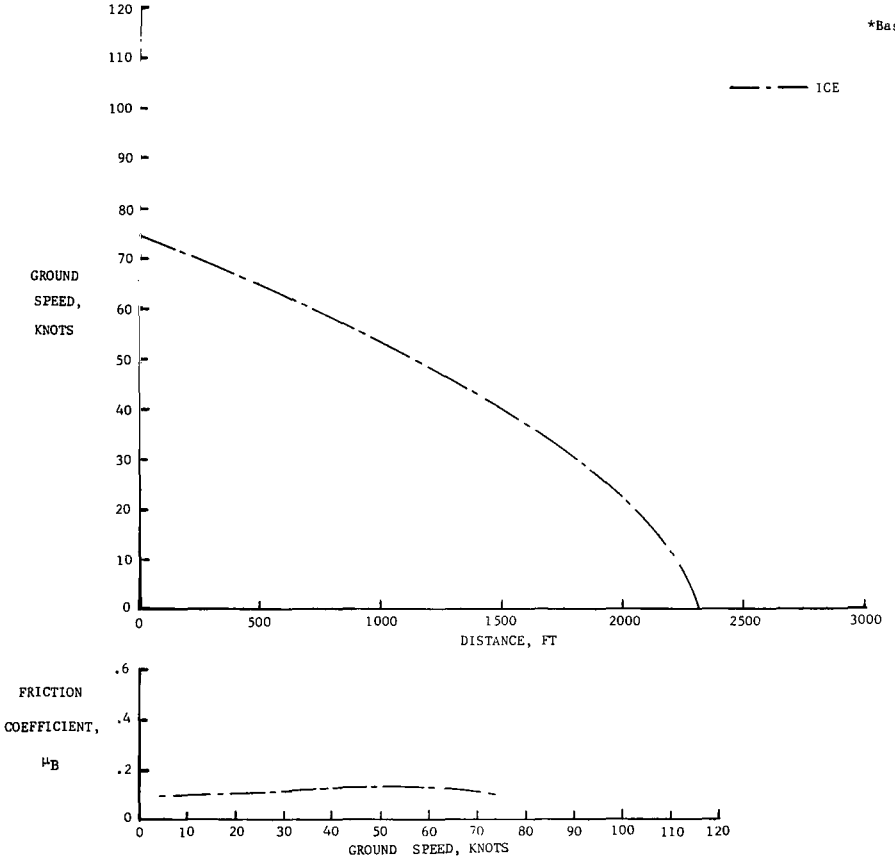

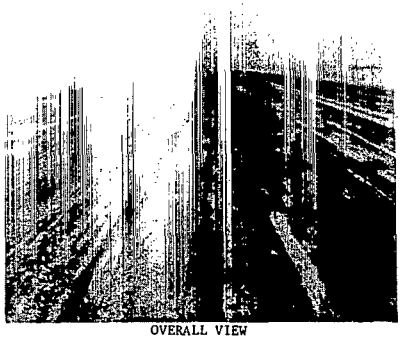

OVERALL VIEW

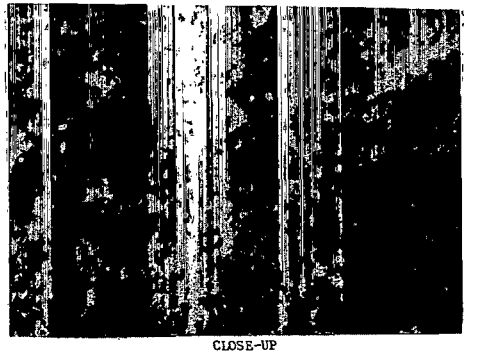

CLOSE-UP

TEST SURFACE

(pp) Runway 44; Grissom Air Force Base.

Figure A1.- Continued.

WRIGHT-PATTERSON AFB, OHIO RUNWAY 5R/23L							DATE 2-3-70		STOPPING DISTANCE, FT			STOPPING DISTANCE RATIO			
R/W REF. NO.	PAVEMENT SURFACE			WIND		TEMP., °F	ALT. SET., in. Hg	AIRCRAFT		AIRCRAFT		TEST VEHICLE	AIRCRAFT		TEST VEHICLE	RCR
	MATERIAL	TEXTURE DEPTH, mm	CONDITION (WATER DEPTH), in.	DIR.	VEL., knots			HEADING	GROSS WEIGHT, lb	REVOLUTION COUNTER	ACCELERATION-TIME	REVOLUTION COUNTER	REVOLUTION COUNTER	ACCELERATION-TIME	REVOLUTION COUNTER	
45	CONCRETE	—	DRY PACKED SNOW WITH ICE	320	5	8	29.91	230	207,700	3160	3030	875	2.87*	2.75*	2.90*	5.5

*Based on S_{DRY} of 1100 ft for aircraft and 302 ft for test vehicle

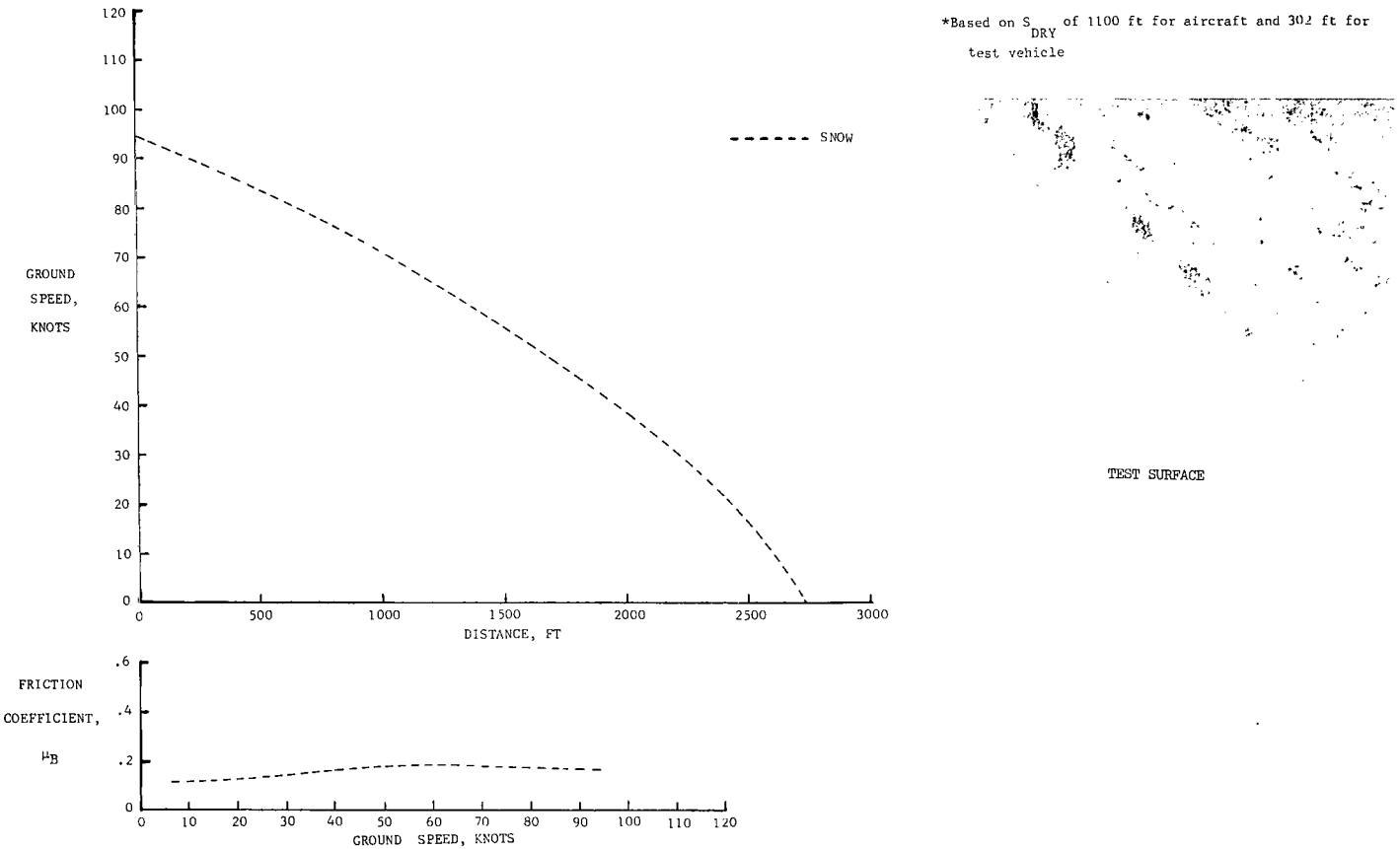

(qq) Runway 45; Wright-Patterson Air Force Base.

Figure A1.- Continued.

GLENVIEW NAS, ILLINOIS RUNWAY 17/35								DATE 2-11-70		STOPPING DISTANCE, FT			STOPPING DISTANCE RATIO			
R/W REF. NO.	PAVEMENT SURFACE			WIND		TEMP., °F	ALT. SET., in. Hg	AIRCRAFT		AIRCRAFT		TEST VEHICLE	AIRCRAFT		TEST VEHICLE	RCR
	MATERIAL	TEXTURE DEPTH, mm	CONDITION (WATER DEPTH), in.	DIR.	VEL., knots			HEADING	GROSS WEIGHT, lb	REVOLUTION COUNTER	ACCELERATION-TIME	REVOLUTION COUNTER	REVOLUTION COUNTER	ACCELERATION-TIME	REVOLUTION COUNTER	
46	CONCRETE & ASPHALT	—	PATCHY ICE AND SNOW	310	9	27	29.98	350	199,000	2425	2840	758	2.20*	2.58*	2.51*	—

*Based on S_{DRY} of 1100 ft for aircraft and 302 ft for test vehicle

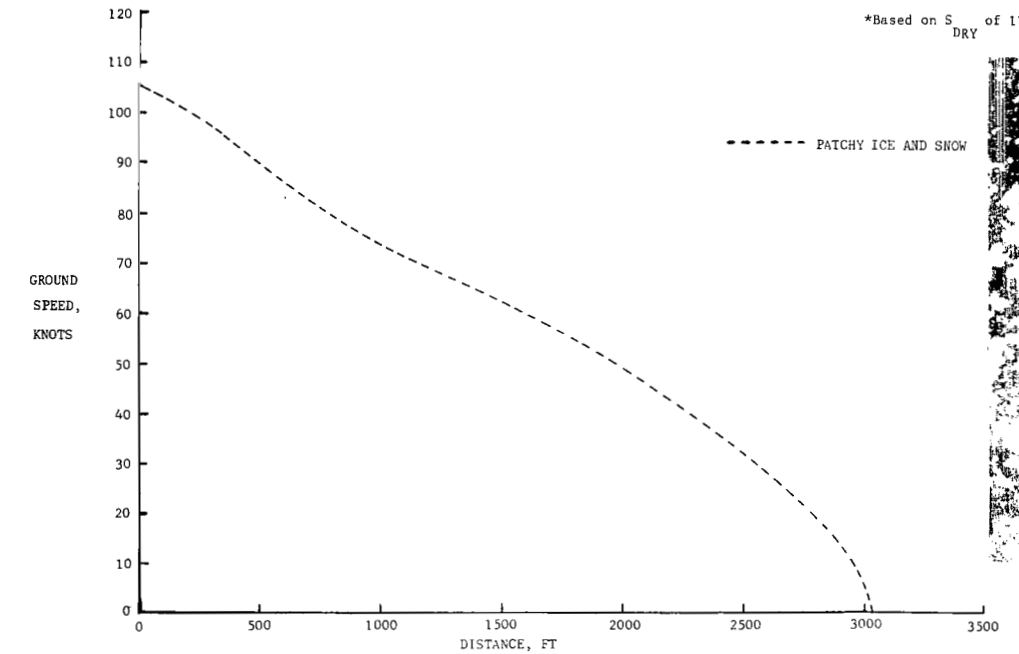

TEST SURFACE

(rr) Runway 46; Glenview Naval Air Station.

Figure A1.- Continued.

K. I. SAWYER AFB, MICHIGAN			RUNWAY 1/19			DATE 1-29-70 & 2-10-70		STOPPING DISTANCE, FT			STOPPING DISTANCE RATIO			RCR
R/W REF. NO.	PAVEMENT SURFACE			WIND		TEMP., °F	ALT. SET., in. Hg	AIRCRAFT		AIRCRAFT		TEST VEHICLE	AIRCRAFT		TEST VEHICLE	
	MATERIAL	TEXTURE DEPTH, mm	CONDITION (WATER DEPTH), in.	DIR.	VEL., knots			HEADING	GROSS WEIGHT, lb	REVOLUTION COUNTER	ACCELERATION-TIME	REVOLUTION COUNTER	REVOLUTION COUNTER	ACCELERATION-TIME	REVOLUTION COUNTER	
47	SLURRY SEAL	—	PATCHY SNOW AND ICE	330	13	11	29.93	010	195,000	2300	2690	493	2.09*	2.45*	1.63*	—
			DRY DRIFTING SNOW	0	18	23	29.90	010	201,000	2220	2730	685	2.02*	2.48*	2.27*	7.5

*Based on S_{DRY} of 1100 ft for aircraft and 302 ft for test vehicle

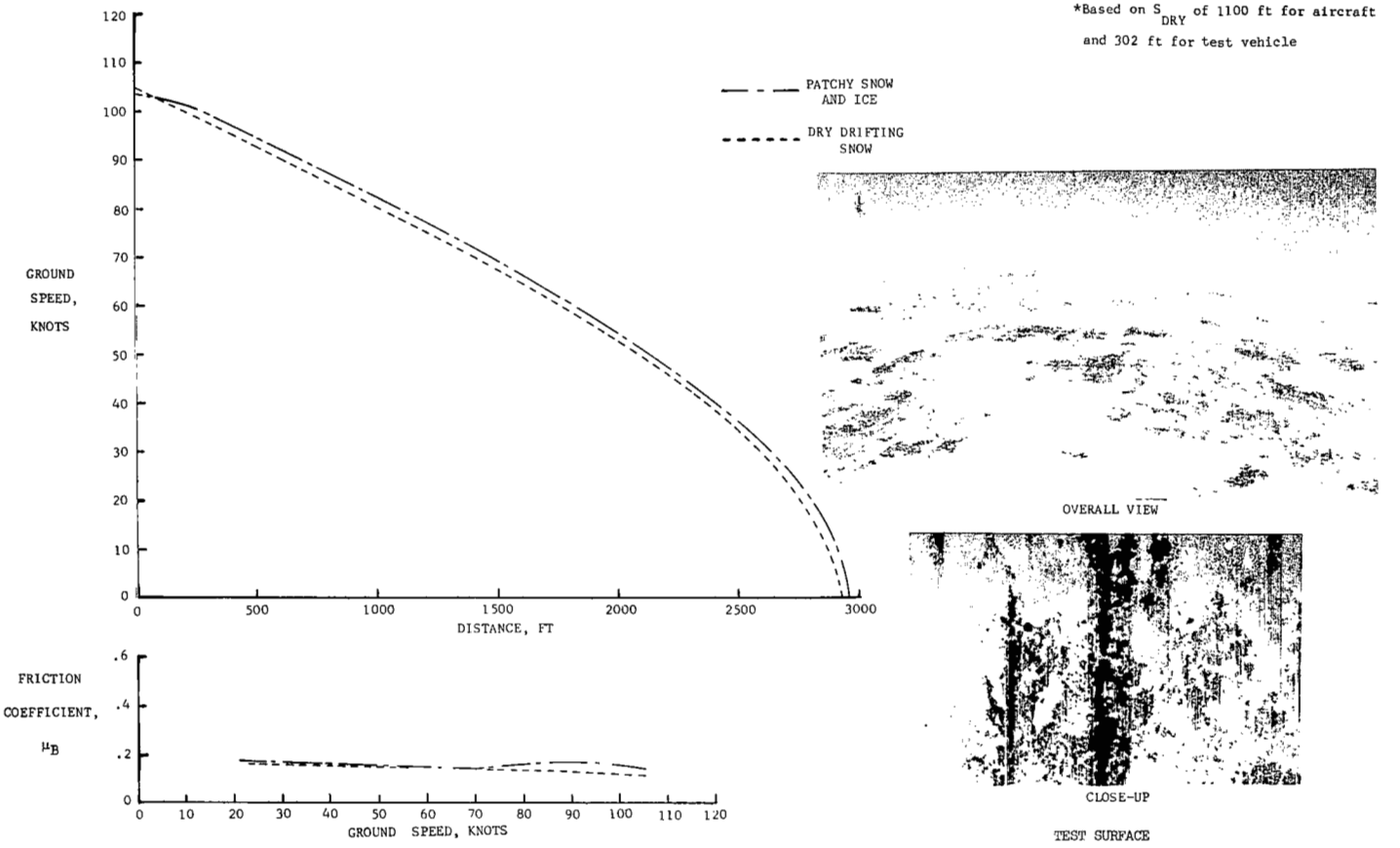

(ss) Runway 47; K. I. Sawyer Air Force Base.

Figure A1.- Continued.

McGUIRE AFB, NEW JERSEY			RUNWAY 18/36				DATE 2-4-70		STOPPING DISTANCE, FT			STOPPING DISTANCE RATIO			RCR
R/W REF. NO.	PAVEMENT SURFACE			WIND		TEMP., °F	ALT. SET., in. Hg	AIRCRAFT		AIRCRAFT		TEST VEHICLE	AIRCRAFT		TEST VEHICLE	
	MATERIAL	TEXTURE DEPTH, mm	CONDITION (WATER DEPTH), in.	DIR.	VEL., knots			HEADING	GROSS WEIGHT, lb	REVOLUTION COUNTER	ACCELERATION-TIME	REVOLUTION COUNTER	REVOLUTION COUNTER	ACCELERATION-TIME	REVOLUTION COUNTER	
48	ASPHALT	——	PATCHY ICE AND SNOW	330	23	14	30.18	360	197,200	1975	2060	656	1.80*	1.87*	2.17*	9.5

*Based on S_{DRY} of 1100 ft for aircraft and 302 ft for test vehicle

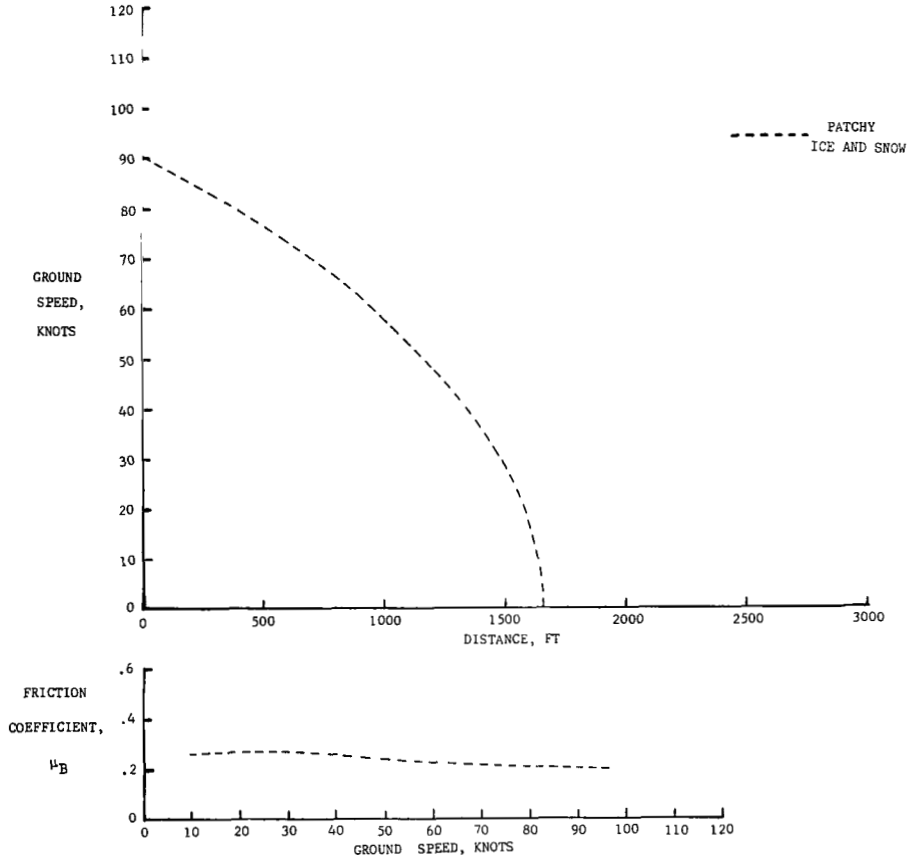

Test surface photograph not available.

(tt) Runway 48; McGuire Air Force Base.

Figure A1.- Concluded.

APPENDIX B

COMPUTATION OF TEST DATA

Aircraft Data Reduction

Accelerometer data obtained onboard the aircraft during the braking tests were reduced by use of a high-speed digital computer to provide time histories of braking distance, friction coefficient, and ground speed. Stopping distance and initial ground speed, $V_{G,O}$, were determined in an alternate manner by utilizing a calibrated nosewheel counter. Corrected stopping distances were then obtained from the appropriate accelerometer time history by either extrapolation or interpolation to $V_{G,O} = 100$ knots and extrapolation to $V_{final} = 0$ knots since the brakes were released prior to achieving a full stop; that is,

$$D_{corr} = D + \Delta D_B + \Delta D_{final} \tag{B1}$$

where

D uncorrected stopping distance from time history

ΔD_B incremental distance above or below $V_{G,O} = 100$ knots where brake engagement occurred, that is,

$$\Delta D_B = \frac{(168.9)^2 - V_{G,B}^2}{-2\vec{a}_{x,B}} \tag{B2}$$

ΔD_{final} incremental distance from brake release to $V_G = 0$, or

$$\Delta D_{final} = \frac{V_{G,final}^2}{-2\vec{a}_{x,final}} \tag{B3}$$

Calculations of braking friction coefficient, velocity, and distance time histories were made.

The braking friction coefficient equation

$$\mu_B = \frac{W}{gF_{z,m}}\left[\frac{T_n}{W}\cos(\alpha + \epsilon) - \vec{a}_x - \frac{C_D q}{W/S}\right] \tag{B4}$$

incorporates the effects of antiskid performance, aerodynamic lift and drag as measured by the accelerometer and removes the effects of idle thrust where μ_B is referred to the main-gear vertical load $F_{z,m}$; that is,

$$F_{z,m} = W\left[\left(1 - \frac{C_L q}{W/S}\right)\left(1 - \frac{\Delta x_g}{\Delta x}\right) + \frac{h_{cg}}{\Delta x}\left(\frac{C_D q}{W/S} - \frac{T_n}{W} + \frac{\bar{a}_x}{g}\right) + \frac{C_{m,g} q \bar{c}}{\Delta x (W/S)}\right]$$

Longitudinal acceleration is determined and corrected for attitude changes:

$$\bar{a}_x = a_x - g \sin(\alpha - \alpha_o) = (a_{x,RDG} - a_{x,Zero}) K_{a,x} - g \sin(\alpha - \alpha_o)$$

T_n is the installed idle thrust obtained from manufacturers' data as a function of airspeed and ambient conditions and $C_{m,g} = 0.072$ (take-off flaps, spoilers deployed). The ground speed time history was obtained from

$$V_G = V_{G,o} + \int_0^t \bar{a}_x \, dt \tag{B5}$$

wherein $V_{G,o}$ was determined from an average of the eight main-gear wheel velocities prior to brake engagement. Distance time histories were then obtained by integration as

$$D = \int_0^t V_G \, dt \tag{B6}$$

A value for three-point aerodynamic drag coefficient was obtained from unbraked tare runs over the test speed range by using

$$C_D = \mu_R C_L - \frac{W/S}{q}\left\{\frac{\bar{a}_x}{g} - \frac{T_n}{W}\cos(\alpha + \epsilon) + \mu_R\left[1 - \frac{T_n}{W}\sin(\alpha + \epsilon)\right] - \sin(\alpha - \alpha_o)\right\} \tag{B7}$$

where

$\mu_R = 0.015$ (assumed)

$C_L = 0.310$ (manufacturers' value with take-off flaps and spoilers deployed)

$\epsilon = 0^o$ (thrust misalinement angle)

T_n manufacturers' installed idle thrust value for velocities and ambient conditions of tare run

APPENDIX B

Auxiliary equations used in the reduction of accelerometer data were as follows:

$$V_A = V_G + V_w \tag{B8}$$

$$q = 0.0002916 \frac{p_a}{T_a} V_A^2 \tag{B9}$$

A three-view drawing of the test aircraft with its pertinent geometric characteristics is shown in figure B1.

Although it is felt that the inclusion of runway slope data in the present computations of friction coefficients, stopping distance, and the overall rating of runways with regard to slipperiness would have been desirable, insufficient civil engineering data were available to incorporate this correction to the present data; that is, only average runway slope data are available for specific runways, wherein, several varying slopes were observed within a region covered by the full-stop tests of the present investigation. Also, ambient corrections to provide stopping distances for each runway at sea level under standard dry conditions were not made since it is generally felt that these corrections would be well within the accuracy of the present data.

The alternate method for determining aircraft stopping distance and initial velocity, as previously mentioned, utilized a nose wheel counter calibrated to measure ground speed at brake engagement and also braking distance. The latter braking distance data were corrected to a brake engagement speed of 100 knots by

$$D_{corr} = \frac{(168.9)^2}{V_{G,B}^2} D \tag{B10}$$

where

$V_{G,B}$ ground speed at brake engagement as determined from calibrated nose wheel counter, ft/sec

D uncorrected counter braking distance, ft

NASA Diagonal-Braked Test Vehicle Data Reduction

Stopping distance data obtained from the test vehicle counter mounted on the fifth wheel were corrected in a manner similar to those obtained from the aircraft instrumented nose wheel; that is,

$$D_{corr} = \frac{(88)^2}{V_{G,B}^2} D \qquad \text{(B11)}$$

wherein the test vehicle data were corrected to a brake engagement speed of 60 mph and D is the uncorrected braking distance for the test vehicle.

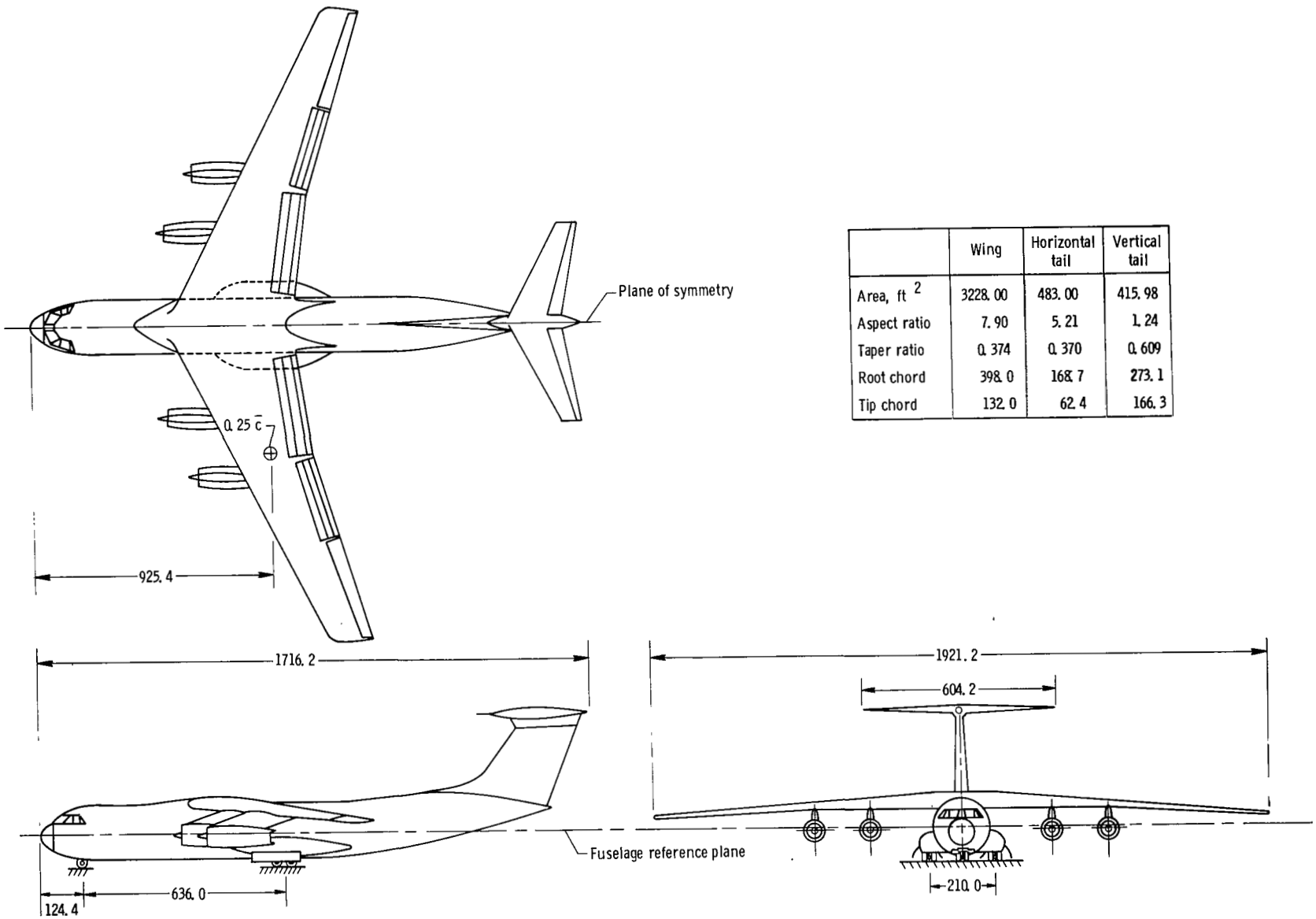

	Wing	Horizontal tail	Vertical tail
Area, ft ^{2}	3228.00	483.00	415.98
Aspect ratio	7.90	5.21	1.24
Taper ratio	0.374	0.370	0.609
Root chord	398.0	168.7	273.1
Tip chord	132.0	62.4	166.3

Figure B1.- Three-view drawing of C-141A test aircraft. All dimensions are in inches unless otherwise specified.

APPENDIX C

CIVIL ENGINEERING DESCRIPTIONS OF RUNWAYS TESTED

This appendix presents the civil engineering descriptions of the runways that were supplied by the specific Airport or Air Force Base. Such data were not available for the following:

Runway	Location
2	England AFB, Louisiana
3	Marham RAFB, England
14	Chicago Midway Airport, Illinois
17	Mildenhall USAFE, England
21	Myrtle Beach AFB, South Carolina
23	Otis AFB, Massachusetts
24	Aviano USAFE, Italy
25	Alconbury USAFE, England
28	Pope AFB, North Carolina
33	Dover AFB, Delaware
35	NASA Wallops Station, Virginia
37	Shemya AFB, Alaska
39	Meigs Airport, Illinois
40	Dyess AFB, Texas
41	Malmstrom AFB, Montana
42	Loring AFB, Maine
43	Wurtsmith AFB, Michigan
44	Grissom AFB, Indiana
45	Wright-Patterson AFB, Ohio
46	Glenview NAS, Illinois
47	K. I. Sawyer AFB, Michigan
48	McGuire AFB, New Jersey
49	Malmstrom AFB, Montana

Data for runways 4 and 15, 10 and 11, and 26 and 36 have been combined.

References in the civil engineering descriptions of the British runways are to items included in the British Ministry of Public Building and Works Airfield Specifications.

APPENDIX C

DYESS AFB, TEXAS – RUNWAY 1

Test runway: 16/34 Length, 13 500 ft Width, 300 ft	Landing approach 34
Construction in 1953	11 700 ft PCC south end, first 1000 ft by 300 ft, rigid 16 in. thick. From north end, first 650 ft, 19 in. thick; next 500 ft, 10 in. thick; next 2300 ft, 15 in. thick. Interior keel, 18 in. thick.
	Surface treatment, rigid nonskid (belt finished). All emulsified asphalt; slurry surface treatment.
	Characteristics of large aggregate: PCC; 2 in. maximum crushed limestone and angular gravel; bituminous, 3/4 in. maximum size.
Construction in 1955	Additional 2300 ft (north extension)
Construction in 1964	Runway widened to 300 ft and 75 ft, interior keel (belted).
Construction in 1965 and 1967	Asphalt runway given slurry surface treatment. Cost less than $0.10 per square yard.
Transverse slope	$1\frac{1}{2}\%$
Longitudinal grade	Varies from 0 to 0.3%
Precipitation	Rain – 22.55 in. Snow – 3.60 in. Highest month – May (3.68 in.) Lowest month – January (0.88 in.)
Drainage	Adequate
Pavement conditions	Good. Some patching needed occasionally on north 3000 ft.

APPENDIX C

OFFUTT AIR FORCE BASE, NEBRASKA – RUNWAYS 4 and 15

Test runway: 12/30 Length, 10 000 ft Width, 300 ft	Landing approach 30
Construction in 1941	Station 0 + 00 to station 57 + 00
Construction in 1954	Station 57 + 00 to station 100 + 00
Construction in 1956	Reconstructed station 0 + 00 to station 57 + 00.
Construction in 1969	Grooved 145 000 sq yd of runway with 1/4 in. by 1/4 in. grooves on $1\frac{1}{4}$ in. centers at a cost of $133 467.
Longitudinal grade	0 + 00 to 20 + 50 -0.985% 20 + 00 to 38 + 00 -0.320% 38 + 00 to 55 + 00 -0.958% 55 + 00 to 80 + 00 -1.00% 80 + 00 to 100 + 00 -0.00%
Precipitation	Rain – 27.85 in. Snow – 27.90 in. Highest rain month – June (4.64 in.) Lowest rain month – January (0.72 in.) Highest snow month – February (6.6 in.) Lowest snow month – May (0.1 in.)
Drainage	Good
Pavement condition	Good. Minor repair of spalling and joint seal each year.

APPENDIX C

ELLINGTON AFB, TEXAS – RUNWAY 5

Test runway: 04/22 Length, 6800 ft Width, 150 ft	Landing approach 04
Construction in 1941	Original 5000 ft runway consisted of 10 to 11 in. of PCC with a burlap drag finish and aggregate from Eagle Lake $1\frac{1}{2}$ in. maximum grain size, very sound and hard.
Construction in 1956	Runway extended on the 04 end consisted of 10 to 11 in. of PCC for 1800 ft with burlap drag finish and aggregate from Eagle Lake $1\frac{1}{2}$ in. maximum grain size, very sound and hard. Also overlayed 2388 ft of 22 end.
Longitudinal grade	0 + 00 to 50 + 00 + 0.6% 50 + 00 to 68 + 00 - 0.6%
Transverse slope	Crowned with 1.5% slope
Precipitation	Annual precipitation – 44.9 in. Annual snowfall – 0.5 in. Highest month – July (4.84 in.) Lowest month – March (2.00 in.)
Drainage	Good; very little puddling.
Pavement condition	Very good to excellent

APPENDIX C

EDWARDS AFB, CALIFORNIA – RUNWAY 6

Test runway: 04/22 Length, 16 800 ft Width, 300 ft	Landing approach 22
Construction history	17 in. thick PCC within test section. Surface finish, belt finished PCC, 5.33 sack mix with W/C = 5.0. Characteristics of large aggregate: 3 in. maximum size to sand, well-graded and sound. 36.9% loss in Los Angeles abrasion test. Total cost of paving and surface $6 578 000. Not much rubber buildup and no removal projects to date.
Transverse slope	Crowned with 0.5% slope
Longitudinal grade	0.140% through test section
Precipitation	Annual precipitation – 8.77 in. Annual snowfall – Trace. Highest month – December (0.95 in.). Lowest month – June and July (0.00 in.).
Drainage	Very effective, no problems
Pavement condition	Good. Has multiple hairline cracks on surface; some oxidation of iron in aggregate; no obvious full-depth cracking.

APPENDIX C

WRIGHT-PATTERSON AFB, OHIO – RUNWAY 7

Test runway: 05L/23R Length, 12 600 ft Width, 300 ft	Landing approach 05L
Construction in 1946	300 ft by 10 000 ft of 21 in. reinforced PCC, burlap drag finish, large aggregate 4 in. maximum from local pits.
Construction in 1956	1000 ft extension on southwest end of 21 in. reinforced PCC, burlap drag finish, large aggregate $1\frac{1}{2}$ in. maximum from local pits.
Construction in 1959	1600 ft extension on southwest end of reinforced PCC; thickness varies with 13 in. on edges and 15 in., 18 in., and 19 in. center portions; burlap drag finish, large aggregate $1\frac{1}{2}$ in. maximum from local pits.
Construction in 1964	Repair of original 10 000 ft; consisting of deteriorated joint and popout repairs with PCC, using quality type 3/4 in. maximum size crushed aggregate, at total cost of $1 116 000 including the architectural engineer inspection and testing. Grinding the center 50 ft width for 2831 linear feet in seven areas between sta. 73 + 85 and sta. 113 + 84 for a total area of 154 241 square feet, costing $125 684.35 at a unit cost of $0.845 per square foot. The finish transverse grooves were cut 1/16 in. deep, 3/16 in. wide, and spaced 3/4 in. center to center.
Construction in 1969	Removed rubber from approximately 80 000 sq yd of pavement on 23R at center line crown, except approximately 1800 ft of warped area at taxiway 12, where crown was eliminated.
Longitudinal grade	Beginning at 05L end, 0.00% from sta. 0 + 85.54 to approximately station 41 + 00, +0.36% from approximately sta. 41 + 00 to sta. 81 + 00, +0.10% from sta. 81 + 00 to sta. 126 + 85.54 end of 23R. Test was entirely in the +0.36% grade.

APPENDIX C

WRIGHT-PATTERSON AFB, OHIO – RUNWAY 7 – Concluded

Precipitation	Annual precipitation, 35.9 in. Annual snowfall, 26.6 in. Highest month – June (4.3 in.) Lowest month – October (2.0 in.).
Drainage	Good, except flat warped area at taxiway 12.
Pavement condition	Fair. Predominant defects are deterioration under and behind the repaired areas, surface sealing, and spalling along joints.

APPENDIX C

LOCKBOURNE AFB, OHIO – RUNWAY 8

Test runway: 23L/05R
Length, 12 100 ft
Width, 200 ft

Landing approach 23L

Construction in 1960

Center 150 ft, 16 in. PCC, 29 in. gravel base. Outer lanes, 25 ft each, 14 in. PCC, 29 in. gravel base.

Surface, broom finish.

Large aggregate – crushed gravel, maximum size 2 in.

Sieve size, U.S. standard square mesh	Percent by weight passing individual sieves	
	No. 4 to 1 in.	1 in. to 2 in.
$2\frac{1}{2}$ in.	---------	100
2 in.	---------	95 to 100
$1\frac{1}{2}$ in.	100	35 to 70
1 in.	95 to 100	0 to 15
1/2 in.	25 to 60	0 to 5
No. 4	0 to 10	
No. 8	0 to 5	

Transverse slope

1% from center line

Longitudinal grade

0.04%

Precipitation

Rain annual – 36.1 in.
Highest month – July (4.3 in.)
Lowest month – October (1.7 in.)
Snow annual – 24.8 in.
Highest month – January (6.3 in.)
Lowest month – May (0.1 in.)

Drainage

Turf side slopes extend approximately 200 in. at 3%. Some puddling in low spots.

Pavement conditions

Excellent, with minor surface popouts. Very little cracking.

APPENDIX C

LANGLEY AFB, VIRGINIA – RUNWAY 9

Test runway: 07/25 Length, 10 000 ft Width, 150 ft	Landing approach 07
Construction in 1940 and 1941 and extension in 1943	8 in., -6 in., -8 in. PCC.
Construction in 1944	Overlayed with 8 in. PCC, burlap drag finish. Large aggregate: Graded with 35% crushed granite from Richmond, Virginia area. During the past 10 years, slabs have been replaced extensively on the runway ends. No slab replacement observed in test area (interior of the runway). Rubber deposits have not been removed.
Transverse slope	1%
Longitudinal grades	07 end 0 + 00 — 0% (level) 10 + 00 — 0.08% down 20 + 00 — 0.14% up 30 + 00 — 0.07% up 40 + 00 — 0.01% up 50 + 00 — 0.06% down 60 + 00 — 0.08% down 70 + 00 — 0.14% up 75 + 00 — 0.10% up 80 + 00 — 0.07% down 90 + 00 — 0.16% down 95 + 00 — 0.08% down 25 end 100 + 00
Precipitation	Annual precipitation – 40.25 in. Snowfall – 5.85 in. Highest month – July (4.91 in.) Lowest month – October (2.25 in.)
Drainage	Good; no ponding observed.
Pavement condition	Numerous slabs repaired with epoxy patches (mostly corner spalls).

APPENDIX C

YEOVILTON RNB, ENGLAND – RUNWAYS 10 AND 11

Test runway – 09/27
Surface – Wire brush texture
Main construction – 8 in. PQ concrete
Date of construction – August 1967

Surface of runways (excluding runway ends): Except for the areas indicated at each runway end, the concrete is to be roughened by drawing a purpose-made wire broom across the pavement at right angles to the side forms, after the finishing operations, but while the concrete is still soft enough to take an impression. The broomhead is to be wire filled, of 24 in. minimum width, with 32 gage by 1/20 in. wire tapes. The contractor is to roughen trial bays for approval of the surface texture by the Specification Officer (S.O.), and thereafter is to reproduce a uniform texture throughout the runway length.

Surface of runway ends and taxiways: The concrete surfacing of runway ends and taxiways is to be slightly roughened or textured. A suitable finish can be obtained by drawing a stiff broom lightly across the pavement at right angles to the side forms, after the finishing operations but while the concrete is still soft enough to take an impression.

Surfaces of concrete surfacing other than runways and taxiways, and of lower slabs of double-slab-concrete construction, and surfaces of concrete which are to receive bituminous surfacing: The surface is to receive no special treatment other than the finishing operations required to produce the specified degree of accuracy of surface level.

Scoring of concrete surfacing: The runway is to be scored transversely by a single pass of a cutting drum incorporating not less than 50 circular segmented diamond saw blades per 12 in. width of drum. The drum is to be set at 1/8 in. depth on a multiwheeled articulated frame with outrigger wheels, fixed to give a uniform depth of scoring over the entire surface of the runway, to ensure the removal of all laitance and the exposure of the aggregate. The blades are nominally 1/8 in. thick, evenly spaced with actual blade thickness of 0.110 in. and space between the blades of 0.133 in. Sawing apparatus is to include water tankers and pressure sprays.

APPENDIX C

J.F. KENNEDY AIRPORT, N.Y. – RUNWAY 12

Test runway: 4R/22L Length 8400 ft Width, 150 ft	Landing approach 22L
Construction in 1959	12 in. PCC burlap drag finish, Aggregate (large) 3 in. minus trap rock. Transverse slope, 1%. Longitudinal grade, 0% (level).
Runway grooved in 1967	3/8 in. width by 1/8 in. depth by $1\frac{3}{8}$ in. pitch with 5/32 in. radius groove 150 ft wide by 8400 ft long. Cost $157 490 or $0.13 per sq ft Rubber deposits removed prior to grooving but not after the grooving project.
Precipitation	Annual precipitation – 40 in. Snow – 14 in. Highest month – March Lowest month – July
Drainage	Fair. After wetting, numerous bird baths or slow draining areas were observed.
Pavement conditions	Considerable number of slabs with cracks along runway center line, and a number of longitudinal edge cracks.